

# **Dynamic culture of osteogenic mesenchymal progenitor cells in a 3D porous scaffold**



The  
University  
Of  
Sheffield.

**Thesis submitted to the University of  
Sheffield for the degree of Doctor of  
Philosophy**

**Mohsen Shaeri**

**Department of Materials Science and  
Engineering**

**November 2013**

# Acknowledgements

The work presented in this thesis has been carried out under the supervision of Dr. Gwendolen Reilly. I would like to thank my supervisor Dr. Gwendolen Reilly for the encouragement and support given to me in the past few years and I am truly grateful for her invaluable advice and help along the way.

A special thanks is owed to Dr. Chuh K Chong for his technical advice, who always explained complicated ideas with great enthusiasm and patience.

Many thanks go to the people in our lab for their companionship and constant support. These include, Alex White, Katie Smith, Nathan Walker, Jennie Robertson, Claire Johnson, Anthony Bullock, Juliet Bell, Sasima Puwanun, William van Grunsven, Nii Armah Armah, Ana Mercedes Campos and Dr Nicola Green. A very special thank to Dr Robin Delaine Smith for his technical knowledge and expertise in teaching me a number of valuable techniques.

I would like to thank Orla Protein Technology and Dr Sion Philips for providing the glass scaffolds without which I would not have been able to carry out this research.

I also wish to thank the UK Engineering and Physical Sciences Research Council and METRC short-term project for providing the funding for this research.

Finally, a very special thank to my friends and family for their endless love and support. My deepest love goes to my parents, who stood by me at all times and without whom none of this would have been possible.

## Acronyms

%	percentage
$\alpha$	alpha
$\beta$	beta
$\mu\text{g}$	microgram
$\mu\text{l}$	microlitre
$\mu\text{M}$	micromolar
2D	two dimensional
3D	three dimensional
AA	ascorbic acid-2-phosphate
ALP	alkaline phosphatase
ANOVA	analysis of variance
ASC	adult stem cell
AR	Alizarin red S
ATP	adenosine triphosphate
BCS	bovine calf serum
$\beta\text{GP}$	$\beta$ -glycerophosphate
BMP	bone morphogenic protein
BMSC	bone marrow stem/stromal cell
BSA	bovine serum albumin
$\text{Ca}^{2+}$	calcium
CH	chloral hydrate
cm	centimetre
$\text{cm}^2$	square centimetre
$\text{CO}_2$	carbon dioxide
COL1	type 1 collagen
COX2	cyclooxygenase 2
DAPI	4',6-diamidino-2-phenylindole
Dex	dexamethasone
dH <sub>2</sub> O	deionised water
DMEM	Dulbecco's Modified Eagle's Medium
DNA	deoxyribonucleic acid

ECM	extracellular matrix
ESC	embryonic stem cell
F	fungizone
FAK	focal adhesion kinase
FBS	fetal bovine serum
FCS	fetal calf serum
FITC	fluorescein isothiocyanate
FSS	fluid shear stress
g	gram
h	hour
HA	hyaluronic acid
HCl	hydrochloric acid
hESMP	human embryonic stem cell-derived mesenchymal progenitor
Hz	hertz
ICT	intraciliary transport
IFT	intraflagellar transport
IGF	insulin-like growth factor
L	litre
M	molar
MAPK	mitogen-activated protein kinase
MC3T3	Mus musculus calvaria cells 3T3
MEM	minimum essential medium
mg	milligram
MG63	human osteosarcoma cells
min	minute
mL	millilitre
MLO-A5	murine long bone osteocyte A5
mm	millimetre
mM	millimolar
MP	multiphoton
MPa	megapascal
mRNA	messenger ribonucleic acid
MSC	mesenchymal stem cells

MTS	3-(4,5-dimethylthiazol-2-yl)-5-(3-carboxymethoxyphenyl)-2-(4-sulfophenyl)-2H-tetrazolium
MTT	3-(4,5-dimethylthiazol-2-yl)-2,5-diphenyltetrazolium bromide
n	number
NaOH	sodium hydroxide
nm	nanometre
nM	nanomolar
nmol	nanomole
NO	nitrogen oxide
O <sub>2</sub>	oxygen
OCN	osteocalcin
OD	optical density
OFF	oscillatory fluid flow
OM	osteogenic media
ON	osteonectin
OPN	osteopontin
P/S	penicillin/streptomycin
Pa	pascal
PBS	phosphate-buffered saline
PGE2	prostaglandin E2
pH	potential of hydrogen
PLGA	poly(lactic-co-glycolic acid)
PU	polyurethane
RNase	ribonuclease
RUNX2	runt-related transcription factor 2
SD	standard deviation
SEM	scanning electron microscopy
siRNA	small interfering ribonucleic acid
SR	Sirius red
t	time
TE	tissue engineering
TGF-β1	transforming growth factor beta-1
TRITC	tetramethyl rhodamine isothiocyanate

# Abstract

There is an increasing need to treat bone defects that arise from disease or trauma and bone tissue engineering offers an alternative solution to the limitations that are present in current treatments. Until now, regenerative medicine strategies rely on the static culture of human mesenchymal stem cells (hMSC) on a three-dimensional (3D) scaffold in the presence of biochemical cues in order to stimulate cell differentiation. However, this approach neglects the importance of mechanical stimuli in the homeostasis of bone tissue. Perfusion bioreactors have been designed to improve the nutrient supply and induce a mechanical stress in *in vitro* cell culture. Within a bioreactor system, many important parameters including flow type, insertion of rest periods, duration, frequency and magnitude of shear stress can create different biomechanical and cellular microenvironments which can accelerate the formation of bone matrix. Therefore, the ultimate aim of this project was to study the effects of a perfusion bioreactor (with particular emphasis on flow parameters) to achieve progenitor cell commitment towards an osteogenic lineage and accelerate the biological process of bone formation.

In order to achieve this, hES-MP cells were seeded on to a novel glass scaffold and subjected to oscillatory and unidirectional flow. It was shown that direct perfusion in combination with oscillatory flow improved cell growth and enhanced genes associated with osteogenic differentiation of hES-MPs in comparison to static cultures.

The methods developed were also used to study the cell's response to a combination of peptide coated scaffolds and bioreactor culture. Scaffolds were received as coated by Orla Protein Technologies with peptides from Tenascin C, Osteopontin and BMP-2. It was shown that the combination of peptide coated scaffolds and oscillatory flow resulted in an improved cell distribution and an upregulation in early and late markers of bone formation.

Finally, the 3D model was used to investigate the role of the primary cilia as a mechanosensory organelle. It was demonstrated that MLO-A5 cells were less responsive and synthesized less matrix in response to fluid shear stress in the absence of the primary cilium. Suggesting that presence of intact primary cilia is essential for load sensing and absence of the cilium (or changes in its morphology), inhibit the ability of cells to respond to fluid flow in a 3D scaffold.

The work in this thesis indicated that short bouts of oscillatory fluid flow may be sufficient to stimulate bone differentiation and maintain cell viability in an open pored scaffold such as used here. Initial data suggested that a combination of coating the scaffolds with peptides from ECM proteins or osteogenic growth factors can act synergistically with fluid flow. Finally it was demonstrated for the first time that the primary cilia of bone cells can be a mechanosensor in a 3D porous scaffold culture system. This work contributes to the ongoing work in the field of bone tissue engineering to optimise in vitro culture conditions for the creation of 3D bone matrix that could be used for future tissue engineering strategies.

# Contents

<b>Acknowledgment</b>	<b>2</b>
<b>Acronyms</b>	<b>3</b>
<b>Abstract</b>	<b>6</b>
<b>Chapter 1: Literature review</b>	<b>17</b>
1.1 Anatomy and physiology	17
1.2 Cell biology	
1.3 Extracellular matrix components	21
1.4 Bone formation, bone modelling and bone remodelling	23
1.5 Cell model for in vitro research	24
1.6 Bone mechanobiology	27
1.7 Mechanically responsive bone cells	29
1.8 Bone mechanotransduction	30
1.9 Candidate mechanoreceptors	31
1.9.1 Integrins	32
1.9.2 The cytoskeleton	32
1.9.3 Ion channels and Connexins	32
1.10 Primary cilia	33
1.11 Role of primary cilia in bone	34
1.12 Bone tissue engineering	36
1.13 Scaffolds for bone tissue engineering	37
1.13.1 Calcium phosphate (CaPs) based bioactive ceramic scaffolds	41
1.13.2 Bioglass based bioresorbable scaffolds	41
1.13.3 Polymeric scaffolds	42
1.13.4 Metallic scaffolds	43
1.14 Peptide-coated scaffolds	44
1.14.1 Osteopontin	45
1.14.2 Tenascin C	46
1.15 Growth factors	46
1.15.1 Bone Morphogenic Proteins (BMP)	47

1.16	Cells for bone tissue engineering	49
1.16.1	Osteoblasts	49
1.16.2	Stem cells	49
1.17	Bioreactors for bone tissue engineering	51
1.18	Fluid Shear Stress	55
1.19	Aims & Objectives	57
1.20	References	59
<b>Chapter 2: Materials and Methods</b>		<b>81</b>
2.1	Materials	81
2.2	methods	83
2.2.1	Cell preparation	83
2.2.1.1	Murine bone marrow derived MSC (BM1)	83
2.2.1.2	Osteoblastic cell line (MLO-A5)	83
2.2.1.3	Human embryonic stem cell derived mesenchymal progenitors (hES-MP)	84
2.2.2	Scaffold Preparation	84
2.2.2.1	Polyurethane Scaffolds (PU)	84
2.2.2.2	Nippon Sheet Glass (NSG) scaffolds	
2.2.3	Cell seeding in 3D scaffolds	87
2.2.4	Fluorescent staining of cell nucleus and cytoskeleton	87
2.2.5	Assessing cell viability	88
2.2.5.1	MTT assay	88
2.2.5.2	MTS assay	89
2.2.5.3	Alamar Blue staining	89
2.2.6	Total DNA assay	90
2.2.7	Assessment of osteogenesis	90
2.2.7.1	Alkaline Phosphatase assay	90
2.2.7.2	Prostaglandin E2 (PGE2) assay	91
2.2.7.3	Alizarin red S staining	92
2.2.8	Sirius red staining (Collagen production)	92
2.2.9	Primary cilia staining	93
2.2.10	Removal of the primary cilia using Chloral Hydrate	94

2.2.11	IBIDI Oscillatory flow pump	94
2.2.12	Peristaltic pump	95
2.2.13	Conduit length	96
2.2.14	Glass scaffolds characterization	98
2.2.15	Estimating the average shear stress for glass scaffolds	100
2.2.16	Statistical analysis	101
2.2.17	References	102

**Chapter 3: Investigating a 3-D in vitro model to study the effects of fluid shear stress on cell behavior** **104**

3.1	Introduction	104
3.2	Investigating the effects of DEX on Mouse MSC cells	110
3.3	Investigating the initial attachment of mouse MSC cells on glass scaffolds	111
3.4	Investigating the initial attachment of hES-MP cells on glass scaffolds	112
3.5	Investigating the effects of different static culture conditions for mouse MSC cells seeded on glass scaffolds	112
3.6	Studying the effects of fluid flow on matrix production and expression of genes associated with osteogenic differentiation for Mouse MSC and hES-MP cells in 3D constructs	114
3.6.1	Short term dynamic culture - Cell viability (MTS)	116
3.6.2	Short-term dynamic culture - Total DNA content and ALP activity	116
3.6.3	Long-term dynamic culture - Collagen and calcium content	119
3.7	Discussion	121
3.8	Conclusion	128
3.9	References	130

**Chapter 4: Mechanical stimulation of mesenchymal stem cells in a 3D glass scaffold using oscillatory and unidirectional flow** **140**

4.1	Introduction	140
4.2	Dynamic culture of hES-MP cells on glass scaffold	144

4.2.1	Methodology	144
4.3	Results	146
4.3.1	Cell viability as assayed by MTT – Day 7	146
4.3.2	Cell viability as assayed by MTS – Day 7 & 14	147
4.3.3	Total DNA content – Day 7	149
4.3.4	ALP activity – Day 7	150
4.3.5	Collagen production (Sirius red staining) – Day 14	151
4.3.6	Calcium deposition (Aliarin red staining) – Day 14	153
4.3.7	Day 14: Live/dead staining	155
4.4	Discussion	157
4.5	Conclusion	164
4.6	References	165

## **Chapter 5: Mechanical stimulation of mesenchymal stem cells seeded on peptide-coated glass scaffolds** **170**

5.1	Introduction	170
5.2	Investigating the effects of serum-containing and serum-free media on hES-MP-peptide-coated constructs with respect to cell attachment, cell viability and matrix mineralisation in static culture	174
5.2.1	Methodology	174
5.2.2	Results	176
5.2.2.1	Cell viability as assayed by MTS – day 7	176
5.2.2.2	Live/dead staining – Day 7	177
5.2.3	Collagen and calcium production – Day 14	179
5.3	Investigating the combination of fluid flow and hES-MP-peptide-coated constructs with respect to matrix mineralisation and expression of genes associated with osteogenic differentiation	181
5.3.1	Methodology	181
5.3.2	Results	183
5.3.2.1	Cell Viability as assayed by MTS – Day 7	183
5.3.2.2	Total DNA content – Day 7	184
5.3.2.3	ALP/DNA – Day 7	185
5.3.2.4	Dapi and phalloidin staining – Day 14	185

5.3.2.5	Collagen and calcium production – day 14	187
5.4	Discussion	189
5.5	Conclusion	193
5.6	References	194

**Chapter 6: Primary cilia of bone cells and its response to 3D dynamic loading** **200**

6.1	Introduction	200
6.2	Methodology	204
6.3	results	205
6.3.1	Cell viability quantified using Alamar Blue	205
6.3.2	CH treatment and MLO-A5 response to FSS	206
6.3.3	Primary cilia of MLO-A5 cells treated with CH and subjected to fluid flow	207
6.3.4	Matrix production	208
6.4	Discussion	210
6.5	Conclusion	214
6.6	References	215

**Chapter 7: Conclusion and Future Work** **219**

7.1	Optimal culturing strategy	219
7.2	Bioreactors for cell seeding	221
7.3	Bone tissue engineering scaffolds	221
7.4	Primary cilia of bone cells	222
7.5	Computational Modeling	223
7.6	Mesenchymal Progenitors	224
7.7	Co-culture of osteoprogenitor cells with endothelial cells	225
7.8	Final Conclusion	226
7.9	References	227

**Appendix 1** **230**

## List of figures

Fig 1.1; Drawing of the proximal end of a human femur	17
Fig 1.2; The ground section of compact bone	18
Fig 1.3; Osteoblasts cultured on LiHA matrix	19
Fig 1.4; MLO-Y4 osteocytic cells	20
Fig 1.5; SEM image of an osteoclast	20
Fig 1.6; Micrograph image of bone cells <i>in vivo</i>	21
Fig 1.7; MSC differentiation pathway <i>in vitro</i>	26
Fig 1.8; Transduction of mechanical strain to osteocytes in bone	28
Fig 1.9; Electron micrograph of the primary cilium	33
Fig 1.10; Scaffold-guided tissue regeneration	37
Fig 1.11; Focal adhesion structure	45
Fig 1.12; Pluripotent of embryonic stem cell	50
Fig 1.13; Schematic of the 8-chamber flow-perfusion bioreactor within a standard cell culture incubator	52
Fig 1.14; Cross section of the scaffold chamber	53
Fig 1.15; Schematic drawing of the chamber within the flow-perfusion bioreactor	54
Figure 2.1; The dimensions of a single PU scaffold and PU scaffolds held in place by steel rings for initial cell attachment	85
Fig 2.2; glass scaffold dimensions	86
Fig 2.3; Oscillatory pump	95
Fig 2.4; Peristaltic pump	96
Fig 2.5; Laminar flow through a pipe	96
Fig 2.6; Estimation of scaffold geometry using a time-collection method	99
Fig 2.7; Comparison of actual flow rate against flow rate collected	99
Fig 2.8; Physiological pressure transducer	101
Fig 3.1; Effect of DEX on Mouse MSC and hES-MP cells as analysed by ALP activity in cell monolayer	110
Fig 3.2; Alamar blue analysis of mouse MSC cells cultured statically on glass scaffolds	111
Fig 3.3; ; Dapi and phalloidin staining of hES-MP cells cultured	

statically on glass scaffolds	112
Fig 3.4; Cell viability and collagen production were analysed on day 7 and day 14 of culture for constructs placed in a 12 well plate and a piece of silicone conduit	113
Fig 3.5; Experimental timeline	115
Fig 3.6; MTS values of cell-seeded scaffolds subjected to fluid flow on day 7 of culture	116
Fig 3.7; Total DNA and ALP activity of cell-seeded scaffolds subjected to oscillatory fluid flow on day 7 of culture	118
Fig 3.8; Collagen and calcium production on day 14 of culture of hES-MP cells seeded on glass scaffolds and subjected to oscillatory fluid flow	119
Fig 3.9; Confocal microscopy of hES-MP constructs subjected to oscillatory fluid flow	120
Fig 4.1; Scaffolds positioned in the vertical and horizontal plane	144
Fig 4.2; Experimental timeline	145
Fig 4.3; MTT staining of scaffolds subjected to transverse oscillatory, transverse unidirectional, parallel oscillatory and parallel unidirectional flow on day 7 of culture	146
Fig 4.4; MTS values of glass scaffolds subjected to transverse and parallel flow on day 7 and 14 of culture	148
Fig 4.5; Normalised MTS values of glass scaffolds subjected to transverse and parallel flow on day 7 and 14 of culture	149
Fig 4.6; Total DNA content normalized to static conditions for scaffolds subjected to transverse and parallel flow on day 7 of culture	150
Fig 4.7; ALP normalised to total DNA for scaffolds subjected to transverse and parallel flow using oscillatory and unidirectional fluid flow	151
Fig 4.8; Normalised collagen production of scaffolds subjected to transverse and parallel flow on day 14 of culture	152
Fig 4.9; Normalised Calcium production of scaffolds subjected to transverse and parallel flow on day 14 of culture	154
Fig 4.10; Live/dead images taken from the top, middle and	

bottom of constructs in static culture and subjected to oscillatory and unidirectional flow	156
Fig 5.1; MTS Absorbance of gelatin and peptide-coated scaffolds in serum free and serum containing media at day 7 of culture	176
Fig 5.2; Live/dead staining of hES-MPs seeded on gelatin, Tenascin C, BMP-2 and osteopontin coated glass scaffolds	178
Fig 5.3; Collagen and calcium production for coated scaffolds in serum free and serum containing media	180
Fig 5.4; Experimental timeline	182
Fig 5.5; Cell activity analysed using MTS for gelatin and peptide coated scaffolds in static and dynamic culture	183
Fig 5.6; Total DNA content for gelatin and peptide coated scaffolds in static and dynamic culture on day 7	184
Fig 5.7; ALP normalized to total DNA for coated scaffolds under static and dynamic culture	185
Fig 5.8; Dapi and phalloidin staining of dynamically cultured hES-MP cells seeded on peptide and gelatin coated scaffolds on day 14 of culture	186
Fig 5.9; Collagen and calcium production for coated scaffolds under static and dynamic culture on day 14	188
Fig 6.1; Experimental design to study the effects of chloral hydrate (CH)	204
Fig 6.2; Cell viability quantified using alamar blue staining for samples treated with 0, 48 and 72 h CH treatment on day 1 and 7 of culture	205
Fig 6.3; Extracellular PGE2 observed after 2 hours of loading on day 7 of culture	206
Fig 6.4; Cell nuclei and anti-acetylated $\alpha$ tubulin staining of MLO-A5 cells with no CH treatment	207
Fig 6.5; Total collagen and calcium production for scaffolds treated with chloral hydrate for 72 hrs	209
Fig7.1; Micro-CT images of glass scaffolds	224

## List of tables

Table 1.1; Components of the organic phase of bone matrix	22
Table 1.2; Signalling factors and their functions	23
Table 1.3; Natural and synthetic scaffolds used for bone tissue engineering	40
Table 1.4; Shear stress values for experimental investigations	56
Table 2.1; Properties of Polyurethane	85
Table 2.2; Properties of glass scaffolds	86

# Chapter 1: Literature review

## 1.1 Anatomy and physiology

Bone is a dynamic, highly vascularised tissue that provides structural support for the body. It also supports muscular contraction (resulting in motion), stores minerals, bears load and protects internal organs. Bone can be divided into two categories; spongy/trabecular/cancellous bone and lamellar/compact/cortical bone [1-3]. The different architectures arise depending on anatomical site and loading conditions.

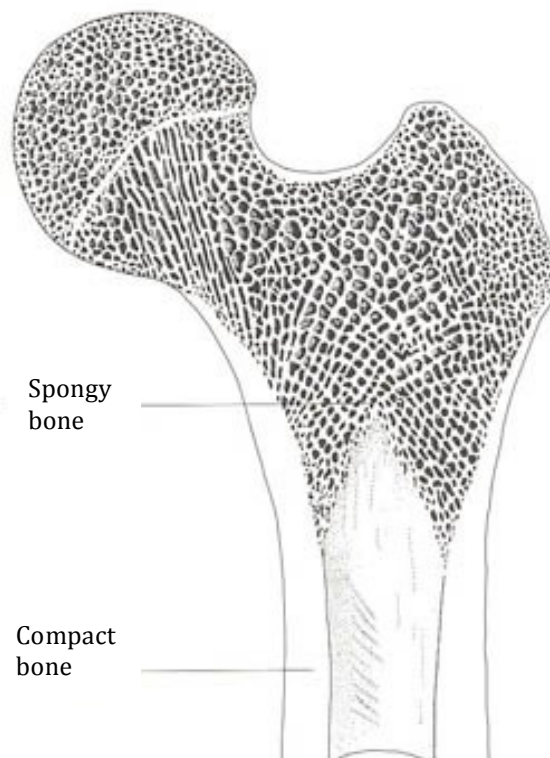


Fig 1.1; Drawing of the proximal end of a human femur showing the location of compact and spongy bone [4].

Cortical bone is located on the external region of bone and appears dense and solid, whereas trabecular bone is located in the internal region and appears as a honeycomb-like network of interconnected trabecular plates [5-8]. These structures serve to provide mechanical stability to the global structure of bone.

This contribution to total bone volume differs at various locations across the body. Cortical bone is only 10% porous containing just microarchitectural channels for blood vessels and bone cells. Trabecular bone has a higher porosity ranging from 50-90% that contain bone marrow, making its compressive strength 20 times less than that of cortical bone [9, 10].

Trabecular bone, contained in the ends of long bones and the site of bone marrow synthesis, exhibits anisotropy (having a different value when measured in different directions) as a result of being composed of rod-shaped and plate-shaped elements. Cortical bone is highly compact and orthotropic (having elastic properties in two or three planes perpendicular to each other) due to the cylindrical, lamellae that make up the osteonal structure. One example of the micro-architectural differences between the two bone types is that cortical bone contains only microscopic channels through the centre of the osteons whereas trabecular bone is highly porous [11].

At the microscopic level, bone can be found in two forms; woven and lamellar. Woven bone is immature bone and is characterised by fibre arrangement with no orientation and contains more randomly arranged cells per unit volume than lamellar bone [12]. This network of randomly oriented fibres results in isotropic mechanical properties (properties of bone are the same in all directions). Lamellar bone contains a high number of organised, stress oriented collagen fibres which give it its anisotropic mechanical behaviour [13].

The Haversian system is the fundamental functional unit of adult human cortical bone. Osteons are cylindrical structures that are normally several millimetres long and roughly 0.2 mm in diameter. Each osteon consists of lamellae that surround a central canal (the Haversian canal), which contains the bone's nerve and blood supply. Within bone, osteocytes live within individual spaces, known as lacuna. Osteocytes make contact with cytoplasmic processes via a network of canals called canaliculi which facilitate the exchange of nutrients and metabolic waste (fig 1.2).

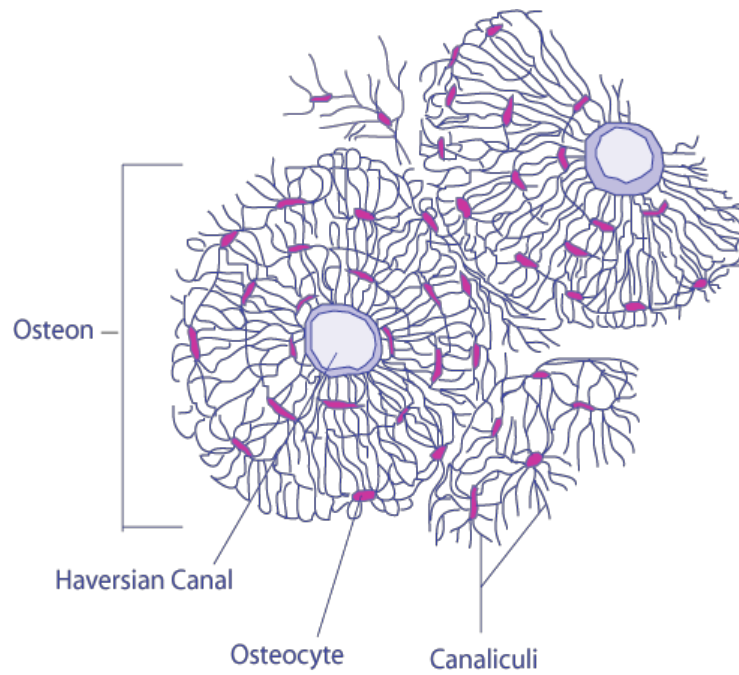


Fig 1.2; Diagram of a ground section of compact bone showing the transverse section of long bone's cortex [14].

## 1.2 Cell biology

*Osteoblasts* are the bone cells that form bone (fig 1.6). They are responsible for the production of the organic matrix of bone and secrete products such as collagen type 1 and also noncollagenous proteins such as osteopontin and osteocalcin (table 1.1). Osteoblasts arise from pluripotent mesenchymal progenitor cells that can also develop into adipocytes, myocytes, and chondrocytes [15]. Figure 1.3 is an SEM micrograph of osteoblasts cultured on a Lithium-Hydroxyapatite (LiHA) matrix.

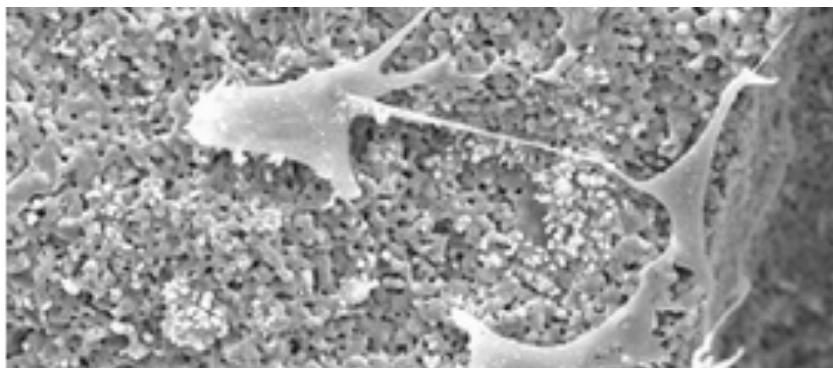


Fig 1.3; SEM micrograph of osteoblasts cultured on LiHA matrix [16].

While osteoblastic cells are perhaps the most widely studied bone cells, by far the most abundant bone cells are the *osteocytes* (fig 1.6). Roughly 90% of all cells in bone are osteocytes. However, due to the difficulties in isolating these cells and culturing them *in vitro*, osteocytes are the least studied bone cells. They arise from osteoblasts that have become entrapped in the mineralised matrix that they have formed. Figure 1.4 is an image of cells from an osteocyte-like cell line MLO-Y4 [17].

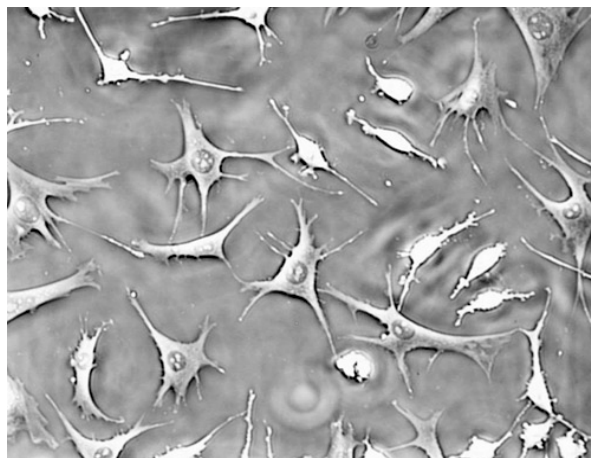


Fig 1.4; Light micrograph of MLO-Y4 osteocytic cells cultured on tissue culture plate [18].

*Osteoclasts* are large multinucleated cells and are responsible for the dissolution and absorption of bone (fig 1.6). They are multinucleated and derive from hematopoietic cells (fig 1.5). They have the ability to secrete lysosomal enzymes which break down mineralized bone. An active osteoclast can resorb 20,000  $\mu\text{m}^3$ /day of bone matrix [17].

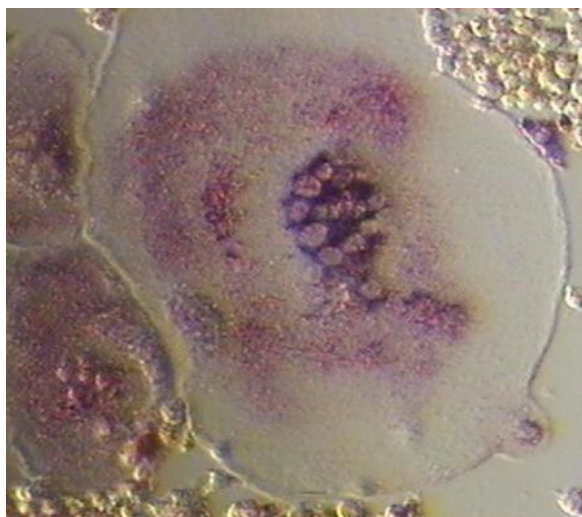


Fig 1.5; Image of an osteoclast in cell culture [19].

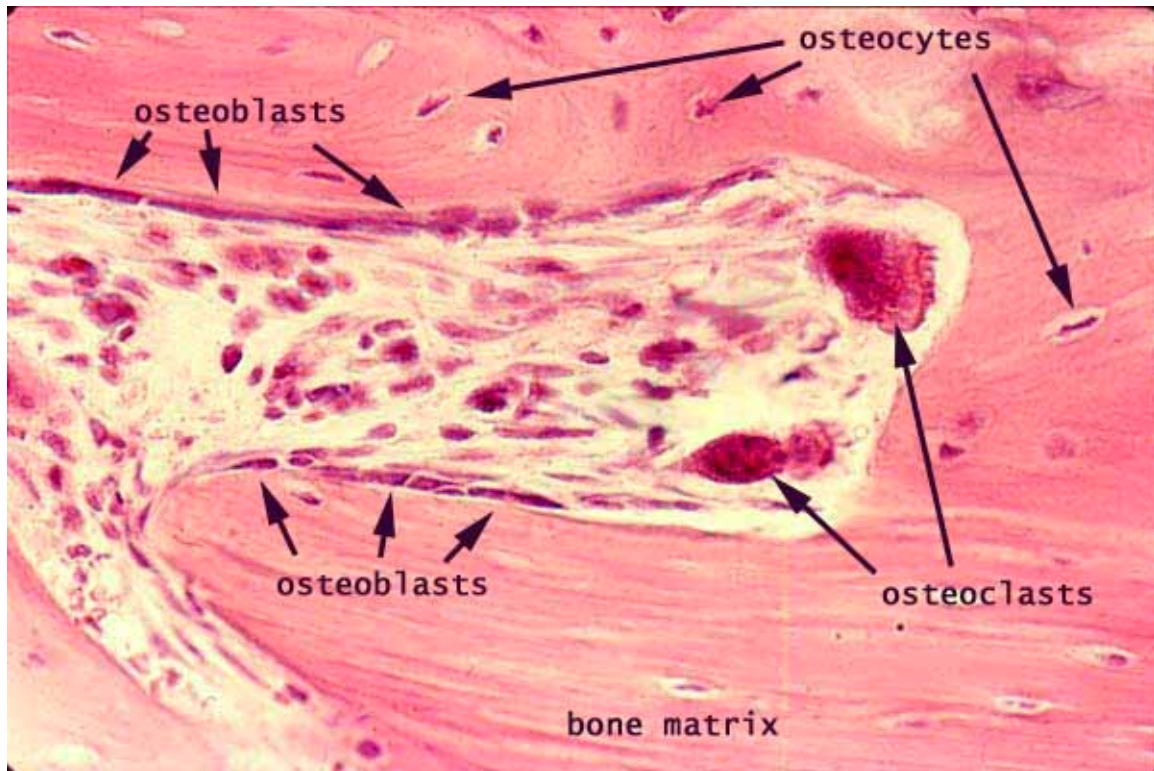


Fig 1.6; Micrograph image of bone cells. *Osteoblasts* lie alongside the surface of the channel and are responsible for the production of the organic matrix of bone. *Osteocytes* arise from osteoblasts and become entrapped in the mineralised matrix they form. *Osteoclasts* remove bone matrix [20].

### 1.3 Extracellular matrix components

Bone matrix has a mineral inorganic component, composed of mostly hydroxyapatite (65-70%) and an organic part, which is composed of collagen, proteoglycans, glycoproteins, bone gla proteins and sialoproteins, that comprises the remaining 25-30% of the total matrix. The newly formed matrix (osteoid) consists roughly 94% collagen [21]. Type I collagen is the principle collagen in mineralized bone, together with type V collagen. The collagen fibrils in bone are stabilized by intermolecular cross-linking which leads to the high tensile strength of collagen fibres [22]. Osteocalcin (OCN), also known as gla protein, is a 5.8-kDa acidic protein which is modified by vitamin-dependent carboxylating enzymes that convert glutamic acids into  $\gamma$ -carboxyglutamic acids (gla group) interacting with hydroxyapatite [23]. Osteopontin (OPN) and Bone sialoprotein (BSP) are 34-kDa proteins with highly glycosylated and phosphorylated sites binding with Hyaluronic acid (HA). BSP is restricted to mineralizing tissues, whereas OPN has been shown to play an important role in both the cell attachment and mechanotransduction responses of osteoblasts *in vitro* [24].

Other components of the bone organic phase are summarized in table 1.1. Some key signaling factors found in bone and their functions are also summarized in table 1.2.

Table 1.1; Components of the organic phase of bone matrix

<b>Bone Extracellular Matrix constituent</b>	<b>Functions and properties</b>	<b>Reference</b>
Collagen I	Provides framework for skeletal structure; matrix calcification	25
Byglican	Proteoglycan; affect collagen fiber growth and diameter, involved in the process of matrix mineralization	26
Decorin		27
Osteonectin	Glycoprotein, binds Ca <sup>2+</sup> and collagen; nucleates hydroxyapatite	28,29
Thrombospondin	Glycoprotein; binds calcium, hydroxyapatite, osteonectin and other cell surface proteins; mediates cell adhesion in a RGD-independent fashion	30
Fibronectin	Osteoblast attachment to substrate	31
Osteopontin	Sialoprotein; constituent of cement line involved in bone remodeling	32,33
Bone Sialoprotein	Sialoprotein; constituent of cement line	34
Osteocalcin	Skeletal gla protein; late marker of osteogenic phenotype; involved in bone remodeling; it may also be involved in the control of mineralization through its inhibition	35

Table 1.2; Signaling factors and their functions during bone development.

<b>Signaling factors</b>	<b>Functions</b>	<b>Reference</b>
Bone Morphogenic Proteins (BMP)	Stimulates osteoblast proliferation Causes increased matrix production Induces MSC differentiation into osteoblasts	36
Fibroblast Growth Factors (FGF)	Stimulates proliferation of MSCs and osteoblasts	13
Dentin matrix protein-1 (DMP1)	Induces MSC differentiation into osteoblasts Mineralization regulator	17
Platelet-derived growth factors (PDGF)	Stimulates proliferation of osteoblasts	17
Insulin-like growth factors (IGF)	Stimulates proliferation of osteoblasts	36
Transforming growth factor- $\beta$ (TGF- $\beta$ )	Induces proliferation of osteoblasts Enhances bone resorption	37
Prostaglandin E2 (PGE2)	Induces osteoblast differentiation, alkaline phosphatase activity, collagen synthesis Stimulates osteoblast proliferation	38
Dexamethasone (DEX)	Promotes osteoblast differentiation	17
Nitric oxide (NO)	Enhances PGE2 release Stimulates osteoblast proliferation	39
Adenosine 3',5'-cyclic monophosphate (cAMP)	Stimulates osteoblast proliferation	17
Extracellular signal-regulated kinase (ERK)	Induces osteoblast differentiation Enhances calcium deposition	40

#### **1.4 Bone formation, bone modelling and bone remodelling**

Bone is initially developed by the process of ossification as a specialised connective tissue. During the process of ossification, osteoblastic cells secrete an

amorphous material gradually becoming osteoid, this is a mixture of collagen 1 (COL1) and non collagenous matrix proteins. Calcium phosphate crystals (synthesised by osteoblasts) are deposited in the osteoid resulting in bone matrix. As the osteoblastic cells become surrounded by the matrix, they differentiate into osteocytes [41]. Chemical and mechanical factors influence the rate of ossification.

Bone modeling is the process by which bone is shaped or reshaped by the action of the osteoblast-osteoclast complex. For example, the radius in the playing arm of a tennis player has a greater diameter and thicker cortex in comparison to the other arm as a result of bone modeling. In the human body, bone modeling occurs less frequently than bone remodeling. Bone modeling differs from bone remodeling in that bone formation does not follow bone resorption.

The remodeling process begins at a quiescent bone surface when the osteoclasts attach to the bone tissue matrix and form a ruffled border at the bone interface [42]. Thus the osteoclast creates an isolated microenvironment and subsequently the osteoclast acidifies the microenvironment and dissolves the organic and inorganic matrices of the bone. Briefly after this resorptive process stops, osteoblasts appear at the same surface site and deposit osteoid and mineralize it and hence forming new bone. Remaining osteoblastic cells continue to synthesize bone until they eventually stop and transform to quiescent lining cells that completely cover the newly formed bone surface [43].

### **1.5 Cell model for *in vitro* research**

Various cell culture models have been employed for studying MSC, osteoblast and osteocyte cell biology, including primary cells from different species, induced osteoblasts from pluripotent stem cells, immortalised and malignant cell lines. The main advantage to using primary human cells is their clinical applicability, they should better represent a 'typical' human osteoblast and one does not need to take into account any interspecies differences, as is the case when other animal cell sources are used. Furthermore, primary human

osteoblasts tend to retain their differentiated phenotype *in vitro*. On the other hand, human isolated cells represent a heterogeneous cell population, and therefore exhibit phenotypic differences relating to the skeletal location from which they were isolated [44, 45]. Many factors influence primary human osteoblast cell behaviour; age, site of isolation and gender differences are the most common. Thus, the time frames for phenotypic changes *in vitro* differ for cells isolated from different origins. Some studies indicate that nodule formation in mineralization of human bone cell cultures may not occur [46].

However primary osteocytes are extremely difficult to work with, firstly they are difficult to isolate from bone since the methods used also release osteoblasts from the same bone. Therefore, osteocytes must be separated via antibody selection. In addition they do not proliferate well in culture and die-differentiate, losing their characteristic morphology of numerous cell processes after prolonged time in plastic. Therefore most of the early work that aimed at understanding the responses of bone cells to fluid flow in fact worked with osteoblast in culture rather than osteocytes. A few specialized laboratories have worked with human primary osteocytes and shown that one hour pulsating fluid flow resulted in a rapid increase in nitric oxide production and mRNA levels for eNOS [47].

Cell-line osteoblasts provide a more homogenous population of cells and allow the study of particular stages of osteoblast phenotype. They are very useful at the early stages of assessing the therapeutic agents or for cytocompatibility testing; however, they do not fully reflect the behaviour of primary cells. The advantages of using immortalized cell lines include ease of maintenance, unlimited number of cells without the need for isolation and relative phenotypic stability. However, some reports present evidence of progressing phenotypic heterogeneity among cell lines, which is correlated with prolonged passaging of cells [48-50]. Additionally, both transformed and non-transformed cell lines, as they are stage-arrested, do not reflect the whole range of phenotypic features of normal osteoblast cells. In the last 10 years a mouse osteocyte cell line (MLO-Y4) was

developed by the Bonewald group and this has become a popular cell line with which to study osteocyte mechanoresponsiveness *in vivo* [51-53]

Mesenchymal stem cells (MSCs) from the bone marrow are multipotent and are capable of differentiating into several lineages including chondrocytes [54], adipocytes [55], fibroblasts [56] and osteoblasts [57]. In order to develop an osteoblastic phenotype, MSCs are cultured in medium supplemented with ascorbic acid (AA),  $\beta$ - glycerophosphate ( $\beta$ GP), and dexamethasone (DEX) [58]. *In vitro* MSC differentiation into an osteoblastic phenotype can be marked by three phases (fig 1.7). During the proliferation phase (growth phase) cells tend to express mRNA for related growth proteins including c-fos, histone, c-myc, transforming growth factor- $\beta$  (TGF- $\beta$ ), procollagen I, and fibronectin [59]. During the matrix maturation phase cells differentiate into osteoblasts and secrete alkaline phosphatase (ALP) and produce type I collagen [60]. Finally, mineralisation is marked by the secretion of collagenous proteins including osteopontin (OPN), osteocalcin (OC), bone sialoprotein (BSP), and deposition of calcium/phosphate minerals [61].

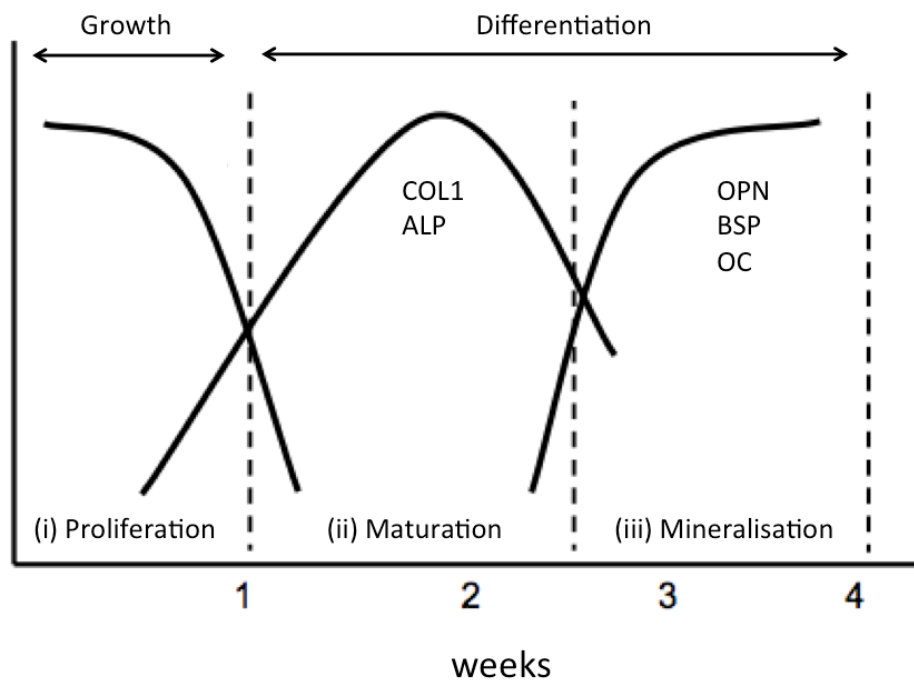


Fig 1.7; MSC differentiation *in vitro* can be marked by the three phases including proliferation, ECM maturation and ECM mineralisation. This development sequence is very useful in monitoring osteoblastic differentiation.

## 1.6 Bone mechanobiology

It is known that cells and tissues in the human body are constantly subjected to a wide variety of external forces, which can influence their growth, development and maintenance. In tissues such as muscles, tendon, skin and vessels, cells continuously recognise alterations in mechanical forces and adapt their biological function accordingly [62]. For example mechanical strain has been found to induce cardiac myocyte hypertrophy [63]. Similarly bone adapts to increased loading by modeling, for example there is greater bone density in the femurs of weightlifters compared to non-weightlifters. *Jones et al.*, compared the dominant arms of professional tennis players with the contralateral bone and found that cortical thickness was increased by 34.9% in men and 28.4% in women. In contrast, reduced loading e.g. due to bed rest, or microgravity can lead to bone loss [64].

It has been advocated over the last several years that the osteocytes are the mechanosensory cells of bone, and the lacuno-canalicular porosity is the structure that allows mechanosensing [65]. The current widely accepted theory of bone mechanotransduction is as follows: mechanical loads *in vivo* cause deformation in bone that induce fluid flow within the bone canaliculae and create shear stresses on the cells (osteocytes) embedded deep within the bone matrix [43]. Osteocytes produce second messengers, which can cause osteoprogenitor cells to differentiate into osteoblasts resulting in new bone formation and/or inhibit osteoclast function resulting in reduced bone resorption. The cyclic loading of bone such as the femur or tibia during walking produces oscillating fluid shear forces in the lacunocanalicular network. This mechanically induced loading not only subjects osteocytes to fluid shear stress but also pumps waste products out of the network and directs oxygenated and nutrient-containing fluid from the blood back to the network. Figure 1.8 illustrates this hypothesis [66, 67].

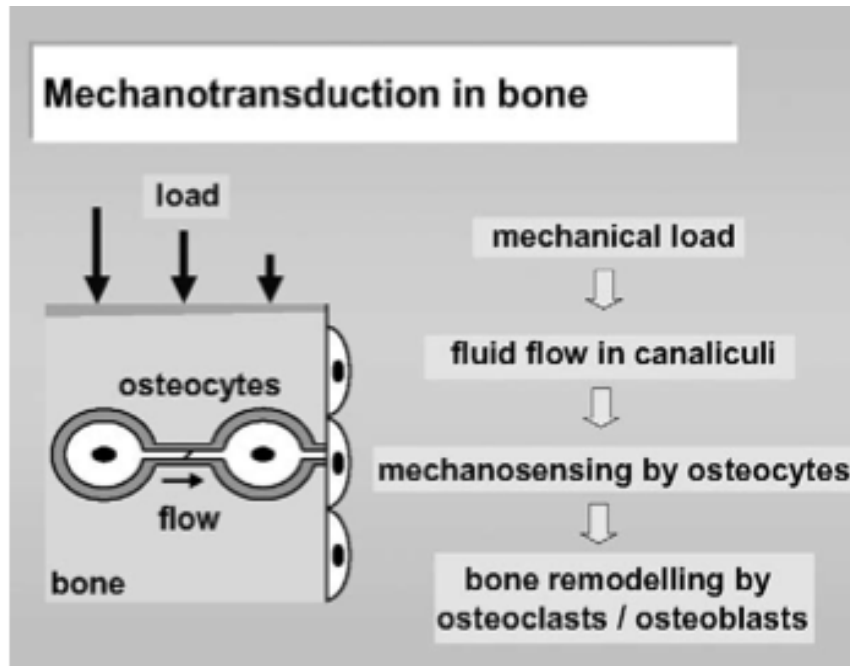


Fig 1.8; Transduction of mechanical strain to osteocytes in bone. Loading results in flow of interstitial fluid in the canalicular complex as indicated by the horizontal arrows.[68].

It has been shown that fluid shear stress plays an important role in normal physiology, e.g. in the adaptation of blood vessels to changes in blood flow. Regular flow of blood results in shear stress, which act on the inner wall of the blood vessel. During exercise, enhanced blood flow results in widening of the vessel, to ensure a constant blood pressure. Endothelial cells sense the increased blood flow (higher shear stress) and produce intercellular messengers such as nitric oxide (NO) and prostaglandins, which enable the blood vessel to adapt to fluid flow. In response to these signaling molecules, the smooth muscle cells around the vessel relax, to allow the vessel to increase in diameter. The capacity of endothelial cells to produce NO in response to fluid flow is related to a specific enzyme called endothelial NO synthase (eNOS). In endothelial cells, eNOS activity is predominantly associated with the plasma membrane and the localisation of this enzyme may be related to the transduction mechanism by which physical forces bring forth the formation of NO [69-71].

Similarly in bone, *in vivo* studies suggest that NO is involved in mechanically induced bone formation. eNOS was found in rat osteocytes and in human bone cells and was found that treatment with pulsating fluid flow increased eNOS mRNA levels in bone cells [72]. The kinetics of this adaptive response are different for the two systems however, it is interesting that two different biological structures would use a similar mechanism to detect mechanical signals. It has been speculated that the detection and signal transduction of NO upregulation (in bone cells and endothelial cells) involves opening of cation channels and an increase in intracellular calcium.

Cell response to mechanical loading depends on various factors including; magnitude, frequency and rate of applied force. High rates of loading and high impact physical activity including jumps in unusual directions have been shown to have a great osteogenic potential in humans [39, 73]. *Bacabac et al.*, suggested the bone cell response to shear stress is rate dependent and demonstrated that increasing shear stress amplitude or frequency on cultured MC3T3-E1 osteoblastic cells, resulted in increased NO production [74].

Other *in vitro* studies have also shown that osteocytes respond to fluid flow by increasing NO levels and stimulating osteoblast proliferation, leading to prostaglandin E2 (PGE2) release [72]. *In vivo*, PGE2 plays an important role in the functional adaptation of bone to mechanical load by inducing cell proliferation, alkaline phosphate activity and collagen synthesis.

## **1.7 Mechanically responsive bone cells**

Bone cells sense and respond to mechanical forces by *at least* four cell types: osteoclasts, osteoblasts, osteocytes, and mesenchymal stem cells. Each of these cell types is independently sensitive to mechanical signals through their interaction with each other and their precursors, can serve as critical regulatory elements in the recruitment, proliferation and differentiation of osteoclasts and osteoblasts.

This regulation is evident in studies which demonstrate that application of mechanical strain to murine marrow derived stromal cells, significantly reduced mRNA expression of receptor activator of NF kappa B ligand (RANKL), a signalling factor that induces osteoclast differentiation [75]. These studies demonstrate the temporal and spatial coordination between multiple cell types in bone, which together regulate adaptive changes in response to alterations in the mechanical environment.

Mechanical control of osteoclast function appears to occur largely through regulation of osteoclast recruitment, which is achieved through osteoprogenitor lineage expression of RANKL [76]. Cells of the osteoprogenitor lineage are located in mechanically active environments, and respond to mechanical cues with alteration in proliferation, differentiation and differentiated function.

MSC cells, which share a hematopoietic niche with blood stem cells, are also sensitive to mechanical stimulation and respond by altering the output of differentiated cell types [77] and increase rates of clonal proliferation [78].

As mentioned previously, osteocytes are uniquely situated in cortical bone and are connected through a network of sister cells [79] which contributes to the perception of these cells to sense and respond to mechanical loading. During unloading (or a decrease in mechanical signals) this network of cells tend to respond with an upregulation in sclerostin and RANKL that control bone remodelling at multiple levels [80, 81]. The long osteocytic processes also pass information between cells and it is likely that they generate soluble factors that modulate MSC differentiation as well as osteoprogenitor recruitment to areas of bone remodelling.

## **1.8 Bone mechanotransduction**

Mechanotransduction is described as the process by which cells convert an external mechanical force into biochemical signals. As mentioned previously, osteocytes are found in the lacunae and form an interconnected network with

one another and also with osteoblasts at the bone surface through canaliculi. *Burger et al*, described mechanotransduction in bone in three different stages [82];

- 1) Mechanical loading must induce a cell-level physical signal that can be sensed by osteocytes,
- 2) The physical signal must be translated to a biochemical signal by osteocytes,
- 3) The biochemical signal must be communicated to effector cells including osteoblasts and osteoclasts.

Subjecting osteocytes to mechanical loading activates multiple signaling pathways that can result in osteogenic and antiresorptive responses. Shortly after exposure to a mechanical load, osteocytes respond with the release of adenosine triphosphate (ATP),  $\text{Ca}^{2+}$  and PGE2. These responses lead to the downstream effects that mediate bone remodeling, including increases in cytochrome oxidase subunit 2 (COX-2) and PGE2 [83-86]. COX-2 is an enzyme maintaining homeostatic levels of prostaglandins and is induced by an array of stimuli including injury, inflammation and mechanical stress.

## **1.9 Candidate mechanoreceptors**

The ability of cells to sense the mechanical signals from the environment requires that mechanoreceptors either directly contact with the extracellular space, or that a mechanoreceptor can distinguish changes in a physical intermediary such as pressure or fluid shear on the plasma membrane. Suggested mechanotransduction mechanisms include junctions between the cell and ECM (integrins and focal adhesions), cell-cell adhesions (cadherins and gap junctions), the cell cytoskeleton (microfilaments, microtubules, and intermediate filaments) and membranes (ion channels and caveolae). Other suggested mechanisms include the pericellular glycocalyx and the primary cilia.

### 1.9.1 Integrins

Integrins are protein complexes that couple the cell to the external environment by spanning the plasma membrane and forming attachments with the ECM. Integrins serve a mechanosensory role in a variety of cells including platelets [87], endothelial cells [88], fibroblasts [89], myocytes [90], chondrocytes [91], and bone cells [92]. The binding of extracellular ligands to integrins may initiate intracellular signaling events. Experiments have shown that integrin manipulation activates RhoA, which induces formation of new focal adhesions which can contribute to remodelling of the cytoskeleton [93].

### 1.9.2 The Cytoskeleton

The actin, intermediate filaments, and microtubules produce a structural framework (the cytoskeleton) by which the cells can mediate functions such as cellular and molecular transport, cell division, and cellular structure. The cytoskeleton provides an inherent means of perceiving and responding to mechanical signals. It has been shown that fluid shear stress across osteoblasts induces reorganization of actin filaments into contractile stress fibers [75] while disruption of the actin cytoskeleton reduces the response of bone cells to fluid shear stress [94, 95]. It has been suggested that cell response to mechanical stimuli is mediated by its cytoskeleton [96]. The stiffness of the cytoskeleton has shown to increase in response to an increase in mechanical stress. *Pavalko et al.*, demonstrated MC3T3-E1 actin cytoskeleton rearranges in response to fluid shear stress [97].

### 1.9.3 Ion channels and Connexins

Ion flow through non-ciliary associated ion channels are responsible for maintaining proper electrochemical gradients and thus are sensitive to membrane depolarization. Connexins are membrane spanning protein complexes that form pores within the plasma membrane of cells. Alignment of connexons with their counterpart on an adjacent cell creates gap junctions that

allows for intracellular communication isolated from the extracellular environment, and can pass small molecules (<1kDA) including calcium, inositol phosphates, ATP, and cAMP [98, 99]. It has been shown that mechanical stimulation increased expression of connexins *in vitro* and *in vivo*, suggesting that cells generate enhanced connections with their neighbours enabling proper transmission of mechanical information within the skeletal network.

### 1.10 Primary cilia

An important aspect of bone cell mechanotransduction, is the mechanism by which these cells sense mechanical loads and translate them to biochemical signals. Although the area is not fully understood, recent studies have suggested that the primary cilium, a microtubule structure that extends from the cell membrane, is a prime candidate for an extracellular sensor of mechanical loading [100-102].

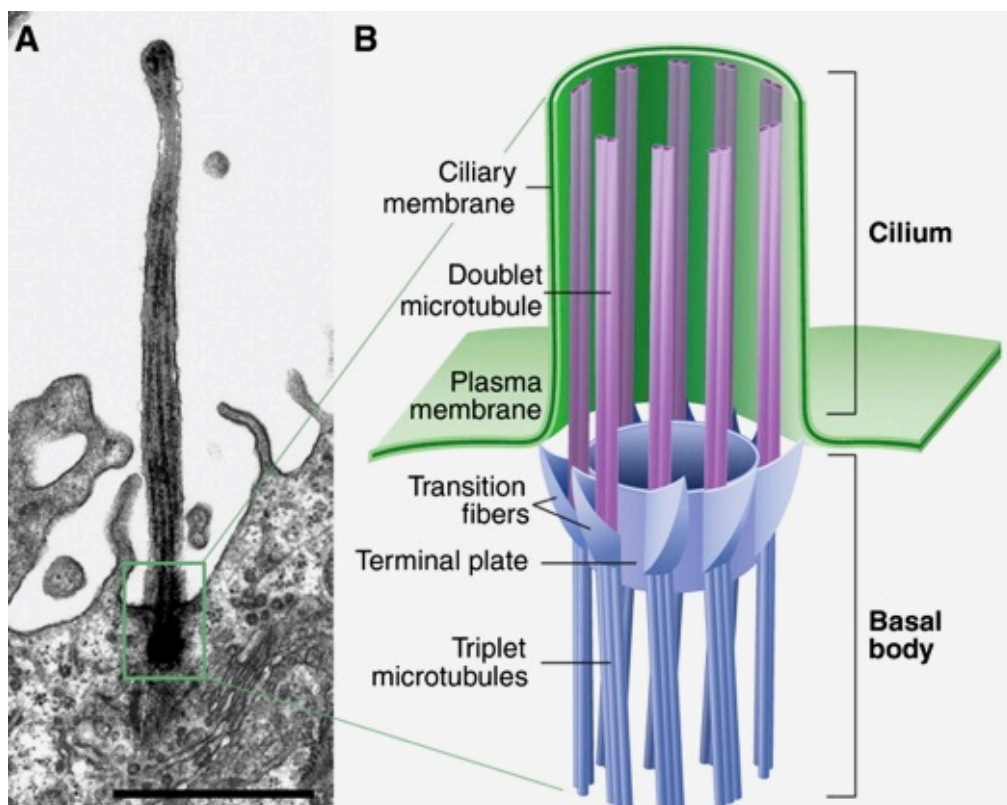


Fig 1.9; (A) An electron micrograph of the primary cilium of a canary brain radial glia. (B) Schematic diagram showing structure of the basal body and primary cilium [103].

The primary cilium is a microtubule-based structure that extends from the cell membrane into the extracellular space. The basal body/mother centriole is well known for its role as a microtubule organising center of mitotic spindles (fig 1.9). When not involved in mitosis, the mother centriole migrates to the cell membrane and acts as an anchor for the primary cilium and as a template of ciliogenesis [104]. Since the primary cilium does not contain the complex machinery to synthesize its own proteins, ciliary proteins are synthesized in the cell body and targeted to the cilia through intraflagellar transport (IFT, a bidirectional system that directs movement along the microtubules of the cilia body).

A typical cilium is approximately 5  $\mu\text{m}$  in length but can be up to 30  $\mu\text{m}$  as seen on cells from a kangaroo rat kidney [105]. Both motile and non motile cilia contain a microtubule doublet that provides structure and stability. Non motile cilia lack a central pair of microtubules (hence designated 9+0 cilia) and other machinery found in motile cilia including radial spokes, central pair projections and inner and outer dynein arms. Unlike motile 9+2 cilia, there is only one primary cilium per cell [103].

### **1.11 Role of primary cilia in bone**

Primary cilia were first discovered over a century ago and until recently their function has been a mystery. They have been shown to have an important role in a number of developmental processes including the establishment of the left-right axis in the embryonic node [106]. *Haycraft and Serra* showed that ciliary dysfunction resulted in extensive polydactyly with loss of anteroposterior digit patterning and shortening of the proximodistal axis [107].

Most previous work that focused on primary cilia as a mechanosensor has focused on the kidney and liver. *Praetorius and Spring* revealed that fluid flow within the kidney resulted in a deflection of the primary cilia, which caused an extracellular calcium dependent increase in intracellular calcium [108]. This response was lost after the removal of the primary cilia. It was found that this

calcium response is mediated by a mechanosensory complex, which is located at the base of the cilium [109]. This complex is made up of polycystin 1 (PC1, a large transmembrane protein) and polycystin 2 (PC2, a cationic channel that is part of the transient receptor potential channel family (TRP)). This mechanosensing mechanism has also been reported in liver cholangiocytes. It was found that the PC1/2 complex and the stretch activated ion channel TRPV4 are situated at the primary cilium and sense fluid shear stress and osmotic pressure respectively [110]. The application of flow not only resulted in an influx of calcium but also suppression of a forskolin stimulated increase in cAMP.

Recent studies have shown that the primary cilia also acts as a mechanosensor in bone cells [111]. Cilia bends under *in vitro* fluid flow and recent reports have found that disruption of the cilia inhibits COX-2 gene expression and PGE2 release in response to fluid flow in osteoblasts [112]. Further studies suggest that the application of flow leads to a cilia-dependent decrease in the second messenger cAMP [113]. Interestingly, flow induced cilia-dependent responses were independent of intracellular calcium [112] suggesting that the mechanotransduction pathway for bone cells differs from the kidney and liver.

*Hoey et al.*, showed that signaling molecules released into culture media by osteoblasts subjected to fluid flow were primary-cilia dependent, suggesting that primary cilia plays a key role in osteogenic responses to flow in osteoblasts [114]. In a similar study the primary cilium was shown to mediate fluid flow-increases in osteogenic genes in human MSCs. Results from this study demonstrate that targeting the primary cilium using oscillatory fluid flow may be beneficial for bone tissue engineering applications and could provide insight regarding ciliopathies and cystic diseases [111].

Although the PC1/2 complex has been shown to play a vital role in cilia-related mechanotransduction in the liver and kidney, its role in bone is still unclear. A recent study showed that heterozygous *pkd1* mutant mice (a mutation in the gene that encodes for PC1) have decreased trabecular bone volume, bone mineral density and cortical thickness [115].

## 1.12 Bone tissue engineering

It is estimated that nearly 1 million cases of skeletal defects a year require bone-graft procedures to achieve union [13]. Bone disease is a major health concern for both USA and the EU, and its incidence will increase in the next years due the ageing of their populations. Current treatments include the use of autologous and autogenous bone grafts or as an alternative to these, polymers and ceramics.

*Autologous bone graft*, that is, bone taken from another part of the patients own body, has been the gold standard of bone replacement for many years because it provides osteogenic cells as well as essential osteoinductive factors needed for bone healing and regeneration. The major disadvantage of this method is the limited amount of autograft that can be obtained and donor site morbidity [116].

*Allograft*, bone taken from somebody else's body, could be an alternative solution. However, the rate of graft incorporation is lower than with the autograft and the bone could also introduce the possibilities of immune rejection and of pathogen transmission from donor to host. Furthermore infections sometimes occur in the recipient's body due to the transplantation [117]. For this reason allograft is usually decellularised and sterilised which compromises both its bioactivity and mechanical properties.

As a result of the limitations of different bone grafts, bone tissue engineering is emerging as a potential alternative [118]. To quote *Langer and Vacanti et al.*, tissue engineering is "an interdisciplinary field of research that applies the principles of engineering and the life sciences towards the development of biological substitutes that restore, maintain, or improve tissue function" [119]. Unlike other approaches (rather than just to implanting new spare parts), tissue engineering is based on the understanding of tissue formation and regeneration, and aims to induce new functional tissues. Researchers hope to reach this goal by combining knowledge from various fields including physics, engineering, chemistry, biology and materials science.

From a biological perspective several key elements must be controlled at all times. These include the cells, extracellular matrix, intercellular communications, cell-matrix interactions and growth factors.

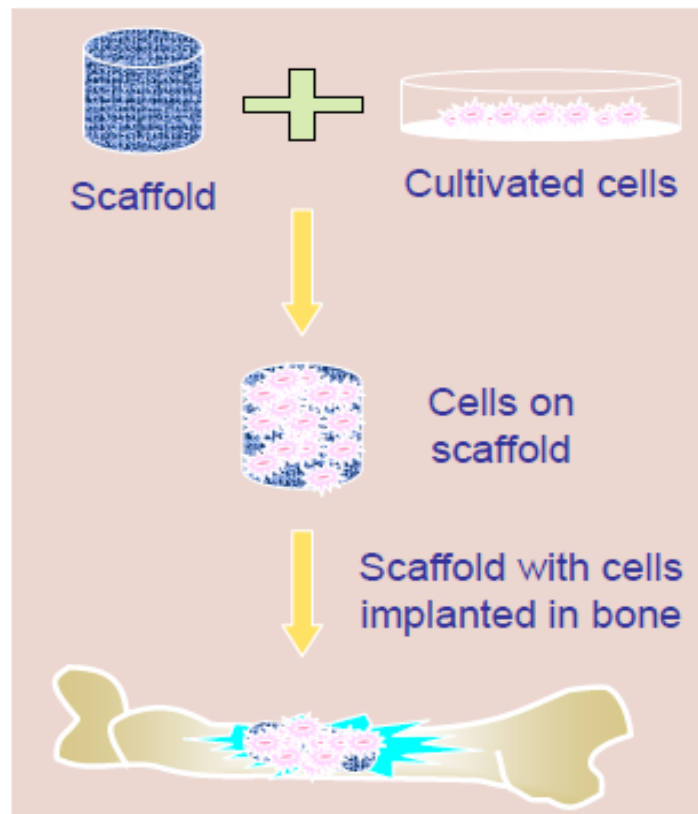


Fig 1.10; Bone tissue engineering technique tends to replicate the natural process of cell signaling involved in cell growth and differentiation. This can be achieved by placing the cells and growth factors in synthetic and biocompatible scaffolds in order to act as temporary extracellular matrices [120].

### 1.13 Scaffolds for bone tissue engineering

Scaffolds are commonly used in bone tissue engineering, acting as a vehicle for the delivery of cells, genetic material and growth factors to the site of interest (table 1.3). The aim is that a scaffold would also support vascular invasion and retain a uniform distribution of cells throughout its 3D lattice. Ideally a scaffold for bone tissue engineering should have the following characteristics:

- **Porosity:** Scaffolds must possess an open pore, fully interconnected geometry in a highly porous structure with large surface to area volume ratio. This will allow cell in-growth and a uniform cell distribution throughout the porous structure. Furthermore, the scaffolds should also exhibit adequate porosity for capillary in-growth.

Porosity and interconnectivity are important for diffusion of nutrients and gases and for the removal of metabolic waste resulting from the activity of the cells that have grown into the scaffold. However, the degree of porosity will influence other properties of the scaffolds such as its mechanical stability, so it should always be balanced with the mechanical needs of the particular tissue that is going to be replaced.

- **Permeability:** Permeability is a term used to measure the ease with which a fluid can flow through the scaffold. A high permeability indicates good diffusion within the scaffold, which would improve the inflow of nutrients and the disposal of waste products. Fluid-material interactions can influence the viscoelastic response of a scaffold and hence change its permeability. This is important when designing scaffolds for bone and articular cartilage repair, since mechanotransduction is affected by fluid flow.

- **Pore Size:** Pore size is also a very important issue. If the pore size is too small, pore occlusion by the cells will prevent cellular penetration and extracellular matrix production. It has been stated that for bone tissue engineering purposes, pore size should be between the 200-900  $\mu\text{m}$  [121-123].

*Holy et al.*, reported bone formation on a 3D temporary matrix (PLGA scaffold) with large macroporous interconnected structure with macro pore size ranging from 1.5-2.2 mm [124]. This approach has advantages due to its high surface to volume ratios that will facilitate cell, tissue and blood vessels ingrowth. However scaffolds with large pores will have lower mechanical properties for a given material so many large pored scaffolds would not be appropriate for load bearing areas.

- **Surface Properties:** Surface properties, both chemical and topographical, are important for cellular adhesion and proliferation [125-127]. Chemical properties affect the ability of proteins and cells to adhere to the material. Topographical properties are of particular interest when considering osteoconduction. As defined by *Davies et al*, osteoconduction “is the process by which osteogenic cells migrate to the surface of the scaffold through a fibrin clot, which is established immediately after the material implantation” [128].

- **Mechanical Properties:** Due to the high levels of pressure that cells are subjected to *in vivo*, the scaffold should have sufficient mechanical strength to withstand this and to maintain the spaces required for cell ingrowth and matrix production. Many researchers suggest that the mechanical properties of the implanted scaffold should ideally match those of living bone [129-131].

- **Biodegradability:** The scaffolds degradation rate must be tuned appropriately with the growth rate of the neotissue, so by the time the injury site is totally regenerated the scaffold is completely degraded [132].

Selecting the most appropriate material to produce a scaffold for bone tissue engineering is a very important step towards the construction of a tissue engineered product. To date, several materials including metals, ceramics and polymers from both natural and synthetic origins have been proposed. Metals and many ceramics are not biodegradable, which leaves the researcher’s choice reduced to a small number of ceramics and to biodegradable polymers. The following table summarises some natural and synthetic polymers used for bone tissue engineering applications.

Table 1.3; Natural and synthetic biocompatible scaffolds used in bone tissue engineering.

<b>Material</b>	<b>Origin</b>	<b>Characteristics</b>	<b>Outcome of study</b>	<b>Reference</b>
Collagen	Natural	- Low immune response - Low mechanical properties	- Good substrate for cell adhesion - Active bone formation	133-136
Fibrin	Natural	- osteoconduction properties	- Promotes migration of vascular endothelial cells - improved regeneration of mature epidermal structure	137-140
Chitosan	Natural	- osteoconduction properties - Hemostatic	- Promotes wound healing - Enhanced periodontal bone regeneration	141, 142
Starch	Natural	- Thermoplastic behavior - Good mechanical properties	- Enhanced cell adhesion	23
Hyaluronic acid (HA)	Natural	- Low mechanical properties	- Minimal immunogenicity	143
Demineralised bone	Natural	- Good mechanical properties	- Promotes osteogenic differentiation of bone marrow stromal cells	144
Poly( $\alpha$ -hydroxy acid)	Synthetic	- Degradation by hydrolysis	- New bone formation - no evidence of significant inflammatory reaction or local tissue damage	145, 146
Polyurethane	Synthetic	- Excellent mechanical properties - Degradable and non degradable	- Enhanced cell adhesion - Promotes tissue ingrowth	147
Titanium	Synthetic	- Excellent mechanical properties	- Promotes bone ingrowth both <i>in vivo</i> and <i>in vitro</i>	148
Bioactive glass	Synthetic	- Degradable and non degradable - Creates a strong bone/implant interface	- Good bone bonding properties - Enhances bone apposition	149

poly(L-lactide-co-D,L-lactide)	Synthetic	- Controllable biodegradability - Low mechanical properties	- Improves the distribution of calcified ECM - Enhanced bone ingrowth	150
Poly( $\epsilon$ -caprolactone)	Synthetic	- Aliphatic polyester - Degraded by hydrolysis - Slow degrading - Good mechanical properties	- Adhesion of bone marrow mesenchymal stem cells	151

### 1.13.1 Calcium phosphate (CaPs) based bioactive ceramic scaffolds

CaPs have been extensively studied as scaffold material for bone tissue engineering since they are a major constituent of bone. Among different CaPs, the majority of research has been focused on hydroxyapatite (HA),  $\beta$ -tricalcium phosphate ( $\beta$ -TCP) or mixture of HA and  $\beta$ -TCP otherwise known as biphasic calcium phosphate (BCP) [152]. Recent studies have shown that BCP scaffolds ( $80 \pm 3\%$  HA and  $20 \pm 3\%$   $\beta$ -TCP) with 70% interconnected porosity (68% pores are  $400 \mu\text{m}$ , and  $\sim 3\%$  are  $0.7 \mu\text{m}$  in size), can successfully support new bone formation in immune-deficient male mice [153].

### 1.13.2 Bioglass based bioresorbable scaffolds

Bioglass scaffolds are silica that contain bioresorbable substances and have been used as an alternative to conventional bioinert materials for bone healing. Studies have shown that a bioglass scaffolds with 70% porosity and  $300\text{--}400 \mu\text{m}$  pore size, exhibited hydroxy carbonate apatite (HCA) layer formation on its surface that significantly enhanced osteoblast activity. The HCA layer was also shown to adsorb protein and growth factors that facilitated new bone formation *in vivo* [154]. Various alterations to bioglass composition have been utilised to enhance its activity, just one recent example is a recent study in which cobalt (Co) was introduced in meso-porous bioglass scaffolds to induce hypoxia

that increased bone marrow-derived stem cell (BMSC) proliferation, differentiation, and bone-related gene expression [155].

### 1.13.3 Polymeric scaffolds

Polymers can be both bioactive and biodegradable. Commonly used natural polymers for bone tissue engineering include collagen, fibrin, alginate, silk, hyaluronic acid, and chitosan. One of the advantages of using these scaffolds is the flexibility in processing and ability to tailor the chemistry of polymers.

*O'Brien et al.*, used a collagen- glycosaminoglycan scaffold to provide a suitable 3D environment on which to culture adult rat mesenchymal stem cells and induce differentiation along the osteogenic and chondrogenic lineages. The results from the study demonstrated that the combination of adult rat mesenchymal stem cells and collagen-glycosaminoglycan scaffold can induce osteogenesis and can be stimulated with osteogenic factors as indicated by the temporal induction of the bone-specific proteins, collagen I and osteocalcin, and subsequent matrix mineralisation [156].

Synthetic polymers are an alternative to natural polymers as a scaffold material and have advantage that their properties can be more closely tailored and manipulated. Degradation of appropriate synthetic polymers can produce monomers which are readily removed by the natural physiological pathway. Some polymers such as poly (propylene fumarate) (PPF) have been shown to have high compressive strength that is comparable to cortical bone and their degradation time can be controlled. However, one of the disadvantages of using polymeric scaffolds is that they show rapid strength degradation *in vivo* even with high initial strength [157]. It has been demonstrated that biodegradable porous poly(DL-lactide-co-glycolide) (P<sub>DL</sub>LGA) hollow fibres in combination with human bone marrow stromal cells (HBMSC) was able to initiate natural bone repair. The results indicated that a high proportion of HBMSC survived when expanded on P<sub>DL</sub>LGA fibres for 6 days and in response to osteogenic stimuli, the cells differentiated along the osteogenic lineage with associated alkaline

phosphatase activity. Following implantation into SCID mice, the combination of P<sub>DL</sub>LGA fibre–HBMSC resulted in type I collagen deposition and associated bone mineralisation and osteoid formation [158].

#### 1.13.4 Metallic scaffolds

Porous metallic scaffolds, predominantly made of titanium (Ti) and tantalum (Ta), have been studied as bone replacement materials since they have high compressive strengths and excellent fatigue resistance [159, 160]. *Xue et al.*, processed 17–58 vol% porous Ti with an average pore size of 800µm allowed strong osteoblast cell attachment and proliferation [161]. However, unlike CaP or polymeric scaffolds, biomolecules cannot be integrated into these scaffolds and they are not biodegradable. Moreover, there are concerns related to metal ion release and surface modification techniques are often employed to improve bioactivity of Ti scaffolds [162].

Polyurethanes are becoming a popular biomaterial for use in bone tissue engineering. This is because of their excellent biocompatibility, great mechanical properties and easy handling during *in vitro* culture and *in vivo* implantation [163]. They also have been shown *in vivo* to support cell growth and proliferation and the in-growth of blood vessels. However, the major disadvantage of using PU as a biomaterial for long term implants is their low rate of biodegradation. Once implanted, several sources were found to contribute to their degradation. One example of this is the aliphatic ester linkage in polyester-urethanes. These are known to be susceptible to hydrolytic degradation, whereas polyether-urethane materials are known to be susceptible to degradative phenomenon involving crack formation and propagation. Furthermore, enzymes in the physiological environment such as hydrolytic enzymes are another factor contributing to PU degradation [164]. Biodegradable PUs can be manufactured through a variety of techniques including carbon dioxide foaming, electrospinning, wet spinning, salt leaching and thermally induced phase separation. Studies have shown that biodegradable PUs can support cell in-growth and hence tissue formation, and can also undergo controllable

degradation to noncytotoxic decomposition products. Since PUs can be modified in terms of their biological, mechanical and chemical properties, they present compelling future opportunities as scaffolds for bone tissue engineering [165-168].

#### **1.14 Peptide-coated scaffolds**

Since 3D scaffolds have a larger interconnected porous structure compared to 2D slides, modification of their surface to improve interaction between cell and surface would have potential to accelerate tissue formation. Cells in tissues constantly sense their environment by binding to molecules of the ECM and cell surface receptors that interact with ligands on neighboring cells. These interactions control cellular behavior and morphology and can therefore influence cell growth and differentiation.

Cell adhesion to a surface is dependent on many factors including, the collection of extracellular matrix (ECM) proteins, the composition of ECM absorbed to the surface and also the intrinsic chemistry of the surface. How a cell attaches to the ECM will depend on its competition of integrins. Integrins are widely expressed and are involved in many biological functions including embryonic development, wound repair and homeostasis [169-171]. Integrin receptors consist of an alpha and a beta subunit and bind to many ECM proteins such as osteopontin (OPN), collagen type I (ColI), fibronectin (FN) and laminin (LN). This binding to the ECM occurs at specific sites known as focal adhesions (fig 1.11).

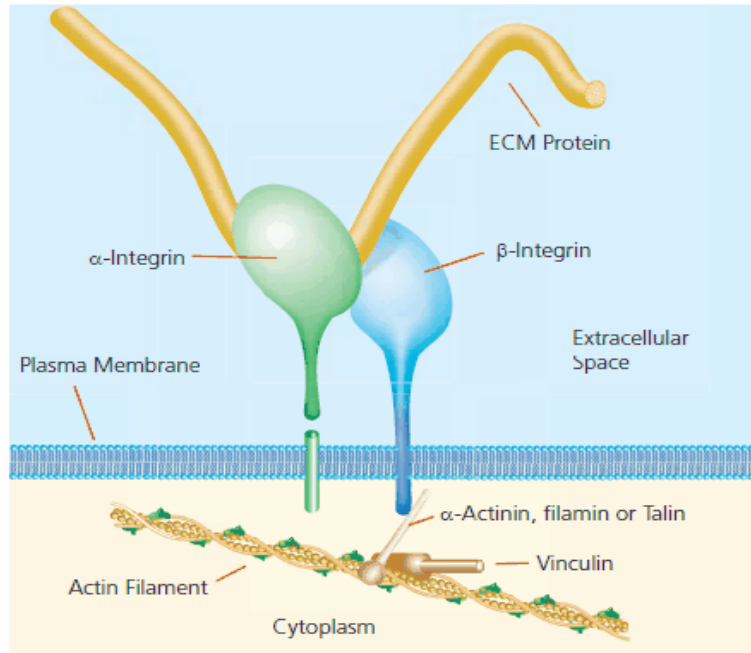


Fig 1.11; The contact areas between the plasma membrane and the extracellular matrix (ECM) are called focal adhesions. Cell-surface integrin molecules associate with intracellular cytoskeleton- proteins and with ECM components [172].

Within a focal adhesion, the cytoplasmic domain of the integrins is linked to the actin cytoskeleton via a complex array of protein-protein interactions. Integrin-ECM binding has the ability to activate multiple signal transduction pathways and regulate gene expression.

#### 1.14.1 Osteopontin

There are many integrins expressed on the surface of human osteoblastic cultured cells, but the major subunits include  $\alpha_3 \beta_1$ ,  $\alpha_4 \beta_1$  and  $\alpha_v \beta_1$  [173-175]. Osteopontin is a bone extracellular matrix protein as mentioned in section 1.3. It is an acidic protein which is highly phosphorylated and glycosylated and has an arginine-glycine-aspartic acid (RGD)-binding domain [176]. Osteopontin binds to cells via the RGD cell adhesion sequence that recognises the  $\alpha_v \beta_1$  integrin. OPN influences bone homeostasis *in vivo* by inhibiting mineral deposition, promoting differentiation of osteoclasts and by enhancing osteoclast activity. It is hypothesised that activated osteoblasts secrete ECM components such as OPN,

which are recognised and bound to by integrins on other osteoblasts to be activated (autocrine). However, osteoclasts also recognise OPN and use it to adhere to the bone surface and resorb bone matrices (paracrine) [177].

#### 1.14.2 Tenascin C

Tenascins are a family of glycoproteins, which are present in many ECMs throughout our bodies. They are synthesised primarily by cells in connective tissue [178]. Tenascin C (TNC) is an ECM protein that displays a restricted pattern of expression *in vivo*. Furthermore, it is highly expressed during embryonic development and organogenesis, it is reduced in developed organs but reappears under pathological conditions caused by infection, inflammation or during tumor development [178]. The fact that TNC is significantly upregulated in tissues adjacent to injury sites, suggests it may play an important role in regulating cellular response to the provisional matrix. Many growth factors have been shown to promote the expression of TNC and another important mechanism to induce TNC expression is by applying a mechanical stress to cells in culture or tissues *in vivo* [178]. In recent experiments employing osteoblast-like cell lines, TNC was shown to stimulate alkaline phosphatase and anti-TNC caused a reduction in alkaline phosphatase and collagen synthesis [179], suggesting that TNC plays an important role in bone cell differentiation.

### 1.15 Growth factors

Growth factors are proteins that serve as signaling agents for cells and they influence critical functions such as matrix synthesis, cell division, and tissue differentiation. Experimental results suggest that growth factors play a vital role in bone and cartilage formation, repair and healing of other musculoskeletal tissues. A wide variety of growth factors including fibroblast growth factors (FGFs), bone morphogenetic proteins (BMPs) and, parathyroid hormone (PTH) have been shown to be expressed during different phases of experimental fracture healing. Therefore, growth factors have been advocated as a potential clinical treatment for bone repair for example, *Joyce et al.*, demonstrated that

injections of TGF-1 in a rat model could stimulate periosteal cells to undergo endochondral ossification [180]. In another study *Kato et al.*, analysed the effect of various doses (0, 50, 100, 200, and 400 µg) of rhFGF-2 on the healing of segmental tibial defects in rabbits. It was shown that concentrations of >100 µg had significant effect on healing, bone volume and mineral content in comparison to controls. It was suggested that a single injection of FGF-2 had the ability to enhance bone formation [181]. In addition to full-length growth factors, truncated peptides of BMP-2 have also demonstrated promising results [182, 183]. *Saito et al.*, reported that a BMP-2-derived peptide in combination with a porous alpha-tricalcium phosphate (TCP) scaffold promoted calcification and induced connection in rabbit bone defects (20-mm long) 12 weeks after implantation [182].

#### 1.15.1 Bone Morphogenetic Proteins (BMP)

Although many growth factors have shown potential for use in bone regeneration and repair, BMPs are the most investigated osteoinductive factors described to date [184]. BMPs are cytokines with important roles during embryonic patterning and early skeletal formation. The various individual BMPs, of which there are more than 30 members, have been shown to induce differentiation of mesenchymal stem cells into cells of osteoblast lineage [185]. However interest has been focused on BMP-2 and -4 in the potential treatment of segmental bone defects, fracture repair and in the fixation of prosthetic implants [186]. Nowadays, recombinant human BMPs (rhBMPs) are widely used in several tissue-engineering products that might serve for the complete regeneration of bone or cartilage. Current applications include rhBMPs loaded in delivery systems made of synthetic or natural polymers and the differentiation of transplanted stem cells from the patient with rhBMPs for later body implantation.

Biodegradable polymers have been widely used as a carrier for BMP delivery including poly(lactic acid) (PLA) [187], polylactic acid-p-dioxanone-polyethylene glycol (PLA-DX-PEG) [188] and, Poly(lactic-co-glycolic acid)

(PLGA) [189]. PLGA has shown successful results in delivering rhBMP-2 and inducing the repair of bone defects several weeks after implantation in alveolar cleft repair in dogs [180], in gelatine sponge composites in a rabbit ulna model [190], in tooth defects of dogs [191] and in combination with bone marrow cells in a rabbit segmental bone defect model [192]. Similarly, an acrylated hyaluronic acid hydrogel was used in combination with human mesenchymal stem cells and rhBMP-2 for healing of rat calvarial defects [193]. Higher levels of osteocalcin expression and bone formation occurred when the BMP-2 and stem cells were tested.

Natural polymers have also been used as carriers for BMP delivery [194]. Recently, rhBMP-2 was immobilised directly on chitosan nanofibres (a guided bone-regenerative membrane surface) that functioned as a bioactive surface to enhance bone healing [195]. It was demonstrated that the BMP-2-conjugated membrane surface retained bioactivity for up to 4 weeks of incubation, promoting cell attachment, proliferation, ALP activity and calcification. In another study, it was shown that electrospun silk fibroin-based scaffolds supported hMSC growth and differentiation towards an osteogenic lineage. Results from the study indicated that scaffolds with the co-processed BMP-2 supported higher calcium deposition, higher transcript levels of collagen type I and enhanced transcript levels of bone-specific markers on day 31 of static culture [196].

Similarly, rhBMP-2 was directly immobilised on silk fibroin films and the effect of the delivery system studied in human bone marrow stromal cells and in critical-sized cranial defects in mice [197] and the rhBMP retained its biological activity. In another report, silk scaffold fibres, prepared by electrospinning, were used to deliver rhBMP-2 and hydroxyapatite nanoparticles for *in vitro* bone formation [196]. The rhBMP-2 induced osteogenesis in cultures of human mesenchymal stem cells. The group also tested BMP-2 delivered via silk fibroin scaffolds in critical size defects in mice [198]. In both studies, the delivered rhBMP-2 increased levels of ALP activity and calcium deposition and transcript levels for bone sialoprotein, osteopontin, osteocalcin and RUNX2.

## 1.16 Cells for bone tissue engineering

An ideal cell source should be easily expandable to higher passages, non-immunogenic and have a protein expression pattern similar to the tissue to be regenerated.

### 1.16.1 Osteoblasts

The isolation of osteoblasts from biopsies taken from the patient is the most obvious choice of cells because of their non-immunogenicity. However there are several limitations to using these cells including: the additional surgery time required, few cells are available after the dissociation of the tissue and their expansion rates are relatively low. Furthermore, for a patient with a bone disease, their osteoblasts may not be appropriate for transplantation [199]. An alternative to this method is the use of cells obtained from other animals which could solve the problem of low cell numbers. However there are also some limitations to this procedure including: the possibilities of the transmission of infectious agents and immunogenicity of the cells. The ethical problems related with use of animal cells have reduced the enthusiasm for this approach [200]. A more promising solution is the use of stem cells.

### 1.16.2 Stem Cells

Stem cells are undifferentiated cells with a high proliferation capability, the ability to self-renew and the ability to differentiate to multiple cell lineages [201]. Stem cells have varying degrees of differentiation potential. The most primitive one being derived from the zygote in the embryonic stage which are also known as embryonic stem cells (ESCs). Adult stem cells (ASCs) are those found in fully differentiated tissues.

#### *- Embryonic Stem Cells*

Undifferentiated ESCs (fig 1.12) have the potential to differentiate into many kinds of tissues including cardiomyocytes, haematopoietic cells, endothelial cells, neurons, chondrocytes, adipocytes, hepatocytes and pancreatic islets [202]. In

the bone tissue engineering field *Buttery et al*, reported how osteoblasts can be differentiated from ES cells in the presence of dexamethasone [203]. However, the criticism against their use because of ethical and social issues is the most difficult barrier to overcome.

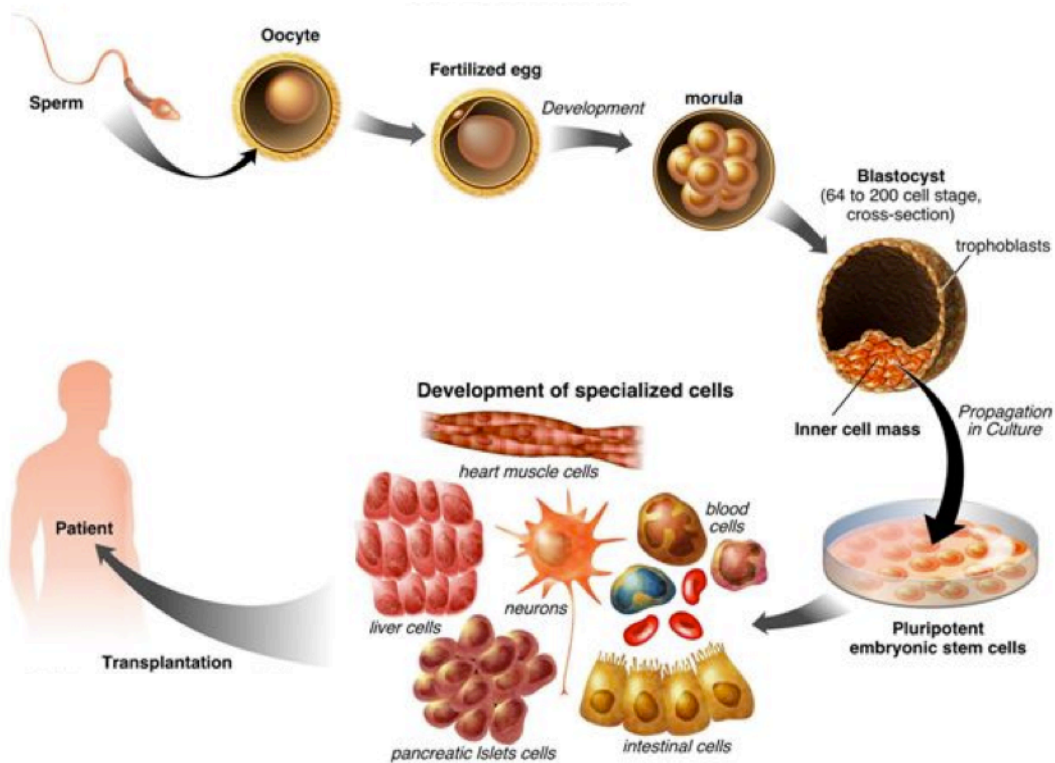


Fig 1.12; Pluripotent of embryonic stem cells. The cells can become into many types of tissues in the body [204].

### - Adult Stem Cells

ASCs are found in the bone marrow, periosteum, muscle, fat, brain and skin [205]. In the bone tissue engineering field there has been a special interest in bone marrow stromal cells (stem cells located in the bone marrow), also known as Mesenchymal Stem Cells (MSC). These are the cells that differentiate into osteoblasts *in vivo*. The bone marrow site is the most exploited source of these cells, however MSCs have also been found in other tissues such as the periosteum and adipose tissue. Apart from their differentiation potential, MSCs present other important properties. *Bruder et al*, described that they can be

extensively expanded *in vitro* [206]. *Pittinger et al*, also showed that with an increased number of passages, they did not spontaneously differentiate. Furthermore it has been suggested that these cells may possess immunosuppressive effects. This may allow them to have immunosuppressive roles *in vivo*, which would make them suitable for allogeneic or xenogeneic transplantation [207].

Although MSCs have several advantages regarding their use for tissue engineering, there are some limitations to their use. It is known that the percentage of MSCs present in the bone marrow is roughly 1 in each 100,000 cells, which makes the expansion time consuming. It was also shown that the number as well as the differentiation potential of MSCs is lower when isolated from elderly patients. Similar to ESCs, the knowledge regarding the mechanisms and pathways that lead to the final osteogenic differentiation is still limited and further research into this field is required [208]. The limitations associated with hMSCs can be overcome by using human embryonic stem cell-derived mesodermal progenitors (hES-MPs). It has been demonstrated that under proper stimulation, hES-MP cells can undergo osteogenic differentiation and have shown to have much higher mineralisation ability in comparison to hMSCs [209]. Several studies have suggested hES-MPs hold great potential for the construction of bone substitutes and can be a suitable alternative cell source to hMSCs [210-212]. The osteogenic differentiation potential of hES-MP cells is further investigated in chapters 3, 4 and 5 of this project.

### **1.17 Bioreactors for bone tissue engineering**

Throughout the past decade, research has shown that traditional 2D cell culture techniques are inadequate for three-dimensional 3D tissue engineering. This is primarily due to the fact that in 2D culture, a monolayer of cells are in continuous contact with the culture medium and because of this, simple diffusion is sufficient to maintain cell viability. However when we are considering 3D scaffolds, the diffusion of nutrients and removal of waste from the inner core becomes very limited and as a result it will lead to central core necrosis with a

layer of live cells on the surface crust of the scaffold [213, 214]. These findings have lead researchers to design various hydrodynamic bioreactors to promote chemotransport for *in vitro* 3D culture. Although the main aim of perfusing 3D scaffold is chemotransport it is likely that fluid flow will also subject the cells to a mechanical signal. As discussed above (section 1.7) bone cells are highly sensitive to fluid flow and therefore it is not surprising that MSCs differentiating to osteoblasts are also highly sensitive to fluid flow. Many of the same mechanisms by which osteoblasts and osteocytes respond to fluid flow seem to be also present in MSCs [215]. Various experimental setups have been utilised to apply flow in 2D systems including parallel plate flow chambers, rotating disc, jet impingement, and microfluidic apparatus. A number of bioreactor types have also been designed for 3D tissue engineering applications including spinner flasks, rotating wall bioreactors and perfusion rigs. These studies have used a range of bone cell types from immature MSCs to mature osteoblasts.

*Warren et al.*, used a flow-perfusion bioreactor to provide chemotransport to thick (6 mm) polyurethane scaffolds (fig 1.13), seeded with murine preosteoblasts. Samples were subjected to flow on days 2, 4, 6 and 8 and analysed for cellular distribution, viability and metabolic activity compared to static conditions. Results demonstrated that constructs subjected to flow had a peripheral cell density of 94% and a core density of 76%, whilst those cultured in static conditions had a peripheral cell density of 67% and a core density of 0.3% [216].

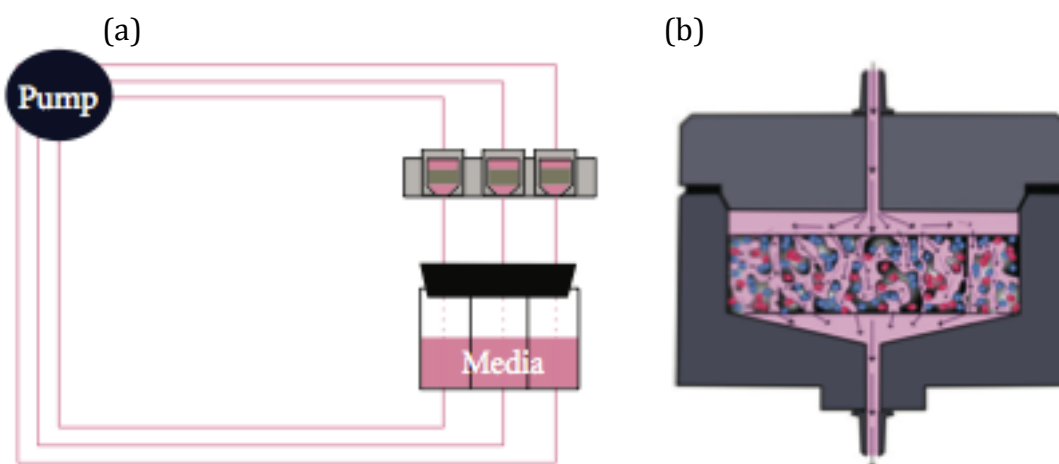


Fig 1.13; (a) Schematic of the 8-chamber flow-perfusion bioreactor within a standard cell culture incubator. (b) Schematic chamber within the flow-perfusion bioreactor whereby media is forced through the entire structure of the scaffold. Arrows indicate direction of flow [216].

In a similar study *Sikavitsas et al.*, seeded rat bone marrow cells onto a titanium fiber mesh and cultured them under static conditions or in a flow perfusion bioreactor for 4, 8 and 16 days [217]. Constructs were examined for DNA content, calcium deposition and alkaline phosphatase activity. Results demonstrated an increase in DNA content from day 4 to day 8 for constructs under perfusion flow and a significant enhancement in DNA on day 8 compared to static conditions. Calcium content was also higher for scaffolds subjected to fluid flow on day 16.

*Jaasma et al.*, investigated the short term (1-49h) effects of various flow regimens including intermittent steady (1 ml/min), pulsatile (0-1 ml/min, 2 Hz) and oscillatory fluid flow (1 ml/min, 1 Hz) on MC3T3-E1 osteoblastic cells on a 3D collagen-glycosaminoglycan scaffold (fig 1.14).

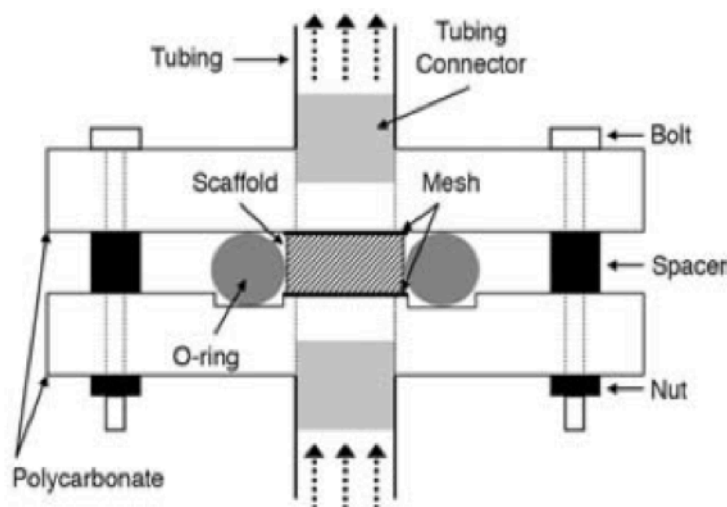


Fig 1.14; Cross section of the scaffold chamber. O-rings hold cell-seeded scaffold in place whilst media is pumped through the tubing. Arrows indicate direction of flow [85].

The results showed that intermittent flow (high flow rate) significantly increased COX-2 expression, PGE2 production and osteopontin expression when compared to steady flow conditions (continuous low flow rate). Pulsatile and oscillatory flow tripled COX-2 expression, whereas under steady flow PGE2 production

dropped at 49h. These results indicate that intermittent flow is advantageous for stimulating osteoblastic cells and that pulsatile and oscillatory flow may be more stimulatory than steady flow over longer periods [85].

A similar short-term study conducted by *Vance et al*, investigated the effects of flow-induced shear stress on the release of PGE2 from osteoblastic cells cultured on 3D calcium phosphate scaffolds in comparison to static culture [84]. Once scaffolds were placed within the bioreactor chamber, medium perfusion was initiated at a rate of 0.025 ml/min for 4 hours daily for 2 days (fig 1.15). Similarly the mechanical stimulation (oscillatory fluid flow) was conducted at a rate of 40 ml/min, with a frequency of 1 Hz for 30 mins. The results showed that scaffolds in the mechanical stimulation group significantly produced more PGE2 than scaffolds in the static and perfusion groups after 24 and 48 hrs. This study found that shorter, more frequent loading sessions separated by adequate resting periods are more osteogenic than continuous loading.

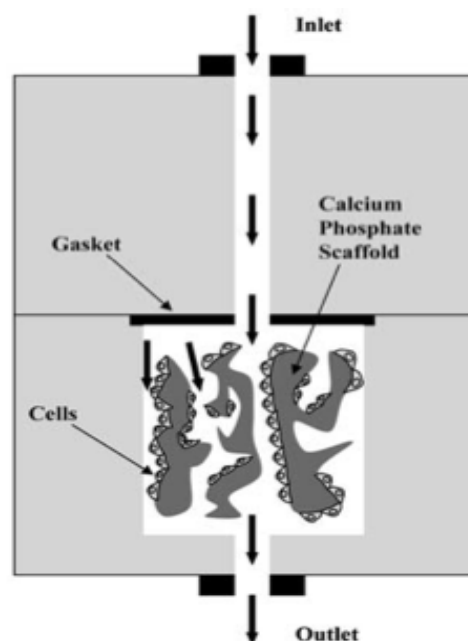


Fig 1.15; Schematic drawing of the chamber within the flow-perfusion bioreactor. Media is forced through the calcium phosphate scaffold providing fresh media and subjecting cells to a mechanical stimuli. Arrows indicate direction of flow [84]

*Kim and Ma.*, demonstrated the importance of media flow in bioreactor systems and how it can create a different cellular and biomechanical environment in 3D porous polyethylene terephthalate (PET) constructs [218]. The influence of different flow patterns (transverse flow and parallel flow) on hMSC's cellular microenvironment was investigated. Results suggested that parallel flow configuration retained ECM proteins however transverse flow induced osteogenic differentiation with higher ALP, higher calcium deposition, and up regulation of bone markers e.g. BMP-2, RUNX2 and OC.

Taking these results into account, it can be concluded that the application of fluid flow can enhance early proliferation and mineralised matrix production of bone marrow stromal osteoblasts as well as mature osteoblasts and also induce osteogenic differentiation in hMSC.

### **1.18 Fluid Shear Stress**

There have been a vast number of studies for non-human and human cell lines/primary cells, detailing the effects of fluid shear stress on directing commitment towards an osteogenic lineage for 2D systems. Fluid shear stress has increased the expression levels of OPN, OC, PGE2, Col1 and NO [219-232]. In 2D systems it appears that a range of 0.1-0.5 Pa [233] is sufficient to induce osteogenic differentiation and in some cases values as high as 2 Pa have produced a positive response. These values show a good correlation with the levels of shear stress expected to occur *in vivo* (0.8-3 Pa) on osteocytes [234], however it is not known whether the optimum shear stress for fully differentiated cells would be the same as for undifferentiated MSCs. Recent studies have also investigated the complex mechanical environment of osteocytes *in vivo* in order to predict average interstitial fluid velocities and average maximum shear stresses [235, 236], which are in agreement with previous studies.

In 3D culture systems, the application of fluid shear stress has resulted in an increase in expression of ALP, PGE2, OPN, OC, COX-2, RunX2, Col1 and

mineralised matrix production [85, 217, 237-240]. These bodies of work suggest that osteogenic differentiation can be achieved with shear stress in the range of 0.0001 to 1.2 Pa (table 1.4). However these are the initial shear forces subjected to the scaffolds under flow perfusion conditions. The effects of continuous stimulation by fluid flow for an extended period of time (weeks as opposed to hour) on osteoblastic cells has not been fully investigated.

Table 1.4; Shear stress values for experimental investigations.

<b>Shear Stress (Pa)</b>	<b>Type of Flow</b>	<b>Cell type</b>	<b>Scaffold type</b>	<b>Results</b>	<b>Reference</b>
$1-2 \times 10^{-1}$	Steady	Rat marrow stromal cells	Titanium fiber mesh	Osteogenic	85
$5 \times 10^{-5}-5 \times 10^{-2}$	Steady	MC3T3-E1	Trabecular bone	Proliferation/osteogenic	84
$2 \times 10^{-2}$	Steady, pulsatile, oscillatory	MC3T3-E1	Collagen GAG	Osteogenic	237
$6.5 \times 10^{-4}$	Steady	Human BECs and LECs	Fiber Gel	Osteogenic	238
$2 \times 10^{-2}$	Steady	MC3T3-E1	Collagen GAG	Osteogenic	239
$2 \times 10^{-2}$	Steady	MC3T3-E1	Collagen GAG	Osteogenic	241
$1-3 \times 10^{-3}$	Steady	Rat MSC	Titanium fiber mesh	Osteogenic	242

## 1.19 Aims & Objectives

The combination of mesenchymal stem cells and 3D scaffolds has become an active area of research into creating functional bone constructs. Cell-seeded scaffolds cultured in static conditions have shown to have major limitations with respect to cell proliferation and cell function. This has lead researchers to design various bioreactors in order to provide a controlled physiochemical and biomechanical microenvironment to maintain the quality of the 3D construct. Fluid flow within bioreactors is important not only for the delivery of oxygen and nutrients on cells within scaffolds but also exerts a hydrodynamic shear stress, which has been shown to enhance genes associated with osteogenesis. In particular, oscillatory and unidirectional flow have demonstrated to direct commitment towards an osteogenic lineage for 2D systems but the signaling mechanisms by which cells convert shear stress into biochemical signals have not been fully investigated in a 3D model. Therefore, the ultimate main aim of this project was to investigate the ability of a perfusion bioreactor to achieve progenitor cell commitment towards an osteogenic lineage and accelerate the biological process of osteogenesis with a particular focus on short bouts of perfusion and the effect of osciallatory verses unidirectional flow.

In order to achieve this aim, the project was broken down into a list of objectives:

- 1. Setup a model system to investigate the *in vitro* culture of MSCs in a 3D environment:**
  - Study the osteogenic differentiation of mouse MSCs and a Mesenchymal progenitor derived from human embryonic stem cell (hES-MP) in static culture
  - Study the effects of fluid flow on the osteogenic response of mouse MSC and hES-MP cells

**2. Investigate the effects of different flow type with respect to hES-MP osteogenesis:**

- Study the biological outcome of hES-MP cells subjected to unidirectional and oscillatory fluid flow

**3. Investigate the response of hES-MP cells on different peptide-coated scaffolds:**

- Study hES-MP cell viability and matrix production in serum-containing and serum-free media
- Study the effects of peptide-coated scaffolds and fluid flow on the osteogenic differentiation of hES-MP cell

**4. Investigate the response of primary cilium to fluid flow in 3D porous scaffolds:**

- Identify the primary cilia of mature bone cells seeded on glass scaffolds
- Study the removal/inhibition of primary cilia using chloral hydrate treatment
- Investigate the response of mature bone cells (lacking a primary cilia) to fluid flow

Results from this study can ultimately be used to better understand the relationship between cell mechanics and mechanotransduction and gives further insight into creating fully developed tissue-engineered constructs for clinical applications.

## 1.20 References

- [1] Michael S, Beate H, David LH: Evidence-Based Orthopedic Surgery: Is It possible? *Orthop Clin N Am*. 2010. vol. 41 (2) 139-43.
- [2] Marieb E, Hoehn K: *Human anatomy & physiology*. 2007, p1814.
- [3] Debbie W: Mechanotransduction Using the force. *Nat Rev Mol Cell Bio*. 2010 vol. 11 (5) 311-311.
- [4] [www.homepage.mac.com/myers](http://www.homepage.mac.com/myers)
- [5] Chao L, Yan Z, Wing-Yee C, Ronak G, Liyun W, Lidan Y: Effects of cyclic hydraulic pressure on osteocytes. *Bone*. 2010 vol. 46 (5) 1449-1456.
- [6] Gang B, Roger D K, Wendy T, Wonmuk H, Daniel AF, Alan JG, Cheng Z, Mohammad RKM: *Molecular Biomechanics: The Molecular Basis of How Forces Regulate Cellular Function*. *Cell Mol Bioeng*. 2010 vol. 3 (2) 91-105.
- [7] Osborne JM, O'Dea RD, Whiteley JP, Byrne HM, Waters H: The Influence of Bioreactor Geometry and the Mechanical Environment on Engineered Tissues. *J Biomech Eng-T Asme*. 2010 vol. 132 (5) 1875.
- [8] Cornelia K, Martijn van G, Ralf P: *Bioreactor Systems for Tissue Engineering*. 2009, 53-61.
- [9] Henri H, Marco H, Hans PM, Lorenz M, Ralph M: Design and validation of a novel bioreactor principle to combine online micro-computed tomography monitoring and mechanical loading in bone tissue engineering. *Rev Sci Instrum*. 2010 vol. 81 (1) 1983-89.
- [10] Kee-Won L, Shanfeng W, Mahrokh D, Michael JY, Lichun L: Enhanced Cell Ingrowth and Proliferation through Three-Dimensional Nanocomposite Scaffolds with Controlled Pore Structures. *Biomacromolecules*. 2010 vol. 11 (3) 682-689.
- [11] Jee W: *Integrated Bone Tissue Physiology: Anatomy and Physiology*. 2001, p. (1)1-(1)68.
- [12] Hong-Zhi Z, Hua Y, Yang X: In vivo self-expanding engineering of bone. *Med Hypotheses*. 2009 vol. 73 (4) 528-530.
- [13] Jeffrey O. Hollinger: *Bone tissue engineering*. 2005, 336-343.
- [14] <http://www.francesdevoe.com/bonecells.htm>
- [15] Ducky, P, Schinke T, Karsenty G: The Osteoblast: A Sophisticated fibroblast under Central Surveillance. *Science*, 2000. 289:5484, 1501-1504.

- [16] <http://www.hindawi.com/journals/amse/2012/650574/fig6/>
- [17] Aubin JE, Liau F: Principles of Bone Biology. 1st E., Academic Press, San Diego 1996, 58-61.
- [18] <http://www.rehab.research.va.gov/jour/00/37/2/mosley.htm>
- [19] <http://www.britannica.com/EBchecked/topic/434277/osteoclast>
- [20] <http://www.siumed.edu/~dking2/ssb/remodel.htm>
- [21] Buckwalter JA: Bone biology part I and II. J bone Jt Surg, 1995. 77A(8): p. 1256-1289.
- [22] Prockop DJ and Kivirikko KI: collagens: molecular biology, diseases, and potentials for therapy. Annu Rev Biochem, 1995. 64: p. 403-34.
- [23] Salgado AJ, Coutinho OP, Reis RL: Bone tissue engineering: state of the art and future trends. Macromol Biosci, 2004. 4(8): p. 743-65.
- [24] Sodek J and McKee MD: molecular and cellular biology of alveolar bone. Periodontology 2000, 2000. 24: p. 99-126.
- [25] Triffitt JT: Principles of Bone Biology. 1st Ed, Academic Press, San Diego 1996, 43-49.
- [26] Termine JD: Primer on the Metabolic Bone Diseases and Disorders of Mineral Metabolism. 2nd Ed, Raven Press, New York, 1993. 43-61.
- [27] Sodek J, Ganss B, McKee MD: Osteopontin. Crit. Rev. Oral Bio. Med, 2000. 11:3, 279-303,
- [28] Boskey AL: Dynamics of Bone and Cartilage Metabolism. 1st Ed, Academic Press, San Diego, 2006, 62-68.
- [29] Sodek J, Cheifetz S: Bone Engineering. 1st Ed, Em squared, Toronto, 1999, 87-90.
- [30] Davies JE: In vitro modeling of the bone/implant interface. Anat. Record, 1996, 245:2, 426-445,
- [31] Davies JE: Mechanisms of endosseous integration. Int. J. Prosthodont., 1998, 11:5, 391-401.
- [32] Davies JE, Baldan N: Scanning electron microscopy of the bone bioactive implant interface. J. Biomed. Mat. 1997, Res., 3:4, 429-440.
- [33] Marks Jr SC, Hermey DC: Principles of bone biology. 1st Ed, Academic Press, San Diego 1996, 35-37.
- [34] Weiner S, Wagner HD: The Material Bone: Structure-Mechanical Function

Relations. *Ann. Rev. Mat. Sci.*, 1998, 28, 271-298.

[35] Weiner S, Traub W, Wagner HD: Lamellar Bone: Structure-Function Relations. *J. Struct. Biol.*, 1999, 126:3, 241-255.

[36] Rawadi G, Vayssière B, Dunn F, Baron R, Roman-Roman S: BMP-2 controls alkaline phosphatase expression and osteoblast mineralization by a Wnt autocrine loop. *J Bone Miner Res.* 2003 Oct;18(10):1842-53.

[37] Chen X, Macica CM, Ng KW, Broadus AE: Stretch-induced PTH-related protein gene expression in osteoblasts. *J Bone Miner Res.* 2005 Aug;20(8):1454-61.

[38] Porter RM, Huckle WR, Goldstein AS: Effect of dexamethasone withdrawal on osteoblastic differentiation of bone marrow stromal cells. *J Cell Biochem.* 2003 Sep 1;90(1):13-22.

[39] Bacabac RG, Smit TH, Mullender MG, Dijcks SJ, Van Loon JJWA, Klein-Nulend J: Nitric oxide production by bone cells is fluid shear stress rate dependent. *Biochem Biophys Res Commun.* 2004; 315: 823-9.

[40] Simmons CA, Matlis S, Thornton AJ, Chen S, Wang CY, Mooney DJ: Cyclic strain enhances matrix mineralization by adult human mesenchymal stem cells. *Tissue Eng.* 2001. 7(1): 89-99.

[41] Lee T, Staines A, Taylor D: Bone adaptation to load: microdamage as a stimulus for bone remodeling. *Journal of anatomy.* 2002, 437-46.

[42] Huiskes R, Ruimerman R, Lenthe G, Janssen J: Effects of mechanical forces on maintenance and adaptation of form in trabecular bone. *Nature.* 2000, 704-6.

[43] Lanyon L: Osteocytes, strain detection, bone modeling and remodeling. *Calcified tissue Calcif Tissue Int.* 1993;53, 106-07.

[44] Kasperk C, Wergedal J, Strong D, Farley J, Wangerin K, Gropp H, Ziegler R, Baylink DJ: Human bone cell phenotypes differ depending on their skeletal site of origin. 1995, *J Clin Endocrinol Metab* 80: 2511-2517.

[45] Martinez ME, Del Campo MT, Medina S, Sanchez M, Sanchez-Cabezudo MJ, Esbrit P, Martinez P, Moreno I, Rodrigo A, Garces MV, Munuera L: Influence of skeletal site of origin and donor age on osteoblastic cell growth and differentiation. 1999, *Calcif Tissue Int* 64: 280-286.

[46] Siggelkow H, Rebenstorff K, Kurre W, Niedhart C, Engel I, Schulz H, Atkinson MJ, Hufner M: Development of the osteoblast phenotype in primary human

osteoblasts in culture: comparison with rat calvarial cells in osteoblast differentiation. 1999, *J Cell Biochem* 75: 22-35.

[47] Klein-Nulend J, Helfrich MH, Sterck JG, MacPherson H, Joldersma M, Ralston S H: Nitric oxide response to shear stress by human bone cell cultures is endothelial nitric oxide synthase dependent. *Biochem Biophys Res Commun* 1998; 250, 108–14.

[48] Grigoriadis AE, Petkovich PM, Ber R, Aubin JE, Heersche JN: Subclone heterogeneity in a clonally derived osteoblast-like cell line. 1985, *Bone* 6: 249-256.

[49] Leis HJ, Hulla W, Gruber R, Huber E, Zach D, Gleispach H, Windischhofer W: Phenotypic heterogeneity of osteoblast-like MC3T3-E1 cells: changes of bradykinin-induced prostaglandin E2 production during osteoblast maturation. 1997, *J Bone Miner Res* 12: 541-551.

[50] Wang D, Christensen K, Chawla K, Xiao G, Krebsbach PH, Franceschi RT: Isolation and characterization of MC3T3-E1 preosteoblast subclones with distinct in vitro and in vivo differentiation/mineralization potential. 1999, *J Bone Miner Res* 14: 893-903.

[51] Cheng B, Kato Y, Zhao S, Luo J, Sprague E, Bonewald LF, Jiang JX. PGE(2) is essential for gap junction mediated intercellular communication between osteocyte-like MLO-Y4 cells in response to mechanical strain. *Endocrinology*. 2001 Aug;142(8):3464-73.

[52] Rosser J, Bonewald LF. Studying osteocyte function using the cell lines MLO-Y4 and MLO-A5. *Methods Mol Biol*. 2012;816:67-81.

Li X, Liu C, Li P, Li S, Zhao Z, Chen Y, Huo B, Zhang D. Connexin 43 is a potential regulator in fluid shear stress-induced signal transduction in osteocytes. *J Orthop Res*. 2013 Jul 22. doi: 10.1002.

[53] Wu D, Schaffler MB, Weinbaum S, Spray DC. Matrix-dependent adhesion mediates network responses to physiological stimulation of the osteocyte cell process. *Proc Natl Acad Sci U S A*. 2013 Jul 16;110(29):12096-101

[54] Bosnakovski D, Mizuno M, Kim G, Takagi S, Okumura M, Fujinaga T. Chondrogenic differentiation of bovine bone marrow mesenchymal stem cells (MSCs) in different hydrogels: influence of collagen type II extracellular matrix on MSC chondrogenesis. *Biotechnol Bioeng*, 2006. 93(6): p. 1152- 63.

- [55] Sekiya I, Larson BL, Vuoristo JT, Cui JG, Prockop DJ. Adipogenic differentiation of human adult stem cells from bone marrow stroma (MSCs). *J Bone Miner Res*, 2004. 19(2): p. 256-64.
- [56] Moreau JE, Chen J, Bramono DS, Volloch V, Chernoff H, Vunjak-Novakovic G, Richmond JC, Kaplan DL, Altman GH. Growth factor induced fibroblast differentiation from human bone marrow stromal cells in vitro. *J Orthop Res*, 2005. 23(1): p. 164-74.
- [57] Deliloglu-Gurhan SI, Vatansever HS, Ozdal-Kurt F, Tuglu I. Characterization of osteoblasts derived from bone marrow stromal cells in a modified cell culture system. *Acta Histochem*, 2006. 108(1): p. 49-57.
- [58] Haynesworth SE, Goshima J, Goldberg VM, Caplan AI. Characterization of cells with osteogenic potential from human marrow. *Bone*, 1992. 13(1): p. 81-8.
- [59] Siggelkow H, Rebenstorff K, Kurre W, Niedhart C, Engel I, Schulz H, Atkinson MJ, Hüfner M. Development of the osteoblast phenotype in primary human osteoblasts in culture: comparison with rat calvarial cells in osteoblast differentiation. *J Cell Biochem*, 1999. 75(1): p. 22-35.
- [60] Bruder SP, Jaiswal N, Ricalton NS, Mosca JD, Kraus KH, Kadiyala S. Mesenchymal stem cells in osteobiology and applied bone regeneration. *Clin Orthop Relat Res*, 1998(355 Suppl): p. S247-56.
- [61] Stein, G.S. and J.B. Lian, Molecular mechanisms mediating proliferation/differentiation interrelationships during progressive development of the osteoblast phenotype. *Endocr Rev*, 1993. 14(4): p. 424-42.
- [62] Kjaer M: Role of extracellular matrix in adaptation of tendon and skeletal muscle to mechanical loading. 2004, *Physiol Rev* 84:649-698.
- [63] Sadoshima J, Xu Y, Slayter HS, Izumo S: Autocrine release of angiotensin II mediates stretch-induced hypertrophy of cardiac myocytes in vitro. *Cell*. 1993 Dec 3;75(5):977-84.
- [64] Jones HH, Priest JD, Hayes WC, Tichenor C, Nagel DA: Humeral hypertrophy in response to exercise. *Journal of bone and surgery*. 1977, Vol: 59, 204-208.
- [65] Nijweide PJ, Burger EH, Klein-Nulend J: The osteocyte: Principles of bone biology. vol. 1. 2002. 93-108. 44.
- [66] Kufahl RH, Saha S. A theoretical model for stress-generated fluid flow in the canaliculi-lacunae network in bone tissue. *J Biomech*. 1990;23(2):171-80.

- [67] Burger EH, Klein-Nulend J. Mechanotransduction in bone role of the lacuno-canalicular network. *FASEB J*. 1999; 13: 101–12.
- [68] Klein-Nulend J, Bacabac RG, Mullender MG: Mechanobiology of bone tissue. *Pathologie Biology* 53, 2005. 576–580.
- [69] Busse R, Fleming I. Regulation and functional consequences of endothelial nitric oxide formation. *Ann Med*. 1995 Jun;27(3):331-40.
- [70] Boje KM, Fung HL. Endothelial nitric oxide generating enzyme(s) in the bovine aorta: subcellular location and metabolic characterization. *J Pharmacol Exp Ther*. 1990 Apr;253(1):20-6
- [71] Busse R, Fleming I: Pulsatile stretch and shear stress: physical stimuli determining the production of endothelium-derived relaxing factors. *J Vasc Res* 1998; 35, 73–84.
- [72] Rubin CT, Lanyon LE: Regulation of bone formation by applied dynamic loads. *J Bone Jt Surg Am*. 1984; 66: 397–402.
- [73] Knippenberg M, Helder MN, Doulabi BZ, Semeins CM, Wuisman PI, Klein-Nulend J: Adipose tissue-derived mesenchymal stem cells acquire bone cell-like responsiveness to fluid shear stress on osteogenic stimulation. *Tissue Eng*, 2005. 11(11-12): 1780-8.
- [74] Bacabac RG, Smit TH, Mullender MG, Van Loon JJ, Klein-Nulend J. Initial stress-kick is required for fluid shear stress induced rate dependent activation of bone cells. *Ann Biomed Eng*. 2005 Jan;33(1):104-10.
- [75] Rubin J, Murphy T, Nanes MS, Fan X: Mechanical strain inhibits expression of osteoclast differentiation factor by murine stromal cells. *American journal of physiology. Cell physiology*. 2000;278:C1126–32.
- [76] Yasuda H, Shima N, Nakagawa N, Yamaguchi K, Kinosaki M, Mochizuki S, Tomoyasu A, Yano K, Goto M, Murakami A, Tsuda E, Morinaga T, Higashio K, Udagawa N, Takahashi N, Suda T: Osteoclast differentiation factor is a ligand for osteoprotegerin/osteoclastogenesis-inhibitory factor and is identical to TRANCE/RANKL. *Proceedings of the National Academy of Sciences of the United States of America*. 1998;95:3597–602.
- [77] David V, Martin A, Lafage-Proust MH, Malaval L, Peyroche S, Jones DB. Mechanical loading down-regulates peroxisome proliferator-activated receptor

gamma in bone marrow stromal cells and favors osteoblastogenesis at the expense of adipogenesis. *Endocrinology*, 2007, 148, 2553–256.

[78] Case N and Rubin J. Beta-catenin a supporting role in the skeleton. *J. Cell. Biochem.* 2010, 110, 545–553

[79] Bonewald LF: The amazing osteocyte. *Journal of bone and mineral research : the official journal of the American Society for Bone and Mineral Research.* 2011;26:229–38.

[80] Tatsumi S, Ishii K, Amizuka N, Li M, Kobayashi T, Kohno K, Ito M, Takeshita S, Ikeda K: Targeted ablation of osteocytes induces osteoporosis with defective mechanotransduction. *Cell metabolism.* 2007;5:464–75.

[81] Xiong J, Onal M, Jilka RL, Weinstein RS, Manolagas SC, O'Brien CA: Matrix-embedded cells control osteoclast formation. *Nature medicine.* 2011;17:1235–41

[82] Klein-Nulend J, van der Plas A, Semeins CM, Ajubi NE, Frangos JA, Nijweide PJ, Burger EH: Sensitivity of osteocytes to biomechanical stress in vitro. 1995, *FASEB J* 9:441–445.

[83] Reilly GC, Haut TR, Yellowley CE, Donahue HJ, Jacobs CR: Fluid flow induced PGE2 release by bone cells is reduced by glycocalyx degradation whereas calcium signals are not. *Biorheology*, 2003. 40(6): 591-603.

[84] Vance J, Galley S, Liu DF, Donahue SW: Mechanical stimulation of MC3T3 osteoblastic cells in a bone tissue-engineering bioreactor enhances prostaglandin E2 release. *Tissue Eng*, 2004. 10(5-6): 1832-9.

[85] Jaasma MJ, O'Brien FJ: Mechanical stimulation of osteoblasts using steady and dynamic fluid flow. *Tissue Eng Part A.* 2008 Jul;14(7):1213-23.

[86] Bonewald, LF: Mechanosensation and transduction in osteocytes. *Bonekey Osteovision*, 2006. 3(10): 7-15.

[87] Goncalves I, Nesbitt WS, Yuan Y, Jackson SP: Importance of temporal flow gradients and integrin alphaIIb beta3 mechanotransduction for shear activation of platelets. *The Journal of biological chemistry.* 2005;280:15430–7.

[88] Shyy JY, Chien S: Role of integrins in endothelial mechanosensing of shear stress. *Circulation research.* 2002;91:769–75.

[89] Tadokoro S, Shattil SJ, Eto K, Tai V, Liddington RC, de Pereda JM, Ginsberg MH, Calderwood DA: Talin binding to integrin beta tails: a final common step in integrin activation. *Science.* 2003;302:103–6.

- [90] Aikawa R, Nagai T, Kudoh S, Zou Y, Tanaka M, Tamura M, Akazawa H, Takano H, Nagai R, Komuro I: Integrins play a critical role in mechanical stress-induced p38 MAPK activation. *Hypertension*. 2002;39:233–8.
- [91] Millward-Sadler SJ, Salter DM: Integrin-dependent signal cascades in chondrocyte mechanotransduction. *Annals of biomedical engineering*. 2004;32:435-46.
- [92] Salter DM, Robb JE, Wright MO: Electrophysiological responses of human bone cells to mechanical stimulation: evidence for specific integrin function in mechanotransduction. *Journal of bone and mineral research : the official journal of the American Society for Bone and Mineral Research*. 1997;12:1133–41.
- [93] Guilluy C, Swaminathan V, Garcia-Mata R, O'Brien ET, Superfine R, BurrIDGE K: The Rho GEFs LARG and GEF-H1 regulate the mechanical response to force on integrins. *Nature cell biology*. 2011;13:722–7.
- [94] Malone AM, Batra NN, Shivaram G, Kwon RY, You L, Kim CH, Rodriguez J, Jair K, Jacobs CR: The role of actin cytoskeleton in oscillatory fluid flow-induced signaling in MC3T3-E1 osteoblasts. *American journal of physiology. Cell physiology*. 2007b;292:C1830–6.
- [95] Myers KA, Rattner JB, Shrive NG, Hart DA. Osteoblast-like cells and fluid flow: cytoskeleton-dependent shear sensitivity. *Biochemical and biophysical research communications*. 2007;364:214–9.
- [96] Wang N, Butler JP, Ingber DE 1993 Mechanotransduction across the cell surface and through the cytoskeleton. *Science* 260(5111):1124-1127.
- [97] Pavalko FM, Chen NX, Turner CH, Burr DB, Atkinson S, Hsieh YF, Qiu J, Duncan RL: Fluid shear-induced mechanical signaling in MC3T3-E1 osteoblasts requires cytoskeleton-integrin interactions. *The American journal of physiology*. 1998;275:C1591–601.
- [98] Genetos DC, Kephart CJ, Zhang Y, Yellowley CE, Donahue HJ: Oscillating fluid flow activation of gap junction hemichannels induces ATP release from MLO-Y4 osteocytes. *Journal of cellular physiology*. 2007;212:207–14.
- [99] Song EK, Rah SY, Lee YR, Yoo CH, Kim YR, Yeom JH, Park KH, Kim JS, Kim UH, Han MK: Connexin-43 hemichannels mediate cyclic ADP-ribose generation and its Ca<sup>2+</sup>-mobilizing activity by NAD<sup>+</sup>/cyclic ADP-ribose transport. *J Biol Chem*. 2011 Dec 30;286(52):44480-90.

- [100] Tonna EA, Lampen NM: Electron microscopy of aging skeletal cells. I. Centrioles and solitary cilia. *J Gerontol.* 1972;27:316–324
- [101] Anderson CT, Castillo AB, Brugmann SA, Helms JA, Jacobs CR, Stearns T: Primary Cilia: Cellular Sensors for the Skeleton. *Anat Rec (Hoboken).* 2008 September ; 291(9): 1074–1078.
- [102] Uzbekov RE, Maurel DB, Aveline PC, Pallu S, Benhamou CL, Rochefort GY: Centrosome fine ultrastructure of the osteocyte mechanosensitive primary cilium. *Microsc Microanal.* 2012 Dec;18(6):1430-41.
- [103] Rikmenspoel R, Sleight MA: Bending moments and elastic constants in cilia. *Journal of Theoretical Biology.* 1970, 28, 81–100.
- [104] Mahoney NM, Goshima G, Douglass AD, Vale RD: Making microtubules and mitotic spindles in cells without functional centrosomes. *Current Biology.* 2006;16:564–569.
- [105] Wheatley DN, Bowser SS: Length control of primary cilia: analysis of monociliate and multiciliate PtK1 cells. *Biol Cell.* 2000 Dec; 92(8-9):573-82.
- [106] Hirokawa N, Tanaka Y and Okada Y: Left–Right Determination: Involvement of Molecular Motor KIF3, Cilia, and Nodal Flow. *Cold Spring Harb Perspect Biol.* 2009 Jul;1(1).
- [107] Haycraft CJ, Zhang Q, Song B, Jackson WS, Detloff PJ, Serra R, Yoder BK: Intraflagellar transport is essential for endochondral bone formation. *Development.* 2007;134(2):307–316.
- [108] Praetorius HA, Spring KR: Bending the MDCK cell primary cilium increases intracellular calcium. *Journal of Membrane Biology.* 2001, 184, 71–79.
- [109] Nauli SM, Alenghat FJ, Luo Y, Williams E, Vassilev P, Li X, Elia AE, Lu W, Brown EM, Quinn SJ, Ingber DE, Zhou J: Polycystins 1 and 2 mediate mechanosensation in the primary cilium of kidney cells. *Nature Genetics.* 2001, 33, 129–137.
- [110] Gradilone SA, Masyuk AI, Splinter PL, Banales JM, Huang BQ, Tietz PS, Masyuk TV, Larusso NF: Cholangiocyte cilia express TRPV4 and detect changes in luminal tonicity inducing bicarbonate secretion. *Proceedings of the National Academy of Sciences USA.* 2007, 104, 19138–19143.
- [111] Hoey DA, Tormey S, Ramcharan S, O'Brien FJ, Jacobs CR. Primary cilia-mediated mechanotransduction in human mesenchymal stem cells.

Stem Cells. 2012 Nov;30(11):2561-70.

[112] Malone AM, Anderson CT, Tummala P, Kwon RY, Johnston TR, Stearns T, Jacobs CR: Primary cilia mediate mechanosensing in bone cells by a calcium-independent mechanism. *Proceedings of the National Academy of Sciences USA*. 2007, 104, 13325–13330.

[113] Kwon RY, Temiyasathit S, Tummala P, Quah CC, Jacobs CR: Primary cilium-dependent mechanosensing is mediated by adenylyl cyclase 6 and cyclic AMP in bone cells. *FASEB J*. 2010 Aug;24(8):2859-68.

[114] Hoey DA, Kelly DJ and Jacobs CR: A role for the primary cilium in paracrine signaling between mechanically stimulated osteocytes and mesenchymal stem cells. 2011, *Biochem Biophys Res Commun* 412(1):182-187.

[115] Qiu N, Cao L, David V, Quarles LD, Xiao Z: Kif3a deficiency reverses the skeletal abnormalities in Pkd1 deficient mice by restoring the balance between osteogenesis and adipogenesis. *PLoS One*. 2010 Dec 2;5(12):e15240.

[116] Petite H, Viateau V, Bensaid W, Meunier A, de Pollak C, Bourguignon M, Oudina K, Sedel L, Guillemain G: Tissue-engineered bone regeneration. *Nat. Biotech*. 2000, 18:9 959-963.

[117] Reece G P, Patrick Jr C W: *Frontiers in Tissue Engineering*. 1st Edition, 1998, 58-72.

[118] Yaszemski MJ, Oldham JB, Lu L, Currier BL: *Bone Engineering*. 1st Ed, 2000, 43-46.

[119] Langer R, Vacanti J P: *Tissue Engineering*. *Science*. 1993, 260:5110,p 920-926.

[120] <http://www.serabyosis.com.au/prod01.htm>

[121] Maquet V, Jerome R: Design of macroporous biodegradable polymer scaffolds for cell transplantation. *Mat. Science Forum*. 1997, 250, 15- 42.

[122] Freed L E, Vunjak-Novakovic G: Culture of organized cell communities. *Adv. Drug. Deliv*. 1998, 33:1-2: 15-30.

[123] Burg KJ, Porter S, Kellam J F: Biomaterial developments for bone tissue engineering *Biomaterials*. 2000, 21:23, 2347-2359.

[124] Holy CE, Schoichet MS, Davies JE: Engineering three-dimensional bone tissue in vitro using biodegradable scaffolds: Investigating initial cell-seeding density and culture period. *J. Biomed. Mat*. 2000, 51:3 376-382.

- [125] Lange R, Luthen F, Beck U, Rychly BJ, Nebe B: Cell-extracellular matrix interaction and physico-chemical characteristics of titanium surfaces depend on the roughness of the material. *Biomol. Eng.* 2002, 19:2-6 255-261.
- [126] He W, Gonsalves KE, Batina N, Poker DB, Alexander E, Hudson M: Micro/nanomachining of Polymer Surface for Promoting Osteoblast Cell Adhesion. *Biomed. Dev.* 2003, 5:2, 101-108.
- [127] Cassinelli C, Morra M, Bruzzone G, Carpi A, Di Santi G, Giardino R, Fini, M: Surface chemistry effects of topographic modification of titanium dental implant surfaces: 1. Surface analysis. *Int. J. Oral & Maxillofac.* 2003, 18:1, 46-50.
- [128] Davies JE: Mechanisms of endosseous integration. *Int. J. Prosthodont.* 1998, 11:5, 391-401.
- [129] Hutmacher DW: Scaffolds in tissue engineering bone and cartilage. *Biomaterials.* 2000, 21:24 2529-2543.
- [130] Agrawal CM, Ray RB: Biodegradable polymeric scaffolds for musculoskeletal tissue engineering. *J. Biomed. Mat. Res.* 2001, 55:2, 141-150.
- [131] Leong KF, Cheah CM, Chua CK: Solid freeform fabrication of three-dimensional scaffolds for engineering replacement tissues and organs. *Biomaterials.* 2003, 24:13: 3262-2378.
- [132] Langer R, Vacanti P: Tissue Engineering. *Science.* 1993, 260:5110, 920-926.
- [133] Deporter DA, Komori N, Howley TP, Shiga A, Ghent A, Hensel P, Parisien K: Reconstituted bovine skin collagen enhances healing of bone wounds in the rat calvaria. *Calcif. Tissue Int.* 1988, 42:5 321-325.
- [134] Murata M, Huang BZ, Shibata T, Imai S, Nagai N, Arisue M: Bone augmentation by recombinant human BMP-2 and collagen on adult rat parietal bone. *J. Oral Maxillofac. Surg.* 1999, 28:3, 232-237.
- [135] Ueda H, Hong L, Yamamoto M, Shigeno K, Inoue M, Toba T, Yoshitani M, Nakamura T, Tabata Y, Shimizu Y: Use of collagen sponge incorporating transforming growth factor- $\beta$ 1 to promote bone repair in skull defects in rabbits. *Biomaterials.* 2002, 23:4, 1003-1010.
- [136] Sachlos E, Reis Ainsley N, Derby B, Czernuszka JT: Novel collagen scaffolds with predefined internal morphology made by solid freeform fabrication. *Biomaterials.* 2003, 24:8, 1487-1497.

- [137] Haisch A, Loch A, David J, Pruss A, Hansen R, Sittinger: Preparation of a pure autologous biodegradable fibrin matrix for tissue engineering. *M., Med. Biol. Eng. Comp.* 2000, 38:6, 686-689.
- [138] Tayapongsak P, O'Brien DA, Monteiro CB, Arceo-Diaz LY: Autologous fibrin adhesive in mandibular reconstruction with particulate cancellous bone and marrow. *J. Oral Maxillofac. Surg.* 1994, 52:2, 161-165.
- [139] Hojo M, Inokuchi S, Kidokoro M, Fukuyama N, Tanaka E, Tsuji C, Myasaka M, Tanino R, Nakazawa H: Induction of Vascular Endothelial Growth Factor by Fibrin as a Dermal Substrate for Cultured Skin Substitute. *Plast. Reconstr. Surg.* 2003, 111:5, 1638-1645.
- [140] Senior RM, Skogen WF, Griffin GL, Wilner GD: Effects of fibrinogen derivatives upon the inflammatory response. Studies with human fibrinopeptide B. *J. Invest.* 1986, 77:3, 1014-1019.
- [141] Zhang M, Haga A, Sekiguchi H, Hirano S: Structure of insect chitin isolated from beetle larva cuticle and silkworm (*Bombyx mori*) pupa exuvia. *Int. J. Biol. Macromol.* 2000, 27:1, 99-105.
- [142] Park YJ, Lee YM, Park SN, Sheen SY, Chung CP, Lee SJ: Platelet derived growth factor releasing chitosan sponge for periodontal bone regeneration. *Biomaterials.* 2000, 21:2, 153-159.
- [143] Brekke JH, Toth JM: Principles of tissue engineering applied to programmable osteogenesis. *J Biomed Mater Res.* 1998 Winter;43(4):380-98.
- [144] Mauney JR, Sjostrom S, Blumberg J, Horan R, O'Leary JP, Vunjak-Novakovic G, Volloch V, Kaplan DL: Mechanical stimulation promotes osteogenic differentiation of human bone marrow stromal cells on 3-D partially demineralized bone scaffolds in vitro. *Calcif Tissue Int.* 2004 May;74(5):458-68.
- [145] Mikos AG, Thorsen AJ, Czerwonka LA, Bao Y, Langer R, Winslow DN, Vacanti JP: Preparation and Characterization of Poly(L-Lactic Acid) Foams. *Polymer. Carbohydrate Polymers.* 2005, 59, 329-337.
- [146] Thomson RC, Mikos AG, Beham E, Lemon JC, Satterfield WC, Aufdemorte TB, Miller MJ: Guided tissue fabrication from periosteum using preformed biodegradable polymer scaffolds. *Biomaterials.* 1999, 20:21, 2007-2018.

- [147] Liao CJ, Chen CF, Chen JH, Chiang SF, Lin YJ, Chang KY: Fabrication of porous biodegradable polymer scaffolds using a solvent merging/particulate leaching method. *J. Biomed. Mat. Res.* 2002, 59:4, 676-681.
- [148] Lopez H, Marco A, Sohier J, Gaillard C, Quillard S, Dorget M, Layrolle P: Rapid prototyped porous titanium coated with calcium phosphate as a scaffold for bone tissue engineering. *Biomaterials*, 2008, Vol.29(17), 2608-2615.
- [149] Farag MM, Rüssel C: Glass-ceramic scaffolds derived from Bioglass® and glass with low crystallization affinity for bone regeneration. *Materials Letters*. 2012, Vol.73, 161-165.
- [150] Oest ME, Dupont KM, Kong HJ, Mooney DJ, Guldborg RE. Quantitative assessment of scaffold and growth factor-mediated repair of critically sized bone defects. *J Orthop Res.* 2007 Jul;25(7):941-50.
- [151] Eichenlaub-Ritter U, Betzendahl I: Chloral hydrate induced spindle aberrations, metaphase I arrest and aneuploidy in mouse oocytes. *Mutagenesis*. 1995 Nov;10(6):477-86.
- [152] Aarvold A, Smith JO, Tayton ER, Lanham SA, Chaudhuri JB, Turner IG, Oreffo RO. The effect of porosity of a biphasic ceramic scaffold on human skeletal stem cell growth and differentiation in vivo. *J Biomed Mater Res A.* 2013 Apr 9. doi: 10.1002/jbm.a.34646
- [153] Teixeira S, Fernandes H, Leusink A, van Blitterswijk C, Ferraz MP, Monteiro FJ, de Boer J: In vivo evaluation of highly macroporous ceramic scaffolds for bone tissue engineering. *J Biomed Mater Res A.* 2010 May;93(2):567-75.
- [154] San Miguel B, Kriauciunas R, Tosatti S, Ehrbar M, Ghayor C, Textor M, Weber FE: Enhanced osteoblastic activity and bone regeneration using surface-modified porous bioactive glass scaffolds. *J Biomed Mater Res A.* 2010 Sep 15;94(4):1023-33.
- [155] Wu C, Zhou Y, Fan W, Han P, Chang J, Yuen J, Zhang M, Xiao Y: Hypoxia mimicking mesoporous bioactive glass scaffolds with controllable cobalt ion release for bone tissue engineering. *Biomaterials.* 2012 Mar;33(7):2076-85.
- [156] Farrell E, O'Brien FJ, Doyle P, Fischer J, Yannas I, Harley BA, O'Connell B, Prendergast PJ, Campbell VA: A collagen-glycosaminoglycan scaffold supports adult rat mesenchymal stem cell differentiation along osteogenic and chondrogenic routes. *Tissue Eng.* 2006 Mar;12(3):459-68.

- [157] Yan J, Li J, Runge MB, Dadsetan M, Chen Q, Lu L, Yaszemski MJ: Cross-linking characteristics and mechanical properties of an injectable biomaterial composed of polypropylenefumarate and polycaprolactone co-polymer. *J Biomater Sci Polym Ed.* 2011;22(4-6):489-504.
- [158] Morgan SM, Tilley S, Perera S, Ellis MJ, Kanczler J, Chaudhuri JB, Oreffo RO: Expansion of human bone marrow stromal cells on poly-(DL-lactide-co-glycolide) (PDL LGA) hollow fibres designed for use in skeletal tissue engineering. *Biomaterials.* 2007 Dec;28(35):5332-43.
- [159] Balla VK, Bodhak S, Bose S, Bandyopadhyay A: Porous tantalum structures for bone implants: fabrication, mechanical and in vitro biological properties. *Acta Biomater.* 2010 Aug;6(8):3349-59.
- [160] Dabrowski B, Swieszkowski W, Godlinski D, Kurzydowski KJ: Highly porous titanium scaffolds for orthopaedic applications. *J Biomed Mater Res B Appl Biomater.* 2010 Oct;95(1):53-61.
- [161] Xue W, Krishna BV, Bandyopadhyay A, Bose S: Processing and biocompatibility evaluation of laser processed porous titanium. *Acta. Biomater.* 2007 Nov;3(6):1007-18.
- [162] Das K, Balla VK, Bandyopadhyay A and Bose S: Surface modification of laser-processed porous titanium for load-bearing implants. *Scripta Materialia* 59 (2008) 822–825.
- [163] Lee CR, Grad S, Gorna K, Gogolewski S, Goessl A, Alini M. Fibrin-polyurethane composites for articular cartilage tissue engineering: a preliminary analysis. *Tissue Eng.* 2005 Sep-Oct;11(9-10):1562-73.
- [164] Santerre JP: Biodegradation evaluation of polyether and polyesterurethanes with oxidative and hydrolytic enzymes. *J Biomed Mater Res,* 1994, vol. 28 (10) 1187-1199.
- [165] Santerre JP, Woodhouse K, Laroche G, Labow RS: Understanding the biodegradation of polyurethanes: From classical implants to tissue engineering materials. *Biomaterials* Vol 26, Issue 35, 2005, 7457-7470.
- [166] Stokes K, McVenes R, Anderson JM: Polyurethane elastomer biostability. *J Biomater Appl,* 1995, vol. 9 (4) 321-354.

- [167] Phillips RE, Smith MC, Thoma RJ: Biomedical applications of polyurethanes: implications of failure mechanisms. *J Biomater.*1988. Vol 3(2) 207-27.
- [168] Slade CL, Peterson HD: Disappearance of the polyurethane cover of the Ashley Natural Y prosthesis. *Plast Reconstr Surg*, 1982, vol. 70 (3) 379-382.
- [169] Buttler WT, Ridall AL, McKee MD: Osteopontin. *Principles of Bone Biology*, Academic Press, California. 1996, 167–181.
- [170] Liu YK, Nemoto A, Feng Y, Uemura T: The binding ability to matrix proteins and the inhibitory effects on cell adhesion of synthetic peptides derived from a conserved sequence of integrins. *J. Biochem.* 1997, 121, 961–96.
- [171] Yabe T, Nemoto A, Uemura T: Recognition of osteopontin by rat bone marrow derived osteoblastic primary cells. *Biosci., Biotechnol., Biochem.* 1997, 61, 754–756.
- [172] <http://www.sigmaaldrich.com/>
- [173] Uemura T, Liu YK, Kuboki Y: mRNA expression of MT1-MMP, MMP-9, cathepsin K, and TRAP in highly enriched osteoclasts cultured on several matrix proteins and ivory surfaces. *Biosci., Biotechnol., Biochem.* 2000, 64 1771–1773.
- [174] Rodan GA, Noda M: Gene expression in osteoblastic cells. *Eukaryotic Gene Expression.* 1991, 1, 85–98.
- [175] Vaananen HK, Liu YK, Lehenkari P, Uemura T: How do osteoclast resorb bone? *Mater. Sci. Eng C.*1998, 6, 205–209.
- [176] Weber GF: The metastasis gene osteopontin: a candidate target for cancer therapy. *Biochem Biophys Acta* 2001; 1552: 61-85.
- [177] Uemura T, Nemoto A, Liu YK, Kojima H, Dong J, Yabe T, Yoshikawa T, Ohgushi H, Ushida T, Tateishi Ta: Osteopontin involvement in bone remodeling and its effects on in vivo osteogenic potential of bone marrow-derived osteoblasts/porous hydroxyapatite constructs. *Materials Science & Engineering C*, 2001, Vol.17(1), 33-36.
- [178] Ruth Chiquet-Ehrisman: Molecules in focus Tenascins. *The International Journal of Biochemistry & Cell Biology* 36 (2004) 986–990.
- [179] Mackie EJ, Ramsey S: Modulation of osteoblast behaviour by tenascin. *J Cell Sci.* 1996, 109: 1597–1604.

- [180] Joyce ME, Jingushi S, Bolander ME. Transforming growth factor-beta in the regulation of fracture repair. *Orthop Clin North Am.* 1990;21:199-209.
- [181] Kato T, Kawaguchi H, Hanada K, Aoyama L, Hiyama Y, Nakamura T, Kuzutani K, Tamura M, Kurokawa T, Nakamura K. Single local injection of recombinant fibroblast growth factor-2 stimulates healing of segmental bone defects in rabbits. *J Orthop Res.* 1998;16:654-9.
- [182] Saito A, Suzuki Y, Kitamura M, Ogata SI, Yoshihara Y, Masuda S, Ohtsuki C, and Tanihara M: Repair of 20-mm long rabbit radial bone defects using BMP-derived peptide combined with an alpha-tricalcium phosphate scaffold. *J Biomed Mater Res A*, 77(4), 2006, 700–706.
- [183] Uludag H, Gao T, Porter TJ, Friess W, and Wozney JM: Delivery systems for BMPs: factors contributing to protein retention at an application site. *J Bone Joint Surg Am* 83-A Suppl 1, 2001, 128–135.
- [184] Franceschi RT: Biological approaches to bone regeneration by gene therapy. *J Dent Res* 84, 2005, 1093–1103.
- [185] Yasko AW, Lane JM, Fellingner EJ, Rosen V, Wozney JM, and Wang EA: The healing of segmental bone defects, induced by recombinant human bone morphogenetic protein (rhBMP-2): A radiographic, histological, and biomechanical study in rats. *J Bone Joint Surg Am.* 1992 Jun;74(5):659-70.
- [186] Yamaguchi A, Komori T, and Suda T: Regulation of osteoblast differentiation mediated by bone morphogenetic proteins, hedgehogs, and Cbfa1. *Endocr. Rev.* 2000, 21, 393-411.
- [187] He XB, Lu WZ, Tang KL, Yang L, He J, Zhu QH, Liu XD, Xu JZ: Effects of bone morphogenic protein and transforming growth factor-beta on biomechanical property for fracture healing in rabbit ulna. *Zhongguo Xiu Fu Chong Jian Wai Ke Za Zhi.* 2003 May;17(3):185-8.
- [188] Murakami N, Saito N, Takahashi J, Ota H, Horiuchi H, Nawata M, Okada T, Nozaki K, Takaoka K: Repair of a proximal femoral bone defect in dogs using a porous surfaced prosthesis in combination with recombinant BMP-2 and a synthetic polymer carrier. *Biomaterials.* 2003 Jun;24(13):2153-9.
- [189] Mayer M, Hollinger J, Ron E, Wozney J: Maxillary alveolar cleft repair in dogs using recombinant human bone morphogenetic protein-2 and a polymer carrier. *Plast Reconstr Surg.* 1996 Aug;98(2):247-59.

- [190] Kokubo S, Fujimoto R, Yokota S, Fukushima S, Nozaki K, Takahashi K, Miyata K: Bone regeneration by recombinant human bone morphogenetic protein-2 and a novel biodegradable carrier in a rabbit ulnar defect model. *Biomaterials*. 2003 Apr;24(9):1643-51.
- [191] Kawamoto T, Motohashi N, Kitamura A, Baba Y, Suzuki S, Kuroda T: Experimental tooth movement into bone induced by recombinant human bone morphogenetic protein-2. *Cleft Palate Craniofac J*. 2003 Sep;40(5):538-43.
- [192] Hu JJ, Jin D, Quan DP, Zhong SZ, Chen JH, Wei KH, Zhao J, Pei GX: Bone defect repair with a new tissue-engineered bone carrying bone morphogenetic protein in rabbits. *Zhongguo Xiu Fu Chong Jian Wai Ke Za Zhi*. 2006 Sep;20(9):931-5.
- [193] Kim J, Kim IS, Cho TH, Lee KB, Hwang SJ, Tae G, Noh I, Lee SH, Park Y, Sun K. Bone regeneration using hyaluronic acid based hydrogel with bone morphogenic protein-2 and human mesenchymal stem cells. *Biomaterials*. 2007 Apr;28(10):1830-7.
- [194] Mano JF, Reis RL: Osteochondral defects: present situation and tissue engineering approaches. *J Tissue Eng Regen Med*. 2007 Jul-Aug;1(4):261-73.
- [195] Park YJ, Kim KH, Lee JY, Ku Y, Lee SJ, Min BM, Chung CP: Immobilization of bone morphogenetic protein-2 on a nanofibrous chitosan membrane for enhanced guided bone regeneration. *Biotechnol Appl Biochem*. 2006 Jan;43(Pt 1):17-24.
- [196] Li C, Vepari C, Jin HJ, Kim HJ, Kaplan DL: Electrospun silk-BMP-2 scaffolds for bone tissue engineering. *Biomaterials*. 2006 Jun;27(16):3115-24.
- [197] Karageorgiou V, Meinel L, Hofmann S, Malhotra A, Volloch V, Kaplan D: Bone morphogenetic protein-2 decorated silk fibroin films induce osteogenic differentiation of human bone marrow stromal cells. *J Biomed Mater Res A*. 2004 Dec 1;71(3):528-37.
- [198] Karageorgiou V, Tomkins M, Fajardo R, Meinel L, Snyder B, Wade K, Chen J, Vunjak-Novakovic G, Kaplan DL: Porous silk fibroin 3-D scaffolds for delivery of bone morphogenetic protein-2 in vitro and in vivo. *J Biomed Mater Res A*. 2006 Aug;78(2):324-34.
- [199] Heath CA: *Cells for tissue engineering*. 2000, 18:1, 17-19.

- [200] Platt JL: The immunological barriers to xenotransplantation. *Critic. Rev. Immunol.* 1996, 16:4, 331-358.
- [201] Blau HM, Brazelton TR, Weimann JM: The Evolving Concept of a Stem Cell Entity or Function? *Cell.* 2001, 105:7, 829-841.
- [202] Shiroy A, Yoshikawa M, Yokota H, Fukui H, Ishizaka S, Tatsumi K, Takahashi Y: Identification of Insulin-Producing Cells Derived from Embryonic Stem Cells by Zinc-Chelating Dithizone. *Stem Cells.* 2002, 20:4, 284-292.
- [203] Buttery LDK, Bourne S, Xynos JD, Wood H, Hughes FJ, Hughes SPF, Episkopou V, Pollak JM: Differentiation of Osteoblasts and in Vitro Bone Formation from Murine Embryonic Stem Cells. *Tissue Eng.* 2001, 7:1, 89-99.
- [204] <http://www.prlog.org>
- [205] Toma JG, Akhavan M, Fernandes KJL, Barnabe-Heider F, Kaplan DR, Miller FD: Isolation of multipotent adult stem cells from the dermis of mammalian skin. *Nat. Cell Biol.* 2001, 3:9, 778-784.
- [206] Bruder SP, Jaiswal N, Hanesworth SE: Growth kinetics, self-renewal, and the osteogenic potential of purified human mesenchymal stem cells during extensive subcultivation and following cryopreservation. *J. Cell. Biochem.* 1997, 64:2, 278-294.
- [207] Pittenger MF, Mackay AM, Beck SC, Jaiswal RK, Douglas R, Mosca JD, Moorman MA, Simonetti DW, Craig S, Marshak DR: Multilineage Potential of Adult Human Mesenchymal Stem Cells. *Science.* 1999, 284:5411, 143-147.
- [208] Caplan A: The mesengenic process. *Clin. Plast. Surg.* 1994, 21:3, 429-425.
- [209] de Peppo GM, Sjoval P, Lenneras M, Strehl R, Hyllner J, Thomsen P, and Karlsson C: Osteogenic potential of human mesenchymal stem cells and human embryonic stem cell-derived mesodermal progenitors: a tissue engineering perspective. *Tissue Eng Part A.* 2010 Nov;16(11):3413-26.
- [210] Bigdeli N, de Peppo GM, Lenneras M, Sjoval P, Lin-dahl A, Hyllner J, and Karlsson C: Superior osteogenic capacity of human embryonic stem cells adapted to matrix-free growth compared to human mesenchymal stem cells. *Tissue Eng Part A.* 2010 Nov;16(11):3427-40.
- [211] de Peppo GM, Svensson S, Lenneras M, Synnergren J, Stenberg J, Strehl R, Hyllner J, Thomsen, P, and Karlson C: Human embryonic mesodermal progenitors highly resemble human mesenchymal stem cells and display high

potential for tissue engineering applications. *Tissue Eng Part A*. 2010 Jul;16(7):2161-82.

[212] de Peppo GM, Sladkova M, Sjövall P, Palmquist A, Oudina K, Hyllner J, Thomsen P, Petite H, Karlsson C. Human Embryonic stem cell derived mesodermal progenitors display substantially increased tissue formation compared to mesenchymal stem cell under dynamic culture conditions in a packed/bed column bioreactor. *Tissue Eng. Part A*. 2013 Jan;19(1-2):175-87.

[213] Al-Munajjed AA, Gleeson JP, O'Brien FJ: Development of a collagen calcium-phosphate scaffold as a novel bone graft substitute. *Stud Health Technol Inform*. 2008;133:11-20.

[214] Lyons FG, Al-Munajjed AA, Kieran SM, Toner ME, Murphy CM, Duffy GP, O'Brien FJ. The healing of bony defects by cell-free collagen based scaffolds compared to stem cell seeded tissue engineered constructs. *Biomaterials*. 2010 Dec;31(35):9232-43.

[215] Taylor AF, Saunders MM, Shingle DL, Cimbala JM, Zhou Z, Donahue HJ: Mechanically stimulated osteocytes regulate osteoblastic activity via gap junctions. *Am J Physiol Cell Physiol*. 2007 Jan;292(1): 545-52.

[216] Warren SM, Alexander M, Sailon AC, Allori EH, Davidson DD, Reformat RJ, Allen Jr: A Novel Flow-Perfusion Bioreactor Supports 3D Dynamic Cell Culture. *Journal of Biomedicine and Biotechnology*. Volume 2009, Article ID 873816, 7 pages.

[217] Sikavitsas VI, Bancroft GN, Holtorf HL, Jansen JA: Mineralized matrix deposition by marrow stromal osteoblasts in 3D perfusion culture increases with increasing fluid shear forces. *Proc Natl Acad Sci USA*. 2003 Dec 9;100(25):14683-8.

[218] Kim J, Ma T. Perfusion regulation of hMSC microenvironment and osteogenic differentiation in 3D scaffold. *Biotechnol Bioeng*. 2012 Jan;109(1): 252-61.

[219] Bouafsoun A, Othmane A, Kerkeni A, Jaffrézic N, and Ponsonnet L: Evaluation of endothelial cell adherence onto collagen and fibronectin: a comparison between jet impingement and flow chamber techniques. *Mater Sci Eng*. 2006, 26, 260-265.

[220] Kapur R, and Rudolph AS: Cellular and cytoskeleton morphology and

strength of adhesion of cells on self- assembled monolayers of organosilanes. *Exp Cell Res.* 1998, 244, 275-283.

[221] Truskey GA, and Pirone JS: The effect of fluid shear stress upon cell adhesion to fibronectin-treated surfaces. *J Biomed Mater Res.* 1990, 24, 1333-53.

[222] Truskey GA, and Proulx TL: Relationship between 3T3 cell spreading and the strength of adhesion on glass and silane surfaces. *Biomaterials* 1993, 14, 243-54.

[223] Van Kooten T, Schakenraad J, van der Mei H, and Busscher H: Influence of substratum wettability on the strength of adhesion of human fibroblasts. *Biomaterials* 1992, 13, 897-904.

[224] Van Kooten T, Schakenraad J, van der Mei H: Fluid shear induced endothelial cell detachment from glass influence of adhesion time and shear stress. *Med Eng Phys.* 1994, 16, 506-12.

[225] Wan Y, Yang J, Yang J, Bei J, and Wang S: Cell adhesion on gaseous plasma modified poly(lactide) surface under shear stress field. *Biomaterials.* 2003, 24, p.3757-64.

[226] Deligianni DD, Katsala ND, Koutsoukos PG, and Missirlis YF: Effect of surface roughness of hydroxyapatite on human bone marrow cell adhesion, proliferation, differentiation and detachment strength. *Biomaterials* 2001, 22, 87-96.

[227] Engler AJ, Chan M, Boettiger D, and Schwarzbauer JE: A novel mode of cell detachment from fibrillar fibronectin matrix under shear. *J Cell Sci.* 2009, 122, 1647-53.

[228] García AJ, Ducheyne P, and Boettiger D: Quantification of cell adhesion using a spinning disc device and application to surface-reactive materials. *Biomaterials.* 1997, 18, 1091-8.

[229] Goldstein AS, and DiMilla PA: Application of fluid mechanic and kinetic models to characterize mammalian cell detachment in a radial-flow chamber. *Biotechnol Bioeng* 1997, 55, 616-29.

[230] Furukawa KS, Ushida T, Nagase T: Quantitative analysis of cell detachment by shear stress. *Mater Sci Eng.* 2001, 17, 55-58.

[231] Christophis C, Grunze M, and Rosenhahn A: Quantification of the adhesion strength of fibroblast cells on ethylene glycol terminated self-assembled

monolayers by a micro- fluidic shear force assay. *Phys Chem Chem Phys*. 2010,12, 4498-504.

[232] Lu H, Koo LY, Wang WM: Microfluidic shear devices for quantitative analysis of cell adhesion. *Anal Chem*. 2004, 76, 5257-64.

[233] McCoy RJ, and O'Brien FJ: Influence of Shear Stress in Perfusion Bioreactor Cultures for the Development of Three-Dimensional Bone Tissue Constructs: A Review. *Tissue engineering*. 2010, 16(6):587-601.

[234] Weinbaum S, Cowin SC, Zeng Y: A model for the excitation of osteocytes by mechanical loading-induced bone fluid shear stresses. *J Biomech*. 1994 Mar;27(3):339-60.

[235] Verbruggen SW, Vaughan TJ, McNamara LM. Fluid flow in the osteocyte mechanical environment: a fluid-structure interaction approach. *Biomech Model Mechanobiol*. 2013 Apr 9.

[236] Song MJ, Brady-Kalnay SM, McBride SH, Phillips-Mason P, Dean D, Knothe Tate ML. Mapping the mechanome of live stem cells using a novel method to measure local strain fields in situ at the fluid-cell interface. *PLoS One*. 2012;7(9):e43601

[237] Plunkett NA, Partap S, and O'Brien FJ: Osteoblast response to rest periods during bioreactor culture of collagen- glycosaminoglycan scaffolds. *Tissue Eng*. 2010, Part A 16, 943-51.

[238] Sikavitsas V, Bancroft G, Lemoine J: Flow perfusion enhances the calcified matrix deposition of marrow stromal cells in biodegradable nonwoven fiber mesh scaffolds. *Ann Biomed Eng*. 2005, 33, 63-70.

[239] Cartmell S, Porter BD, García AJ, and Guldberg RE: Effects of medium perfusion rate on cell-seeded three- dimensional bone constructs in vitro. *Tissue Eng*. 2003, 9, 1197-203.

[240] Holtorf HL, Datta N, Jansen JA, and Mikos AG: Scaffold mesh size affects the osteoblastic differentiation of seeded marrow stromal cells cultured in a flow perfusion bioreactor. *J Biomed Mater Res*. 2005, Part A 74A, 171-80.

[241] Bancroft GN, Sikavitsas VI, van den Dolder J: Fluid flow increases mineralized matrix deposition in 3D perfusion culture of marrow stromal osteoblasts in a dose-dependent manner. *Proc Natl Acad Sci USA*. 2002, 99, 12600-5.

[242] Helm CE, Fleury ME, Zisch AH, Boschetti F, and Swartz MA: Synergy between interstitial flow and VEGF directs capillary morphogenesis in vitro through a gradient amplification mechanism. Proc Natl Acad Sci USA. 2005, 102, 15779-84.

# Chapter 2: Materials and Methods

## 2.1 Materials

1. Polyether polyurethane (PU) foam grade XE1700V (department of chemistry, University of Sheffield, UK)
2. Glass-based 3D cell matrix (kindly donated by Dr. Sion Philips, Orla Protein Technologies Ltd, Newcastle, UK)
3. BM1 murine bone marrow derived MSC (donated by University of Sheffield, Medical School, Sheffield, UK)
4. BM1 murine bone marrow derived MSC culture media: DMEM supplemented with 10% (v/v) fetal bovine serum (FBS), 1% penicillin/streptomycin (P/S) and 1% Glutamine (G)
5. MLO-A5 osteoblastic cell (kindly donated by Professor Lynda Bonewald, University of Missouri, Kansas City, USA)
6. MLO-A5 basal culture media: Alpha minimum essential medium ( $\alpha$ -MEM) supplemented with 5% FBS, 5% bovine calf serum (BCS), 1% P/S and 0.25% fungizone (F)
7. Human embryonic stem cell mesenchymal progenitor cells (hES-MP 0025) (Cellartis, Gothenburg, Sweden)
8. hES-MP serum-free media: Stemline® Pluripotent Stem Cell Culture Medium (Sigma Aldrich, Roset, UK).
9. hES-MP basal culture media:  $\alpha$ -MEM supplemented with 10% FCS, 1% P/S and 1% Glutamine
10. hES-MP osteogenic differentiation media: hES-MP basal culture media supplemented with dexamethasone at final concentration 10 nM, ascorbic acid-2-phosphate (AA) 50  $\mu$ g/ml and 5mM of  $\beta$ -glycerophosphate ( $\beta$ GP)
11. Loading media:  $\alpha$ -MEM supplemented with 10% FCS, 1% P/S and 1% Glutamine
12. Medical grade stainless steel rings (internal diameter 1 cm)
13. Porcine gelatine (Sigma, UK)

14. MTT (Sigma Aldrich, Roset, UK)
15. MTS (Promega, Southampton, UK)
16. DAPI [4'-6-Diamidino-2-phenylindole] (Sigma Aldrich, Roset, UK)
17. ALP Yellow (pNPP) Liquid Substrate system for ELISA (Sigma, UK) for measuring alkaline phosphatase (ALP) activity in cells.
18. Oscillatory fluid flow pump (ibidi, Germany)
19. Peristaltic fluid pump (fisher, UK)
20. Silicone tubing/conduit (cole-parmer, UK)
21. Sirius Red (Sigma Aldrich, Roset, UK)
22. Alizarin red (Sigma Aldrich, Roset, UK)
23. PGE2 Assay kit (Parameter, R&D Systems, Abingdon, UK) for quantitative determination of Prostaglandin E<sub>2</sub> in cell culture supernates.
24. Mouse antibody to Acetylated alpha tubulin [6-11B-1] (2mg/ml) (Sigma Aldrich, Roset, UK)
25. FITC-conjugated rabbit anti-mouse immunoglobulins (green) or rhodamine-conjugated goat anti-mouse immunoglobulins (red) (400mg/L) (Sigma Aldrich, Roset, UK)
26. Micro CT scanner (SKYSCAN)
27. ImageJ software (National institute of Health, Maryland, USA)
28. Simpleware software (Exeter, UK)
29. All other chemicals were from Sigma Aldrich (Dorset, UK) unless stated.

## 2.2 Methods

### 2.2.1 Cell preparation

All cells were examined daily to observe their morphology, colour of media and density of cells. To passage cells, cell media was removed and cells were washed with PBS twice before adding 2 ml of trypsin-EDTA and incubated for 5 minutes to detach cells. Media was added to halt the trypsin-EDTA reaction and detached cells in suspension were centrifuged at 1000 rpm for 5 minutes to form a cell pellet. The supernatant was poured off and cells were resuspended in a known volume of media. A cell count was performed using a haemocytometer and cells were then split 1:10 to new flasks.

#### 2.2.1.1 Murine bone marrow derived MSC (BM1)

Murine bone marrow derived MSCs, previously isolated in the lab from 5-8 weeks old Balb/c mice by our collaborator Ilaria Bellantuono, were cultured in DMEM media supplemented with 10% (v/v) FBS, 1% Penicillin (P) and 2 mM L-Glutamine (G) in a 37°C incubator with a humidified atmosphere of 95% air and 5% CO<sub>2</sub> in 0.1% gelatin coated T75 flasks. Cells were used for experiments between passages 3-10 in most cases.

#### 2.2.1.2 Osteoblastic cell line (MLO-A5)

MLO-A5 cells are postosteoblast-preosteocyte cells and are thought to behave similarly to the cells that are responsible for mineralisation in bone. *Kato et al*, have also described these cells as spontaneously producing more bone like matrix faster in culture than other osteoblastic cell lines, even in the absence of additional chemical factors normally added to induce cell differentiation and matrix production [1]. MLO-A5 cells utilised in this study were cultured in media supplemented with  $\alpha$ -MEM (Alpha Modified Eagles Medium), 10% Fetal Calf Serum (FCS) on 0.1% gelatin coated surfaces and used between passages 25-30.

### 2.2.1.3 Human embryonic stem cell derived mesenchymal progenitors (hES-MP)

hES-MP cells were shown to be very similar to mesenchymal stem cells with regards to morphology and expression of markers. These cells also have the potential to differentiate towards the osteogenic, adipogenic, and chondrogenic lineage *in vitro* [2]. These cells were cultured in media supplemented with  $\alpha$ -MEM (Alpha Modified Eagles Medium), 10% Fetal Calf Serum (FCS) on 0.1 % gelatine coated surfaces and expanded in 4nM fibroblast growth factor-basic recombinant human (bFGF) as stated by the manufacturer (Cellartis). Cells were used for experiments between passages 3-10 in most cases. Cells could be expanded up to passage 20 but were observed to begin to lose their fibroblastic morphology after passage 12 and ALP activity and mineral depositing ability also reduced.

## 2.2.2 Scaffold Preparation

### 2.2.2.1 Polyurethane Scaffolds (PU)

A previous study [3] measured the average pore size and strut width of the PU foams using imageJ (an image analysis package). The average pore size was shown to be 400  $\mu\text{m}$  (varies between 150-1000  $\mu\text{m}$ ) and the average strut width was shown to be 65  $\mu\text{m}$  (varies between 43-96  $\mu\text{m}$ ). In the same study the mechanical properties were tested by a single cycle of loading to 50% strain at 0.2 mm/sec. Properties of the PU scaffolds are shown in the following table;

Table 2.1; Properties of Polyurethane used in this study

<b>Properties of PU scaffold</b>	
Density (Kg/M <sup>3</sup> )	15-18
Tensile Strength (kPa)	80
Elongation at break (%)	100
Porosity %	80
Young's modulus of elasticity (kPa)	2.87±0.02
Strut width (µm)	43-96
Pore size (µm)	150-1000

From a single block of PU, a hole-punch (size 10) was used in order to create long PU cylinders with 10 mm diameters. A ruler was used to cut the long samples into 10 mm thicknesses (fig 2.1). This resulted in PU cylindrical scaffolds having dimensions of 10 mm x 10 mm. Scaffolds were sterilised using peracetic acid (acetic acid, 40-45%) for 3 hours after which they were washed with phosphate buffered saline (PBS). Scaffolds being prepared for seeding with hESMPs or MLO-A5s were soaked in 0.1 % gelatine solution. All scaffolds were then left to rock gently over night under sterile conditions at room temperature. Excess gelatine solution was removed before cell seeding. Scaffolds were removed and gently squeezed to remove excess PBS or gelatine solution and placed in 10 mm internal diameter steel rings which support the scaffolds during the initial cell seeding and attachment phase.

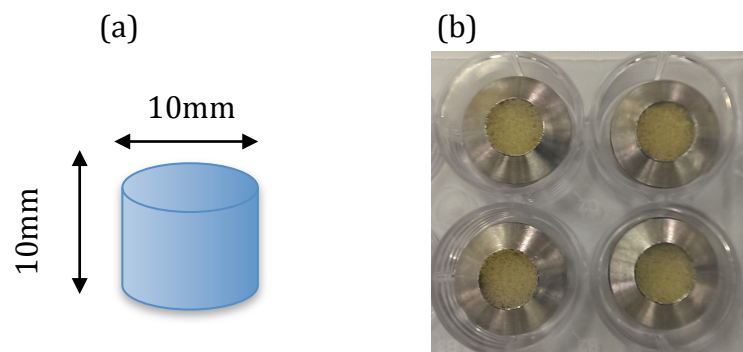


Fig 2.1; (a) The dimensions of a single PU scaffold and (b) PU scaffolds were hole-punched, sterilized and washed with PBS. Steel rings held the PU scaffolds in place for the for initial cell seeding which contained 100 µl media with 500,000 cells per scaffold.

### 2.2.2.2 Nippon Sheet Glass (NSG) scaffolds

*Orla Protein Technologies* provided Nippon Sheet Glass (NSG) scaffolds made from the same high optical grade borosilicate glass used for the production of 2D microscope slides and coverslips (fig 2.2).

These scaffolds were sterilised in the same manner as the PU scaffolds, however they could not be placed within the steel rings for cell seeding due to their geometry and fragility. Instead glass scaffolds were placed on a thin and hollow silicone ring for sterilisation and initial cell attachment.

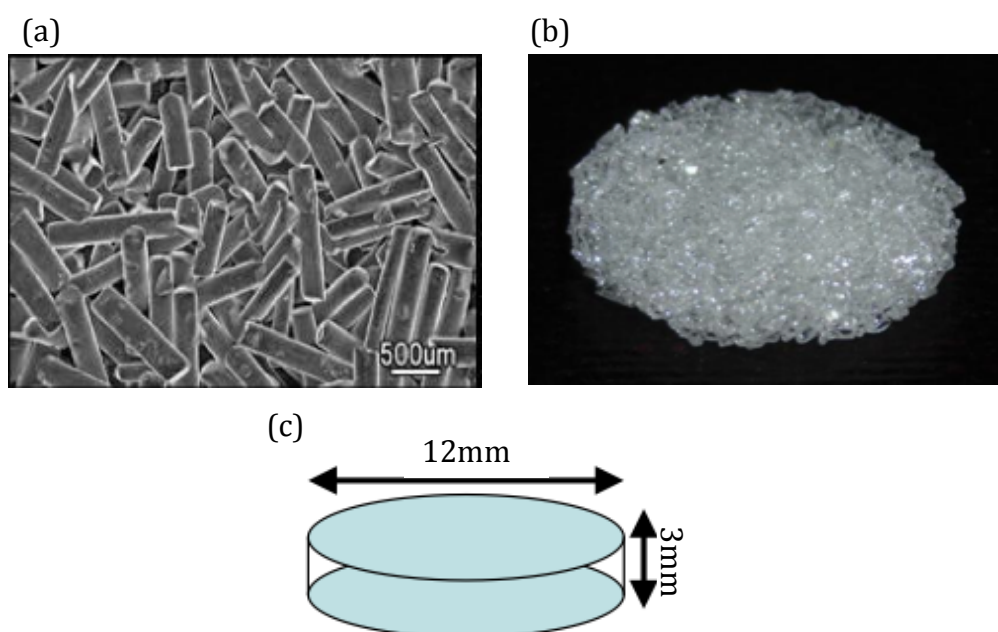


Fig 2.2; (a) Image of cylindrical glass rods, which are sintered to create randomly oriented glass scaffolds. The result is a highly porous material, with pores of variable size making up approximately 60% of the total volume. (b) image of a single glass scaffold (c) dimensions of a single glass scaffold (12 mm x 3 mm).

Table 2.2; Properties of glass scaffolds used in this study

<b>Properties of glass scaffold</b>	
Pore volume (%)	60
Glass volume (%)	40
Density (g/mL)	2.5
Pore size (µm)	100-500

### **2.2.3 Cell seeding in 3D scaffolds**

Initially cells were passaged under standard culture conditions in basal medium and at 80% confluency, cells were enzymatically released using Trypsin/EDTA. Cells were pelleted by centrifugation at 1000 rpm for 5 minutes and resuspended in 1 ml media and cell number was determined using hemocytometer. From a previous study the optimum cell density and volume of cell suspension for PU scaffolds was determined at  $5 \times 10^5$  cells in 100  $\mu$ l of media. Having a smaller volume, it was found that  $2.5 \times 10^5$  cells in 50  $\mu$ l of media was sufficient to seed glass scaffolds. The cell suspension volume was able to spread throughout the scaffold structure, cells were retained and had the opportunity to attach. After incubating for 1 hour, sufficient media was added to cover scaffolds and stainless steel rings. Cells were allowed to attach for 3-4 hours, removed from stainless steel or silicone rings and held in place using stainless steel wires (if PU). Cell seeded scaffolds were cultured in the incubators for the experimental period and supplied with fresh media every 3 days. Cell seeded scaffolds were assessed for cell viability, osteogenesis or further investigated at specific time points depending on experimental design.

### **2.2.4 Fluorescent staining of cell nucleus and cytoskeleton**

DAPI (4',6-Diamidino-2-phenylindole dihydrochloride) is a tool used for various cytochemical investigations. DAPI is known to form fluorescent complexes with natural double-stranded DNA. When DAPI binds to DNA, it is fluorescent under the blue wavelength. Cell cytoskeletal staining was performed using phalloidin-TRITC (phalloidin-Tetramethylrhodamine B isothiocyanate). Phalloidin is a fungal toxin that binds to polymeric and oligomeric forms of actin. TRITC conjugate allows for imaging under the orange-red wavelengths.

Samples were carefully washed with PBS and fixed with 10% formalin, for 10 minutes under room temperature. This was followed by washes with PBS 3 times, allowing the cells to keep their structures and preventing degradation. To increase cell membrane permeability, a 0.5% Triton-X solution was applied to

samples for 5 minutes and then washed away. A solution of 1 µg/ml of DAPI and 1 µg/ml phalloidin-TRITC in PBS was added to each well to cover the samples. The well plates were covered with aluminum foil and incubated for 30 minutes. The DAPI solution was removed and replaced by PBS, and cells were imaged on an epifluorescent or confocal microscope.

### **2.2.5 Assessing cell viability**

There have been a number of methods developed in order to measure cell proliferation including direct counting of viable cells, measurement of DNA content and measurement of metabolic activity. The traditional methods of using trypan blue dye exclusion assay (using a hemacytometer) are very simple and inexpensive however, they can be time consuming and inaccurate [4]. Mitochondrial metabolic rate can be measured using MTT (3-(4,5-Dimethylthiazol-2-yl)-2,5-diphenyltetrazolium bromide) and MTS (3-(4,5-dimethylthiazol-2-yl)-5-(3-carboxymethoxyphenyl)-2-(4-sulfophenyl)-2H-tetrazolium). These assays do indirectly reflect viable cell number and have been widely used [5-7]. However, cell metabolic activity can change due to different conditions or addition of chemical treatments, which can ultimately vary the results obtained from these assays.

#### **2.2.5.1 MTT assay**

MTT (3-(4,5-dimethylthiazol-2-yl)-2,5-diphenyltetrazolium bromide) is a method used for measuring cell growth and viability. The yellow MTT solution is reduced to a dark blue formazan insoluble salt due to the active mitochondria in live cells. The optical density of dissolved salt is measured by using a plate reader at a wavelength of 540 nm. The absorbance is directly related to the amount of formazan salt formed and is assumed to represent the number of live cells. For the experiments conducted in this study, the cell seeded scaffolds were washed with PBS several times and incubated with 1 mg/ml MTT in PBS for 40 minutes at 37°C. The solution was then removed and dissolved with 0.125%

acidified isopropanol and the absorbance of the resulting solution was determined using a 96-well plate reader at 570nm referenced at 630nm.

#### 2.2.5.2 MTS assay

Similar to MTT assay, MTS (3-(4,5-dimethylthiazol-2-yl)-5-(3-carboxymethoxyphenyl)-2,4-(sulphophenyl)-2H-tetrazolium) assay is another colorimetric method to determine the number of viable cells in culture. The yellow MTS tetrazolium compound is reduced to a pink formazan product that is soluble in culture medium. This conversion is achieved by NADPH which is produced by dehydrogenase enzymes in metabolically active cells. The cell-seeded scaffolds were washed several times until there was no colour present in the solution. Scaffolds were placed in 1cm diameter stainless steel rings and the assay was performed by adding 0.5 ml of 1:10 MTS in PBS mixture directly to the scaffolds. After 3 incubating for 3 hours at 37°C, two 200 µl samples were pipetted out from the scaffolds and absorbance was read at 490 nm.

#### 2.2.5.3 Alamar Blue staining

Alamar blue is also another colorimetric method designed to provide a rapid and sensitive measure of cell viability, which can be used to estimate proliferation, and cytotoxicity in various human and animal cell lines, bacteria and fungi. It is simple to use as the indicator dye is water soluble, thus eliminating the washing/fixing and extraction steps required in other commonly used cell proliferation assays. It also produces a clear, stable and distinct change, which is easy to interpret. Alamar Blue has several characteristics that make this dye an attractive candidate for use as a quantitative assay of cell proliferation. This dye is nonradioactive, nontoxic, water-soluble (eliminating the need for extraction), and readily detectable by either absorbance or fluorescence spectroscopy. Assay was performed by washing samples several times with PBS and adding 1 ml of 0.4:1 alamar blue in PBS mixture. Specimens were incubated for 4 hours and optical density was measured measured at 520 nm and 630 nm.

## 2.2.6 Total DNA assay

Total DNA was measured using a fluorescent Quant-iT™ PicoGreen® dsDNA reagent assay kit (Invitrogen, UK). This was used as a measure of total cell number through the binding of a fluorescent dye to double stranded DNA in the cells.

Cell-seeded scaffolds were washed with PBS several times (5 minutes each) and placed in a bijou that contained a known volume of buffer solution. Scaffolds were vortexed for 10 seconds followed by centrifugation at 10,000 rpm and left at 4°C overnight. To extract cellular DNA, cell-seeded scaffolds were freeze-thawed 3 times, 100 µl of cell lysate was added to 200 µl of Tris-buffered EDTA solution (provided in kit, diluted 1:20) containing the Quant-iT™ PicoGreen® (diluted 1:400). Fluorescence intensity was recorded using a fluorescence reader (BioTek, UK) using 485 nm excitation and 520 nm emission.

## 2.2.7 Assessment of osteogenesis

### 2.2.7.1 Alkaline Phosphatase assay

Alkaline phosphatase (ALP) has been shown to be a biochemical indicator of bone turnover and the assay involves the conversion of p-nitrophenol phosphate substrate to p-nitrophenyl and recording the rate of colour change from colourless to yellow. Cell lysate for ALP assessment was taken from the same cell solution used to extract total DNA using the same extraction techniques (See 2.2.6).

Cell lysate was incubated for 30 min before adding 10 µl ( $V_{\text{sample}}$ ) to 190 µl of p-nitrophenol phosphate substrate followed by incubation for 5 minutes. The mixture was then briefly vortexed and centrifuged. 200 µl ( $V_{\text{total}}$ ) of mixture was transferred into a well of a 96 well plate and the subsequent conversion to p-nitrophenyl was measured by recording the rate of colour change from

colourless to yellow at 405 nm. ALP activity was expressed as nmol of p-nitrophenol converted per minute where 22.5 nmol (K) equals 1 absorbance value ( $A_{405}$ ). ALP activity was calculated using the following formula:

$$\text{ALP activity (nmol pNPP converted per min)} = \Delta A_{405} * K * V_{\text{total}}/V_{\text{sample}}$$

ALP activity was then normalised to total DNA.

#### 2.2.7.2 Prostaglandin E2 (PGE2) assay

This assay is based on the forward sequential competitive binding technique in which PGE2 present in a sample competes with horseradish peroxidase (HRP)-labeled PGE2 for a limited number of binding sites on a mouse monoclonal antibody. The PGE2 kit was obtained from R&D Systems, UK and all reagents are provided in the kit.

PGE2 has diverse actions on various organs, including inflammation, bone healing, bone formation and embryo implantation. It also plays an important role in the functional adaptation of bone cells to mechanical loading. PGE2 release into the media by MLO-A5 cells after application of flow was determined using a Parameter PGE2 assay kit following the manufactures protocol. Media was extracted from well plates and a goat anti-mouse was then used to coat the base of a 96-well plate. A mouse monoclonal antibody was then added to the wells to bind to the anti-mouse antibody. Media samples were then added to the well plate and after 2 hours the well plate was washed 3 times using a wash buffer. Well plates were left in room temperature for 30 minutes, an acid solution was added to stop any enzymatic activity, which was seen by a change in colour. The plate were then placed on a plate reader and read at a wavelength of 450 nm. PGE2 concentration was calculated from the formula of a plotted standard curve:

$$\text{PGE2 concentration} = \text{EXP} ((A_{405} - 0.2146)/-0.025)$$

This assay was used in chapter 6 and cells subjected to fluid flow were incubated in fresh medium for 2 hours before collection of the medium.

#### 2.2.7.3 Alizarin red S staining

Alizarin red S is a dye that binds to  $\text{Ca}^{2+}$  ions to form a strong red complex and is commonly used as an indicator of calcium deposition in mineralising cells and tissues. Scaffolds were washed three times with PBS and fixed with 10% formalin for 10 minutes at room temperature. The Solution was removed and again washed with PBS several times. Alizarin red S dye was added to  $\text{dH}_2\text{O}$  (10 mg/ml) and the pH adjusted to 4.1 using ammonium hydroxide before applying to fully cover each sample and placing under mild shaking for 15 minutes at room temperature. Scaffolds were removed and washed under distilled water. For qualitative analysis, samples were air dried in a fume cupboard and observed under a light microscope or normal magnification with a digital camera. For quantitative analysis, samples were destained with 5% perchloric acid and subjected to 15 minutes of mild shaking. The optical density was then measured at 490 nm.

#### 2.2.8 Sirius red staining (Collagen production)

Picro-sirius red staining is a routine method for the qualitative identification of collagen in tissue sections or that deposited by cells. If collagen is present it will form a strong red staining complex that can then be destained for semi-quantitative analysis. Sirius red is a strong anionic dye and aligns itself parallel to the long axis of the collagen molecules. The dye is not specific and so stains all types of collagen but it can be used as a fluorescent marker of collagen and suffers very little from photo-bleaching. Cell seeded scaffolds were washed several times with PBS and fixed with 10% formalin for 15 minutes, which was then removed and three PBS washes were performed again. Sirius red dye was mixed with saturated picric acid solution (1 mg/ml) and added to fully cover each sample. Samples were then left to shake mildly for 18 hours at room temperature. Dye solution was removed and each well was washed with distilled

water several times until no more red colouring was eluted. For qualitative analysis, samples were air dried in a fume cupboard and observed under a light microscope or normal magnification with a digital camera. For quantitative analysis, the scaffolds were destained with 0.2M NaOH/Methanol in a 1:1 ratio and subjected to mild shaking for 15 minutes and optical density was measured at a wavelength of 490 nm.

### **2.2.9 Primary cilia staining**

As mentioned in chapter 1, primary cilia have axonemes containing alpha tubulin and can therefore be detected by immunostaining with anti-acetylated alpha tubulin antibodies. Alpha tubulin immunostaining shows the microtubular cytoskeleton which is dense around the centrosome region in which primary cilia occur [8].

1. Samples were washed with PBS 3 times and fixed in 3.7% formaldehyde solution for 10 minutes,
2. Cells were permeabilised by 0.1% triton-X-100 solution and incubated in primary blocking solution (containing 0.1% Albumin bovine serum and 0.2% Igepal in PBS for 2 hours at room temperature),
3. Samples were incubated with primary antibody solution (1:2000 of 2 mg/ml mouse antibody to acetylated alpha tubulin in primary blocking solution) for 24 hours,
4. Samples were then washed with primary blocking solution 3 times,
5. Secondary antibody containing 1:30 of FITC-conjugated rabbit anti-mouse immunoglobulins in primary blocking solution was applied to samples for 1 hour at room temperature,
6. Samples were then washed with primary blocking solution 3 times,
7. DAPI solution (1:1000 DAPI in PBS) was added to the samples and left for 30 minutes,
8. Samples were then washed with PBS 3 times and imaged using confocal microscopy.

### **2.2.10 Removal of the primary cilia using Chloral Hydrate**

It has been shown that long exposure to chloral hydrate will completely remove the cilia in MDCK cells, from the early embryo phase of the sea urchin and also bone cells. The mechanisms by which chloral hydrate destabilises the primary cilium is still unclear, however it has been proposed that it disrupts the junction between the cilium and basal body through disassembly of microtubules. It has been suggested that the primary cilia does weaken when exposed to chloral hydrate. Deciliation in this study (chapter 6) was achieved by incubating constructs in culture media containing 4mM chloral hydrate for 48 and 72 hrs. After which samples were washed with PBS 3 times and placed in normal culture medium for 24 hrs before subjecting them to fluid flow.

### **2.2.11 IBIDI Oscillatory flow pump**

The oscillatory perfusion bioreactor (fig 2.3) consists of a pump system (Ibidi, Germany) that was controlled by a computer software provided by the same company. The reservoir pots were connected to filters and air pressure tubings, which in turn connected to a bottle containing silicate beads. A conduit was connected to this unit to hold the cell-seeded scaffolds in place during the action of the fluid flow. After confirming the absence of air bubbles, the whole system was placed in a 37°C incubator and samples were subjected to 1 hour of fluid flow at a frequency of 1 Hz. A frequency of 1 Hz was chosen since it is commonly advocated as a 'biomimetic loading frequency that represents walking pace. It is a standard loading frequency used to study bone cell mechanotransduction in the author's laboratory and many others. A previous preliminary study showed that short bouts of oscillatory flow (5 ml/min, 1 Hz, 1 hour loading session) were able to induce osteogenic differentiation of hMSCs in PU scaffolds. It was shown that ALP activity and collagen per cell was significantly enhanced in comparison to static cultures. Following from this work, this project examined a range of flow rates in order to analyse the flow-induced shear stress on cell response including; cell growth and matrix production [9].

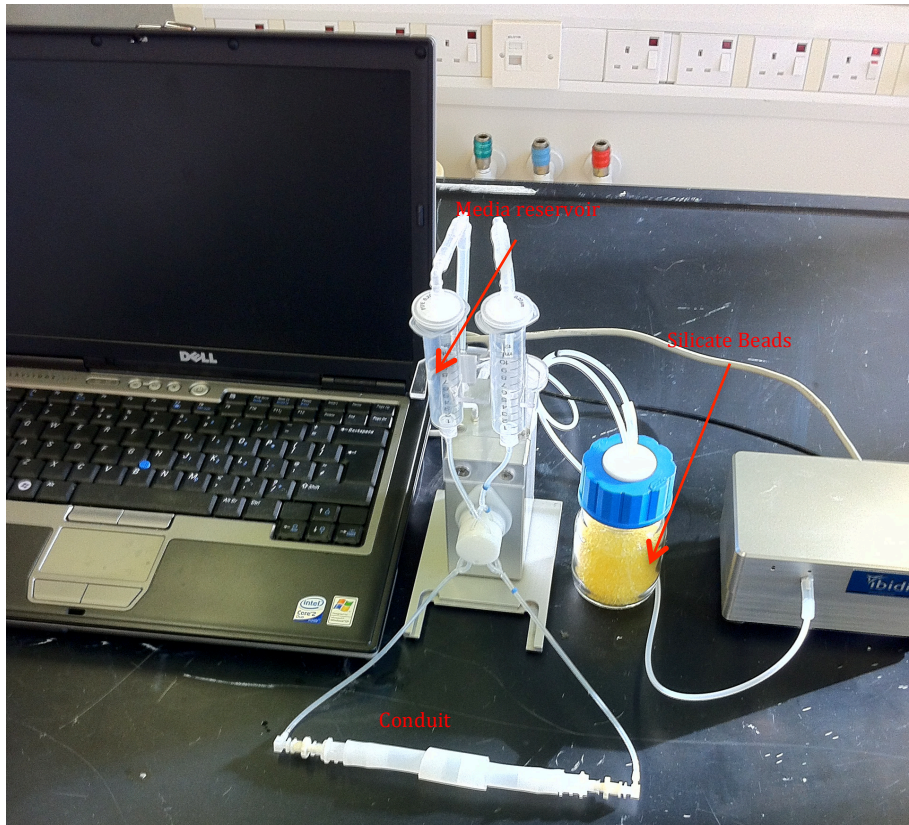


Figure 2.3; Photograph of the IBIDI oscillatory pump system. All tubing were sterilized in advance to prevent contamination. A single scaffold would be placed in the conduit and subjected to fluid flow for 1 hour at a frequency of 1 Hz.

### 2.2.12 Peristaltic pump

The peristaltic pump (Watson Marlow, UK) is setup in the same manner as the previous system however it only applies flow in one direction. Figure 2.4 shows the setup of this system, whereby rotating cylinders squeeze fluid through a cassette and finally deliver media to the conduit holding the cell seeded scaffold. The pump is connected to a reservoir pot which contains an inlet and outlet (for media circulation) and also a 0.2  $\mu\text{m}$  filter for gas exchange.

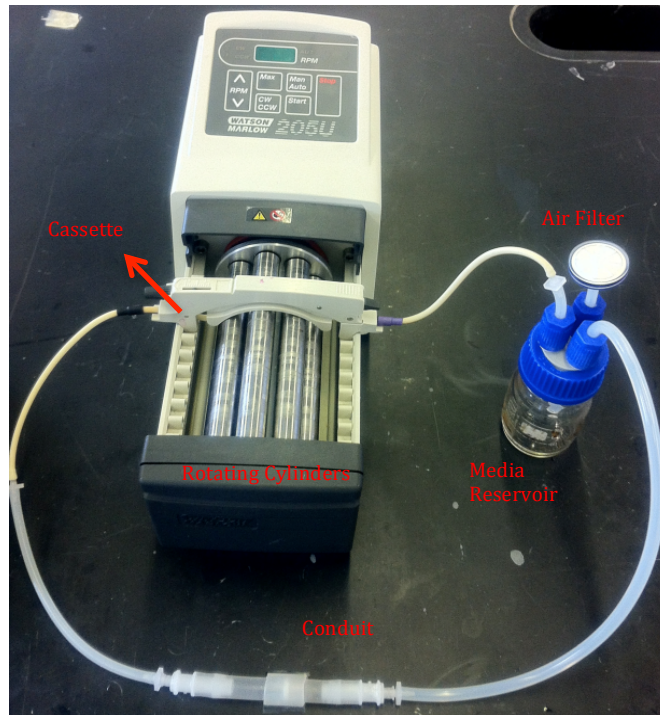


Figure 2.4; Photograph of the peristaltic pump system. Rotating cylinders pump media from the media reservoir towards the conduit in which scaffolds were held in place.

### 2.2.13 Conduit length

The conduit was the piece of silicone tubing that holds the cell-seeded scaffold in place whilst being subjected to fluid flow. Equations 2.1 and 2.2 were used to verify its length to make sure that the flow is fully developed before it enters the scaffold. Since the highest flow rate for these experiments was 10 ml/min, a conduit length according to this flow rate was calculated.

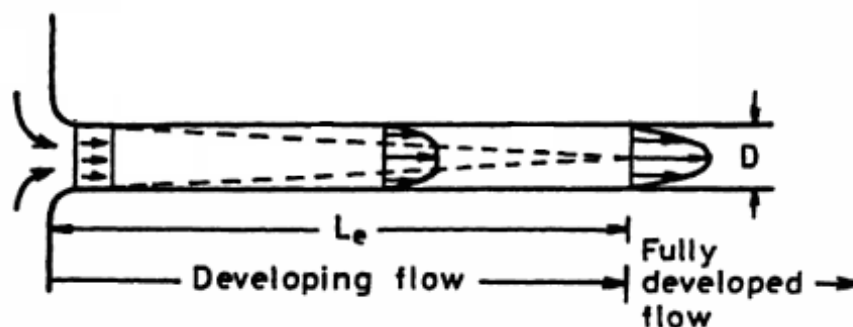


Fig 2.5; Flow in the entry region for laminar flow.  
<http://www.mdp.eng.cam.ac.uk>

The following equation was used to calculate the entry length (fig 2.5) within a pipe based on steady flow;

$$L_e = 0.06 Re D \quad (\text{Equation 2.1})$$

Where,  $Re$  = Reynolds number

$D$  = Tube diameter (m)

In order to calculate the Reynolds number the following equation was used;

$$Re = \frac{\rho V D}{\mu} \quad (\text{Equation 2.2})$$

Where,  $Re$  = Reynolds Number

$\rho$  = Fluid density ( $\text{kg/m}^3$ )

$V$  = Average fluid velocity (m/s)

$D$  = Tube diameter (m)

$\mu$  = Fluid viscosity (kg/ms)

The volume flow rate (ml/min) was first converted to  $\text{m}^3/\text{s}$  and divided by pipe cross-sectional area ( $\text{m}^2$ ) to achieve an average velocity (m/s). The values were then substituted in equation 2.2 to calculate the Reynolds number.

$$Re = \frac{(1000.2 \text{ kg/m}^3) (0.00212 \text{ m/s}) (0.01\text{m})}{(0.00899 \text{ Pa s})}$$

$$Re = 2.36$$

Given the flow characteristics, flow type can be expected to be *laminar* based on the Reynolds number. Using this  $Re$  value and equation 2.1, the entry length ( $L_e$ )

of the system was calculated to be **1.416 mm** for a flow rate of 10 ml/min and **0.425 mm** for a flow rate of 3 ml/min ( $0.71 \leq Re \leq 2.36$ ). However for ease of handling and to reduce the risk of bacterial infection to cell-seeded scaffolds, a length of 120 mm was chosen which guarantees a fully developed flow before coming into contact with the scaffold.

#### **2.2.14 Glass scaffolds characterisation**

Since every glass scaffold is different in terms of internal geometry (to a certain extent) an experiment was devised to determine how much the scaffolds varied from one another. In order to achieve this, each scaffold was housed inside the silicone conduit and connected to the peristaltic pump. Scaffolds were subjected to 3, 5 and 10 ml/min unidirectional flow for 1 minute. At the end of each experiment the fluid was collected in an empty container and weighed.

Figure 2.6 illustrates the mass of fluid collected for 198 scaffolds subjected to 3 (blue dots), 5 (red dots) and 10 ml/min (green dots) flow. An average mass of  $3.26 \pm 0.28$  g,  $5.2 \pm 0.3$  g and  $10.15 \pm 0.45$  g of fluid was collected respectively.

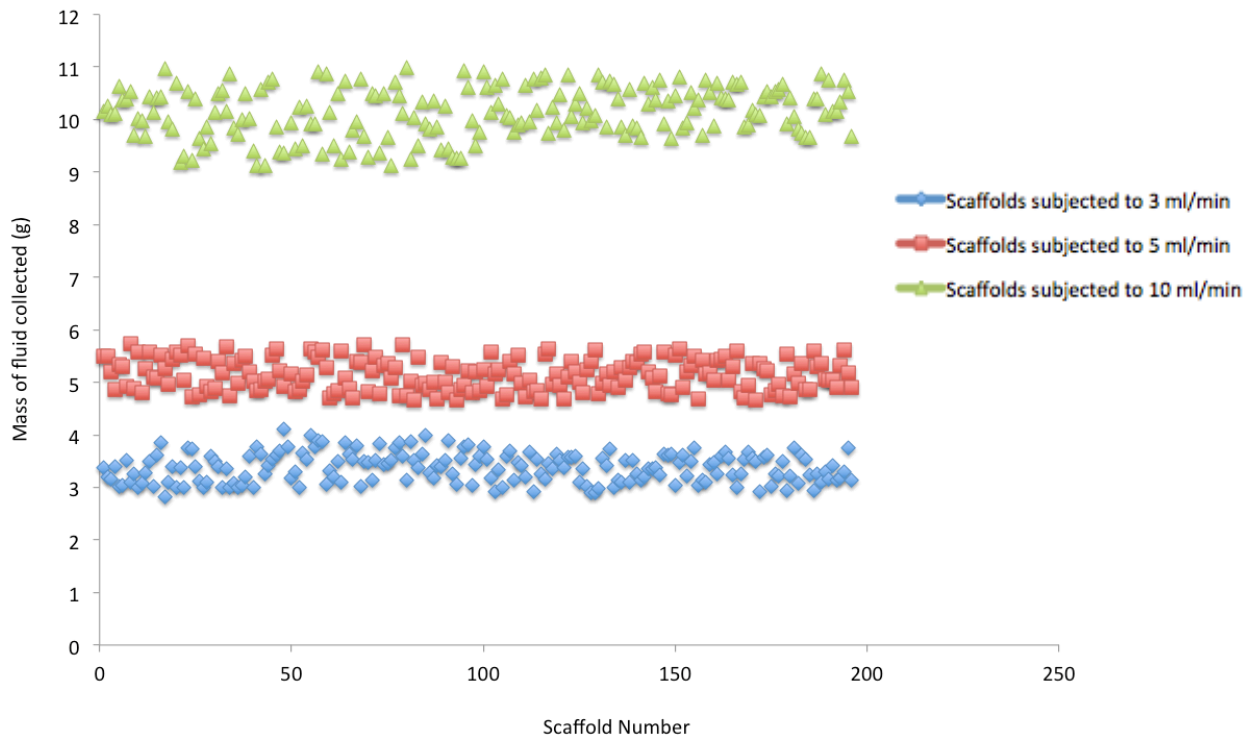


Fig 2.6; Scaffold geometry was roughly estimated using a time-collection method with the peristaltic pump. Individual scaffolds were subjected to flow rates of 3, 5 and 10 ml/min for one minute. The fluid would then be collected in a small tub and weighed. The blue, red and green dots represent the amount of fluid collected for scaffolds subjected to 3, 5 and 10 ml/min respectively.

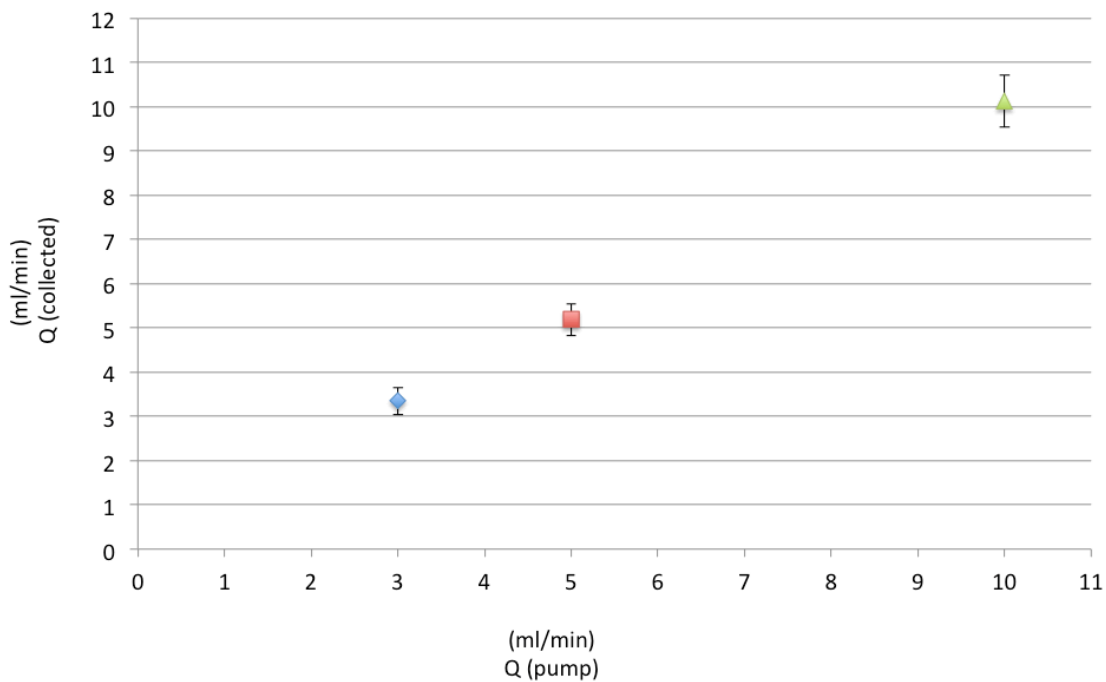


Fig 2.7; Results from the time-collection method were used to compare the actual flow rate ( $Q$  collected) to the flow rate applied by the pump system ( $Q$  pump). Scaffolds subjected to 3 (blue), 5 (red) and 10 ml/min (green) produced a flow rate of  $3.352 \pm 0.309$ ,  $5.19 \pm 0.361$  and  $10.12 \pm 0.584$  ml/min respectively.

Results from figure 2.6 were used to calculate the average flow rate in the outlet tube. Figure 2.7 illustrates that scaffolds subjected to 3, 5 and 10 ml/min produced a flow rate of  $3.352 \pm 0.309$ ,  $5.19 \pm 0.361$  and  $10.12 \pm 0.584$  ml/min respectively in the outlet tube. This indicates that the actual flow rates (Q collected) are very close to the applied value (Q pump).

### 2.2.15 Estimating the average shear stress for glass scaffolds

The average shear stress can be calculated using Wang and Tarbell's equation (equation 2.3) [10].

$$\bar{\tau} = \frac{\mu v}{\sqrt{k}} \quad \text{Equation 2.3}$$

Where,  $\bar{\tau}$  is the mean shear stress value,  $\mu$  is the fluid viscosity,  $v$  is the flow average velocity at the scaffold inlet and  $K$  is the permeability. This only applies for flows obeying Darcy's law (equation 2.4) and requires pressure drop measurements.

$$Q = - \frac{kA(P_b - P_a)}{\mu L} \quad \text{Equation 2.4}$$

Where,  $Q$  is the flow rate,  $A$  is the scaffold surface area (area in which fluid flow first comes into contact with),  $P_b - P_a$  is the pressure drop and  $L$  is the thickness of the scaffold. Figure 2.8 illustrates how the pressure drop was measured in order to calculate the permeability ( $k$ ). A physiological pressure transducer was used to measure the pressure drop before the flow enters the scaffold (point a) and immediately after it leaves (point b). The measurements were taken for all three flow rates on 6 different glass scaffolds.

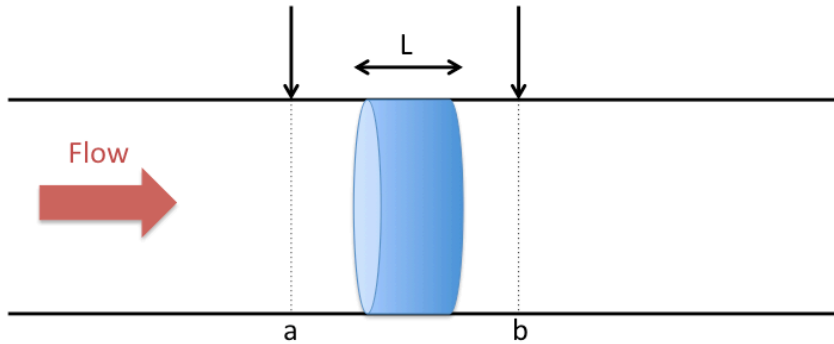


Fig 2.8; A physiological pressure transducer was used to measure the pressure drop before the flow enters the scaffold (point a) and immediately after it leaves (point b) for flow rates of 3, 5 and 10 ml/min.

Equation 2.4 was rearranged to find the value of  $k$  for each scaffold at different flow rates i.e. 6 ' $k$ ' values for each flow rate. These values were then placed in equation 2.3 to calculate the average shear stress. Cell-seeded scaffolds subjected to 3, 5 and 10 ml/min fluid flow experienced an average shear stress levels of peak flow of  **$0.111 \pm 0.002$** ,  **$0.647 \pm 0.05$**  and  **$1.398 \pm 0.02$  Pa** respectively.

### 2.2.16 Statistical analysis

Most experiments were performed a minimum of three times ( $N=3$ ) with two samples for each condition ( $n=2$ ). To test for significant differences between two group means, an unpaired Student's  $t$ -test was performed and differences were considered statistically significant if the  $p$ -value was less than 0.05 ( $p < 0.05$ ). For comparisons between multiple groups, one-way ANOVA was performed followed by Tukey's post-hoc test. All graphs were plotted as mean  $\pm$  SD. For imaging of samples, some experiments were limited to one sample per condition per experimental run due to time constraints. Single images are always chosen to be representative of the experimental outcome.

### 2.2.17 References

- [1] Kato Y, Boskey A, Spevak L, Dallas M, Hori M, Bonewald LF: Establishment of an osteoid preosteocyte-like cell MLO-A5 that spontaneously mineralizes in culture. *J Bone Miner Res.* 2001;16:1622–1633.
- [2] Karlsson C, Emanuelsson K, Wessberg F, Kajic K, Axell MZ, Eriksson PS, Lindahl A, Hyllner J, Strehl R: Human embryonic stem cell-derived mesenchymal progenitors-Potential in regenerative medicine. *Stem Cell Research*, 2009, vol. 3, no. 1, 39–50.
- [3] Sittichokechaiwut A, Scutt AM, Ryan AJ, Bonewald LF, Reilly GC: Use of rapidly mineralising osteoblasts and short periods of mechanical loading to accelerate matrix maturation in 3D scaffolds. *Bone.* 2009 May;44(5):822-9.
- [4] Kanemura Y, Mori H, Kobayashi S, Islam O, Kodama E. Evaluation of in vitro proliferative activity of human fetal neural stem/ progenitor cells using indirect measurements of viable cells based on cellular metabolic activity. *J Neurosci Res*, 2002, 69: 869–879.
- [5] Thangapazham RL, Singh AK, Sharma A, Warren J, Gaddipati JP, et al. Green tea polyphenols and its constituent epigallocatechin gallate inhibits proliferation of human breast cancer cells in vitro and in vivo. *Cancer Lett*, 2007, 245: 232–241.
- [6] Yu HN, Shen SR, Yin JJ. Effects of interactions of EGCG and Cd(2+) on the growth of PC-3 cells and their mechanisms. *Food Chem Toxicol*, 2007, 45: 244–249.
- [7] Farabegoli F, Barbi C, Lambertini E, Piva R. Epigallocatechin-3-gallate downregulates estrogen receptor alpha function in MCF-7 breast carcinoma cells. *Cancer Detect Prev*, 2007, 31: 499–504
- [8] Wheatley DN, Wang AM, and Strugnell GE: Expression of primary cilia in mammalian cells. *Cell Biol Int*, 1996. 20(1): 73-81.
- [9] Matsiko A, Edwards J, Reilly GC. Human mesenchymal stem cell responses to steady and oscillatory fluid flow in a porous scaffold. *Regenerative Medicine.* 2009;4:S159.

[10] Wang S, Tarbell JM: Effect of fluid flow on smooth muscle cells in a 3-dimensional collagen gel model. *Arteriosclerosis, Thrombosis, and Vascular Biology*, 20 (10) (2000), 2220–2225.

# Chapter 3: Investigating a 3-D *in vitro* model to study the effects of fluid shear stress on cell behavior

## 3.1 Introduction

A bone tissue engineering strategy that involves seeding marrow stromal cells (MSCs) onto a porous biodegradable scaffold before implantation into the body represents a promising alternative to current clinical treatments for bone defects such as using autologous or allogeneic bone grafts [1, 2]. A common tissue engineering strategy involves cell-seeded scaffolds to be cultured *in vitro* to increase cell number and to allow for cell differentiation of stem cells into osteoblasts.

Human mesenchymal stem cells (hMSCs) from bone marrow and other adult tissues have been shown to differentiate *in vitro* and *in vivo* into several cell types, including the adipogenic, myogenic, chondrogenic, and osteogenic lineages [3] and have been suggested to be a suitable cell type for bone tissue engineering applications [3-7]. Despite their great potential, isolating hMSCs after aspiration from patients or donors has been shown to have its limitations. Adult MSCs exhibit wide variability both within a bone marrow population and between different people making their clinical usefulness unpredictable [8-11]. Furthermore, after protracted *ex vivo* expansion, hMSCs have been shown to lose their replicative capability [11, 12] which limits their bulk production for tissue engineering applications and have been associated with significant alterations in the pattern of gene expression, karyotypic instability [13], spontaneous malignant transformation [14, 15], and an impaired differentiation capacity [16].

Human embryonic stem cells (hESC) have been shown to provide a homogeneous and unlimited source of cells for bone tissue engineering

applications [17,18]. Unfortunately hESC's tend to form teratoma *in vivo* which limits their potential use in clinical applications [19]. On the other hand, an alternative could be the use of progenitor cells derived from hESCs. Human embryonic stem cell derived mesodermal progenitor cells (hES-MPs) do not form teratoma *in vivo* and resemble adult hMSCs with respect to gene expression, surface markers and ability to differentiate towards mesodermal tissues [20,21]. hES-MPs display significantly higher proliferation ability than hMSCs and have been demonstrated to display lower amount of human leukocyte antigen (HLA) class II proteins than hMSCs, suggesting that hES-MPs may be well qualified for the successful treatment of musculoskeletal conditions [20]. In a recent study, *de Peppo et al.*, showed that under proper stimulation, hES-MPs can be directed towards an osteogenic lineage with an increase in mineralisation when compared to hMSCs [21]. In a follow up study, *de Peppo et al.*, demonstrated that dynamic culture of hES-MPs in a packed bed/column bioreactor had the potential to induce proliferation, expression of genes involved in osteogenic differentiation, and matrix mineralisation, which resulted in increased bone-like tissue formation [22]. Therefore, hES-MPs have the potential to be a model cell line with greater reproducibility than adult MSCs which to test a range of osteogenic stimulation. In addition hES-MPs may in themselves have clinical applications should the barriers to the use of embryonic stem cells in medicine be removed.

Animal Marrow stromal cells are multipotential progenitor cells that can commit to the osteoblast lineage and have been used quite extensively for *in vitro* studies in bone tissue engineering. Rat and mouse MSC osteogenesis has been demonstrated on a number of scaffolds including PLGA [23-25] and Calcium phosphate-coated bioactive glass [26, 27]. In spite of the attention given to the study of mesenchymal stem cells derived from bone marrow of humans and other species, there is still a lack of information regarding murine MSCs. As mouse cells are often used in basic science experiments as a model cell type it is important to understand and compare mouse MSC responses to osteogenic conditions with those of human MSCs. It has been shown that *in vitro* expanded cells from murine bone marrow have the ability to differentiate along the

osteogenic and adipogenic lineages [28]. In a recent study the differentiation potential of primary MSCs derived from adult mouse bone was investigated. It was shown that cell population was maintained over 30 passages and under proper stimulation these cells were able to induce osteoblastic differentiation as confirmed by the expression of osteopontin and accumulation of a bone-like mineralised matrix [29].

There are many factors that influence the expression of osteoblast phenotype in culture, including: cell source, culture medium, culture time and the presence of compounds that influence cell proliferation and differentiation [30]. Furthermore, several systemic and local hormones, growth factors and cytokines have also been shown to be involved in the osteoblast differentiation process [31]. The most commonly used osteogenic medium for MSCs usually consists of ascorbic acid/ vitamin C (AA) or its phosphate salt, beta-glycerophosphate ( $\beta$ GP), and dexamethasone (DEX). AA is essential for the production of stable collagen, the major matrix protein of bone, and plays a key role as a cofactor in the hydroxylation of proline residues in the collagen molecule [32].  $\beta$ GP is known to provide inorganic phosphates for synthesis of bone-like mineral by the cells [33]. Dexamethasone (DEX) is a synthetic glucocorticoid and is a component of multiple differentiation media formulae including osteogenic, chondrogenic, and adipogenic media. Data regarding the effects of glucocorticoids on cell activity *in vitro* are conflicting, as they appear to depend upon concentration, time and duration of exposure to the drug [34]. Results of *in vitro* investigations using bone-derived cells of adult human origin have suggested that glucocorticoids reduce cell proliferation and increase ALP activity [35] and its effect on collagen expression seems to be controversial, as both stimulation and inhibition have been reported depending on the cell source and culture conditions [36, 37]. Despite this, it has been well documented that human bone marrow cells, including actively proliferating osteoprogenitors, can be induced to differentiate into cells exhibiting the osteoblast phenotype by DEX at both 10 nM and 100 nM concentrations [38, 39].

Traditional static cultures of 3D scaffolds have been shown to have a major limitation in that there is insufficient transport of nutrients into the inner regions of the construct. Because of this a thin layer (crust) of live cells tend to cover the exterior surface of the scaffold [40]. Lyons *et al.*, evaluated collagen-glycosaminoglycan (CG) and biomimetic collagen-calcium phosphate (CCP) scaffolds (cell-free and cultured with MSCs prior to implantation) for bone repair in rat cranial defects. They noted that for MSC-seeded groups, the location of the resorption response was confined to the construct periphery. The authors suggested that the matrix produced by the MSCs *in vitro* may act as a barrier to bone healing [40].

The use of bioreactors such as the spinner flask [41] and rotatory vessel [42] have not demonstrated an improvement in the distribution of bone cells on 3D scaffolds since there is limited mass transport of nutrients to the inner core of the construct [43, 44]. Flow perfusion bioreactors have been shown to induce fluid flow throughout the entire structure of a 3D scaffold allowing for a more efficient nutrient and waste exchange to take place, which will subsequently increase cell viability. Furthermore, perfusion bioreactors can mechanically stimulate cultured bone cells to accelerate the formation of increased bone matrix in constructs. Previous work performed on monolayers of cells seeded on slides has shown that the application of fluid flow has biological effects on cultured bone cells [45-47] such as upregulating osteopontin expression, ALP activity and expression of COX-2 and release of PGE2.

Highly porous scaffolds used for bone tissue engineering would ideally have load bearing properties once implanted *in vivo*. As mentioned previously (chapter 1), selecting the most appropriate material to produce a scaffold for bone tissue engineering is a very important step towards the construction of a tissue-engineered product. PU scaffolds have sufficient elasticity, resiliency and stiffness to deal with *in vitro* mechanical loading. The advantage of using this material is that it can be used to create a highly porous structure, and it is biocompatible with bone cells [48-50]. Furthermore, this non-degradable industrially produced foam has been shown to support MLO-A5 osteoblast

culture in 3D [51]. In other studies, an osteosarcoma cell line was shown to grow and mineralise on laboratory synthesised PU foams [52]. Using non-degradable PU for cell culture purposes means that it maintains its mechanical properties over time and does not leach degradation products into the culture media, which may complicate the experimental set-up.

Orla Protein Technologies initially developed their protein coatings for flat surfaces. To enable their coating to be relevant for biomaterials and tissue engineering purposes, it was important to develop a process for coating 3D materials. The first porous scaffold on which they applied their coatings is manufactured from Nippon Sheet Glass (NSG) and is made from the same high optical grade borosilicate glass used for the production of 2D microscope slides and cover slips. The glass scaffolds have good light transmissibility useful for microscopy. They can be supplied uncoated or peptide coated which provides a foundation for studying various aspects of cell matrix interaction, mechanotransduction and cell behavior relevant to *in vitro* 3D culture systems. Ceramic and glass based scaffolds have been widely used in the biomedical engineering and bone regeneration field due to their osteoconductive and osteoinductive properties [53]. While the glass for the Orla coated scaffolds was chosen for its bioinertness and is not intended to be an implantable scaffold it would have similar material properties to other glass based scaffolds made of clinical grade glasses.

In this chapter, the intention is to set up a system in which the effect of short bouts of dynamic loading on MSCs in a 3D environment can be investigated.

The main hypothesis was:

The porous glass scaffold supplied by Orla Protein Technologies would be a suitable substrate for MSC cell growth and cells would respond to fluid flow through the scaffold in a similar way to previous experiments on PU foams.

In order to test this hypothesis a suitable cell model was first established. To date, little is known about the behaviour of hES-MP and mouse MSC cells cultured on 3D scaffolds. Furthermore, the effects of dynamic culture conditions

with respect to cell proliferation and expression of genes involved in osteogenic differentiation have not been fully investigated. Therefore the aim of this chapter was to analyse and compare the effects of dynamic culture in terms of cell growth and osteogenic differentiation of hES-MP and mouse MSC cells seeded on PU and glass scaffolds.

The experiments were divided into 2 stages:

Stage 1: Investigating the osteogenic differentiation of mouse MSC and hES-MP cells in the presence of DEX. Furthermore, studying the effects of different static culture conditions and initial attachment of mouse MSC and hES-MP cells seeded on glass scaffolds.

Stage 2: Studying the effects of fluid flow on matrix production and expression of genes associated with osteogenic differentiation for mouse MSC and hES-MP cells in 3D constructs comparing responses within the previously established PU scaffold to the novel glass scaffold.

### 3.2 Investigating the effects of DEX on Mouse MSC cells

The aim of this experiment was to investigate the effects of dexamethasone (DEX, commonly used to induce osteogenic differentiation of MSCs *in vitro*) on mouse MSC and hES-MP cells as analysed by alkaline phosphatase (ALP) activity. A simple 2D static experiment was devised whereby 50,000 cells of each cell type were seeded in 0.1% gelatin coated well-plates and cultured in DEX containing (100 nM) and DEX free media (both culture conditions contained AA and  $\beta$ GP). Fresh media was supplied every 3 days and on day 7 and 14 of culture, cells were analysed for ALP activity as described in chapter 2. Figure 3.1 indicates that on day 7 and day 14 of static culture, mouse MSC cells have a higher ALP activity in the absence of DEX. However, ALP is upregulated for hES-MP cells cultured in the presence of DEX.

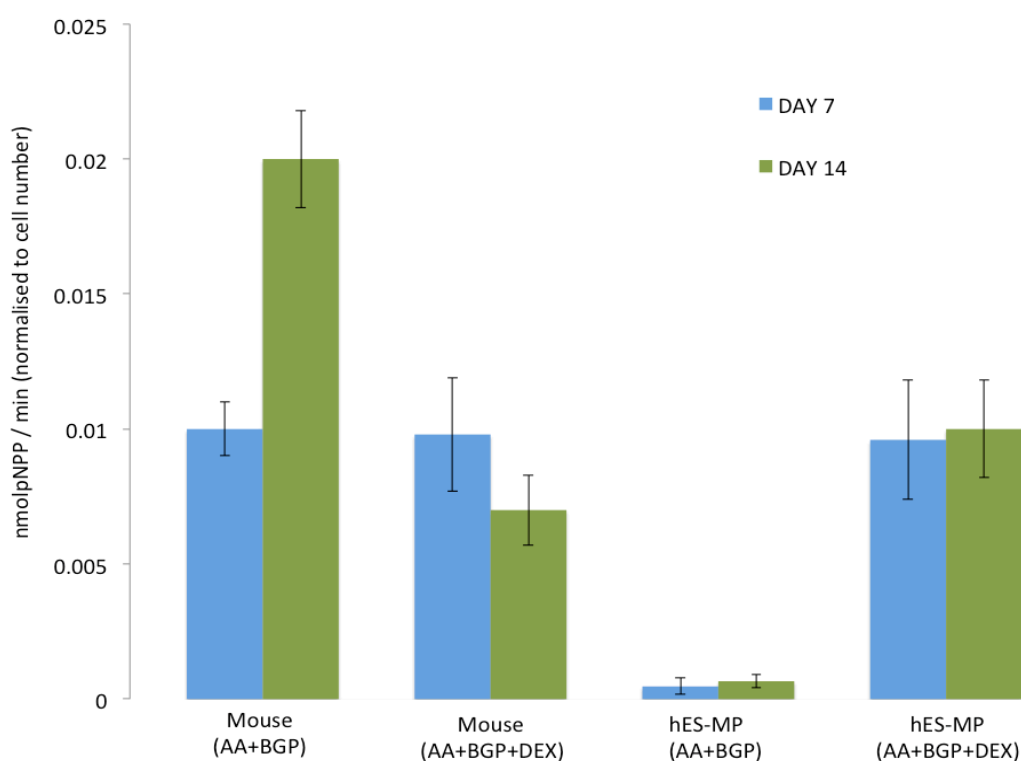


Fig 3.1; hES-MP and mouse MSC cells cultured for 7 and 14 days on 12 well-plates in DEX free and DEX containing media were assayed for ALP activity (normalized to DNA). All data is mean  $\pm$  SD (n=4).

### 3.3 Investigating the initial attachment of mouse MSC cells on glass scaffolds

The aim of this experiment was to investigate the initial cell attachment of mouse MSC cells seeded on glass scaffolds. Briefly, mouse MSC cells were statically seeded at a density of 250,000 cells per glass scaffold (12 mm in length and 3 mm in thickness) using the seeding and culture methods described in chapter 2. Cell-seeded scaffolds were analysed for cell activity using Alamar Blue staining for a period of 5 consecutive days. Figure 3.2 demonstrates that cell activity increased up until day 5, indicating that cells had attached and proliferated within the glass scaffold.

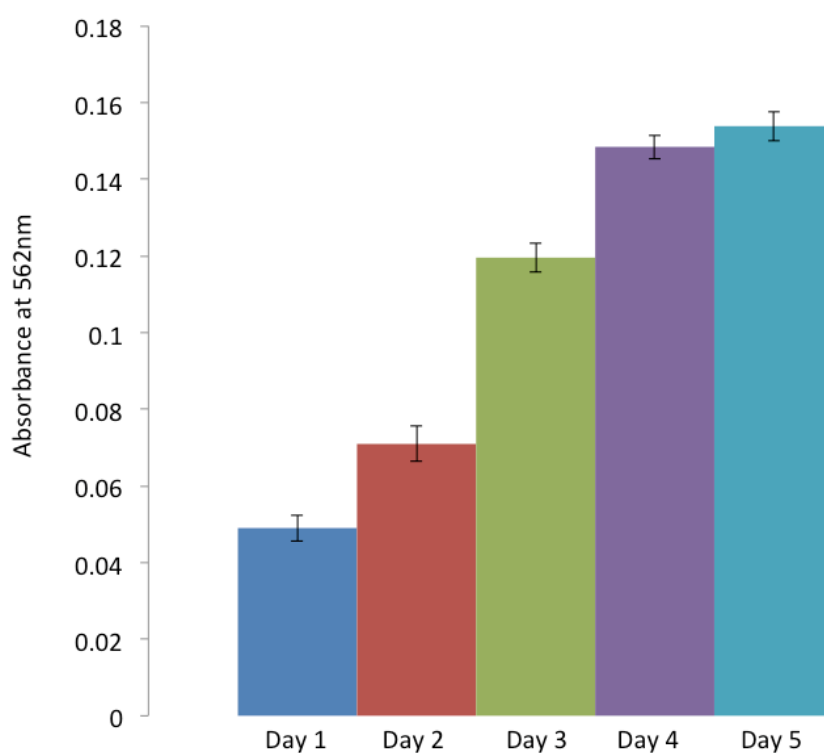


Fig 3.2; Mouse MSC cells were statically cultured on glass scaffolds for 5 days and assayed for cell viability on each day using Alamar blue. All data is mean  $\pm$  SD (n=4).

### 3.4 Investigating the initial attachment of hES-MP cells on glass scaffolds

The aim of this experiment was to investigate the initial cell attachment of hES-MP cells seeded onto glass scaffolds. hES-MP cells were statically seeded at a density of 250,000 cells per glass scaffold using the seeding and culture methods described in chapter 2. The cell-seeded scaffolds were cultured in standard media supplemented with AA,  $\beta$ GP and DEX (100 nM). Fresh media was supplied every 3 days and on day 7 of culture, cell-seeded scaffolds were stained with dapi and phalloidin to analyse the distribution of cells. From figure 3.3 it can be noted that more cells were seen on the outer surfaces than the inner core as normally seen in porous scaffolds. Furthermore, cell morphology did not seem to vary within different locations in the scaffold.

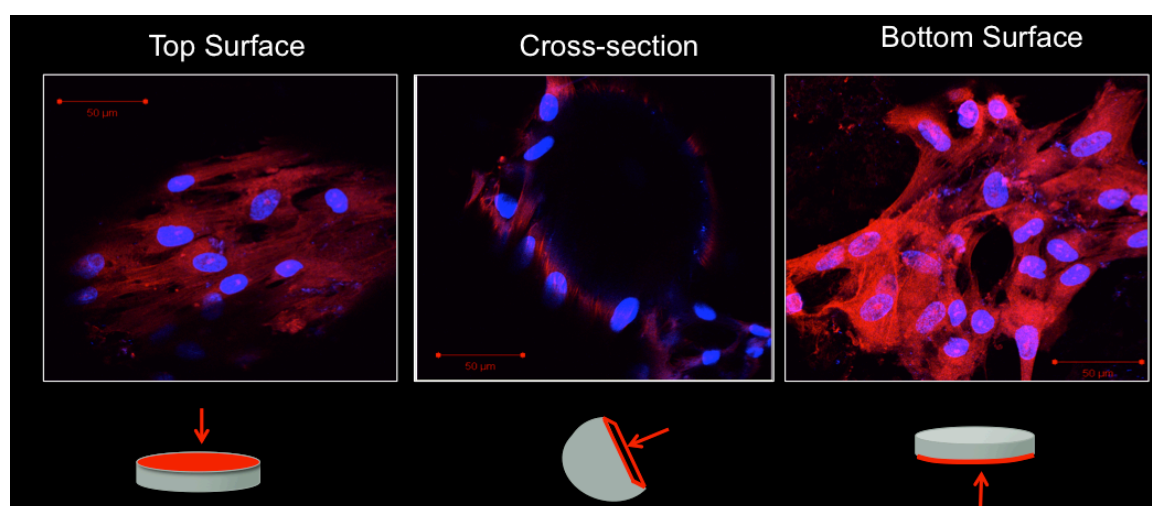


Fig 3.3; Morphology of hES-MP cells on glass scaffolds at day 7 of culture. Cell nucleus (DAPI-blue) and actin cytoskeleton (Phalloidin TRITC-red) shows cell morphology at different locations within the glass scaffold including the top, middle and bottom section. Representative images are shown (n=2). Scale bar = 50  $\mu$ m.

### 3.5 Investigating the effects of different static culture conditions for mouse MSC cells seeded on glass scaffolds

The aim of this experiment was to investigate the effects of different culture environments of Mouse MSC cells seeded on glass scaffolds with respect to cell viability and matrix production. In order to do this, Mouse MSC cells were

statically seeded with 250,000 cells per glass scaffold using the seeding and culture method as described in chapter 2. The cell-seeded scaffolds were cultured in standard media supplemented with AA and  $\beta$ GP. Cell seeded scaffolds were statically cultured in a well-plate or in a piece of silicone tubing (10 mm in diameter, 240 mm in length). Fresh media was supplied every 3 days for both conditions, which were 3 ml for samples in well plates, and 10 ml for samples in the piece of silicone tubing. The cell viability (as assayed by MTS) and collagen content (as assayed by sirius red staining) were evaluated on day 14 of culture.

It is evident that there was no significant difference between culturing scaffolds in well-plates or in a piece of tubing (fig 3.4). It was therefore decided for future experiments, cell-seeded scaffolds should be statically cultured in a well plate rather than a piece of silicone tubing to reduce manipulation steps.

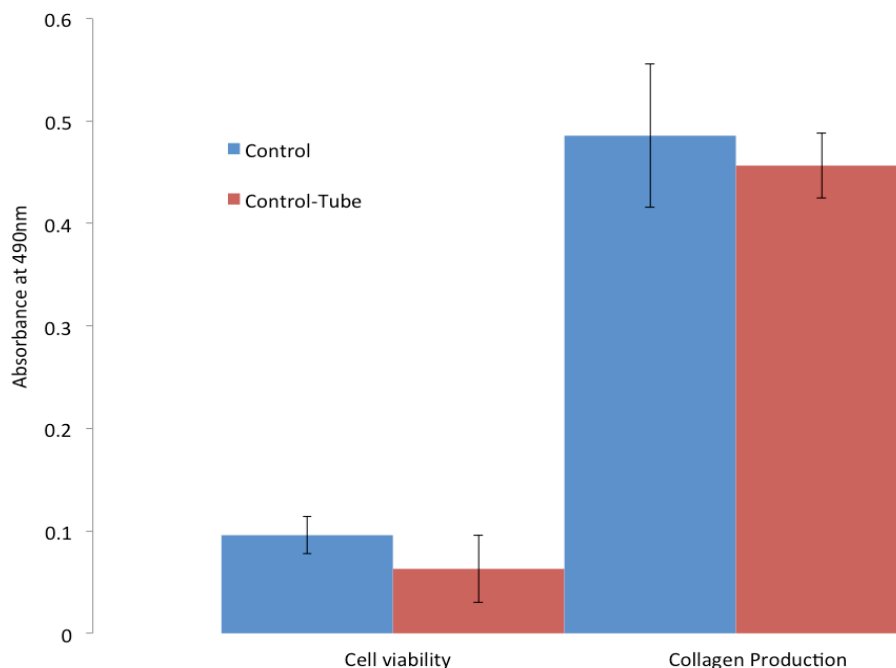


Fig 3.4; Mouse MSC cells seeded on glass scaffolds and cultured in well plates (blue bar) or silicon tubing (red bar). On day 14 of static culture samples were assayed for cell viability (MTS) and collagen production (Sirius red). All data is mean  $\pm$  SD (n=4).

### **3.6 Studying the effects of fluid flow on matrix production and expression of genes associated with osteogenic differentiation for Mouse MSC and hES-MP cells in 3D constructs**

The aim of these experiments was to study the effect of oscillatory fluid flow on cell viability, ALP activity, collagen production and calcium deposition of mouse MSC and hES-MP cells in 3D constructs. To study this effect, glass scaffolds were seeded with 250,000 cells and PU scaffolds (having a larger volume, 10 mm x 10 mm) were seeded with 500,000 cells using the seeding and culture methods described in chapter 2. Samples seeded with mouse MSC cells were cultured in standard culture media and supplemented with AA and  $\beta$ GP. Samples seeded with hES-MP cells were cultured in standard culture media and supplemented with AA,  $\beta$ GP and DEX. Fluid flow was applied using the oscillatory pump (chapter 2, figure 2.3) at a frequency of 1Hz for a loading period of 1 hour.

In short-term dynamic culture, samples were subjected to oscillatory fluid flow (3 ml/min, 1 Hz, 1 hour loading session) on day 4 and analysed for cell viability, total DNA content and ALP activity on day 7 (figure 3.5a). In long-term culture, samples were subjected to fluid flow on day 4, 7, 10 and analysed collagen production and calcium deposition on day 14 (figure 3.5b). Between loading sessions, cell-seeded scaffolds were cultured statically in an incubator in standard conditions. The experiment was conducted once (N=1) with 3 scaffolds (n=3) for each condition. Therefore, statistical analysis was not performed due to the low number of repeats.

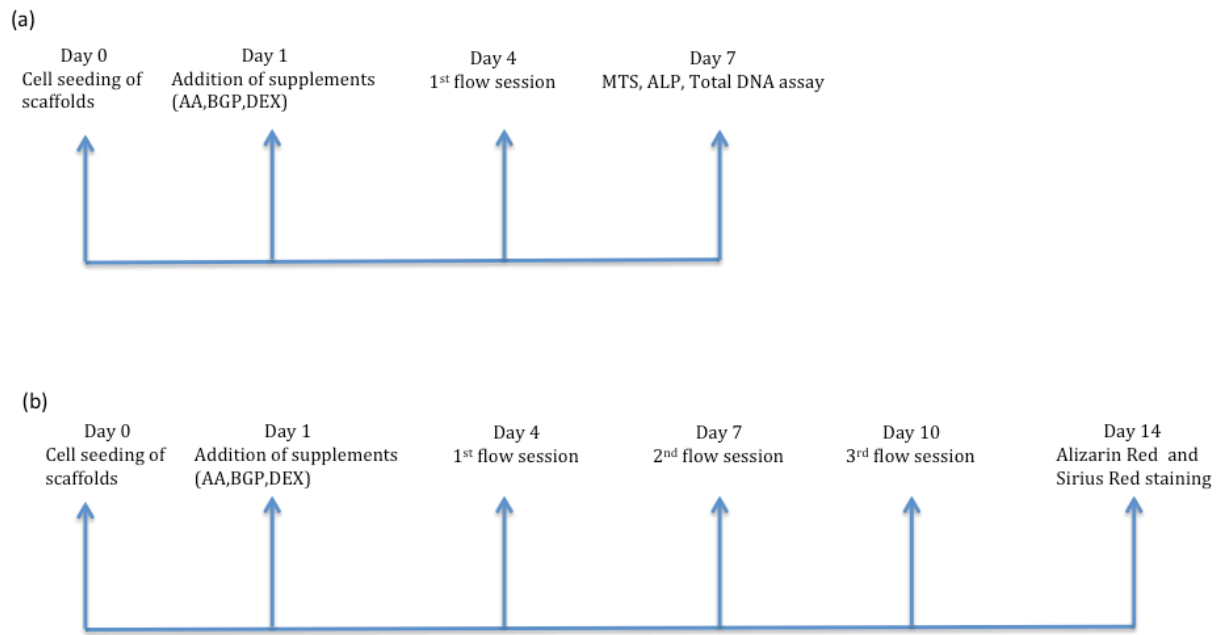


Figure 3.5; The experimental time line. (a) Short term dynamic culture, samples were subjected to flow on day 4 of culture and analysed for cell viability, total DNA content, and ALP activity on day 7. (b) Long term dynamic culture, samples were subjected to flow on days 4, 7 and 10 and analysed for cell viability, collagen and calcium content on day 14.

### 3.6.1 Short term dynamic culture - Cell viability (MTS)

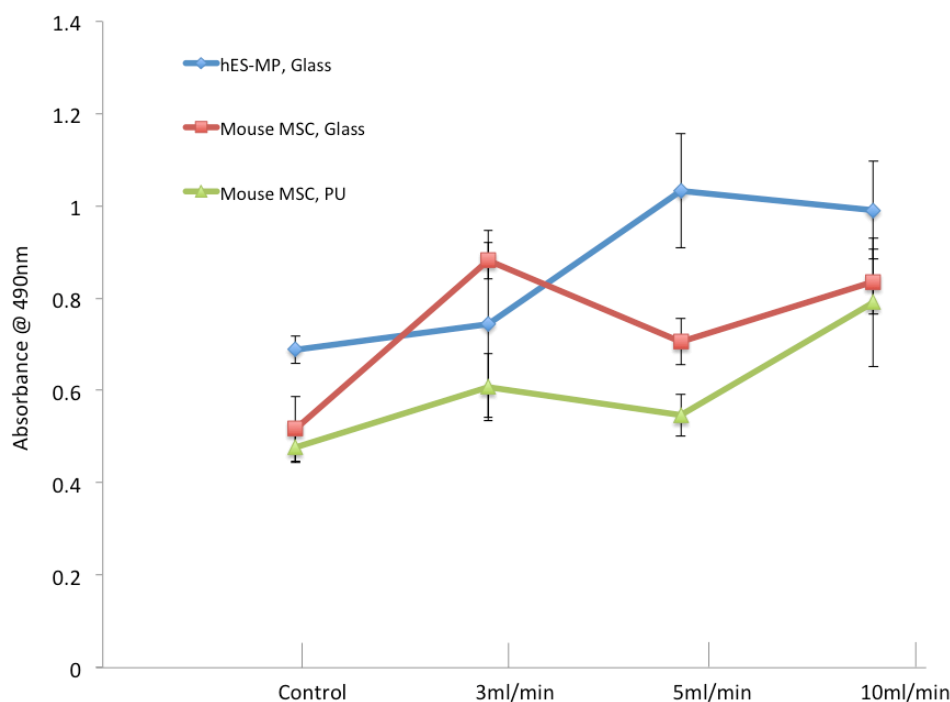


Fig 3.6; Cell-seeded scaffolds were subjected to three different flow rates on day 4 and analyzed for cell viability (MTS) on day 7 of culture. All data is mean  $\pm$  SD (n=2).

From figure 3.6 it appears that regardless of scaffold or cell type, the application of flow caused higher cell viability compared to static conditions. hES-MP cells seeded on glass scaffolds and subjected to 5 ml/min had the highest cell viability, whereas mouse MSC cells seeded on the same scaffold showed highest cell viability when subjected to 3 ml/min fluid flow. Moreover, mouse MSC cells seeded on PU foam demonstrated the highest cell viability when subjected to 10 ml/min oscillatory fluid flow.

### 3.6.2 Short-term dynamic culture - Total DNA content and ALP activity

Total DNA and ALP activity of cell-seeded scaffolds subjected to oscillatory fluid flow was analysed on day 7 of culture. DNA content of Mouse MSC cells seeded on glass scaffolds (fig 3.7a) was higher for all scaffolds subjected to fluid flow when compared to static culture. It appears that scaffolds subjected to 5 ml/min had the highest DNA content. ALP activity (fig 3.7b) appears to be relatively

consistent between flow groups and static culture except for scaffolds under 10 ml/min, where the activity of ALP was lowest.

The total DNA content for Mouse MSCs seeded on PU scaffolds (fig 3.7c) appears to be consistent throughout all flow and static conditions, whereby scaffolds subject to 3 ml/min had a slightly higher DNA content than other groups. In general, ALP activity (fig 3.7d) was lower for all scaffolds subjected to fluid flow when compared to static conditions.

DNA content for hES-MP cells seeded on glass scaffolds (fig 3.7e) and subjected to 3 ml/min appears to be lowest compared to other flow conditions and static cultures. Furthermore, scaffolds subjected to 5 ml/min and 10 ml/min fluid flow have a higher DNA content than static culture. ALP activity (fig 3.7f) also appears to be consistent throughout all flow and static conditions.

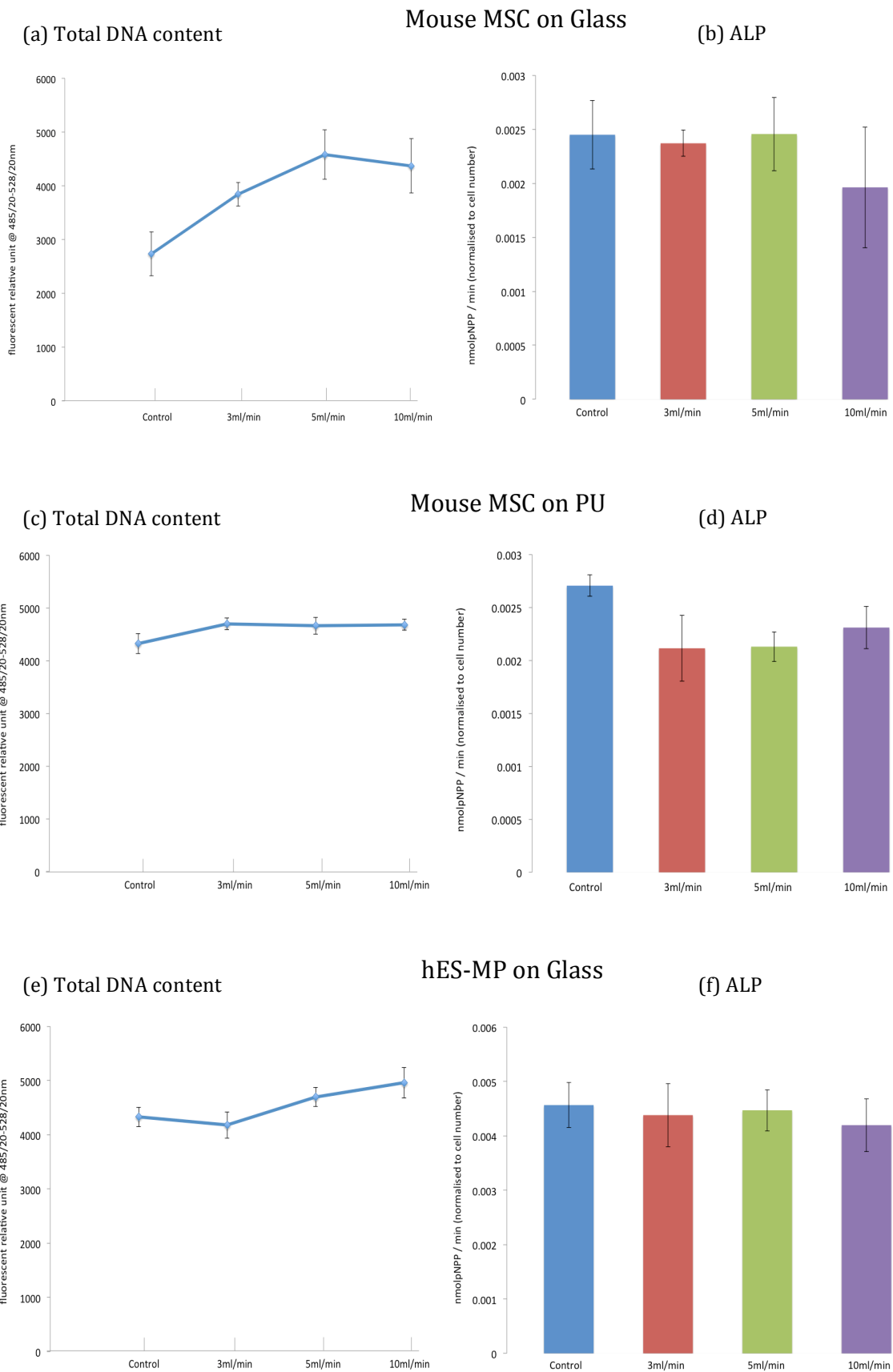


Fig 3.7; Affect of fluid flow on (a) total DNA content and (b) ALP activity (normalized to DNA) for mouse MSCs cultured on glass scaffolds (c) total DNA content and (d) ALP activity (normalized to DNA) for mouse MSCs cultured on PU scaffolds (e) total DNA content and (f) ALP activity (normalized to DNA) for hES-MP cells cultured on glass scaffolds at day 7. All data is mean  $\pm$  SD (n=2).

### 3.6.3 Long-term dynamic culture - Collagen and calcium content

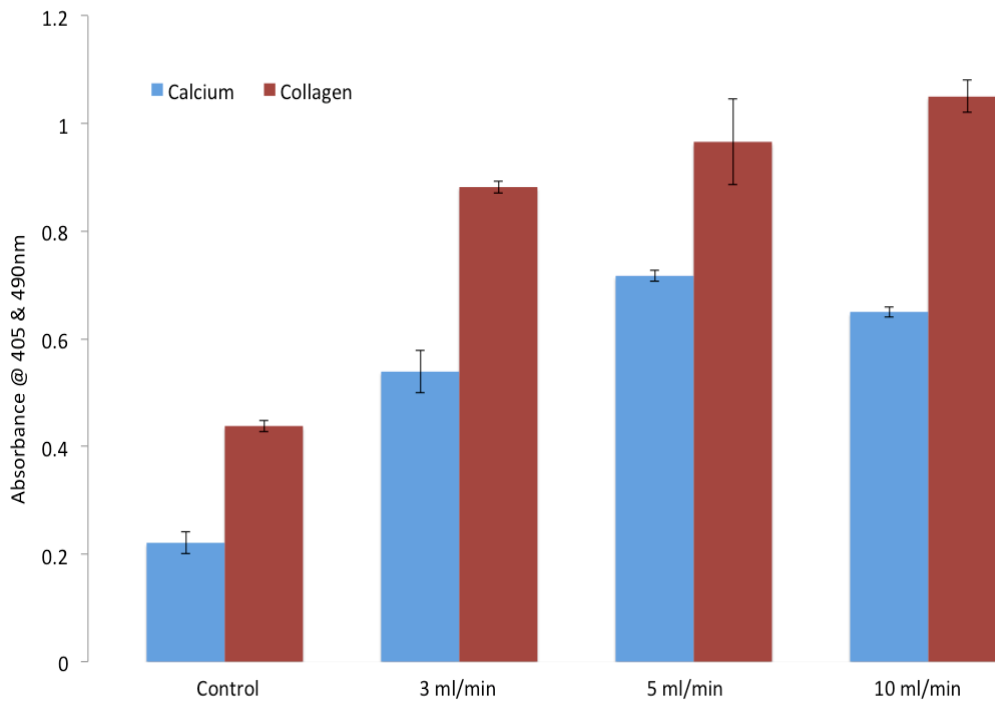


Fig 3.8; hES-MP cells cultured on glass scaffolds and subjected to three different flow rates on day 4, 7 and 10. Collagen production (Sirius red) and calcium deposition (Alazarin red) were analyzed on day 14. All data is mean  $\pm$  SD (n=2).

Late markers of osteogenic differentiation were also analysed using Sirius red (for collagen production) and alizarin red (calcium deposition) staining on day 14 of culture (Figure 3.8). In general, it seems that the application of flow increased matrix production in comparison to static culture. Scaffolds subjected to 5 ml/min flow deposited the most calcium whereas scaffolds subjected to 10 ml/min flow produced the highest collagen.

Fluorescent microscopy was also used to look at mouse MSC cell distribution across the glass scaffold surface on day 14 of culture. From figure 3.9 it appears that there were more cells on the surface for scaffolds in static culture when compared to flow conditions. This arrangement has also been witnessed in other fluid flow studies where it is thought that effects of fluid flow tend to shear off cells from the scaffold surface.

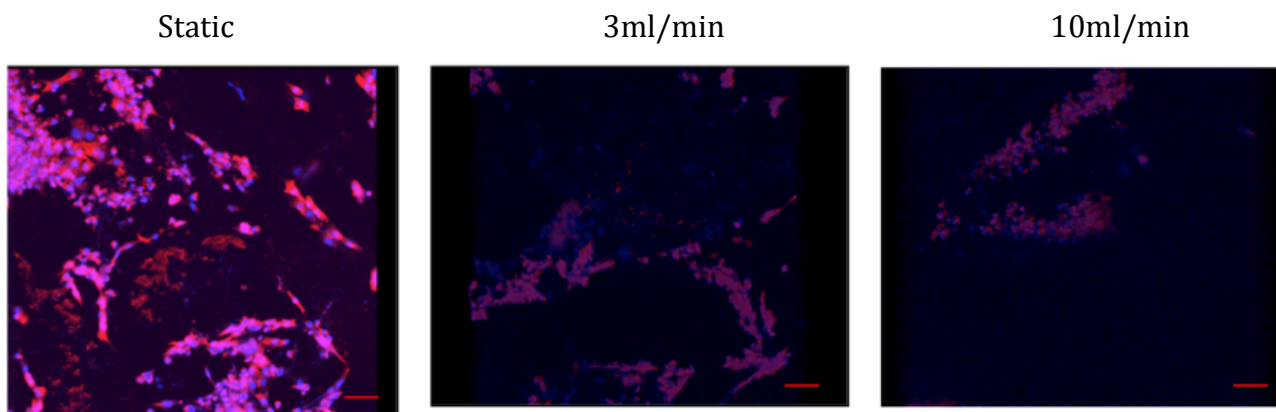


Fig 3.9; Mouse MSCs cultured on glass scaffolds and subjected to fluid flow on day 4,7 and 10. On day 14, images produced using confocal microscopy reveal a higher number of cells on the surface of scaffolds in static culture in comparison to samples subjected 3 and 10 ml/min oscillatory flow. Representative images are shown (n=2). Scale bar = 100  $\mu$ m.

### 3.7 Discussion

In this chapter it was demonstrated that mouse MSC and hES-MP cells can be cultured on an industrially produced PU and novel glass based scaffold, which has not previously been reported for use in 3D tissue culture. A non-dynamic method to culture cells in a 3D static environment was designed, allowing to further investigate selected mechanical stimuli and mechanotransduction in bone tissue constructs. Culturing cells on a 3D scaffold can better mimic the bone environment providing a better physiological model than cells cultured in 2D monolayer. The model in this study can be used to better understand bone tissue constructs and other *in vitro* studies of bone cells in a 3D environment.

It has been well demonstrated that MSCs can be stimulated towards osteogenesis *in vitro* by addition of ascorbic acid, dexamethasone, and  $\beta$ -glycerophosphate. For example MSC proliferation and the number of colony forming units were increased by the addition of ascorbic acid. DEX was shown to enhance ALP activity and was critical for mineral deposition [54]. However hES-MPs are a new commercially available mesenchymal progenitor cell for which there was limited literature available at the beginning of this study, other than papers authored by the company that market the cells. Therefore, experiments were conducted to verify the osteogenic potential of these cells using standard laboratory conditions.

In this study it was shown that hES-MP cells treated with 100 nM DEX, increased ALP activity on day 7 and day 14 of static culture (fig 3.1). Interestingly, this effect was not seen for the mouse MSCs obtained from the collaborator where the addition of DEX reduced ALP activity on day 14 of culture. Dr. Delaine-Smith also investigated the osteogenic differentiation of hES-MP cells when exposed to different DEX concentrations (0, 10 nM and 100 nM) and showed that lower DEX concentration corresponded to higher total DNA, indicating that DEX affects cell number. ALP activity of samples treated with 10 nM and 100 nM showed no difference at days 7-14. However, on day 21 of culture, samples treated with 100 nM DEX displayed 1.5-fold higher ALP activity than those treated with 10 nM.

Cells with 0 nM dex exhibited a much lower ALP activity at all time points. Sirius red staining of collagen at day 14 indicated that increasing DEX concentration resulted in less staining [55]. *Beresford et al.* also demonstrated that DEX can inhibit expression of collagen type I (COL 1) and enhance maturation adipocytes in culture [56].

The results from this investigation showed an inhibition of ALP activity of mouse MSC cells treated with DEX. It has also been indicated that the effects of DEX may vary depending on the species origin, maturation stage of the cells as well as culture conditions [57, 58]. In a similar study it was shown that mice and rats are different in their response to the cell proliferation effects of DEX [59]. It showed that instead of increasing the number of calcified nodules as seen in rat cells, calvarial osteoblasts from mice produced fewer calcified colonies in the presence of dexamethasone. The data further indicated that DEX might not be beneficial for the growth and differentiation of bone marrow stromal cells culture as reported for rat cells or human MSCs. It is interesting to note these strong differences in the two species responses to a biochemical agent since mice are the most common source of transgenic and knockout animals for biomedical research. The mechanism by which DEX and mechanical stimuli induce osteogenic differentiation in human MSC cells is poorly understood. However, it has been proposed that one of the potential signal transduction pathways which could direct the human MSC cells towards a osteogenic lineage is the mitogen-activated protein kinase (MAPK) pathway [60]. Extracellular signal related kinase (ERK, a member of the MAPK family) stimulates the differentiation of human MSCs into osteoblasts via phosphorylation of the osteogenic transcription factor RUNX2/Cbfa1 [60].

Metabolic assays such as MTS, MTT or alamar blue are widely used to assess cell viability and cell proliferation. Furthermore, assays such as ALP, sirius red and alizarin red staining are used to evaluate cell differentiation in 2D and 3D culture [61]. Although the non-dynamic model showed acceptable results with regards to mouse MSC proliferation as seen by alamar blue analysis (fig 3.2), the

distribution of cells was not homogenous. Confocal images (fig 3.3) revealed more cells on the top and bottom surface than in the cross-section of the glass scaffold. Alternative techniques such as application of flow can induce fluid into the culture system to improve growth, migration and distribution of cells [62-70]. During the assay protocol it was noticed that not all the solutions may be able to diffuse out of the interior of scaffolds whether its the quantification of cell number by dissolving MTS or measuring calcium deposition by alizarin red staining. In the case of MTT, the assay relies on the cells metabolising a solution of a colored substrate. Studies have shown that the accuracy of assays in 3D scaffolds is dependent on the efficiency of solution diffusion into and out of constructs [71, 72]. Therefore in later chapters it was decided that scaffolds would be separated into several sections to maximise diffusion out of the interior.

Results from this chapter suggest that the application of flow to both mouse MSC and hES-MP cells promoted cell proliferation as indicated by higher MTS over time and general increase in DNA content. This observation has also been reported by others culturing hMSCs under dynamic conditions in bioreactor systems [73, 74]. Perfusion systems are known to affect cell proliferation through two main mechanisms, enabling mass transport and applying a fluid-driven mechanical stimulation. Similarly, the increase in cell proliferation in this study maybe due to the short increase in nutrient transport and fluid shear stress associated with flow perfusion [75]. On the other hand, it has been reported by *Lynch et al*, that upon osteogenic differentiation and bone-like tissue formation *in vitro*, cells undergo programmed cell death [76]. In the present study it was unclear whether the increase in DNA content is due to an actual increase in proliferation or reduced cell death. However in the current system there is no continuous perfusion so effects of nutrient transport are likely to be small.

In this investigation cell morphology did not seem to alter with respect to location on glass scaffolds as hES-MP cells demonstrated an elongated fibroblast-like shape at the top, cross-section and bottom part of the scaffold (fig 3.3).

Extracellular matrix (ECM) stiffness has also been shown to play an important role in a variety of cell behaviours such as migration, proliferation, and differentiation in both osteogenic and non-osteogenic cells [77-79]. Engler *et al.*, demonstrated that MSC differentiation along different phenotypic lineages is partially dependant on substrate stiffness. It was shown that MSCs would differentiate into osteoblast-like cells when cultured on collagen coated polyacrylamide substrates that would mimic the stiffness of osteoid (25–40 kPa). Furthermore, cells would take the characteristics of neurons when cultured in substrates with stiffness values similar to brain (1 kPa). MSCs cultured on matrices with stiffness range of 8-17 kPa became spindle-shaped in morphology, similar to myoblasts [80]. In these studies the stiffness of the struts of the scaffold were not measured, however the glass scaffold would have been very stiff, well above the range tested by Engler's group and therefore it is not really possible to compare these results with theirs. It would be interesting in the future to investigate whether the differences in stiffness between glass and PU have any effect on cell differentiation, however it would be difficult to separate stiffness effects from chemical effects in these two very different materials.

In this study, two different cell seeding densities were chosen due to the difference in scaffold size. Glass scaffolds (12 mm x 3 mm) were seeded with 250,000 cells while PU scaffolds (10 mm x 10 mm) having a larger volume were seeded with 500,000 cells, as per a previously established protocol in the laboratory. The separation distance of cells, as controlled by cell seeding density, has been shown to play a key role in the differentiation of osteogenic cells during *in vitro* cell culture experiments due to changes in paracrine signaling distance among the cells. Kim *et al.* established the importance of seeding density for the differentiation of BMSCs into osteoblasts on 2D culture plates. It was shown that ALP activity in rat bone marrow stromal cells was higher when cells were seeded at a lower initial seeding density ( $3 \times 10^4$  per  $\text{cm}^2$ ) in comparison to a high seeding density ( $14.9 \times 10^4$   $\text{cm}^2$ ) [81]. Cell seeding density has been shown to influence osteoblast proliferation and matrix mineralisation in 3D constructs *in vitro* [82]. It was demonstrated that bone formation was increased when a higher number of goat bone marrow cells ( $47.8 \times 10^6$  cells/ $\text{cm}^3$ ) were seeded on to HA scaffolds

(2.8x3.6x5.2 mm<sup>3</sup>) [83]. Therefore, choosing a suitable seeding density is important as cell-cell interactions may be controlled by this factor which would eventually induce a specific cell differentiation needed for each tissue type. Due to the limited number of glass scaffolds available it was not possible to extensively examine density effects however this would be an interesting variable to include in future studies.

ALP activity is used as a marker of osteogenic differentiation and plays a vital role in the early phases of mineralisation of newly formed bone [84]. In this study the activity of ALP in constructs was slightly different when cultured under static and dynamic conditions. Higher ALP activity was observed for scaffolds under static conditions compared to dynamic conditions. This difference may be due to the cell lysate not diffusing well out of the inner core of the constructs. Another reason could be complex biological factors underlying gene expression and protein synthesis [85]. Interestingly, ALP exists as membrane-bound and as a released enzyme, therefore the application of fluid flow may contribute to the removal of the released isoform and resulting in an underestimation of its activity [86]. ALP is generally upregulated in the early phase of osteoblast differentiation and the positive correlation between ALP activity and matrix mineralisation indicates a relationship between the two markers. This has been supported by many other authors [68, 87-90] and is suggested that greater ALP activity would result in bone-like formation. Once this level is reached, an upregulation in ALP activity will not result in an increase in matrix mineralisation. However this relationship was not observed in this study, and it may be speculated that there would be a specific level of ALP activity that is required to induce bone formation. Since calcium deposition was higher for samples subjected to fluid flow in comparison to static controls, it can be speculated that the peak in ALP activity could have occurred either before or after day 7. Thus, highlighting the complex biology underlying gene expression, as well as the possibility that additional components control its regulation. This has also been observed in other studies whereby a significant decrease in the ALP activity occurs at a later stage when osteoblastic cells mature and form mineralised extracellular matrix [91, 92].

Osteogenic differentiation of hES-MP cells was further assessed by investigating the collagen and calcium production on day 14 of culture. It is evident that matrix production was higher for constructs under dynamic conditions compared to static conditions. In a recent study, rat stromal cells were seeded on a titanium scaffold and placed in a perfusion bioreactor. It was shown that the rate of osteoblastic differentiation and calcium deposition significantly increased [87]. As calcium is deposited in the late stages of osteoblastic differentiation, it was suggested that the application of flow greatly enhanced the differentiation of stem cells into mature osteoblasts. It was proposed that the cells were responding to the fluid shear stress caused by the fluid movement into and out of the scaffold. This will eventually cause a cascade of events that would finally result in an upregulation of survival and matrix producing genes. Furthermore, an improved nutrient supply only for a short time could contribute to the mechanosensitive response however the mechanical stimuli subjected to the cells would also play a key role as has been demonstrated in 2D monolayers [93, 94].

The use of PU scaffolds for tissue engineering purposes are limited due to their lack of biodegradation during long-term *in vivo* culture [95]. However these have good mechanical properties and allows them to withstand *in vitro* mechanical loading, while at the same time being cost-effective and highly reproducible. It was previously shown that PU scaffolds supported MLO-A5 mouse osteoblastic cell growth [51] and therefore, it was predicted that this scaffold would also be biocompatible with MSCs. Furthermore, it was demonstrated that PU foams can support MSC adhesion, proliferation and differentiation into osteoblastic cells by observing the CaP deposition in *in vitro* static culture [96].

A wide variety of both natural and synthetic materials are being investigated for the design and construction of scaffolds for bone tissue engineering. Scaffolds made from calcium phosphate have been used for bone engineering application for more than two decades. Hydroxyapatite and other calcium phosphates including; tricalcium phosphate ( $\beta$ -TCP), have been widely used as bone substitutes in the clinical area due to their osteoconductive properties. *Cancedda*

*et al.* demonstrated that marrow derived osteoprogenitor cells seeded onto hydroxyapatite (HA) scaffolds provided better bone repair over a short period of time in comparison to cell-free HA scaffolds [97]. Even with the promising results gained from using synthetic calcium-based ceramics, their use in the clinical area is limited since they do not combine good mechanical properties with an open porosity and have been shown to be prone to fragile failure [98, 99].

The combination of bioactive ceramics in combination with polymers have shown to improve the mechanical properties of scaffolds. *In vitro* culture studies have shown promising results when osteoblastic cells were seeded on to Highly porous PLLA and PLLA-HA scaffolds. Osteoblasts penetrated deep into the PLLA-HA scaffolds and demonstrated uniform distribution with a higher cell survival count when compared to PLLA scaffolds. In addition, cells seeded on PLLA-HA scaffolds showed higher expression of bone-specific markers [100]. Similar synthesised collagen derived gelatin-HA nanocomposites were investigated for osteoblastic cellular responses; the scaffolds retained less crystallised and smaller-sized apatite crystals and a more well-developed pore configuration than the conventional ones [101]. *Kim et al.*, synthesised collagen-derived gelatin/hydroxyapatite (HA) nanocomposites for tissue engineering purposes. MG63 osteoblastic cells seeded on nanocomposites were shown to attach and proliferate to a much higher degree when compared to conventional composite scaffolds. Furthermore, the ALP activity and osteocalcin produced by the MG63 cells were significantly higher on the nanocomposite scaffolds in comparison to conventional composite scaffolds [101].

hES-MP cells utilised in this study were used as a model for human MSCs however it also possible they have future clinical applications. As mentioned previously, human mesenchymal stem cells (hMSCs) are a promising candidate for musculoskeletal regeneration and tissue engineering. In a study that compared the osteogenic potential of human MSCs with hES-MP cells, *de peppo et al.*, demonstrated faster mineralisation of matrix produced by hES-MP cells in comparison to hMSCs. In addition hES-MP cells displayed good proliferation and high mineralisation potential after protracted expansion. ALP activity was also

observed from week 1 with peak of intracellular ALP activity measured after 6 weeks. Interestingly, hES-MP cells displayed a significantly lower ALP activity with greater mineralisation ability than hMSCs. It was suggested that when considering hES-MP cells, ALP activity may not be crucial for matrix mineralisation as different cells may be subjected to different signaling pathways and dynamics in relation to their differentiation towards the osteogenic lineage [21].

Another study successfully incorporated hES-MP cells with Electron beam melting (EBM) fabricated cp-Ti and Ti6Al4V scaffolds under *in vitro* conditions. It was shown that hES-MPs distributed uniformly within the geometrical features of both scaffolds. It demonstrated that increasing cell density inhibits cell proliferation, as cell-cell communication is essential for tissue formation. In addition, the expression of RUNX2, OPN and OC increased after 2 weeks of culture in both scaffolds [102].

In a follow up study, the researchers investigated the behaviour of hES-MP and hMSC cells cultured in coral scaffolds (3x3x3 mm, volume porosity: 49%–2%, pore diameter 150–400  $\mu\text{m}$ ) under dynamic conditions. The data demonstrated a significant increase in cell proliferation for both cell types subjected to flow in comparison static culture. Interestingly, ALP activity was higher for hES-MP constructs cultured in static conditions compared to dynamic conditions. Suggesting that this difference may in part be due to technical limitations and in part to complex biological factors underlying gene expression or may result from a washout effect as a result of fluid flow. Furthermore, it was shown that hES-MP constructs subjected to flow deposited nodules of calcium phosphate deep inside the scaffold pores in comparison to static conditions [22].

### **3.8 Conclusion**

In this chapter it was shown that hES-MP and mouse MSC cells can attach and proliferate on an industrial grade PU and a novel glass scaffold. Glass scaffolds possessed good properties including an adequate pore size to provide enough

media perfusion to take place and stimulate cells using fluid shear stress. Therefore, it was decided to further investigate specific flow parameters using these glass scaffolds in order to address future aims of comparing the effects of flow with those of specific peptide coatings. Dexamethasone induced an osteogenic response in hES-MP cells, and increased ALP activity. Furthermore, it was possible to analyse cell morphology and cell distribution on glass scaffolds since they have good light transmissibility. It was shown that hES-MP and mouse MSC cells can survive and distribute well through out both scaffolds for upto 14 days in static culture. However the response of mouse MSCs to DEX was different from the response of hES-MPs in these experiments and the observed response of adult MSCs seen in our laboratory and others. Therefore, it was decided to use hES-MPs for further follow up work on specific flow parameters using the glass scaffolds. Finally, these preliminary experiments indicated that short bouts of fluid flow could increase cell viability and calcium deposition of hES-MP-glass constructs. Therefore it is important to further establish which flow parameters are osteogenic in this system in a systematic way. The work of this chapter leads to the following chapter in which the hES-MPs and glass scaffolds are used as a model system with which to test a range of bioreactor flow conditions.

### 3.9 References

- [1] Rowley JA, Madlambayan G, and Mooney D J: Alginate hydrogels as synthetic extracellular matrix materials. *Biomaterials*. 1999 Jan;20(1):45-53.
- [2] Petite HV, Viateau W, Bensaid A, Meunier C, de Pollak M, Bourguignon M, Oudina P, Sedel L, Guillemin G: Tissue-engineered bone regeneration. *Nature Biotech*. 2000, 18:959– 963.
- [3] Pittenger, M.F., Mackay, A.M., Beck, S.C., Jaiswal, R.K., Douglas, R., Mosca, J.D., et al. Multilineage potential of adult human mesenchymal stem cells. *Science* 284, 143, 1999.
- [4] Tapp H, Hanley EN Jr, Patt JC, Gruber HE: Adipose-derived stem cells: characterization and current application in orthopaedic tissue repair. *Exp Biol Med (Maywood)*. 2009, Jan;234(1):1-9.
- [5] Matsumoto T, Kuroda R, Mifune Y, Kawamoto A, Shoji T, Miwa M, Asahara T, Kurosaka M: Circulating endothelial/skeletal progenitor cells for bone regeneration and healing. *Bone*. 2008, 434-9.
- [6] Jäger M, Zilkens C, Bittersohl B, Krauspe R: Cord blood-an alternative source for bone regeneration. *Stem Cell Rev*. 2009 Sep;5(3):266-77.
- [7] Danisovic L, Varga I, Polak S, Ulicna M, Bohmer D, Vojtassak J: Morphology of in vitro expanded human muscle-derived stem cells. *Biomed Pap Med Fac Univ Palacky Olomouc Czech Repub*. 2008 Dec;152(2):235-8.
- [8] Ho AD, Wagner W, Franke W: Heterogeneity of mesenchymal stromal cell preparations. *Cytotherapy*. 2008;10(4):320-30.
- [9] Wagner W, and Ho AD: Mesenchymal stem cell preparations comparing apples and oranges. *Stem Cell Rev*. 2007 Dec;3(4):239-48.
- [10] Bonab MM, Alimoghaddam K, Talebian F, Ghaffari SH, Ghavamzadeh A, and Nikbin B: Aging of mesenchymal stem cell in vitro. *BMC Cell*. 2006, Biol 7.
- [11] Baxter MA, Wynn RF, Jowitt SN, Wraith JE, Fair-bairn LJ, and Bellantuono I: Study of telomere length reveals rapid aging of human marrow stromal cells following in vitro expansion. *BMC Cell Biol*. 2006 Mar 10;7:14.
- [12] Wagner W, Horn P, Castoldi M, Diehlmann A, Bork S, Saffrich R. Replicative senescence of mesenchymal stem cells: a continuous and organized process. *PLoS ONE* 3, e2213, 2008.

- [13] Izadpanah R, Kaushal D, Kriedt C, Tsien F, Patel B, Dufour J. Long-term in vitro expansion alters the biology of adult mesenchymal stem cells. *Cancer Res.* 2008, 68, 4229.
- [14] Rosland GV, Svendsen A, Torsvik A, Sobala E, McCormack E, Immervoll H. Long-term cultures of bone marrow-derived human mesenchymal stem cells frequently undergo spontaneous malignant transformation. *Cancer Res.* 2009, 69, 5331.
- [15] Rubio D, Garcia-Castro J, Martin MC, de la Fuente R, Cigudosa JC, Lloyd AC. Spontaneous human adult stem cell transformation. *Cancer Res.* 2005, 65, 3035.
- [16] Kim J, Kang JW, Park JH, Choi Y, Choi KS, Park KD. Biological characterization of long-term cultured human mesenchymal stem cells. *Arch Pharm Res.* 2009, 32, 117.
- [17] Sottile V, Thomson A, and McWhir J: In vitro osteogenic differentiation of human ES cells. *Cloning Stem Cells.* 2003;5(2):149-55.
- [18] Bigdeli N, de Peppo GM, Lenneras M, Sjövall P, Lindahl A, Hyllner J, and Karlsson C: Superior osteogenic capacity of human embryonic stem cells adapted to matrix-free growth compared to human mesenchymal stem cells. *Tissue Eng Part A.* 2010 Nov;16(11):3427-40.
- [19] Przyborski SA: Differentiation of human embryonic stem cells after transplantation in immune-deficient mice. *Stem Cells.* 2005 Oct;23(9):1242-50.
- [20] de Peppo GM, Svensson S, Lenneras M, Synnergren J, Stenberg J, Strehl R, Hyllner J, Thomsen, P, and Karlsson C: Human embryonic mesodermal progenitors highly resemble human mesenchymal stem cells and display high potential for tissue engineering applications. *Tissue Eng Part A.* 2010 Jul;16(7):2161-82.
- [21] de Peppo GM, Sjövall P, Lenneras M, Strehl R, Hyllner J, Thomsen P, and Karlsson C: Osteogenic potential of human mesenchymal stem cells and human embryonic stem cell-derived mesodermal progenitors: a tissue engineering perspective. *Tissue Eng Part A.* 2010 Nov;16(11):3413-26.
- [22] de Peppo GM, Sladkova M, Sjövall P, Palmquist A, Oudina K, Hyllner J, Thomsen P, Petite H, Karlsson C. Human Embryonic stem cell derived mesodermal progenitors display substantially increased tissue formation

compared to mesenchymal stem cell under dynamic culture conditions in a packed/bed column bioreactor. *Tissue Eng. Part A*. 2013 Jan;19(1-2):175-87.

[23] Yoshikawa T, Ohgushi H, Dohi Y, Davies JE: Viable bone formation in porous hydroxyapatite marrow cell-derived in vitro bone on the surface of ceramics. *Biomed Mater Eng*, 7 (1) (1997), 49–58.

[24] Ishaug SL, Crane GM, Miller MJ, Yasko AW, Yaszemski MJ, Mikos AG: Bone formation by three-dimensional stromal osteoblast culture in biodegradable polymer scaffolds. *J Biomed Mater Res*, 36 (1) (1997), 17–28.

[25] Martin I, Shastri VP, Padera RF, Yang J, Mackay AJ, Langer R, Vunjak-Novakovic G, Freed LE: Selective differentiation of mammalian bone marrow stromal cells cultured on three-dimensional polymer foams. *J Biomed Mater Res*, 55 (2) (2001), 229–235.

[26] Ducheyne P, el-Ghannam A, Shapiro I: Effect of bioactive glass templates on osteoblast proliferation and in vitro synthesis of bone-like tissue. *J Cell Biochem*, 56 (2) (1994), 162–167.

[27] Ozawa S, Kasugai S: Evaluation of implant materials (hydroxyapatite, glass ceramics, titanium) in rat bone marrow stromal cell culture. *Biomaterials*, 17 (1) (1996), 23–29.

[28] Meirelles Lda S, Nardi NB. Murine marrow-derived mesenchymal stem cell: isolation, in vitro expansion, and characterization. *Br J Haematol*. 2003 Nov;123(4):702-11

[29] Sreejit P, Dilip KB, Verma RS. Generation of mesenchymal stem cell lines from murine bone marrow. *Cell Tissue Res*. 2012 Oct;350(1):55-68

[30] Chavassieux PM, Chenu C, Valentin-Opran A, Marle B, Delmas PD, Hartmann DJ, Saez S, Meunier PJ. Influence of experimental conditions on osteoblast activity in human primary bone cell cultures. *J Bone Miner Res* 1990;5:337- 343.

[31] Fromingué O, Marie PJ, Lonri A. Differential effects of transforming growth factors b2, dexamethasone and 1,25- dihydroxivitamin D3 on human bone marrow stromal cells. *Cytokine* 1997;9:613-623.

[32] Kielty, C. M., I. Hopkinson and M. E. Grant. "Collagen: The collagen family: Structure, assembly, and organization in the extracellular matrix." In *Connective tissue and its heritable disorders: Molecular, genetic, and medical aspects*. 1993.

- [33] Chang, Y. L., C. M. Stanford and J. C. Keller. Calcium and phosphate supplementation promotes bone cell mineralization: Implications for hydroxyapatite (HA)-enhanced bone formation. *J. Biomed. Mater. Res.* 2000, 52(2):270-278.
- [34] Bellows CG, Aubin JE, Heersche JNM. Physiological concentrations of glucocorticoids stimulate formation of bone nodules from isolated rat calvaria cells in vitro. *Endocrinology* 1987;121:1985-1992.
- [35] Wong MM, Rao LG, Ly H, Hamilton L, Tong J, Sturtridge W, McBroom R, Aubin JE, Murray TM. Long -term effects of physiologic concentrations of dexamethasone on human bone-derived cells. *J Bone Miner Res* 1990;5:803-813.
- [36] Shalhoub V, Conlon D, Tassinari M, Quinn C, Partridge N, Stein GS, Lian JB. Glucocorticoids promote development of the osteoblast phenotype by selectively modulating expression of cell growth and differentiation associated genes. *J Cell Biochem* 1992;50:425-440.
- [37] Kasugay S, Todescan R Jr, Nagata T, Yao K-L, Butler WT, Sodek J. Expression of bone matrix proteins associated with mineralized tissue formation by adult rat bone marrow cells in vitro: inductive effects of dexamethasone on the osteoblastic phenotype. *J Cell Physiol* 1991; 147:111-120.
- [38] Scutt A, Bertram P, Brautigam M. The role of glucocorticoids and prostaglandin E2 in the recruitment of bone marrow mesenchymal cells to the osteoblastic lineage: positive and negative effects. *Calcif Tissue Int* 1996;59:154-162.
- [39] Haynesworth SE, Goshima J, Goldberg VM, Caplan AI. Characterization of cells with osteogenic potential from human marrow. *Bone* 1992;13:81-88
- [40] Lyons FG, Al-Munajjed AA, Kieran SM, Toner ME, Murphy CM, Duffy GP, O'Brien FJ. The healing of bony defects by cell-free collagen based scaffolds compared to stem cell seeded tissue engineered constructs. *Biomaterials*. 2010 Dec;31(35):9232-43.
- [41] Sikavitsas V, Bancroft GN, Mikos AG: Formation of three-dimensional cell/polymer constructs for bone tissue engineering in a spinner flask and a rotating wall vessel bioreactor. *J Biomed Mater Res.* 2002 Oct;62(1):136-48.
- [42] Schwarz RP, Goodwin TJ, and Wolf DA: Cell culture for three-dimensional modeling in rotating-wall vessels: An application of simulated microgravity. *J.*

Tissue Cult Methods. 1992;14:51–58.

[43] Lappa M: Organic tissues in rotating bioreactors: fluid-mechanical aspects, dynamic growth models, and morphological evolution. *Biotechnol Bioeng*. 2003 Dec 5;84(5):518-32.

[44] Li YJ, Batra NN, You L, Meier SC, Coe IA, Yellowley CE, Jacobs CR: Oscillatory fluid flow affects human marrow stromal cell proliferation and differentiation. *Journal of Orthopaedic Research* 22 (2004) 1283-1289.

[45] Qin YX, Kaplan T, Saldanha A, Rubin C: Fluid pressure gradients, arising from oscillations in intramedullary pressure, is correlated with the formation of bone and inhibition of intracortical porosity. *Journal of Biomechanics*. Volume 36, Issue 10, October 2003, Pages 1427–1437.

[46] Wu CC, Li YS, Haga JH, Wang N, Lian IY, Su FC, Usami S, Chien S: Roles of MAP Kinases in the Regulation of Bone Matrix Gene Expressions in Human Osteoblasts by Oscillatory Fluid Flow. *Journal of Cellular Biochemistry*. 2006, 98:632–641.

[47] Batra NN, Li YJ, Yellowley CE, You L, Malone AM, Kim CH, Jacobs CR: Effects of short-term recovery periods on fluid-induced signaling in osteoblastic cells. *Journal of Biomechanics* 38 (2005) 1909–1917.

[48] Fassina L, Visai L, Asti L, Benazzo F, Speziale P, Tanzi MC, Magenes G: Calcified matrix production by SAOS-2 cells inside a polyurethane porous scaffold, using a perfusion bioreactor. *Tissue Eng*, 2005. 11(506): 685-700.

[49] Gorna K, and Gogolewski S: Biodegradable polyurethanes for implants. II. In vitro degradation and calcification of materials from poly(epsilon-caprolactone)-poly(ethylene oxide) diols and various chain extenders. *J Biomed Mater Res*, 2002. 60(4): 592-606.

[50] Zhang J, Doll BA, Beckman EJ, Hollinger JO: A biodegradable polyurethane-ascorbic acid scaffold for bone tissue engineering. *J Biomed Mater Res A*, 2003. 67(2): 289-400.

[51] Sittichokechaiwut A, Scutt AM, Ryan AJ, Bonewald LF, Reilly GC: Use of rapidly mineralising osteoblasts and short periods of mechanical loading to accelerate matrix maturation in 3D scaffolds. *Bone*, 2009, Vol.44(5), 822-829.

[52] Gorna K, and Gogolewski S: Preparation, degradation, and calcification of biodegradable polyurethane foams for bone graft substitutes. *J Biomed Mater*

Res A. 2003 Dec 1;67(3):813-27.

[53] Quarto R, Mastrogiacomo M, Cancedda R, Kutepov SM, Mukhachev V, Lavroukov A, Kon E, Marcacci M: Repair of large bone defects with the use of autologous bone marrow stromal cells. *N Engl J Med*. 2001 Feb 1;344(5):385-6.

[54] Fiorentini E, Granchi D, Leonardi E, Baldini N, Ciapetti G. effects of osteogenic differentiation inducers on in vitro expanded adult mesenchymal stromal cells. *Int J Artif Organs*. 2011 Oct;34(10):998-1011.

[55] Delaine-Smith RM: Mechanical and physical guidance of osteogenic differentiation and matrix production. 2013, PhD thesis, University of Sheffield.

[56] Beresford JN, Bennett JH, Devlin C, Leboy PS, Owen ME. Evidence for an inverse relationship between the differentiation of adipocytic and osteogenic cells in rat marrow stromal cell cultures. *J Cell Sci*. 1992 Jun;102 ( Pt 2):341-51.

[57] Canalis E, Giustina A. Glucocorticoid-induced osteoporosis: summary of a workshop. *J Clin Endocrinol Metab* 2001;86:5681 – 5.

[58] Patschan D, Loddenkemper K, Buttgereit F. Molecular mechanisms of glucocorticoid-induced osteoporosis. *Bone* 2001;29:498 – 505.

[59] Chen TL, Fry D. Hormonal regulation of the osteoblastic phenotype expression in neonatal murine calvarial cells. *Calcif Tissue Int* 1999; 64:304 – 9.

[60] Jaiswal RK, Jaiswal N, Bruder SP, Mbalaviele G, Marshak DR, Pittenger MF. Adult human mesenchymal stem cell differentiation to the osteogenic or adipogenic lineage is regulated by mitogen-activated protein kinase. *J Biol Chem*. 2000 Mar 31;275(13):9645-52.

[61] Barralet JE, Wang L, Lawson M, Triffitt JT, Cooper PR, Shelton RM: Comparison of bone marrow cell growth on 2D and 3D alginate hydrogels. *J Mater Sci Mater Med*, 2005. 16(6): 515-9.

[62] Grayson WL, Fröhlich M, Yeager K, Bhumiratana S, Chan ME, Cannizzaro C: Engineering anatomically shaped human bone grafts. *Proc Natl Acad Sci USA* 2010; 107(8):3299-304.

[63] Holtorf HL, Jansen JA, Mikos AG: Modulation of cell differentiation in bone tissue engineering constructs cultured in a bioreactor. *Adv Exp Med Biol* 2006; 585: 225-41.

[64] Liu C, Abedian R, Meister R, Haasper C, Hurschler C, Krettek C: Influence of

perfusion and compression on the proliferation and differentiation of bone mesenchymal stromal cells seeded on polyurethane scaffolds. *Biomaterials* 2012; 33(4): 1052-64.

[65] Kim J, Ma T: Perfusion regulation of hMSC microenvironment and osteogenic differentiation in 3D scaffold. *Biotechnol Bioeng* 2012; 109(1): 252-61.

[66] Lim JY, Loisel AE, Lee JS, Zhang Y, Salvi JD, Donahue HJ: Optimizing the osteogenic potential of adult stem cells for skeletal regeneration. *J Orthop Res* 2011; 29(11):1627-33.

[67] Glowacki J, Mizuno S: Collagen scaffolds for tissue engineering. *Biopolymers* 2008; 89(5): 338-44.

[68] Cartmell SH, Porter BD, García AJ, Guldberg RE: Effects of medium perfusion rate on cell-seeded three-dimensional bone constructs *in vitro*. *Tissue Eng* 2003; 9(6): 1197-203.

[69] Jaasma MJ, O'Brien FJ: Mechanical stimulation of osteoblasts using steady and dynamic fluid flow. *Tissue Eng Part A* 2008; 14(7):1213-23.

[70] Grayson WL, Bhumiratana S, Grace Chao PH, Hung CT, Vunjak-Novakovic G: Spatial regulation of human mesenchymal stem cell differentiation in engineered osteochondral constructs: effects of pre-differentiation, soluble factors and medium perfusion. *Osteoarthritis Cartilage* 2010; 18(5): 714-23.

[71] Ng KW, Leong DT, Hutmacher DW: The challenge to measure cell proliferation in two and three dimensions. *Tissue Eng*, 2005. 11(1-2): 182-91.

[72] Strehl R, Schumacher K, de Vries U, Minuth WW: Proliferating cells versus differentiated cells in tissue engineering. *Tissue Eng*, 2002. 8(1): 37042.

[73] Zhao F, and Ma T: Perfusion bioreactor system for human mesenchymal stem cell tissue engineering: dynamic cell seeding and construct development. *Biotechnol Bioeng*. 2005 Aug 20;91(4):482-93.

[74] Mygind T, Stiehler M, Baatrup A, Li H, Zou X, Flyvbjerg A, Kassem M, and Bunger C: Mesenchymal stem cell ingrowth and differentiation on coralline hydroxyapatite scaffolds. *Biomaterials*. 2007 Feb;28(6):1036-47.

[75] Holzwarth C, Vaegler M, Pfister SM, Handgretinger R, Kerst G, Muller I: Low physiologic oxygen tensions reduce proliferation and differentiation of human multipotent mesenchymal stromal cells. *BMC Cell Biol*. 2010 Jan 28;11:11.

- [76] Lynch MP, Capparelli C, Stein JL, Stein GS, Lian JB. Apoptosis during bone-like tissue development in vitro. *J Cell Biochem.* 1998 Jan 1;68(1):31-49.
- [77] Pelham RJ Jr, Wang YI. Cell locomotion and focal adhesions are regulated by substrate flexibility. *Proc Natl Acad Sci U S A.* 1997 Dec 9;94(25):136615-5.
- [78] Khatiwala CB, Peyton SR, Metzke M, Putnam AJ. The regulation of osteogenesis by ECM rigidity in MC3T3-E1 cells requires MAPK activation. *J Cell Physiol.* 2007 Jun;211(3):661-72.
- [79] Hsiong SX, Carampin P, Kong HJ, Lee KY, Mooney DJ. Differentiation stage alters matrix control of stem cells. *J Biomed Mater Res A.* 2008 Apr;85(1):145-56.
- [80] Engler AJ, Sen S, Sweeney HL, Discher DE. Matrix elasticity directs stem cell lineage specification. *Cell.* 2006 Aug 25;126(4):677-89.
- [81] Kim K, Dean D, Mikos AG, Fisher JP. Effect of initial cell seeding density on early osteogenic signal expression of rat bone marrow stromal cells cultured on cross-linked poly(propylene fumarate) disks. *Biomacromolecules.* 2009 Jul 13;10(7):1810-7.
- [82] Holy CE, Shoichet MS, Davies JE. Engineering three-dimensional bone tissue in vitro using biodegradable scaffolds: investigating initial cell-seeding density and culture period. *J Biomed Mater Res.* 2000 Sep 5;51(3):376-82.
- [83] Wilson CE, Dhert WJ, Van Blitterswijk CA, Verbout AJ, De Bruijn JD. Evaluating 3D bone tissue engineered constructs with different seeding densities using the alamarBlue assay and the effect on in vivo bone formation. *J Mater Sci Mater Med.* 2002 Dec;13(12):1265-9.
- [84] Siffert RS: The role of alkaline phosphatase in osteogenesis. *J Exp Med.* 1951 May;93(5):415-26.
- [85] Fraser HB, Hirsh AE, Giaever G, Kumm J, and Eisen MB: Noise minimization in eukaryotic gene expression. *PLoS Biol.* 2004, 137.
- [86] Moss DW: Release of membrane-bound enzymes from cells and the generation of isoforms. *Clin Chim Acta.* 1994 May;226(2):131-42.
- [87] Bancroft GN, Sikavitsast VI, van den Dolder J, Sheffield TL, Ambrose CG, Jansen JA: Fluid flow increases mineralized matrix deposition in 3D perfusion culture of marrow stromal osteoblasts in a dose-dependent manner. *Proc Natl Acad Sci U S A* 2002;99:12600–5.
- [88] Sikavitsas, V.I., Bancroft, G.N., Holtorf, H.L., Jansen, J.A., and Mikos, A.G.

Mineralized matrix deposition by marrow stromal osteoblasts in 3D perfusion culture increases with increasing fluid shear forces. *Proc Natl Acad Sci U S A* 100, 14683, 2003.

[89] Zhao, F., Chella, R., and Ma, T. Effects of shear stress on 3- D human mesenchymal stem cell construct development in a perfusion bioreactor system: experiments and hydrody- namic modeling. *Biotechnol Bioeng* 96, 584, 2007.

[90] Mueller, S.M., Mizuno, S., Gerstenfeld, L.C., and Glowacki, J. Medium perfusion enhances osteogenesis by murine osteosarcoma cells in three-dimensional collagen sponges. *J Bone Miner Res* 14, 2118, 1999.

[91] Vehof JW, de Rujiter AE, Spauwen PH, Jansen JA. Influence of rhBMP-2 on rat bone marrow stromal cells cultured on titanium fiber mesh. 2001, *Tissue Eng* 7:373-383.

[92] Mark, M.P.& Butler, W.T.& Prince, C.W.& Finkelman, R.D.& Ruch, J.V., Developmental expression of 44-kDa bone phosphoprotein (osteopontin) and bone gamma-carboxyglutamic acid (Gla)-containing protein (osteocalcin) in calcifying tissues of rat, *Differentiation: Research in Biological Diversity*, vol. 37, 2, 1988, p.123-136.

[93] Donahue TL, Haut TR, Yellowley CE, Donahue HJ, Jacobs CR: Mechanosensitivity of bone cells to oscillating fluid flow induced shear stress may be modulated by chemotransport. *J. Biomech.*, 36 (2003), pp. 1363–137.

[94] Riddle RC, Hippe KR, Donahue HJ: Chemotransport contributes to the effect of oscillatory fluid flow on human bone marrow stromal cell proliferation. *J. Orthop. Res.*, 26 (2008), pp. 918–924.

[95] Santerre JP, Woodhouse K, Laroche G, Labow RS. Understanding the biodegradation of polyurethanes: from classical implants to tissue engineering materials. *Biomaterials*. 2005 Dec;26(35):7457-70.

[96] Zanetta M, Quirici N, Demarosi F, Tanzi MC, Rimondini L, Farè S. Ability of polyurethane foams to support cell proliferation and the differentiation of MSCs into osteoblasts. *Acta Biomater*. 2009 May;5(4):1126-36.

[97] Cancedda R, Mastrogiacomo M, Bianchi G, et al. 2003; Bone marrow stromal cells and their use in regenerating bone. *Novartis Found Symp* 249: 133–143

- [98] Grundel RE, Chapman MW, Yee T, Moore DC. 1991; Autogeneic bone marrow and porous biphasic calcium phosphate ceramic for segmental bone defects in the canine ulna. *Clin Orthop* 266: 244–258.
- [99] Bruder SP, Kraus KH, Goldberg VM, Kadiyala S. 1998; The effect of implants loaded with autologous mesenchymal stem cells on the healing of canine segmental bone defects. *J Bone Joint Surg Am* 80: 985–996.
- [100] Ma PX, Zhang R, Xiao G, Franceschi R. 2001; Engineering new bone tissue in vitro on highly porous poly( $\alpha$ -hydroxyl acids)/hydroxyapatite composite scaffolds. *Biomed Mater Res* 54(2): 284–293.
- [101] Kim HW, Kim HE, Salih V. 2005; Stimulation of osteoblast responses to biomimetic nanocomposites of gelatin–hydroxyapatite for tissue engineering scaffolds. *Biomaterials* 26(25): 5221–5230.
- [102] de Peppo GM, Palmquist A, Borchardt P, Lennerås M, Hyllner J, Snis A, Lausmaa J, Thomsen P, Karlsson C. Free-form-fabricated commercially pure Ti and Ti6Al4V porous scaffolds support the growth of human embryonic stem cell-derived mesodermal progenitors. *ScientificWorldJournal*. 2012;2012:646417.

# Chapter 4: Mechanical stimulation of mesenchymal stem cells in a 3D glass scaffold using oscillatory and unidirectional flow

## 4.1 Introduction

The combination of hMSCs and 3D scaffolds has become an attractive approach to creating functional constructs for therapeutic outcomes and correcting critical bone defects [1]. For this reason bioreactors play a vital role in the development of 3D constructs as they provide an instructive stimulus and regulate the cell growth environment [2]. Bioreactors such as rotating wall vessels and spinner flasks have been extensively reviewed and investigated in the field of bone tissue engineering [3]. These bioreactors increase homogeneity of nutrient distribution only on the surface of constructs. Bioreactors which subject direct perfusion through the constructs have the ability to expose cells throughout the scaffold to the interstitial fluid flow as opposed to cells only on the exterior of the construct [2]. The outcome is that these flow configurations create different cellular and biochemical microenvironments in the 3D constructs [4-6].

Bone cells *in vivo* are believed to be subjected to two forms of fluid shears stress at the cellular level; an outward radial unidirectional flow, driven by a hydrostatic pressure drop across the cortex [7] and an oscillatory flow induced by mechanical loading [8]. 2D flow chamber studies have shown an osteogenic response of bone cells when subjected to unidirectional flow by increasing the amounts of ALP [9] and expression of osteocalcin [10].

3D constructs have also been subjected to unidirectional fluid flow whereby the media is forced through the interconnected pores of the scaffold, which continuously removes waste and introduces fresh nutrients, as well as applying a

physical stimulus by the shear stress [11]. Studies that incorporated unidirectional flow have had a positive effect on osteogenic differentiation by increasing the amount of PGE2 [12] and mineralised matrix production [13] on MSCs in 3D scaffolds. *Botchwey et al.*, cultured cells on 3D scaffold and demonstrated that subjecting constructs to unidirectional flow (interior flow velocity  $1 \times 10^{-3}$  and  $1 \times 10^{-2}$  cm/s) significantly increased cell growth in the interior as well as retaining osteoblastic phenotype as measured by ALP activity [14].

*Wang et al.*, investigated the osteogenic differentiation of bone marrow-derived osteoblasts (BMOs) in porous ceramics (dimensions:  $5 \times 5 \times 5$  mm<sup>3</sup>, porosity: 75%, pore size: 100 to 400  $\mu$ m) under dynamic conditions. Constructs were subjected to a continuous flow rate of 2 ml/hr by a peristaltic pump and the ALP activity and OCN content were measured at the end of 1, 2, 3, and 4 weeks of subculture. The results demonstrated that levels of ALP activity and OCN in groups subjected to flow were significantly higher in comparison to static culture [15]. *Sikavitsas et al.*, seeded rat bone marrow stromal cells in 3D porous titanium fiber mesh disk scaffolds (diameter = 10 mm, thickness = 0.8 mm, porosity = 86%, average pore size = 250  $\mu$ m) and cultured for up to 16 days in a flow perfusion bioreactor. The study involved perfusing culture media of different viscosities through the construct, whilst maintain a constant flow rate of 0.3 ml/min. It was shown that increasing the viscosity led to an increase in mineral deposition with a better spatially distributed extracellular matrix inside the 3D scaffolds in comparison to static conditions [16].

Previous 2D experiments have shown that the application of oscillatory fluid flow has biological effects on cultured bone cells such as increased osteopontin expression [17-21]. However few studies have examined the effect of oscillatory flow on cell-seeded scaffolds and fewer have also directly compared the two flow types with respect to cell distribution, cell proliferation and osteogenic differentiation. Where this has been studied it has mostly been using bone cell lines such as MC3T3. *O'Brien et al.*, designed a novel flow perfusion bioreactor that can hold up to six constructs and can be cultured simultaneously. Osteoblast-seeded collagen-GAG scaffold discs (diameter = 12.7 mm, thickness =

3.5 mm, pore diameter = 95  $\mu\text{m}$ , porosity  $\sim 99\%$ ) were subjected to steady, pulsatile and oscillatory flow (0.1-2.0 ml/min). It was demonstrated that cell-seeded scaffolds under dynamic culture maintained cell viability and that mechanical stimulation led to an 800-1200% increase in PGE2 production in comparison to static culture [22]. In a follow up study, *O'Brien et al.*, and researchers investigated the effects of intermittent steady (1 ml/min), pulsatile (0–1.0 mL/min at 2 Hz), and oscillatory ( $\pm 1.0$  mL/min at 1 Hz) fluid flow on MC3T3-E1 activity with the same collagen-GAG scaffold. Cell-seeded scaffolds were analysed after 1, 25 and 49 hours of continuous flow or static culture. Results indicated that scaffolds subjected to fluid flow (regardless of flow profile) had a 40% to 52% decrease in cell number. However, cellular spatial distribution was much improved for cell-seeded scaffolds subjected to fluid flow. In addition, the mechanical stimulation induced the production of early stage bone formation markers including COX-2, PGE2 and OPN. It was also suggested that oscillatory and pulsatile fluid flow could be more stimulatory for long-term bioreactor culture compared to steady flow however there were no strong differences between oscillatory and pulsatile flow [23].

In a similar study, mouse osteoblast-like MC3T3-E1 were seeded onto porous ceramic scaffolds (diameter = 10 mm, height = 8 mm, porosity = 75%) and cultured *in vitro* for 6 days under oscillatory (0.5 and 1 ml/min), unidirectional (1 ml/min) and static conditions. The results demonstrated that cells proliferated on the scaffold surface in static culture. The proliferation for samples subjected to unidirectional flow was significantly higher than other groups but was very inhomogeneous. Only samples subjected to oscillatory fluid flow displayed a uniform distribution of cells throughout the scaffolds with an increase in ALP activity [24].

Since an important function of a bioreactor system is to create a suitable microenvironment for the development of functional 3D constructs, understanding the effects of flow on hMSC phenotype can provide further insight for engineering 3D bone constructs. For this reason the aim of this chapter was to investigate the effect of different flow regimes, oscillatory and unidirectional flow, for stimulating proliferation and osteogenic differentiation of Human

Embryonic Mesenchymal Progenitor (hES-MP) cells seeded on 3D glass scaffolds. Furthermore, two types of perfusion flow will also be investigated including parallel flow (PF, where the scaffold is positioned in the horizontal plane) and transverse flow (TF, where the scaffold is positioned in the vertical plane). A study of the difference in biological effects between these two types would be important not only for the design of a bioreactor but will provide useful information on how bone cells respond to different flow conditions for the creation of a clinically effective engineering bone tissue.

## 4.2 Dynamic culture of hES-MP cells on glass scaffold

### 4.2.1 Methodology

The human embryonic cell-derived mesenchymal progenitor cell line (hES-MP) was used between passages 3-7 for all assays. Glass scaffolds (12 mm x 3 mm, 60% porosity, 100-500  $\mu\text{m}$  pore size) were seeded with 250,000 cells using the seeding and culture methods described in chapter 2. Cell-seeded scaffolds were cultured in standard culture media and supplemented with AA,  $\beta\text{GP}$  and DEX. Fluid flow was applied using the oscillatory (chapter 2, figure 2.3) and unidirectional pump (chapter 2, figure 2.4) at a frequency of 1 Hz for a loading period of 1 hour with three different flow rates (3, 5 and 10 ml/min). Cell-seeded scaffolds in static culture remained in 24 well-plates, whilst scaffolds subjected to fluid flow were either placed in the horizontal plane (fig 4.1a, whereby the direction of flow is parallel to the scaffold surface) or positioned in the vertical plane (fig 4.1b, whereby direction of flow is perpendicular to the scaffold surface) within the conduit. The conduit consisted of 2 silicone rubber tubes (10 mm in diameter, 120 mm in length), which were inserted into a wider tube (12 mm in diameter) to sandwich and hold the scaffold in place before placing it in the circuit. The length of the inlet tube was determined from theoretical calculations required to ensure a fully developed laminar flow as described in chapter 2. Prior to setup, the conduit and all tubing was sterilised overnight with 70% ethanol and washed with PBS.

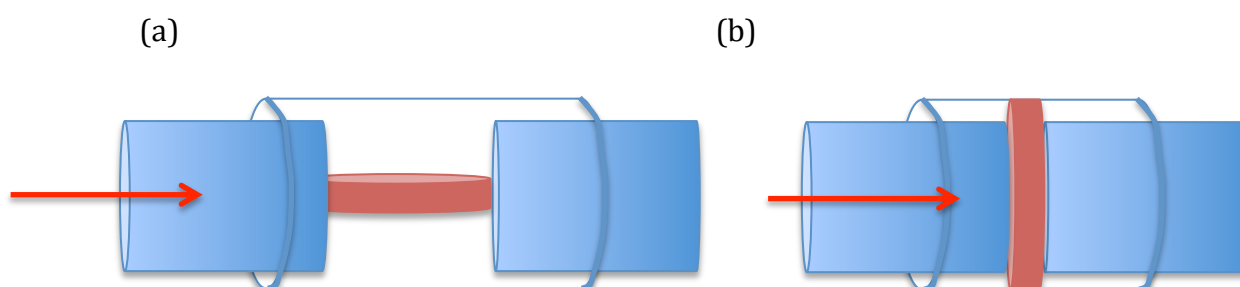


Fig 4.1; Scaffolds where subjected to fluid flow whilst positioned in two different planes. (a) Horizontal plane (parallel flow, whereby the direction of flow is parallel to scaffold surface), (b) vertical plane (transverse flow, whereby direction of flow is perpendicular to scaffold surface). Arrows indicate direction of flow.

In short-term dynamic culture, samples were subjected to fluid flow on day 4 and analysed for cell viability (MTS and MTT), total DNA content and ALP activity on day 7 (figure 4.2a). In long-term culture, samples were subjected to fluid flow on day 4, 7, 10 and analysed for cell viability (MTS), collagen production, and calcium deposition on day 14 (figure 4.2b). Between loading sessions, cell-seeded scaffolds were cultured statically in an incubator in standard conditions. The experiment was conducted three times (N=3) with 2 scaffolds (n=2) for each condition. Results presented in this chapter were normalised to static conditions and a one-way ANOVA followed by Tukey's post-hoc test were performed. Results are expressed as mean  $\pm$  standard deviation.

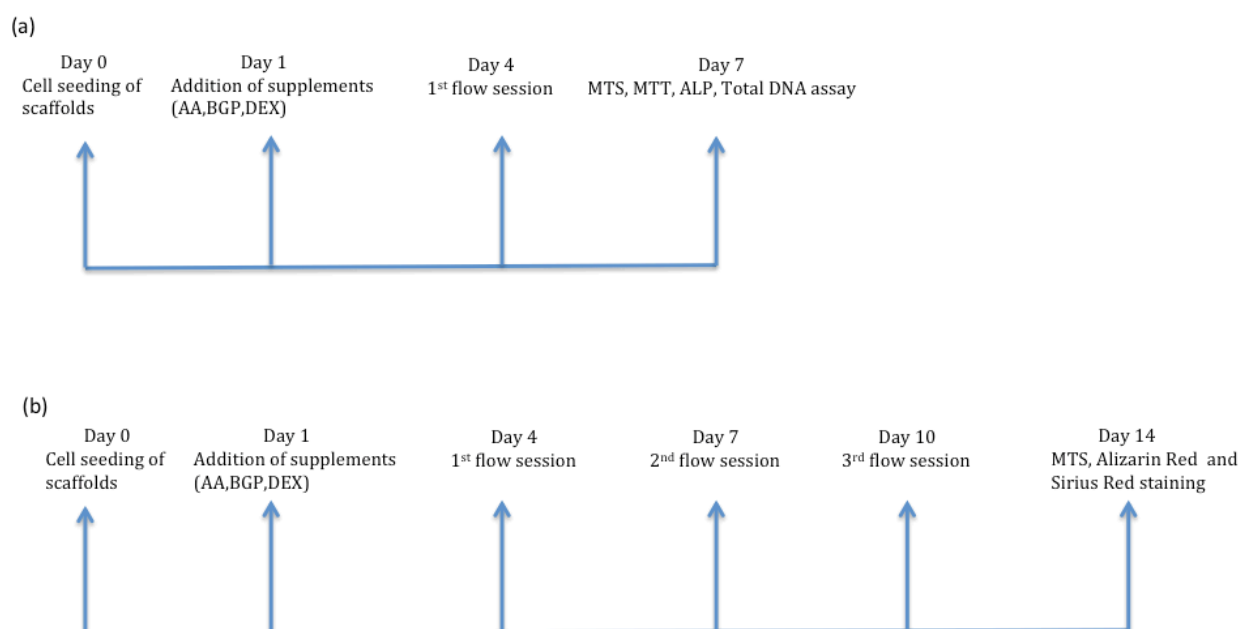


Figure 4.2; The experimental time line. (a) Short term dynamic culture, samples were subjected to flow on day 4 of culture and assayed for cell viability (MTS, MTT), total DNA content and ALP activity on day 7. (b) Long term dynamic culture, samples were subjected to flow on days 4, 7 and 10 and assayed for cell viability (MTS), collagen production (SR) and calcium deposition (AR) on day 14.

## 4.3 Results

### 4.3.1 Cell viability as assayed by MTT – Day 7

As shown in figure 4.3, the qualitative study of cell viability confirms the findings of uniform cell distribution across the glass scaffolds under perfusion flow. Scaffolds subjected to flow displayed higher cell viability than static conditions, except for scaffolds subjected to a transverse unidirectional flow of 10 ml/min (fig 4.3b). Although it is very difficult to distinguish which condition created the most uniform distribution, it is quite clear that scaffolds subjected to 3 and 5 ml/min perfusion flow have a higher cell viability as indicated by a stronger purple staining than other conditions (fig 4.3a).

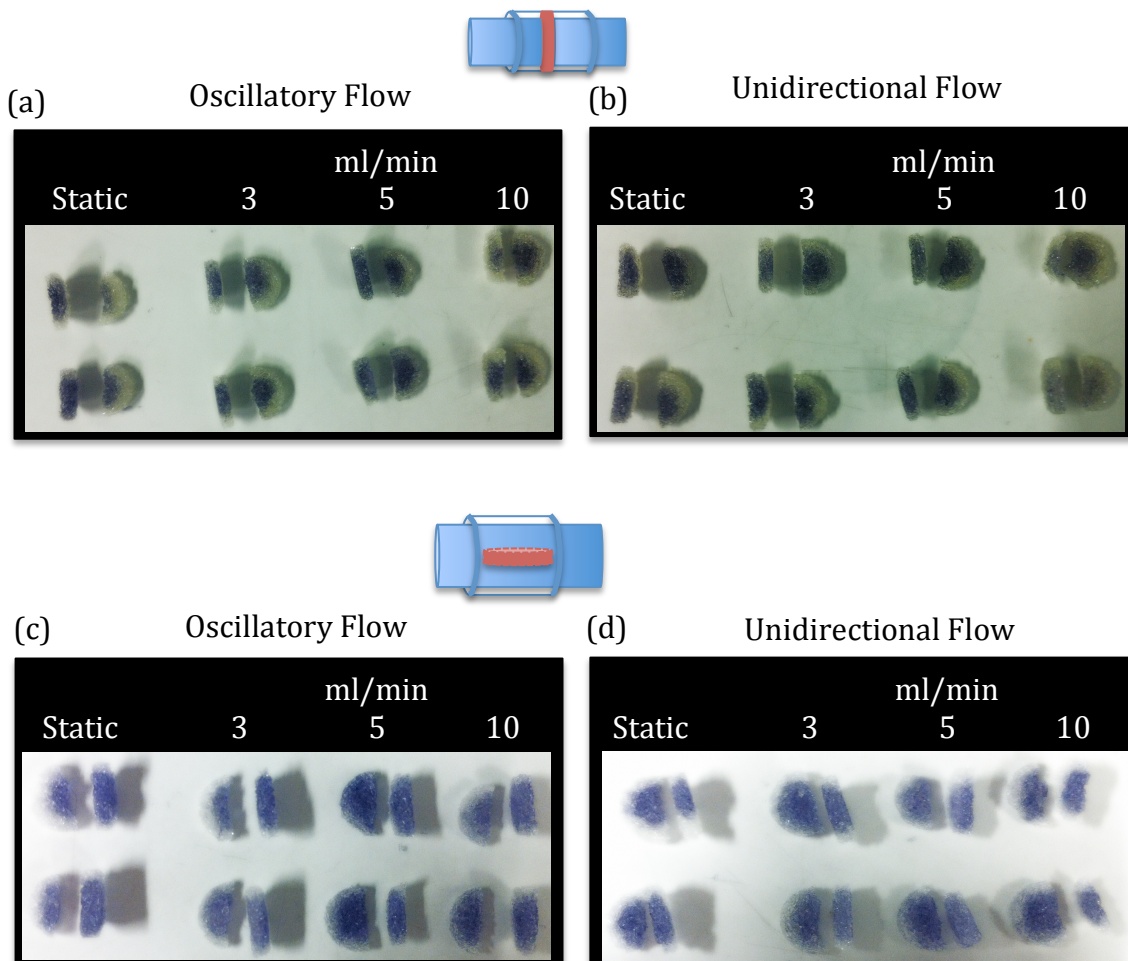


Fig 4.3; hES-MP cells cultured on glass scaffolds and subjected to 3, 5 and 10 ml/min fluid flow (unidirectional and oscillatory) on day 4. On day 7 of culture, samples were analyzed for cell viability (MTT) for cell-seeded scaffolds subjected to (a) transverse oscillatory flow, (b) transverse unidirectional flow, (c) parallel oscillatory flow and (d) parallel unidirectional flow.

#### 4.3.2 Cell viability as assayed by MTS – Day 7 & 14

From figure 4.4a and 4.5a it is evident that on day 7 of culture, samples subjected to transverse oscillatory flow exhibited much higher ( $p < 0.05$ ) cell viability than static culture. More specifically, cell-seeded scaffolds subjected to a transverse oscillatory flow of 5 ml/min demonstrated a significantly ( $P < 0.05$ ) higher MTS value than other samples subjected to transverse oscillatory flow. hES-MP-constructs subjected to a transverse unidirectional flow of 3 ml/min also exhibited a much higher ( $P < 0.05$ ) cell viability than static and other samples subjected to transverse unidirectional flow. Furthermore, cell-seeded scaffolds subjected to a transverse oscillatory flow of 5 ml/min showed significantly higher ( $P < 0.05$ ) cell viability than samples subjected to a transverse unidirectional flow of 5 ml/min.

On day 14 of culture (fig 4.4a and 4.5a), cell viability was significantly higher ( $P < 0.05$ ) for cell-seeded scaffolds subjected to a transverse oscillatory flow of 5 and 10 ml/min in comparison to static and samples subjected to 3 ml/min transverse oscillatory flow. hES-MP-constructs under transverse unidirectional flow of 3 and 10 ml/min, displayed a 10% and 12 % decrease in cell viability in comparison to static conditions. Samples subjected to a transverse oscillatory flow rate of 3, 5 and 10 ml/min, displayed significantly higher ( $P < 0.05$ ) cell viability than samples under transverse unidirectional flow of 3, 5 and 10 ml/min respectively.

Scaffolds subjected to parallel flow did not demonstrate such high cell viability as with the transverse flow group (fig 4.4b and 4.5b). On day 7 of culture, cell-seeded scaffolds subjected to a parallel oscillatory flow of 3 and 10 ml/min displayed significantly higher ( $P < 0.05$ ) cell viability than samples under parallel unidirectional flow of 3 and 10 ml/min respectively. On day 14 of culture (fig 4.4b and 4.5b), samples in all flow groups did not show any significant increase in cell viability with respect to samples in static conditions.

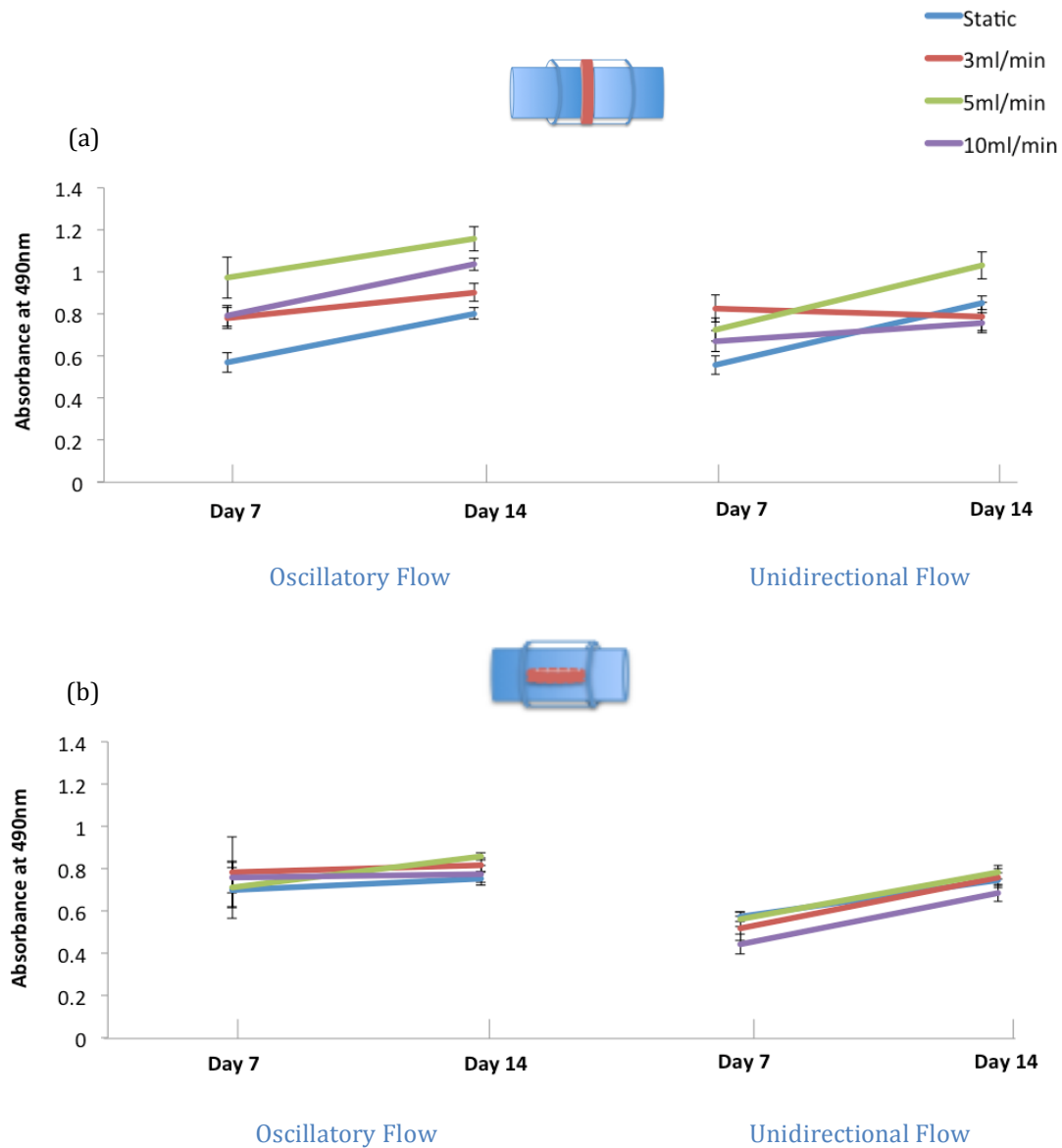


Fig 4.4; Non-normalised (raw) data for hES-MP cells cultured on glass scaffolds and subjected to 3, 5 and 10 ml/min fluid flow (unidirectional and oscillatory). On day 7 and 14 of culture, samples were analyzed for cell viability (MTS, normalized to static conditions) for constructs under (a) transverse flow and (b) parallel flow. All data is mean  $\pm$  SD (n=6). Lines are used to link the two data points for ease of visualization and are not intended to imply continuous data.

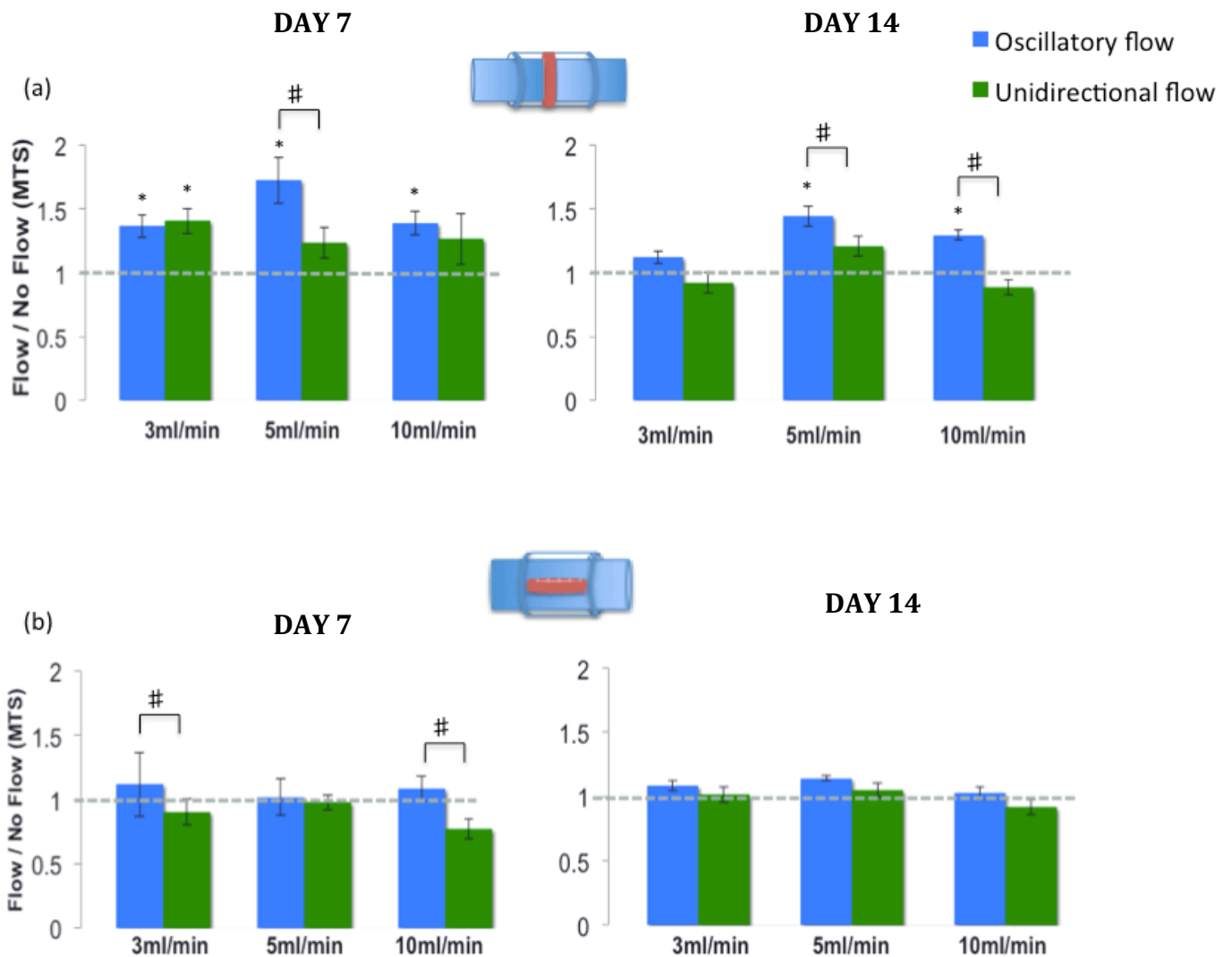


Fig 4.5; hES-MP cells cultured on glass scaffolds and subjected to 3, 5 and 10 ml/min fluid flow (unidirectional and oscillatory). On day 7 and 14 of culture, samples were analyzed for cell viability (MTS, normalised to static conditions) for constructs under (a) transverse flow and (b) parallel flow. \*= Significantly different compared to static culture (dashed line) and #=Significantly different to corresponding flow rate. All data is mean  $\pm$  SD (n=6).

#### 4.3.3 Total DNA content – Day 7

From figure 4.6a, it is clear that cell-seeded scaffolds subjected to a transverse oscillatory flow of 3 and 5 ml/min had a much higher ( $p < 0.05$ ) DNA content than those of static culture. It is also evident that the same samples subjected to transverse oscillatory flow of 3 and 5 ml/min, showed significantly higher ( $P < 0.05$ ) total DNA content than samples under 3 and 5 ml/min transverse

unidirectional flow. hES-MP constructs subjected to parallel oscillatory flow exhibited higher DNA content than static conditions (fig 4.6b). More specifically, scaffolds subjected to a parallel oscillatory flow of 5 ml/min significantly ( $P<0.05$ ) had a higher DNA content than static culture. Furthermore, Samples subjected to a transverse oscillatory flow rate of 3, 5 and 10 ml/min, displayed significantly higher ( $P<0.05$ ) total DNA content than samples under transverse unidirectional flow of 3, 5 and 10 ml/min respectively.

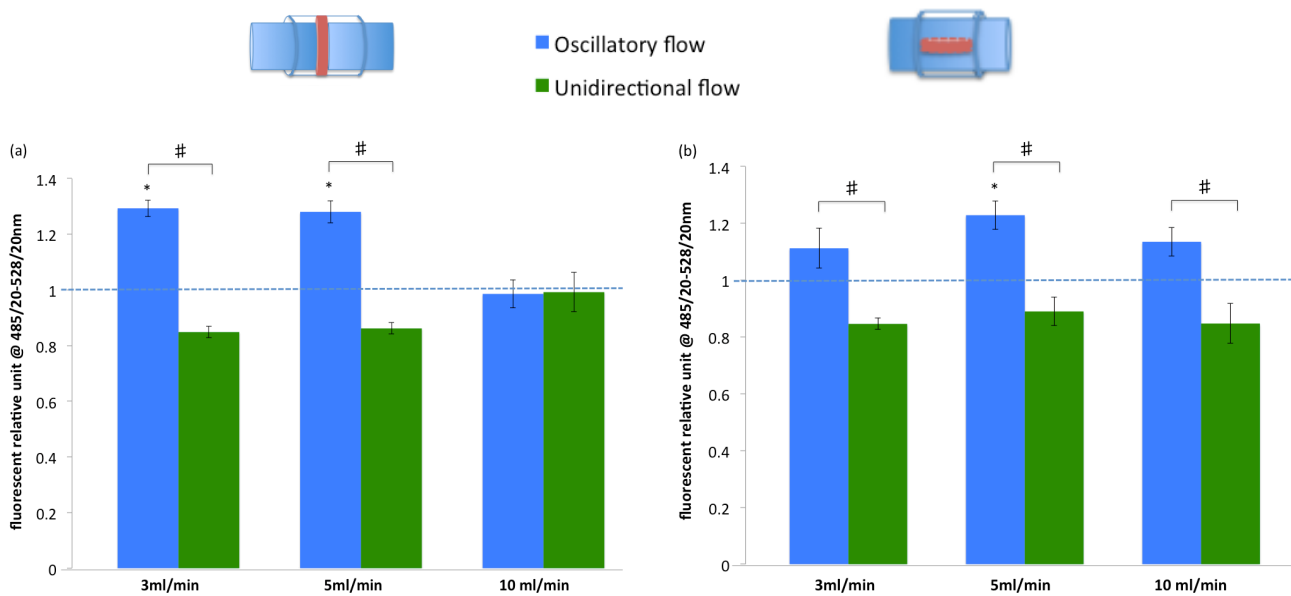


Fig 4.6; hES-MP cells cultured on glass scaffolds and subjected to 3, 5 and 10 ml/min fluid flow (unidirectional and oscillatory) on day 4. On day 7 of culture, total DNA content (normalised to static conditions) was measured for cell-seeded scaffolds under (a) transverse flow and (b) parallel flow. \*= Significantly different compared to static culture (dashed line) and #=Significantly different to corresponding flow rate. All data is mean  $\pm$  SD ( $n=6$ ).

#### 4.3.4 ALP activity – Day 7

In general, cell-seeded scaffolds subjected to transverse perfusion (oscillatory and unidirectional) exhibited higher ALP activity than static culture. More specifically, scaffolds subjected to transverse oscillatory and unidirectional flow of 5 ml/min demonstrated significantly ( $P<0.05$ ) higher ALP activity in comparison to static culture (fig 4.7a). Scaffolds subjected to parallel flow also

had a higher ALP activity than static culture. Although not significant, but the highest value of ALP activity was 13% more than the static group and was seen in constructs subjected to a unidirectional flow of 3 ml/min (fig 4.7b).

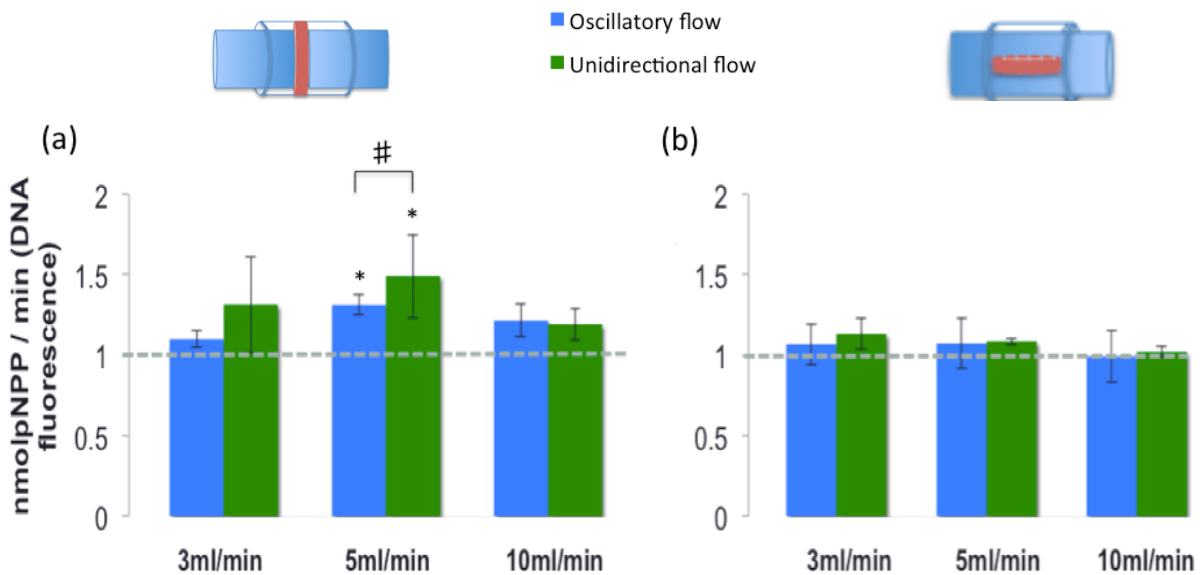


Fig 4.7; hES-MP cells cultured on glass scaffolds and subjected to 3, 5 and 10 ml/min fluid flow (unidirectional and oscillatory) on day 4. On day 7 of culture, ALP activity (normalised to DNA) was measured for cell-seeded scaffolds under (a) transverse flow and (b) parallel flow. \*= Significantly different compared to static culture (dashed line) and #=Significantly different to corresponding flow rate. All data is mean  $\pm$  SD (n=6).

#### 4.3.5 Collagen production (Sirius red staining) – Day 14

In general, transverse perfusion increased collagen production for samples subjected to a flow rate of 3 and 5 ml/min. More specifically, hES-MP-constructs subjected to transverse oscillatory flow of 5 ml/min produced significantly higher ( $P < 0.05$ ) collagen in comparison to static culture (fig 4.8a). From the data it is clear that a large variance exists in collagen production for samples subjected to transverse unidirectional flow. Similarly, cell-seeded scaffolds subjected to parallel oscillatory flow also produced more collagen than static culture. Samples under parallel oscillatory flow of 5 ml/min produced much higher ( $P < 0.05$ ) collagen in comparison to static conditions (fig 4.8b).

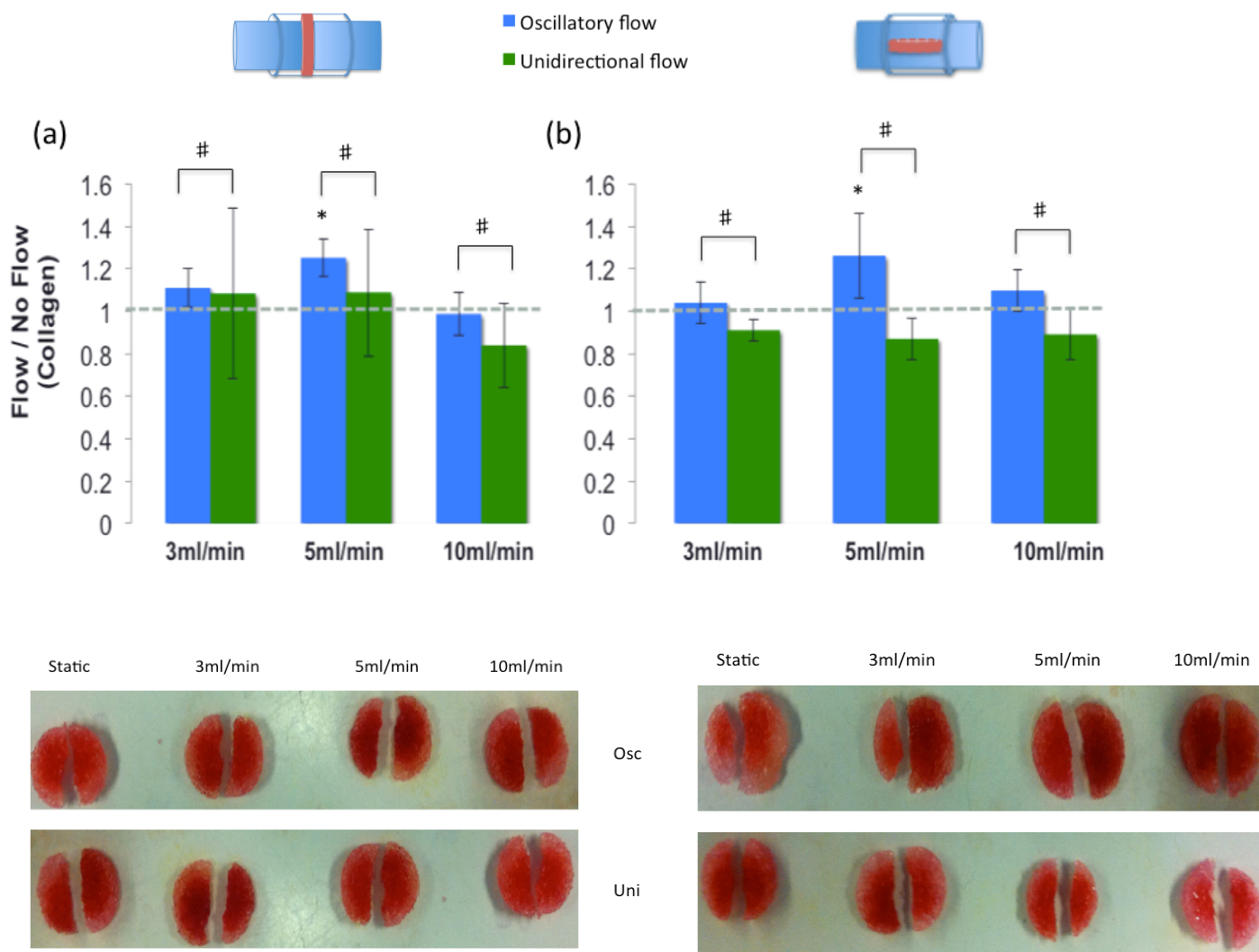


Fig 4.8; hES-MP cells cultured on glass scaffolds and subjected to 3, 5 and 10 ml/min fluid flow (unidirectional and oscillatory) on day 4, 7 and 10. On day 14 of culture, samples were analysed for collagen production (Sirius red) for constructs under (a) transverse flow and (b) parallel flow. Cell-seeded scaffolds stained with Sirius red provide a qualitative measure of collagen production for different flow conditions. \*= Significantly different compared to static culture (dashed line) and #=Significantly different to corresponding flow rate. All data is mean  $\pm$  SD (n=6).

#### 4.3.6 Calcium deposition (Aliarin red staining) – Day 14

It is interesting to note that the pattern for calcium deposition for both flow types (oscillatory and unidirectional) was very similar for all flow groups when subjected to either transverse or parallel flow. More specifically, scaffolds subjected to a transverse oscillatory flow of 3 and 5 ml/min deposited 119% and 370% more calcium than static cultures ( $p < 0.05$ ) (fig 4.9a). Scaffolds subjected to a transverse unidirectional flow of 5 ml/min also deposited a much higher amount of calcium ( $p < 0.05$ ) than static conditions. Furthermore, Samples subjected to a transverse oscillatory flow rate of 3 and 5 ml/min, displayed significantly higher ( $P < 0.05$ ) calcium deposition than samples under transverse unidirectional flow of 3 and 5 ml/min respectively.

Similarly, cell-seeded scaffolds subjected to a parallel oscillatory flow of 3 and 5 ml/min deposited 154% and 377% more calcium ( $p < 0.05$ ) in comparison to static conditions respectively (fig 4.9b). Furthermore, samples subjected to a parallel oscillatory flow rate of 3 and 5 ml/min, displayed significantly higher ( $P < 0.05$ ) calcium deposition than samples under parallel unidirectional flow of 3 and 5 ml/min respectively.

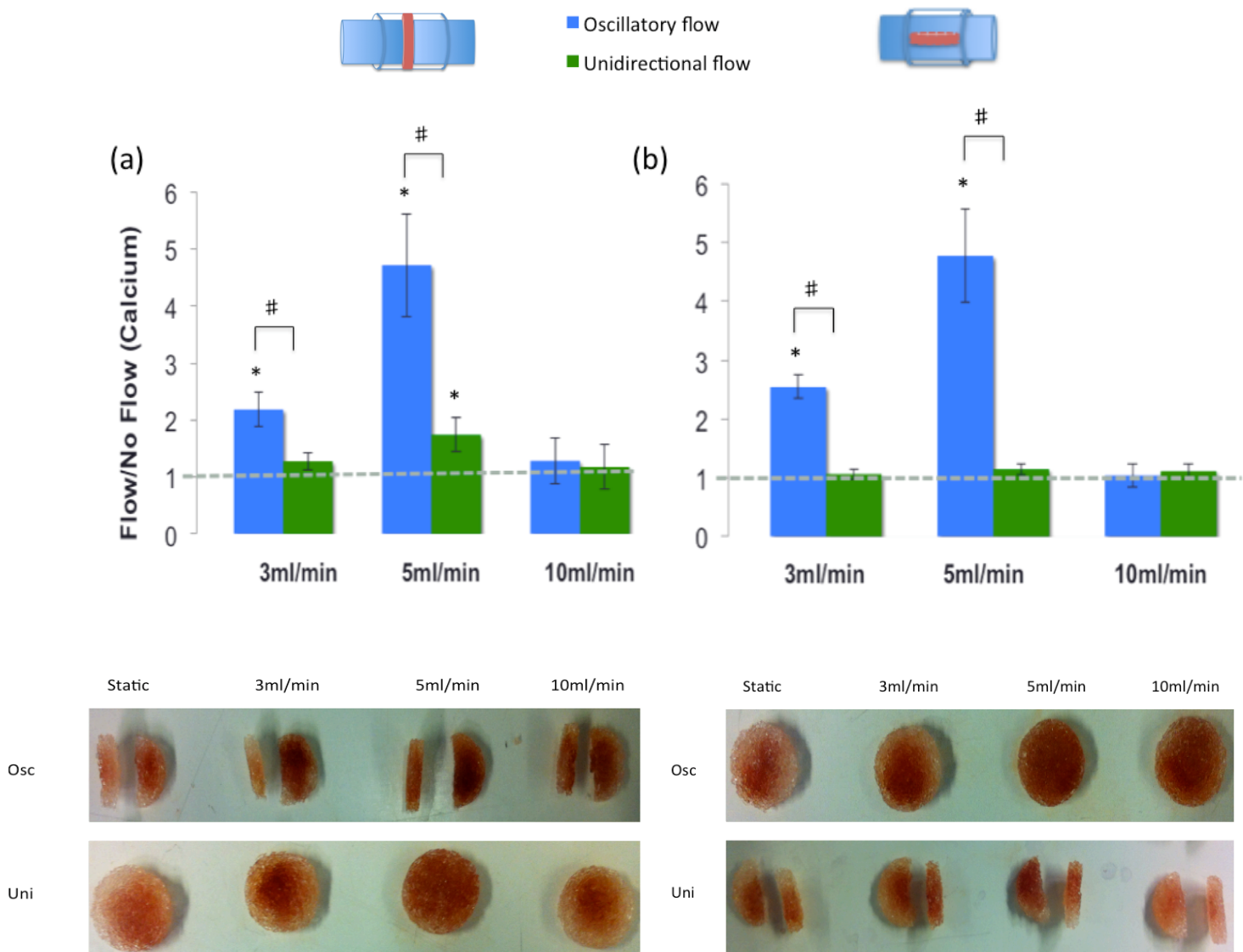


Fig 4.9; hES-MP cells cultured on glass scaffolds and subjected to 3, 5 and 10 ml/min fluid flow (unidirectional and oscillatory) on day 4, 7 and 10. On day 14 of culture, samples were analysed for calcium deposition (Alizarin red) for constructs under (a) transverse flow and (b) parallel flow. Cell-seeded scaffolds stained with Alizarin red provide a qualitative measure of calcium content for different flow conditions. \*= Significantly different compared to static culture (dashed line) and #=Significantly different to corresponding flow rate. All data is mean  $\pm$  SD (n=6).

#### 4.3.7 Day 14: Live/dead staining

A live/dead staining technique (described in chapter 2) was used to compare the location and attachment of viable and dead cells on three different sections within the glass scaffold for the different experimental setups. Images were taken from the top, cross-section and bottom of the constructs (fig 4.10). There were more dead cells visible (stained as red) in the cross section cells grown in static conditions. As where this does not seem to be apparent for scaffolds subjected to flow. In the unidirectional perfusion system, cells spread uniformly but living cells favored the top surface of the scaffold and more dead cells were visible at the bottom surface. Constructs subjected to oscillatory fluid flow displayed a uniform cell distribution with fewer dead cells visible in the bottom surface of the scaffold.

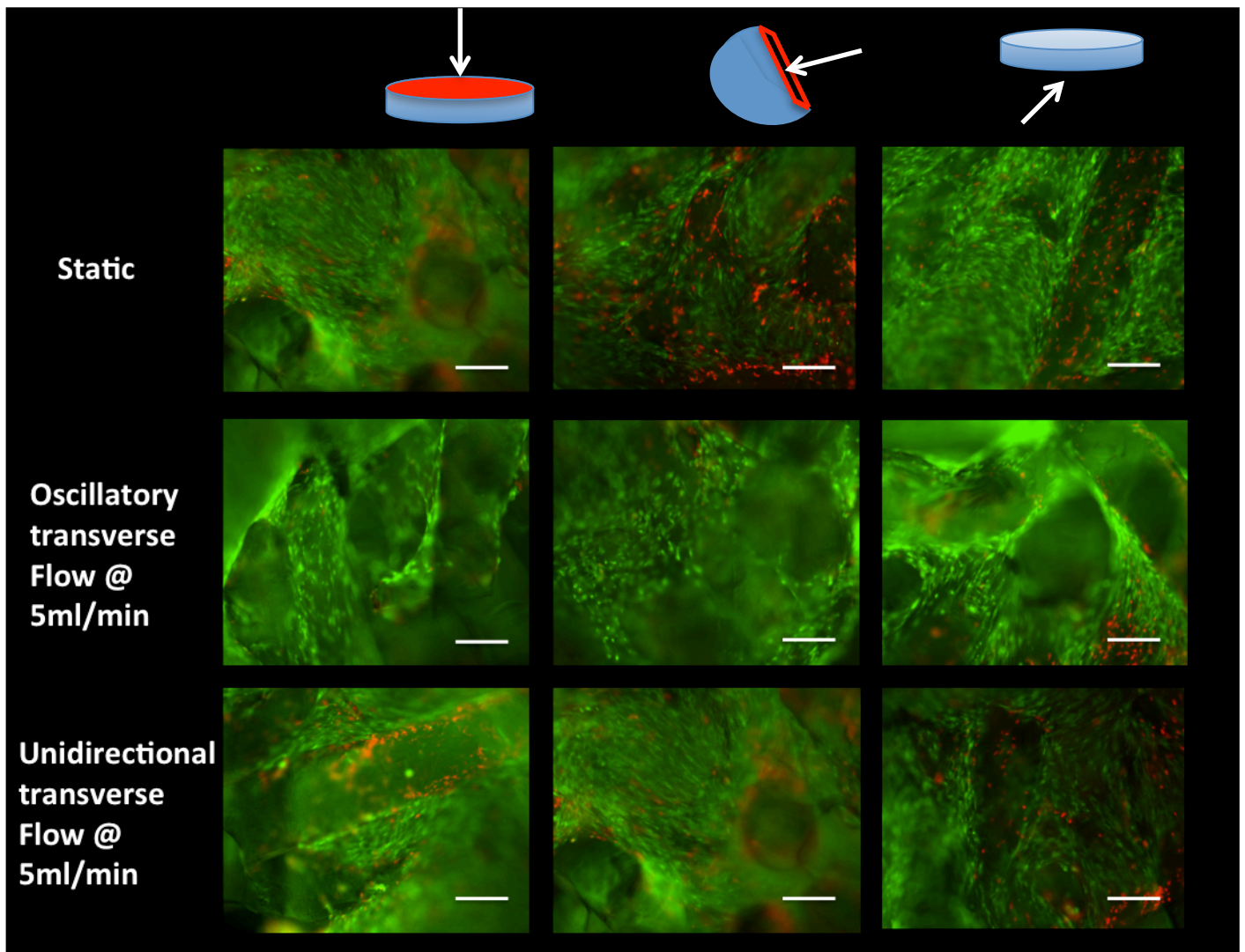


Fig 4.10; hES-MP cells cultured on glass scaffolds and distribution was analysed using Live/Dead imaging technique for samples under static, transverse oscillatory flow of 5 ml/min, and transverse unidirectional flow of 5 ml/min on day 14 of culture. Images were taken from the top, middle and bottom location of cell-seeded scaffolds. Live cells are stained as green and dead cells are stained as red. Representative images are shown (n=2). Scale bar = 200  $\mu$ m.

#### 4.4 Discussion

Numerous studies have investigated the effect of fluid flow on cell cultures. The effect of mechanical stimulation has been analysed in 2D [9, 18, 19, 25-27] and in 3D [11, 12, 16, 28, 29] *in vitro* conditions.

The aim of this study was to examine flow type and scaffold orientation on a human mesenchymal stem cell line (hES-MP) seeded on a novel glass scaffold. Constructs were subjected either to oscillatory, unidirectional or no flow upto a period of 14 days to compare the biological outcomes for each condition. To this end it was shown that short bouts of transverse oscillatory flow ensures cell survival, proliferation and osteogenic differentiation of hES-MP cells inside a porous glass scaffold.

Although short bouts of flow were beneficial for cell growth and survival, transverse flow seems to accelerate the early stages of bone formation in comparison to parallel flow. Due to a simple mechanical design of the system, transverse flow forces fluid through the construct thus creating a more homogenous environment, rather than just improving convection at the scaffold surface. The reason could be that this setup will allow a biomechanical stimulus to be applied to cells throughout the entire structure of the scaffold. Therefore the applied shear stress leads to a better cell survival and proliferation of hES-MP cells.

Overall, cell-seeded scaffolds subjected to transverse flow appeared more uniformly distributed than samples subjected to parallel flow as seen by the MTT staining on day 7 of culture (fig 4.3). Although from the images it is difficult to make a direct comparison between oscillatory and unidirectional flow samples, it does appear that hES-MP-constructs subjected to 5 ml/min transverse flow seem to have the highest cell viability as indicated by a stronger purple staining (fig 4.3a & 4.3b). On the other hand, samples subjected to 10 ml/min transverse flow (fig 4.3b) had a very light purple staining implying that the shear stress created might have been too high and as a result cells were washed from the scaffold, as seen by other research groups for different scaffold type [11]. Samples under

static conditions appeared to have an inhomogeneous cell distribution with a high density of cells in the core part of the scaffold and very few cells in the outer regions. During the seeding phase cells were directly pipetted onto the glass scaffolds, which probably led to a higher density of cells in the centre/core of the scaffold than the periphery.

From the MTS data it appears that scaffold orientation (TF vs PF) had an effect on cell viability. In transverse flow, it is evident that samples subjected to oscillatory flow had much higher cell viability than static and unidirectional flow groups (fig 4.4a and 4.5a). More specifically, it appears that cell activity was highest for samples under oscillatory flow rate of 5 ml/min. The cell viability data for cell-seeded scaffolds under transverse oscillatory flow were also in agreement with the total DNA content (fig 4.6a), implying that the metabolic activity and total cell number are correlated in this system. MTS was slightly higher at day 14 than day 7 indicating that the cells also proliferated over time in culture, however the change between day 7 and day 14 was rather small, probably because of the high initial seeding density. The higher cell numbers in oscillatory transverse flow groups compared to their static counterparts on day 7 indicates that oscillatory flow either increased the proliferation rate or reduced cell death during that first week of culture. A more specific assay such as the cell proliferation assay bRDU would be needed to determine which of these had occurred. Other research groups have also reported on the same findings whereby the application of flow has increased cell viability, however these groups used longer flow durations, different loading times and different scaffolds [13, 30, 31]. It is interesting that such short times in dynamic culture (3 hours within a 14 day culture period) also has a significant effect on cell viability. The effect of flow on viability was more apparent at day 7 than day 14 for example only samples subjected to transverse oscillatory flow of 5 and 10 ml/min had higher MTS values than static controls. Whereas the low flow rate of 3 ml/min had been sufficient to induce higher cell numbers by day 7 in transverse flow both oscillatory and unidirectional, those cell numbers did not increase between day 7 and 14 and therefore cell numbers equalised with static controls. This 7-14 day period resembles later osteoblastic differentiation and matrix

mineralisation. Other studies such as one that subjected marrow stromal cells cultured on titanium fiber mesh scaffolds to flow perfusion also showed the an effect on cell number only occurred in the early stages of cell culture, here it seems this effect is also flow rate dependant [13, 32].

*Bancroft et al.*, seeded marrow stromal osteoblasts on 3D titanium fiber mesh scaffolds (diameter=10 mm, thickness=8 mm, porosity= 86%, pore size ~ 250  $\mu\text{m}$ ) to study the effects of different flow rates (static, 0.3, 1 and 3 ml/min) on osteoblast differentiation. Samples were subjected to continuous unidirectional flow for a period of upto 16 days and analysed on day 4, 8 and 16 of culture. The results demonstrated that with an increase in flow rate, mineralised matrix production was also increased in comparison to static conditions. Furthermore, it was suggested that long-term culture was beneficial in order to enhance and create a uniform distribution of cells throughout the scaffolds [13]. Similarly, *Olivier et al.*, investigated the efficiency of a new bioreactor system for the *in vitro* development of large bone substitutes. Human MG63 osteoblast-like cells were seeded on beta tricalcium phosphate ( $\beta$ -TCP) cylinders (33 mm in length and 14 mm in diameter, macroporosity with spherical pores of 500–630  $\mu\text{m}$ ) and subjected to unidirectional flow of 3 ml/min for upto 28 days. In general, the results demonstrated that long-term culture enhances the bone matrix production of MG63 osteoblast-like cells and improves their distribution in 3D scaffolds [31].

On the other hand, samples subjected to parallel flow displayed contradictory results with respect to cell viability (MTS) and total DNA content. The results show that cell viability for samples subjected to parallel oscillatory flow (fig 4.4b and 4.5b) are relatively the same as static conditions, however the total DNA content was significantly higher for the same comparison (fig 4.6b). The differences in DNA content compared to metabolic activity as measured by MTS may be due to dead cells remaining within the scaffold. The MTS data does shows the predicted effect as subjecting hES-MP-constructs to parallel flow may limit the amount of media entering the scaffold due to its orientation. The limited flow of media into the scaffold might lead to a non-uniform distribution of cells.

Reports in the literature indicate that insufficient oxygenation in the core of the scaffold could correlate to nonuniform distribution of cells and as a result nonuniform bone matrix deposition can occur [33, 34]. In general, uniform cell distribution is very important for uniform formation of bone matrix. Unfortunately, due to limited numbers of glass scaffolds it was not possible to undertake live-dead staining on the samples subjected to parallel flow which would have helped address this question.

In this study live cells were present deep within the core of the glass scaffolds for groups subjected to transverse fluid flow (fig 4.10). It was shown that scaffolds cultured in either static or unidirectional flow had more dead cells compared to samples subjected to oscillatory flow. Moreover, static cultured constructs contained a large number of dead cells in the core and bottom surface of scaffolds. This is also in confirmation with other studies whereby the application of flow has shown to improve cell distribution [13, 29]. It is interesting that unidirectional flow alone does not improve cell survival indicating that cell survival is not enhanced simply by improved nutrient flow but is an effect of the specific mechanical stimulus of oscillatory flow. Others have shown live cells to be present within the periphery of cell-seeded scaffold (200-300  $\mu\text{m}$ ) [35] or live cells at millimeter depths depending on scaffold geometry [36]. Confocal images from this study demonstrate that flow conditions (in particular oscillatory fluid flow) allow for a better distribution of live hES-MP cells inside the glass scaffold than static culture conditions. In a similar study, *Du et al.*, studied the effects of different flow profiles (unidirectional and oscillatory) on 3D porous cellular constructs. Mouse osteoblast-like MC3T3-E1 cells were cultured on Porous b-TCP ceramic scaffold disks (10 mm in diameter and 8 mm in height, porosity of 75%) *in vitro* for 6 days under static, oscillatory (0.5 ml/min) and unidirectional flow (1 ml/min). The results demonstrated that proliferation of cells was highest for cells subjected to unidirectional flow in comparison to other groups but was very inhomogeneous. However, it was seen that samples subjected to oscillatory flow allowed cells to proliferate in a uniform manner, (even with a scaffold thickness of 8 mm) and also increased ALP activity when compared to other groups [37]. The reason for the findings in this study can be explained through

the simple mechanical design of the perfusion system. The scaffolds positioned in the vertical plane (TF) are placed in such a manner that media is forced through the whole internal structure of the scaffold in both oscillatory and unidirectional systems, creating a more homogenous microenvironment which has led to better survival and proliferation of hES-MP cells.

As mentioned in chapter 1, ALP is an enzyme involved in the early phases of mineralisation of newly formed bone tissue [38]. Results in this study (4.7a) showed a high activity of the enzyme on day 7 of culture for samples subjected to transverse flow when compared to parallel flow. In the transverse configuration, cell-seeded scaffolds under oscillatory and unidirectional flow had a higher ALP activity in comparison to their static control. However this is not the case for scaffolds arranged in parallel. *Goldstein et al.*, showed an increase in ALP expression when marrow stromal osteoblasts were seeded in 3D porous PLGA scaffolds (12.7 mm diameter, 6.0 mm thick, 78.8% porous) and cultured for 7 days in a continuous flow perfusion bioreactor [39]. *Mai et al.*, also confirmed that one single load of oscillatory fluid flow (1 h, 1.2 Pa) subjected to MC3T3-E1 cells seeded on a parallel plate, was capable of inducing terminal differentiation by up-regulating osteogenic genes, elevating ALP and inducing secretion of type I collagen [40]. The findings in this chapter are in confirmation with other studies [5, 11, 38] and some have found that on days 14 and 21 the ALP activity in perfused samples was three times the corresponding amount in static cultures. However variable levels of ALP have been observed in other studies of MSCs. *Peter et al.*, [41] demonstrated the differentiation of rat MSCs on poly(propylene fumarate) disks and noticed that ALP activity was not enhanced until day 21 for static conditions. The high expression of ALP in both oscillatory and unidirectional flow groups suggests that continuous perfusion is not required in order to upregulate ALP activity or matrix production of hES-MP cells. Short bouts of fluid flow (in particular oscillatory flow) can increase ALP activity and mineralisation of hES-MPs in porous scaffolds. It seems this could be possible if flow is directed through the scaffold hence stimulating cells in the core/centre of the construct however in parallel arrangement this would not be the case since flow is mainly restricted to the periphery of the scaffold.

It is interesting to note that scaffold orientation (TF vs PF) did not have any significant effect on matrix deposition as measured by collagen and calcium assays. Despite not having an ALP response to flow at day 7, cells subjected to parallel oscillatory flow did produce as much matrix as cells subjected to transverse oscillatory flow at day 14. As discussed in the previous paragraph this may be related to the peak of ALP expression occurring at different times in different culture conditions.

From the data (fig 4.8 & 4.9) it seems that flow type plays a key role in mineral production of hES-MP cells. From these results it appears that subjecting cells to oscillatory flow offers a greater benefit than placing them in a unidirectional perfusion system for producing and depositing the most matrix. Although 5 ml/min unidirectional flow has an effect (60 % higher) on mineral deposition, this was much less than the effect observed for samples subjected to an oscillatory flow of 5 ml/min (370%). Effect of 5 ml/min oscillatory was also stronger in comparison to samples subjected to an oscillatory flow of 3 ml/min (fig 4.9). The presence of newly formed mineral in glass scaffolds further confirms mature osteoblast-like characteristics of hES-MP constructs.

It is difficult to make direct comparisons with these results and others. For example *Bancroft et al.*, investigated the effects of different perfusion rates on rat marrow stromal osteoblasts and found that higher flow rates enhanced calcium deposition in a dose dependent manner [13]. A recent study investigated the effects of intermittent steady, pulsatile, and oscillatory fluid flow on MC3T3-E1 activity within a collagen-GAG scaffold. The results demonstrated that an oscillatory flow of 1 ml/min for 49 hours resulted in uniform cell distribution and enhanced the production of early stage bone formation markers [23]. The inconsistency between this study and other studies may be explained in terms of differences in cell types. However, differences in system geometries, scaffold material and scaffold architecture further makes direct comparisons difficult since similar volumetric rates can result in highly different shear stresses imparted to the cells.

The production of a mineralised matrix is considered the end-point of full maturation of differentiating marrow stromal cells, and flow perfusion culture at this range appeared to have accelerated this differentiation [13]. Others have described oscillatory flow being the dominant flow type in physiological bone conditions, it maybe because of this reason that the results in this study show oscillatory flow as a much more efficient flow type than unidirectional flow [42].

The results presented in this study suggest that shear stresses created by oscillatory flow might be more beneficial than shears stresses created by unidirectional flow for directing hES-MPs towards an osteogenic lineage. A wealth of literature exists focusing on the effects of fluid shear stress on osteoblastic differentiation that have shown that the application of fluid flow affects osteogenic signal expression of mesenchymal stem cells [2, 43-46]. Predicting shear stress distribution for different scaffold architecture, in combination with the knowledge of how these local stresses affect cell attachment and cell growth can ultimately lead to scaffold design procedures that would maximise cell and tissue growth. In this study (chapter 2, section 2.2.15), Wang and Tarbell's model was used to approximate the average stress values subjected to the cells by unidirectional flow. It was found that flow rates of 3, 5 and 10 ml/min produced average stress values of 0.111, 0.647 and 1.398 Pa respectively. Since oscillatory flow has a back and forth motion, it was not possible to use the same model to predict shear stress values. The variation in cell types, 3D scaffold geometry and bioreactor setup has increased the complexity of defining the optimum shear stress. Nevertheless, up to now the bodies of work suggest that osteogenic differentiation can be achieved with shear stresses in the range of  $1 \times 10^{-4}$ -1.2 Pa, showing a good correlation with levels of shear stress expected to occur in bone (0.8-3 Pa) [8].

## 4.5 Conclusion

The aim of this chapter was to investigate the effects of different bioreactor systems in order to create a suitable microenvironment for the development of functional 3D constructs. In particular it was predicted, based on previous work in the laboratory, that cells would respond to short bouts of oscillatory flow. It was shown that short bouts of direct perfusion can direct the differentiation of a progenitor cell line towards an osteogenic lineage as demonstrated by an increase in ALP activity and an upregulation in mineral deposition. The combination of direct perfusion (scaffolds positioned in the vertical plane) and oscillatory fluid flow significantly enhanced bone formation markers and improved cell distribution in comparison to unidirectional flow groups and static conditions. Although cells in scaffolds orientated parallel to the flow direction also produced collagen and calcium in response to flow, these cells did not have the increased cell number in response to flow seen in scaffold orientated in the transverse direction. Therefore taking all the data together the best conditions for bone matrix production of those examined here was 5 ml/min of oscillatory flow with the scaffold orientated transversely to the flow direction. These conditions will be used for the further experiments in this thesis.

## 4.6 Reference

- [1] Burdick JA, Vunjak-Novakovic G: Engineered microenvironments for controlled stem cell differentiation. *Tissue Eng.* 2009, A 15:205–219.
- [2] Yeatts AB, Fisher JP: Bone tissue engineering bioreactors: Dynamic culture and the influence of shear stress. *Bone.* 2011, 48:171–181.
- [3] McCoy RJ, O'Brien FJ: Influence of shear stress in perfusion bioreactor cultures for the development of three-dimensional bone tissue constructs. *Tissue Eng.* 2010. B Rev 16:587 601.
- [4] Crowe JJ, Gran, SC, Logan TM, Ma T: A magnetic resonance- compatible perfusion bioreactor system for three-dimensional human mesenchymal stem cell construct development. *Chem Eng Sci.* 2011, 66:4138– 4147.
- [5] Sikavitsas VI, Bancroft GN, Lemoine JJ, Liebschner MAK, Dauner M, Mikos AG: Flow perfusion enhances the calcified matrix deposition of marrow stromal cells in biodegradable nonwoven fiber mesh scaffolds. *Ann Biomed Eng.* 2005 Jan;33(1):63-70.
- [6] Stiehler M, Bunger C, Gaatrup A, Lund M, Kassem M, Mygind T: Effect of dynamic 3-D culture on proliferation, distribution, and osteogenic differentiation of human mesenchymal stem cells. *J Biomed Mater Res A.* 2009 Apr;89(1):96-107.
- [7] McAllister TN, Du T, Frangos JA: Fluid Shear Stress Stimulates Prostaglandin and Nitric Oxide Release in Bone Marrow-Derived Preosteoclast-like Cells. *Biochemical and Biophysical Research Communications.* *Biochem Biophys Res Commun.* 2000 Apr 13;270(2):643-8.
- [8] ] Weinbaum S, Cowin SC, and Zeng, Y: A model for the excitation of osteocytes by mechanical-induced bone fluid shear stresses. *J Biochem,* 1994. 27(3): 339-60.
- [9] Jessop HL, Rawlinson SC, Pitsillides AA, Lanyon LE: Mechanical strain and fluid movement both activate extracellular regulated kinase (ERK) in osteoblast-like cells but via different signaling pathways. *Bone.* 2002, 31(1):186–194.
- [10] Lan CH, Wang FF, Wang YJ: Osteogenic enrichment of bone-marrow stromal cells with the use of flow chamber and type I collagen-coated surface. *Journal of Biomedical Materials Research.* 2003, Part A Volume 66A, Issue 1, pages 38–46.

- [11] Cartmell SH, Porter BD, García AJ, and Guldberg RE: Effects of Medium Perfusion Rate on Cell-Seeded Three-Dimensional Bone Constructs in Vitro. *Tissue Engineering*. December 2003, 9(6): 1197-1203.
- [12] Vance J, Galley S, Liu DF, and Donahue SW: Mechanical Stimulation of MC3T3 Osteoblastic Cells in a Bone Tissue-Engineering Bioreactor Enhances Prostaglandin E<sub>2</sub> Release. *Tissue Engineering*. November/December 2005, 11(11-12): 1832-1839.
- [13] Bancroft GN, Sikavitsas VI, van den Dolder J, Sheffield TL, Ambrose CG, Jansen JA, Mikos AG: Fluid flow increases mineralized matrix deposition in 3D perfusion culture of marrow stromal osteoblasts in a dose-dependent manner. *PNAS* October 1, 2002 vol. 99 no. 20 12600-12605.
- [14] Botchwey EA, Pollack SR, El-Amin S, Levine EM, Tuan RS, Laurencin CT. Human osteoblast-like cells in three-dimensional culture with fluid flow. *Biorheology*. 2003;40(1-3):299-306.
- [15] Wang Y, Uemura T, Dong J, Kojima H, Tanaka J, Tateishi T. Application of perfusion culture system improves in vitro and in vivo osteogenesis of bone marrow derived osteoblastic cells in porous ceramic materials. *Tissue Eng*. 2003 Dec ;9(6):1205-14.
- [16] Sikavitsas VI, Bancroft GN, Holtorf HL, Jansen JA, Mikos AG. Mineralized matrix deposition by stromal osteoblasts in 3D perfusion culture increases with increasing fluid shear forces. *Proc Natl Acad Sci U S A*. 2003 Dec 9;100(25):14683-8.
- [17] Ponik SM, Triplett JM, and Pavalko FM: Osteoblasts and Osteocytes Respond Differently to Oscillatory and Unidirectional Fluid Flow Profiles. *Journal of Cellular Biochemistry*. 2007, 100:794–807.
- [18] Li YJ, Batra NN, You L, Meier SC, Coe IA, Yellowley CE, Jacobs CR: Oscillatory fluid flow affects human marrow stromal cell proliferation and differentiation. *Journal of Orthopaedic Research* 22 (2004) 1283-1289.
- [19] Qin YX, Kaplan T, Saldanha A, Rubin C: Fluid pressure gradients, arising from oscillations in intramedullary pressure, is correlated with the formation of bone and inhibition of intracortical porosity. *Journal of Biomechanics*. Volume 36, Issue 10, October 2003, Pages 1427–1437.
- [20] Wu CC, Li YS, Haga JH, Wang N, Ian YZ, Su FC, Usami S, and Chien S: Roles of

MAP Kinases in the Regulation of Bone Matrix Gene Expressions in Human Osteoblasts by Oscillatory Fluid Flow. *Journal of Cellular Biochemistry*. 2006, 98:632–641.

[21] Batra NN, Li YJ, Yellowley CE, You L, Malone AA, Kim CH, Jacobs CR: Effects of short-term recovery periods on fluid-induced signaling in osteoblastic cells. *Journal of Biomechanics* 38 (2005) 1909–1917.

[22] Jaasma MJ, Plunkett NA, O'Brien FJ. Design and validation of a dynamic flow perfusion bioreactor for use with compliant tissue engineering scaffolds. *J Biotechnol*. 2008 Feb 29;133(4):490-6.

[23] Jaasma MJ, O'Brien FJ. Mechanical stimulation of osteoblasts using steady and dynamic fluid flow. *Tissue Eng Part A*. 2008 Jul;14(7):1213-23.

[24] Du D, Furukawa KS, Ushida T. 3D culture of osteoblast-like cells by unidirectional or oscillatory flow for bone tissue engineering. *Bioetchnol Bioeng*, 2009 Apr 15 102 (6): 1670-8.

[25] Kaspar D, Seidl W, Neidlinger-Wilke C, Ignatius A, Claes L: Dynamic cell stretching increases human osteoblast proliferation and CICP synthesis but decreases osteocalcin synthesis and alkaline phosphatase activity. *Journal of Biomechanics*, 33 (2000), 45–51.

[26] Kreke MR, Huckle WR, Goldstein AS: Fluid flow stimulates expression of osteopontin and bone sialoprotein by bone marrow stromal cells in a temporally dependent manner. *Bone* 2005;36:1047–55.

[27] Kreke MR, Sharp LA, Lee YW, Goldstein AS: Effect of intermittent shear stress on mechanotransductive signaling and osteoblastic differentiation of bone marrow stromal cells. *Tissue Eng A* 2008;14:529–37.

[28] Porter B, Zael R, Stockman H, Guldberg R, Fyhrie D. 2005. 3D computational modeling of media flow through scaffolds in a perfusion bioreactor. *J Biomech* 38(3):543–549.

[29] Sikavitsas VI, van den Dolder J, Bancroft GN, Jansen JA, Mikos AG: Influence of the in vitro culture period on the in vivo performance of cell/titanium bone tissue-engineered constructs using a rat cranial critical size defect model. *J Biomed Mater Res A*. 2003 Dec 1;67(3):944-51.

[30] Gomes ME, Sikavitsas VI, Behraves E, Reis RL, Mikos AG: Effect of flow perfusion on the osteogenic differentiation of bone marrow stromal cells

cultured on starch-based three-dimensional scaffolds. *Journal of Biomedical materials, Research Part A*. 2003, Vol.67, 87-95.

[31] Olivier V, Hivart P, Descamps M, Hardouin P: In vitro culture of large bone substitutes in a new bioreactor: importance of the flow direction. *Biomed Mater*. 2007Sep;2(3):174-80.

[32] Sikavitsas V, Bancroft GN, Mikos AG: Formation of three-dimensional cell/polymer constructs for bone tissue engineering in a spinner flask and a rotating wall vessel bioreactor. *J Biomed Mater Res*. 2002 Oct;62(1):136-48

[33] Malladi P, Xu Y, Chiou M, Giaccia AJ, and Longaker MT: Effect of reduced oxygen tension on chondrogenesis and osteogenesis in adipose-derived mesenchymal cells. *Am J Physiol Cell Physiol*. 2006 Apr;290(4): 1139-46

[34] Xu Y, Malladi P, Chiou M, Bekerman E, Giaccia AJ, and Longaker MT: in vitro expansion of adipose-derived adult stromal cells in hypoxia enhances early chondrogenesis. *Tissue Eng*. 2007 Dec;13(12):2981-93.

[35] Ishaug-Riley SL, Crane-Kruger GM, Yaszemski MJ, Mikos AG: Three-dimensional culture of rat calvarial osteoblasts in porous biodegradable polymers. *Biomaterials*. 1998 Aug;19(15):1405-12.

[36] Fröhlich M, Grayson WL, Marolt D, Gimble JM, Kregar-Velikonja N, Vunjak-Novakovic G: Bone grafts engineered from human adipose-derived stem cells in perfusion bioreactor culture. *Tissue Eng Part A*. 2010 Jan;16(1):179-89.

[37] Du D, Furukawa KS, Ushida T. 3D culture of osteoblast-like cells by unidirectional or oscillatory flow for bone tissue engineering. *Biotechnol Bioeng*. 2009 Apr 15;102(6):1670-8.

[38] Bjerre L, Bünger CE, Kassem M, Mygind T: Flow perfusion culture of human mesenchymal stem cells on silicate-substituted tricalcium phosphate scaffolds. *Biomaterials*, 2008, Vol.29(17), 2616-2627.

[39] Goldstein AS, Juarez TM, Helmke CD, Gustin MC, Mikos AG: Effect of convection on osteoblastic cell growth and function in biodegradable polymer foam scaffolds. *Biomaterials*. 2001 Jun: 33(11):1279-88.

[40] Mai Z, Peng Z, Wu S, Zhang J, Chen L, Liang H, Bai D, Yan G, Ai H: Single Bout Short Duration Fluid Shear Stress Induces Osteogenic Differentiation of MC3T3-E1 Cells via Integrin  $\beta$ 1 and BMP-2 Signaling Cross-Talk. *PLoS One*. 2013 Apr 11;8(4).

- [41] Peter SJ, Lu L, Kim DJ, Mikos AG: Marrow stromal osteoblast function on a poly(propylene fumarate)/  $\beta$ -tricalcium phosphate biodegradable orthopaedic composite. *Biomaterials*, 2000, Vol.21(12), 1207-1213.
- [42] Chao L, Yan Z, Wing-Yee C, Ronak G, Liyun W, Lidan Y: Effects of cyclic hydraulic pressure on osteocytes. *Bone*. 2010 vol. 46 (5) 1449-1456.
- [43] Grellier M, Bareille R, Bourget C, Amedee J: Responsiveness of human bone marrow stromal cells to shear stress. *J Tissue Eng Regen Med* 2009;3:302-9.
- [44] Kapur S, Baylink DJ, Lau KHW: Fluid flow shear stress stimulates human osteoblast proliferation and differentiation through multiple interacting and competing signal transduction pathways. *Bone* 2003;32:241-51.
- [45] Scaglione S, Wendt D, Miggino S, Papadimitropoulos A, Fato M, Quarto R: Effects of fluid flow and calcium phosphate coating on human bone marrow stromal cells cultured in a defined 2D model system. *J Biomed Mater Res A* 2008;86A:411-9.
- [46] Boschetti F, Raimondi MT, Migliavacca F, Dubini G: Prediction of the micro-fluid dynamic environment imposed to three-dimensional engineered cell systems in bioreactors. *J Biomech* 2006;39:418-25.

# Chapter 5: Mechanical stimulation of mesenchymal stem cells seeded on peptide-coated glass scaffolds

## 5.1 Introduction

Human and animal cells are grown in serum in order to enable growth and proliferation. The most commonly used serum for cell culture is fetal calf serum. Serum, which is extracted from blood, is an extremely complex mixture of many small and large molecules with different physiologically balanced growth promoting and growth inhibiting activities. Serum provides an enormous variety of substances necessary for cultivating a wide variety of animal cells, such as hormones, growth factors, transport proteins and attachment factors. Advantages of using serum in media is to provide basic nutrients in soluble or in protein-bound forms and also contains albumin, hormones, vitamins, minerals, fatty acids which promote proliferation of cells. However, Batch testing is necessary due to variability and Specific cell lines require specific fetal calf serum. Recent developments in formulating media show that a variety of cells can be cultured in the absence of a serum supplement, provided various combinations of hormones, nutrients and purified proteins are added to the medium to replace serum [1]. Some reasons for using serum-free media include the avoidance of serum toxicity and in the absence of serum, the phenotype of cell can be better controlled. However, Serum-free media are highly specific to one cell type, as cell type from each species has its own characteristics and requirements and reliable serum-free media are not readily available commercially.

Many factors contribute to the maintenance of a biomimetic microenvironment for cell growth *in vitro* including consistency of the growth medium, addition of supplements and the surface in which cells attach and grow. The nature of the

surface to which cells attach and are cultured is important for their ability to proliferate, migrate and function. Components of the ECM have recently been used to coat glass or plastic surfaces to enhance and promote cell attachment *in vitro*. These fragments represent binding sites that are known to allow cell attachment and can be immobilised on surfaces in order to mimic the effects seen by the binding sites on whole molecules [2].

Tenascin C is known to be a hexameric glycoprotein and each of its disulphide-linked subunits consists of a series of domains with homology to other proteins including fibrinogen, fibronectin, and epidermal growth factors [3,4]. The multi domain structure of tenascin C demonstrates the many potential sites of interaction with cells and other matrix proteins. A variety of functions have been associated with tenascin C on the basis of *in vitro* findings. In the developing nervous system, tenascin C has been shown to stimulate granule cell migration and neurite outgrowth [5, 6]. Tenascin C also inhibits milk protein synthesis by mammary epithelial cells [7, 8] and inhibits T lymphocyte activation [9]. In the developing skeleton, tenascin C encourages chondrogenic differentiation in limb and mesenchymal cell culture [10]. Cells of the osteoblast lineage have been shown to express tenascin C from the onset of ossification, however tenascin C is undetectable in mineralised bone. The expression of tenascin C appears to be enhanced at sites of remodeling and/or bone formation [10-12]. In a recent study, tenascin C was found to stimulate ALP activity of osteosarcoma-derived osteoblast-like cell lines and anti-tenascin C resulted in a reduction in collagen synthesis and ALP activity [13].

Osteopontin (OPN) is an extracellular matrix protein and it has been demonstrated to play a key role in inflammation and immunological responses, [14] as well as remodeling of mineralised tissue. *In vitro* experiments have shown that OPN binds to the cells via cell adhesion sequences that recognise integrins including  $\alpha_v\beta_{1,3,5,6}$  [15]. In rat calvarial osteoblast cells, OPN expression is increased during the initial stages of differentiation and has also upregulated ALP activity [16]. Therefore, OPN has been proposed not only as a linker between hydrophobic surfaces and the cell, but as an activator on the surfaces. In

a recent study, osteoblastic MG63 cells were seeded on to surfaces that were covered with recombinant osteopontin (rOPN17-169) fragments (containing the cell adhesion motifs). The results demonstrated that rOPN17-169 precoated on the hydrophobic surface can promote cell adhesion, generate mitogen activated protein kinases (MAPK) and cytokine activation for osteoblastic cells [17].

Bone morphogenetic protein-2 (BMP-2) is a member of the transforming growth factor (TGF)  $\beta$  superfamily and is an essential factor for enhancing osteogenic differentiation. Recombinant BMPs can offer the early stage signals for pluripotent cells in order to differentiate into mineral depositing osteoblasts [18]. Under the influence of locally administered BMPs, stem cell differentiation is accelerated and functional properties of regenerated bone tissue are enhanced [19-22]. A previous study demonstrated the repair of a 20-mm long rabbit radial bone defect by using a BMP-2 derived peptide combined with porous  $\alpha$ -tricalcium phosphate (TCP) scaffold. *In vivo* experiments showed that a combination of BMP-2 derived peptide and  $\alpha$ -TCP scaffold promoted calcification in the implanted area [23]. Another study demonstrated bone marrow-derived mesenchymal stem cell (BMMSC) adhesion on chitosan-grafted titanium (Ti-CS) coated with immobilised BMP-2. Furthermore, it was shown that Ti-CS-BMP-2 enhanced ALP activity and had higher level of transcription activity of the bone transcription factor Runx2, compared with that of bone cell-derived osteoblasts. Alizarin red staining also confirmed calcium deposition, suggesting that the BMMSCs were actively differentiating into osteoblasts [24].

Studying the effects of peptide-coated surfaces should give further insight into cell attachment, cell migration and cell function on biomaterials. For this reason it is of interest to investigate cell responses to a combination of peptide coated scaffolds cultured in different serum conditions. In this chapter, the hypothesis is that the combination of peptide-coated scaffolds and application of fluid flow (established in chapter 4) will have a synergistic effect on hES-MP cell distribution, proliferation and osteogenic differentiation in 3D dynamic culture. To test this hypothesis, the experiments were divided into 2 stages:

- 1) Investigating the effects of scaffold coatings, containing bone-relevant peptides with respect to hES-MP cell attachment, cell viability and matrix mineralisation in static culture in serum-containing and serum-free media.
- 2) Investigating the combination of fluid flow and hES-MP-peptide-coated constructs with respect to matrix mineralisation and expression of genes associated with osteogenic differentiation.

## **5.2 Investigating the effects of serum-containing and serum-free media on hES-MP-peptide-coated constructs with respect to cell attachment, cell viability and matrix mineralisation in static culture.**

### 5.2.1 Methodology

Peptide coating was performed by the commercial company Orla Protien Technologies. The peptide motifs derived from Tenascin C (VFDNVKL), BMP-2 (IPKASSVPTELSAISTLY) and Osteopontin (VVYGLRGSGSGSS) were modified first by silanisation then treated with colloid gold, which gives the scaffolds an invisible gold coating across the entire exposed surface. All the proteins used have a single exposed cysteine on the bottom of the molecule and it is the binding of the SH group in the cysteine to the gold that gives scaffolds the ability to form oriented protein monolayers on substrates, simply by placing the substrate in an aqueous Orla protein solution.

Neutron reflection data demonstrates that the proteins dimensions are estimated as 5nm x 2.5nm making the theoretical thickness of the coating 5nm [25]. There is no easy way to show that the coating of each material has worked without in effect destroying the coating. Therefore confidence in the coating process comes from the control tests Orla perform in their labs. These include analytical tests such as surface plasmon resonance (SPR), surface acoustic wave (SAW) or quartz crystal microbalance (QCM) chips, combined with the biological effects and changes in wettability observed on coated 2D/3D surfaces. These assays were all performed by Orla Protein Technologies, in house.

The aim of this experiment was to investigate the effects of growing hES-MP cells in serum-containing and serum-free media on hES-MP-peptide-coated scaffolds with respect to cell viability and matrix production. Peptide-coated scaffolds were sterilised using 70% ethanol rather than 0.1% peracetic acid (as recommended by Orla Protein Technologies to avoid any damage to the surface coatings) and washed with PBS several times. hES-MP cells were statically

seeded with 250,000 cells per glass scaffold, using the seeding and culture method as described in chapter 2 (section 2.2.2.2). The cell-seeded scaffolds were cultured in serum-free and serum-containing media (the standard basal media detailed in chapter 2) supplemented with AA,  $\beta$ GP and DEX. The serum free medium was designed by the company specifically for mesenchymal stem cell growth, It is supplied with a substrate which was not used in these experiments as it would mask the effects of the peptide coatings. Cell-seeded scaffolds were statically cultured for upto 14 days and fresh media was supplied every 3 days. Samples were assessed for cell viability (MTS) and proliferation (LIVE/DEAD staining) on day 7 of culture and matrix production was analysed on day 14. Due to the limited number and expensive nature of the coated scaffolds, it was only possible to use 3 scaffolds for each condition (n=3, N=1) hence, statistical analysis was not performed due to the low number of repeats.

## 5.2.2 Results

### 5.2.2.1 Cell viability as assayed by MTS – day 7

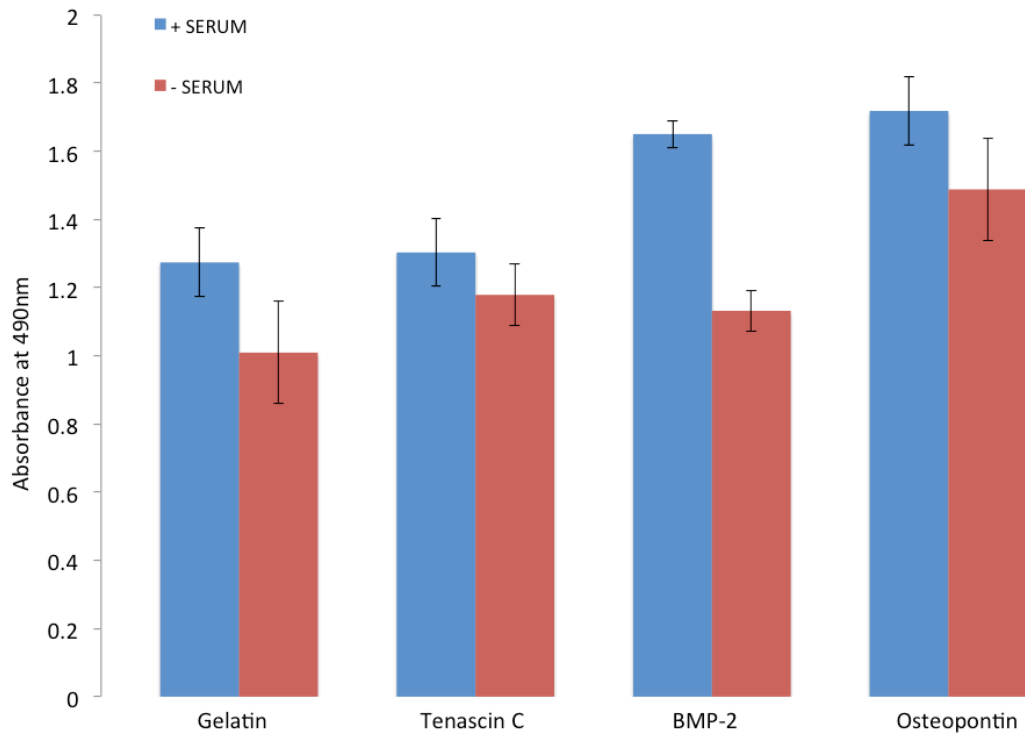


Fig 5.1; MTS absorbance of hES-MP cells cultured on gelatin and peptide-coated glass scaffolds in serum-free (-serum) and serum-containing (+serum) media at day 7 of static culture. All data is mean  $\pm$  SD (n=4).

In general, hES-MP cell viability was higher for scaffolds in serum-containing media (blue bar) as opposed to serum-free media (red bar). The data suggests that cell viability was highest for scaffolds coated with BMP-2 and osteopontin cultured in serum-containing media. Overall, cells seeded on coated scaffolds had a higher cell viability (whether in serum-free or serum-containing media) than control (gelatin coated) scaffolds.

#### 5.2.2.2 Live/dead staining – Day 7

According to the previous results (fig 5.1), constructs cultured in serum-containing media showed better cell viability than samples cultured in serum free media. Therefore a live/dead staining technique was used to visualise cell proliferation and uniformity on day 1, 3 and 7 for samples statically cultured in serum-containing media. The images reveal that on day 1, gelatin coated scaffolds contained more dead cells (red dots) than other peptide-coated scaffolds. By day 7, very few dead cells seem to be present however a much higher number of live cells (green dots) seem to be present on peptide-coated constructs, more specifically on those coated with osteopontin. hES-MP cells also tended to have a much more uniform distribution on peptide-coated scaffolds than gelatin coated samples, whereby cells had dominated and covered most of the surface area of a scaffold strut (fig 5.2).

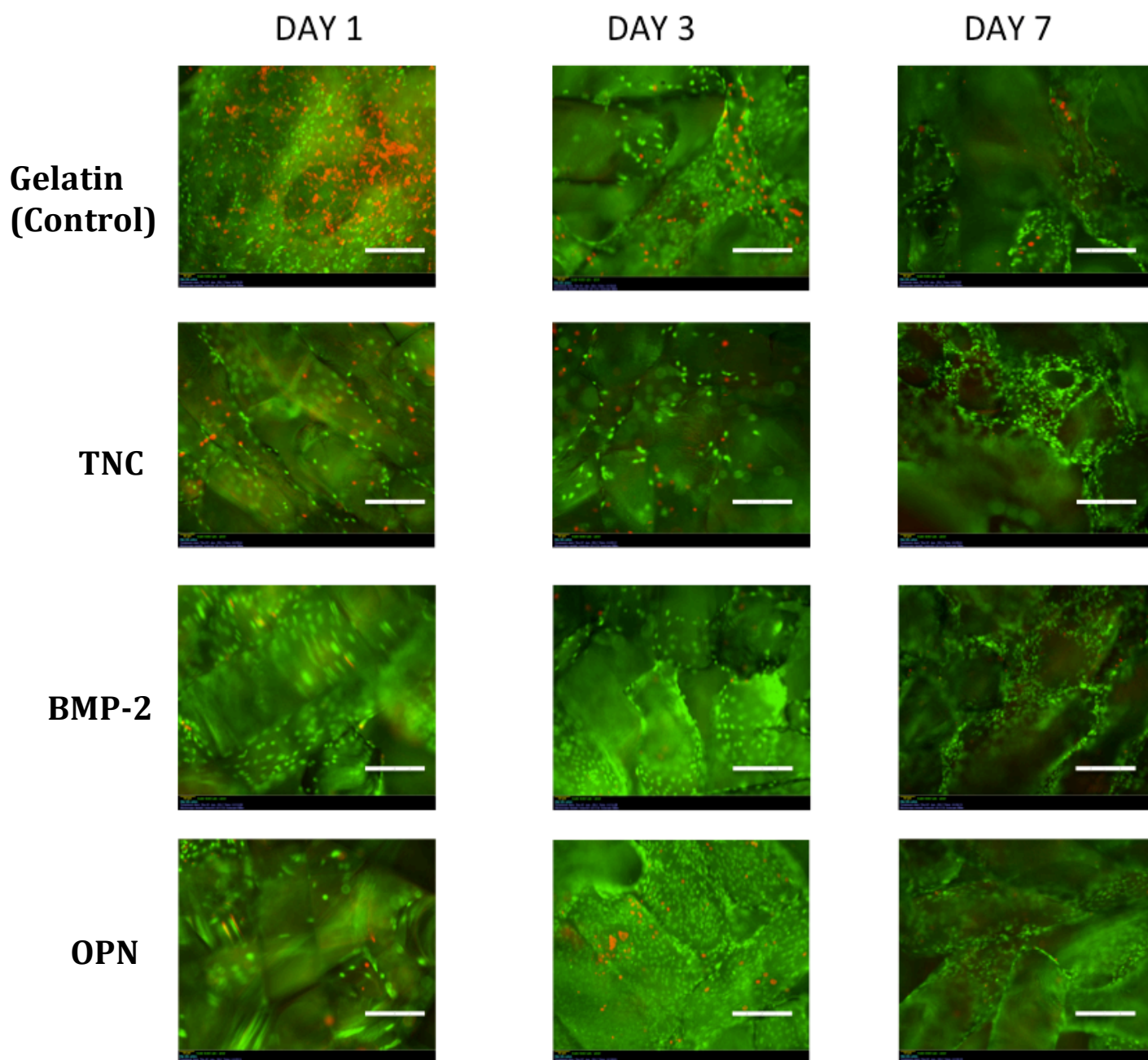
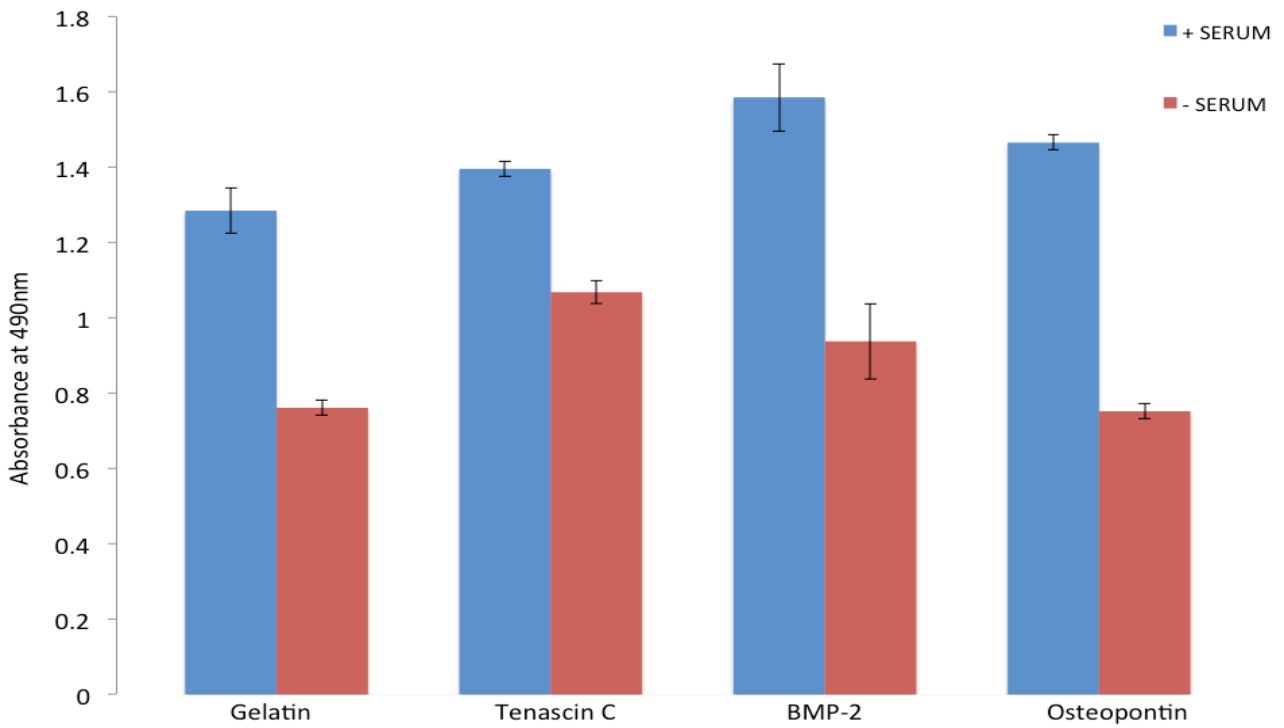


Fig 5.2; Live/Dead staining technique was used to analyse cell distribution on day 1, 3, and 7 of static culture for hES-MP cells seeded on gelatin and peptide-coated glass scaffold. Live cells are stained as green, whereas dead cells are stained as red. Representative images are shown (n=2). Scale bar = 200  $\mu$ m.

### 5.2.3 Collagen and calcium production – Day 14

Collagen production (fig 5.3a) and calcium deposition (fig 5.3b) were analysed using sirius red and alizarin red staining respectively. It is interesting to note that collagen and calcium production was highest for scaffolds coated with BMP-2 in serum-containing media. Furthermore, collagen and calcium production seemed to be lowest for scaffolds coated with osteopontin in serum-free media. Overall, peptide-coated scaffolds cultured in serum-containing media enabled cells to produce more collagen and calcium than gelatin-coated scaffolds.

(a) Collagen production



(b) Calcium deposition

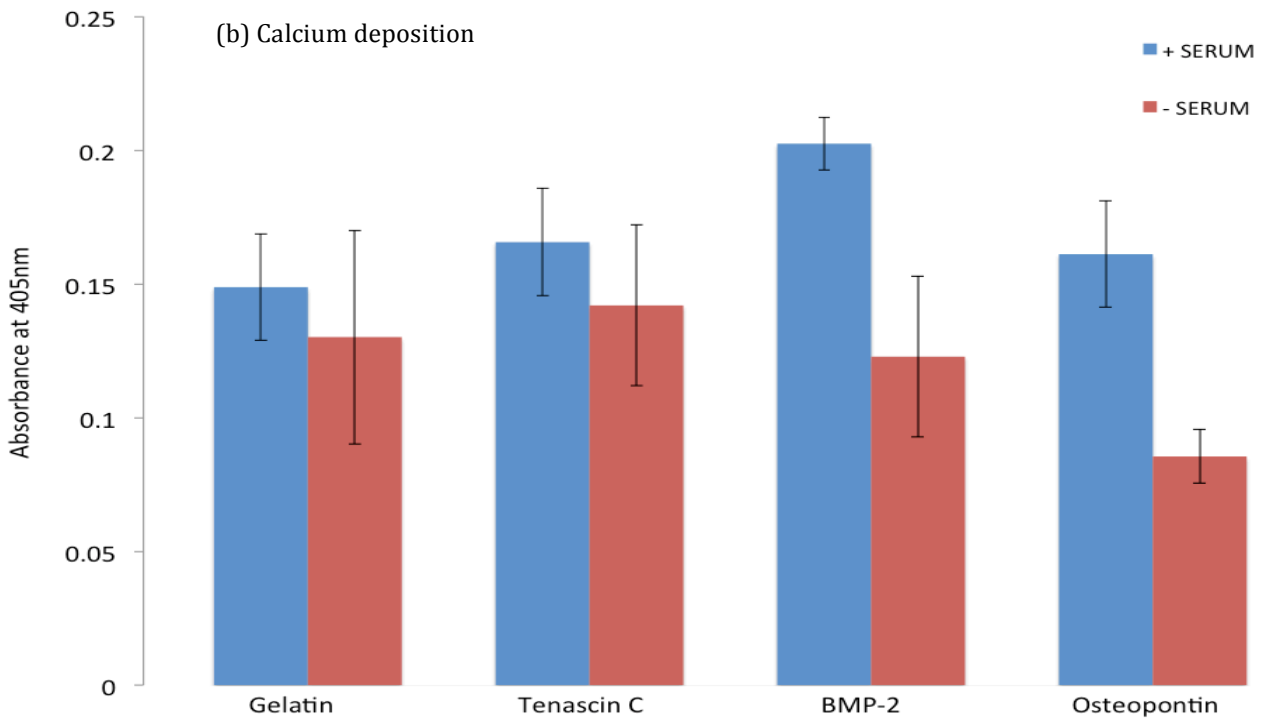


Fig 5.3; Collagen production (SR) and calcium deposition (AR) was analysed on day 14 of static culture for hES-MP cells seeded on gelatin and peptide-coated scaffolds supplemented with serum-free (-serum) and serum-containing (+serum) media. All data is mean  $\pm$  SD (n=3).

### **5.3 Investigating the combination of fluid flow and hES-MP-peptide-coated constructs with respect to matrix mineralisation and expression of genes associated with osteogenic differentiation.**

#### 5.3.1 Methodology

Although it was promising that cells could survive almost as well in serum-free than serum-containing media, the serum-free media did inhibit collagen and calcium production. The effects of protein coating were still evident in serum-containing media therefore it was decided to use serum-containing media for the following experiments. The hES-MP cells were used between passages 8-12 for ALP activity and total DNA analysis. However, for all other assays the cells were used between passages 3-7. Glass scaffolds were seeded with 250,000 cells using the seeding and culture methods described in chapter 2. Cell-seeded scaffolds were cultured in standard culture media and supplemented with AA,  $\beta$ GP and DEX. Fluid flow was applied using the oscillatory pump (chapter 2, figure 2.3) and cell-seeded scaffolds were arranged inside of the conduit as defined in chapter 4.

In short-term dynamic culture, samples were subjected to oscillatory fluid flow (5 ml/min, 1 Hz, 1 hour loading session) on day 4 and analysed for cell viability (MTS), total DNA content and ALP activity on day 7 (figure 5.4a). In long-term culture, samples were subjected to fluid flow on day 4, 7, 10 and analysed for cell distribution (DAPI and Phalloidin staining), collagen production, and calcium deposition on day 14 (figure 5.4b). Between loading sessions, cell-seeded scaffolds were cultured statically in an incubator in standard conditions. The experiment was conducted three times (N=3) with 2 scaffolds (n=2) for each condition. A one-way ANOVA followed by Tukey's post-hoc test were performed, since there were comparisons of more than two sample means. Results were expressed as mean  $\pm$  standard deviation.

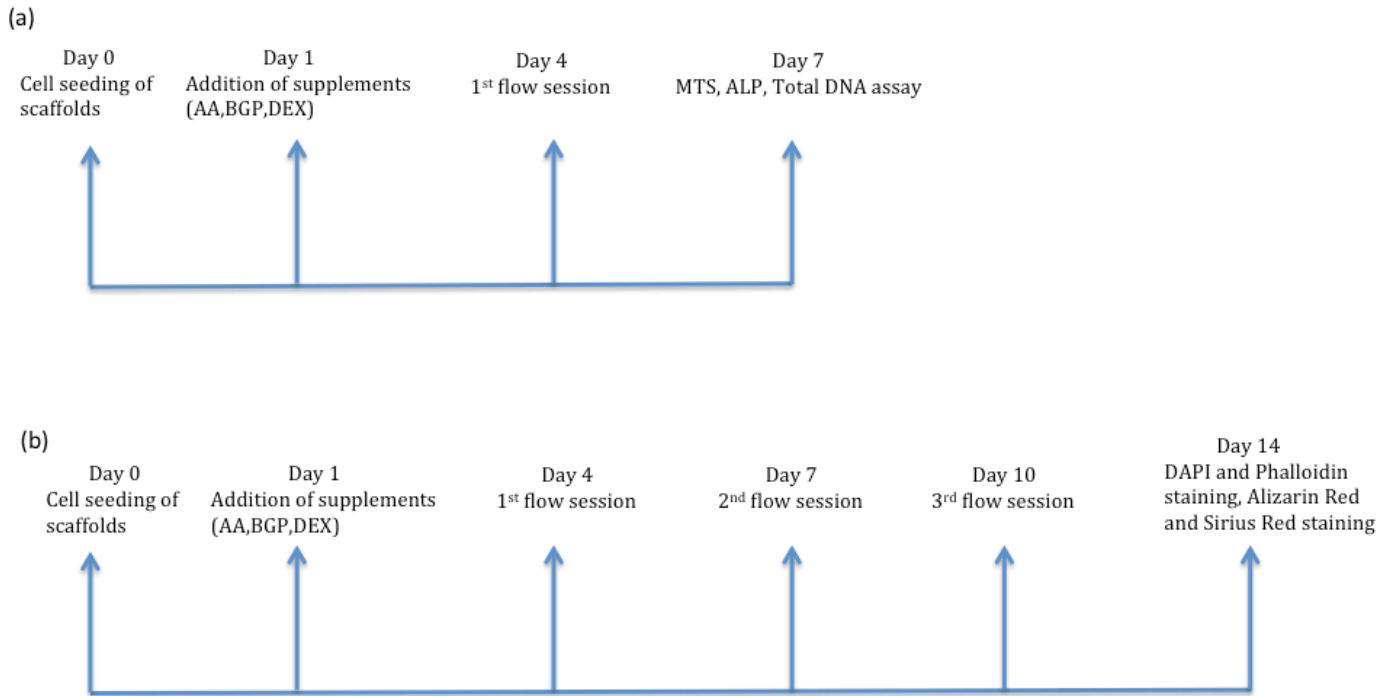


Figure 5.4; The experimental time line. (a) Short term dynamic culture, samples were subjected to flow on day 4 of culture and assayed for cell viability (MTS), total DNA content and ALP activity on day 7. (b) Long term dynamic culture, samples were subjected to flow on days 4, 7 and 10 and assayed for collagen production (SR) and calcium deposition (AR) content on day 14 of culture.

## 5.3.2 Results

### 5.3.2.1 Cell Viability as assayed by MTS – Day 7

As seen previously there was a small effect of the peptide coatings on cell number. However, the application of fluid flow significantly enhanced cell viability compared to static control (fig 5.5). All peptide-coated samples subjected to fluid flow had significantly higher cell viability than the fluid flow gelatin group. However, only Tenascin C and gelatin-coated samples showed significantly higher cell viability compared to their respective static cultures. However, overall it does appear that the application of flow increased cell viability by day 7 of culture as seen in the previous chapter (chapter 4).

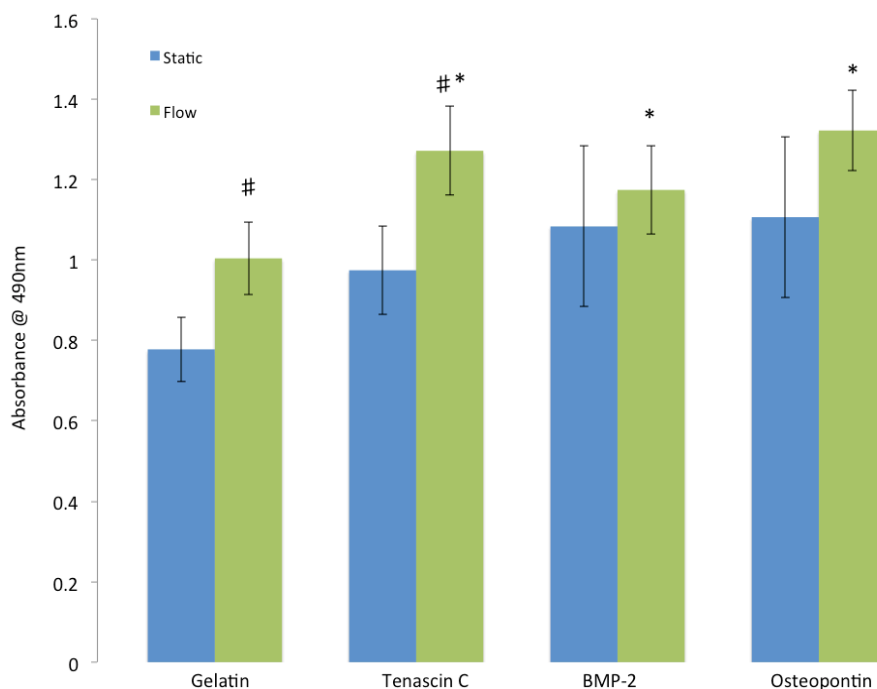


Fig 5.5; Cell viability (MTS) analysed on day 7 for hES-MP cells cultured on gelatin and peptide-coated scaffolds subjected to 5 ml/min oscillatory fluid flow. \*= Significantly different compared to gelatin flow group and #=Significantly different to corresponding static culture. All data is mean  $\pm$  SD (n=4).

### 5.3.2.2 Total DNA content – Day 7

Total DNA content was measured on day 7 of culture for gelatin and peptide-coated scaffolds under static and/or dynamic culture. From figure 5.6 it is evident that DNA content was significantly lower for osteopontin-coated scaffolds subjected to fluid shear stress in comparison to its own static culture and also to gelatin coated scaffolds subjected to dynamic flow. Tenascin C coated scaffolds too had a significantly lower DNA content when compared to gelatin coated scaffolds subjected to fluid flow. Interestingly, the application of fluid flow did not have an effect on the DNA content for gelatin coated scaffolds as seen in the previous chapter (chapter 4, fig 4.3). It is important to note that the passage number of the hES-MP cells utilised for these experiments to quantify DNA content and analyse ALP activity was relatively high and may explain the discrepancy compared to previous chapters.

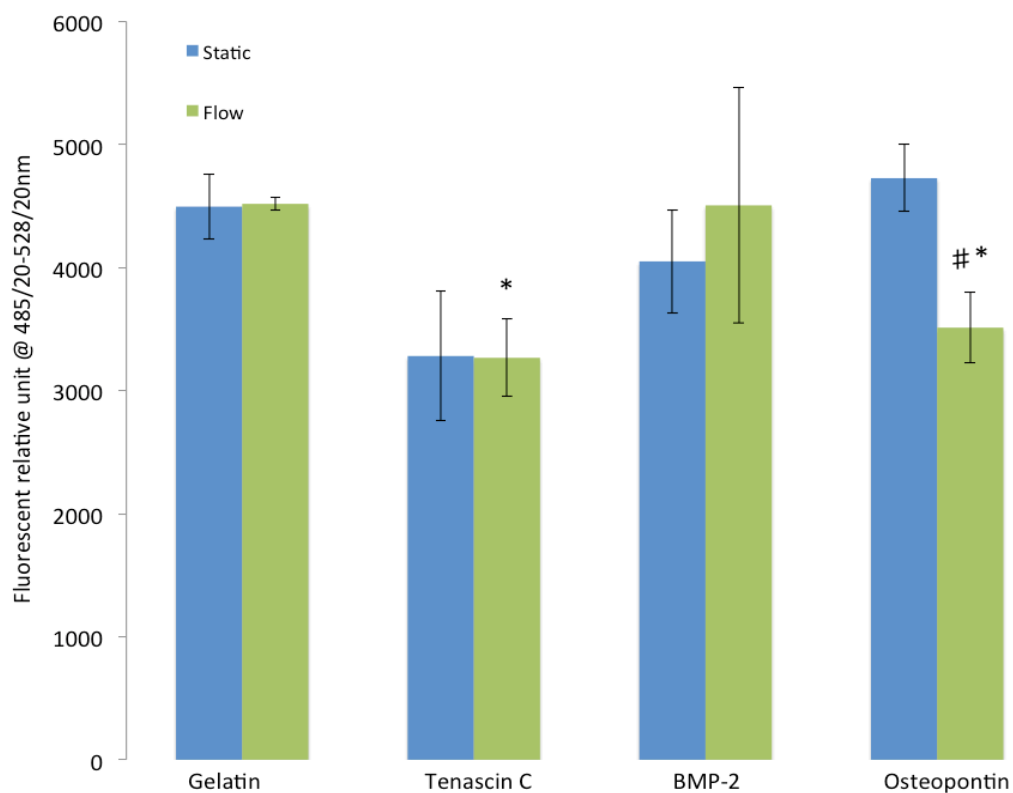


Fig 5.6; Total DNA content analysed on day 7 for hES-MP cells cultured on gelatin and peptide-coated scaffolds subjected to 5 ml/min oscillatory fluid flow. \*= Significantly different compared to gelatin flow group and #=Significantly different to corresponding static culture. All data is mean  $\pm$  SD (n=4).

### 5.3.2.3 ALP/DNA – Day 7

The ALP was normalised to total DNA content on day 7 of culture and these results can be seen in figure 5.7. This data does however contradict results from the previous chapter whereby the application of flow significantly increased the activity of ALP (chapter 4, fig 4.6). The reason for this discrepancy could again be due to the high passage number of hES-MP cells.

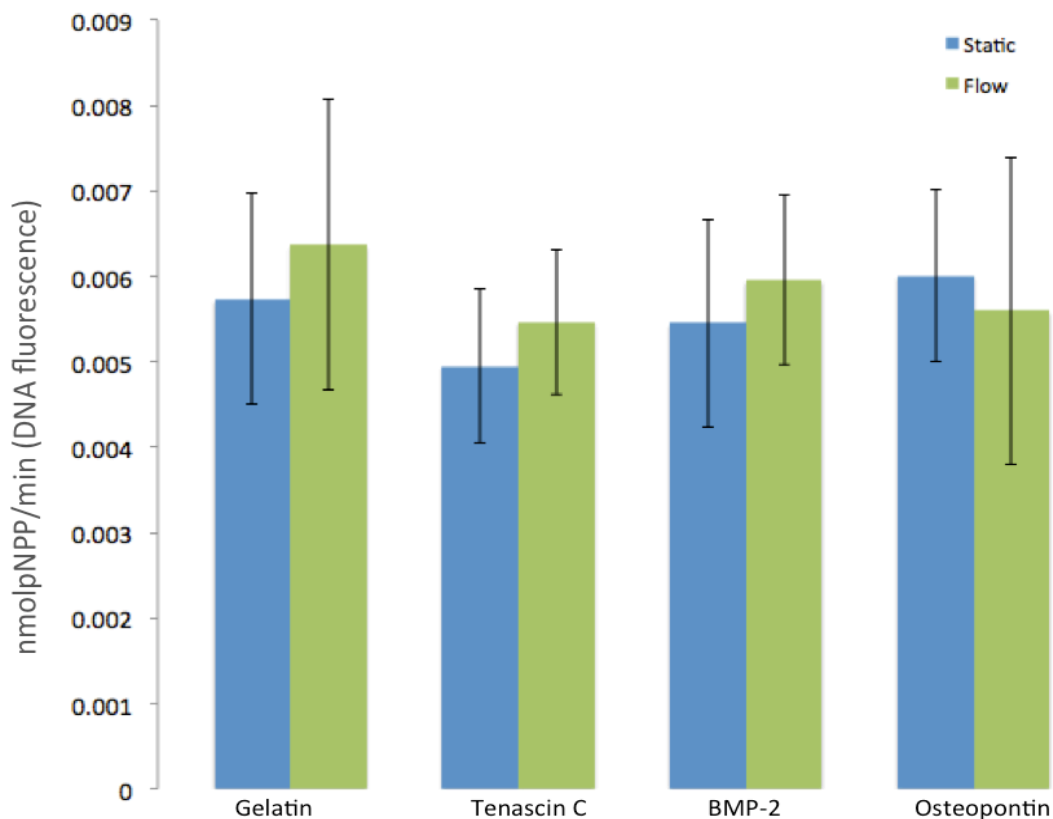


Fig 5.7; ALP activity (normalised to DNA) analysed on day 7 for hES-MP cells cultured on gelatin and peptide-coated scaffolds subjected to 5 ml/min oscillatory fluid flow. \*= Significantly different compared to gelatin flow group and #=Significantly different to corresponding static culture. All data is mean  $\pm$  SD (n=4).

### 5.3.2.4 Dapi and phalloidin staining – Day 14

Dapi and phalloidin staining was used on coated scaffolds to analyse cell distribution and cell uniformity, images were taken from the top, cross-section

and bottom part of the constructs on day 14 of culture (post loading session). Figure 5.8 clearly shows that cell distribution is very uniform for both peptide and gelatin coated scaffolds after being subjected to oscillatory fluid flow. Throughout all scaffolds it is evident that by day 14, cells have successfully penetrated through the core and distributed towards the bottom section of the scaffold. More specifically, scaffolds coated with BMP-2 and osteopontin seem to contain the most cells when compared to Tenascin C and gelatin coated scaffolds, as there seems to be a much higher number of cell nuclei within the different points of the constructs.

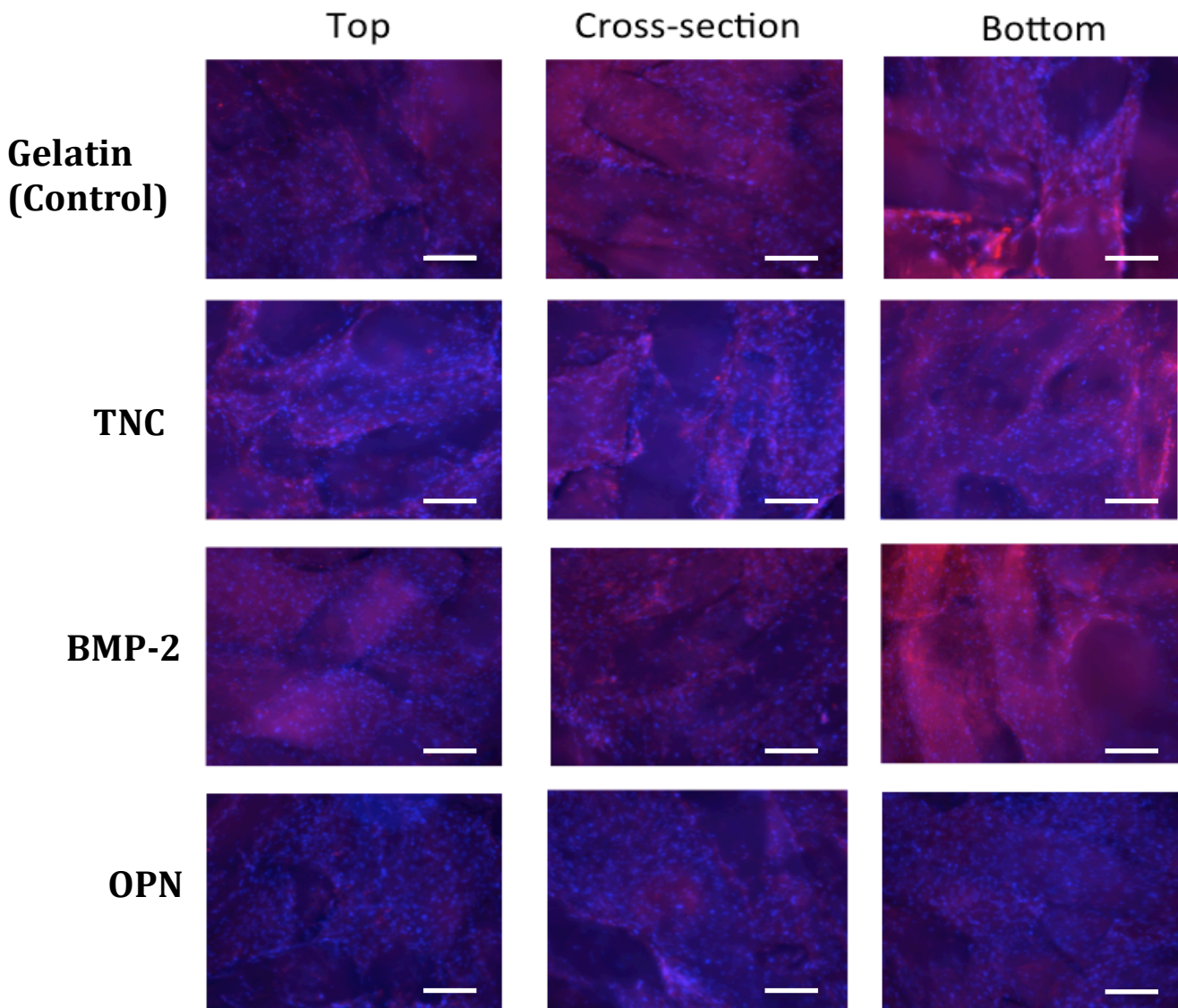
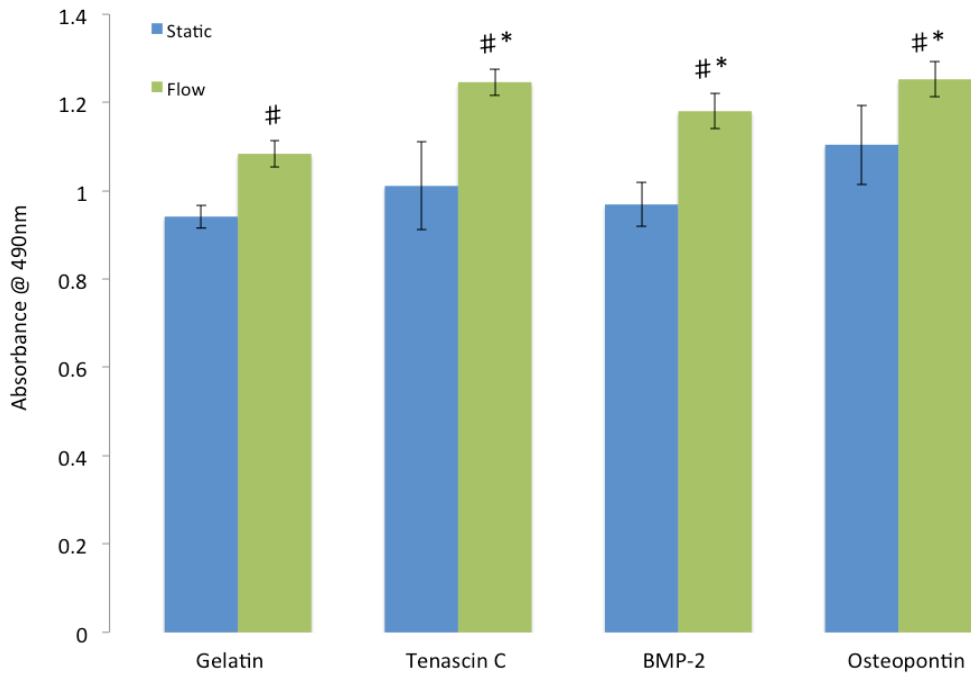


Fig 5.8; Dapi and phalloidin staining of dynamically cultured hES-MP cells seeded on peptide and gelatin coated scaffolds on day 14 of culture. Images were taken from the top, middle and bottom part of the constructs. Bar = 200  $\mu$ m, representative of n=2. Each image is a merged image of 5 slices 10  $\mu$ m depth.

#### 5.3.2.5 Collagen and calcium production – day 14

Interestingly, cells on all coated scaffolds subjected to flow (including gelatin coated scaffolds) significantly produced higher collagen and calcium compared to their static cultures (fig 5.9a, 5.9b). Cells seeded on peptide-coated scaffolds under dynamic conditions significantly produced more collagen and calcium than gelatin coated scaffolds. Furthermore, hES-MP's seeded on osteopontin coated scaffolds under static conditions significantly produced the highest collagen and calcium compared to other static cultures.

(a) Collagen production



(b) Calcium deposition

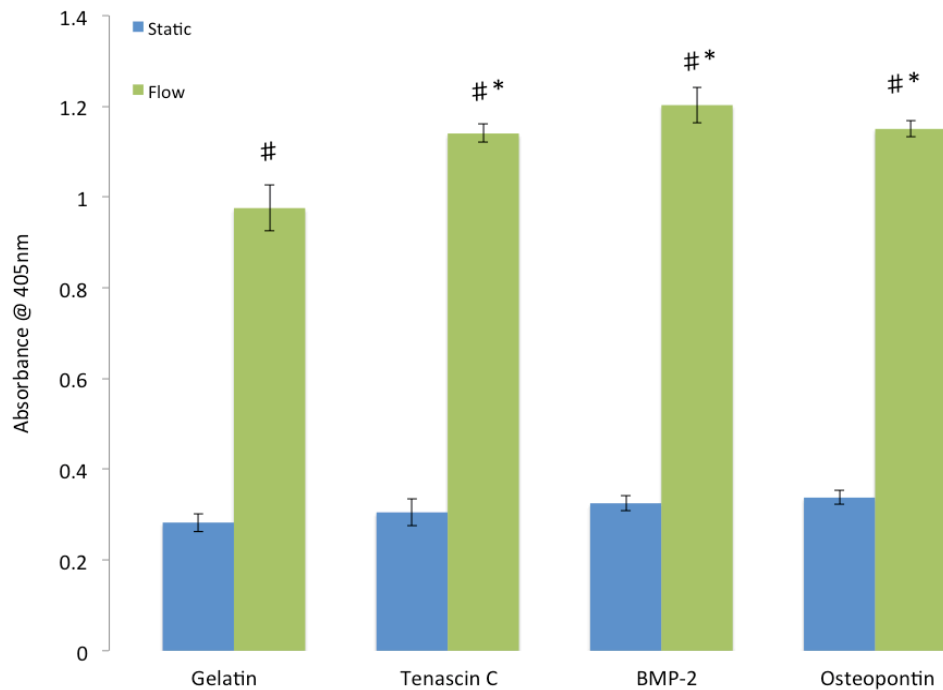


Fig 5.9; Collagen production (SR) and calcium deposition (AR) analysed on day 14 for hES-MP cells cultured on gelatin and peptide-coated scaffolds subjected to 5 ml/min oscillatory fluid flow. \*= Significantly different compared to gelatin flow group and #=Significantly different to corresponding static culture. All data is mean  $\pm$  SD (n=4).

## 5.4 Discussion

The aim of this chapter was to investigate the response of hES-MP cells seeded on peptide coated and standard coated glass scaffolds under dynamic conditions with respect to cell distribution and various markers of osteogenic differentiation.

Short term static experiments, revealed that Tenascin C, BMP-2 and osteopontin coated scaffolds cultured in serum-containing media enabled better adherence of hES-MP cells, exhibited higher cell viability as assayed by MTS on day 7 of culture and produced more collagen and calcium compared to hES-MPs seeded on gelatin coated scaffolds. Conventional media has been used for isolating and expanding human MSCs with supplementing FBS at 10%. FBS contains nutritional and physiochemical compounds as well as a high content of attachment and growth factors required for cell growth and cell maintenance. However, due to the inherent problems associated with ill-defined FBS there is a need for the development of defined serum-free media. Efforts have been made to develop a defined serum-free media for animal or human MSC growth. [26-29].

Additionally, cells exposed to serum during the isolation/expanding phase could lead to serum-derived contaminants, which will probably be carried over with the cells when placed under serum-free conditions and ultimately limiting their therapeutic use. Previous researchers developed a defined serum-free medium (PPRF-msc6) for hMSC isolation and expansion that contains key attachment and growth factors required for both primary and passaged cultures [30]. It was shown that PPRF-msc6 medium supported hMCS generation from multiple bone marrow samples in a rapid and consistent manner whilst maintaining their multipotency and hMSC-specific immunophenotype. Interestingly, in comparison to serum-containing media, hMSCs cultured in PPRF-msc6 media exhibited a greater colony capacity, lower population doubling time, greater number of population doublings and a more homogeneous cell population. The serum free media used in this study has been optimised for adult MSC and contains an

attachment substrate, which can mask and interfere with peptide-coated scaffolds. This could explain the lower cell number in samples cultured in serum free media. A combination of peptide coatings may better resemble the critical ECM molecules needed for cell survival and proliferation and enable the cells to achieve as high a number as in serum containing medium.

*In vivo* studies have shown that the application of mechanical loading is a potent stimulus for new bone formation. Furthermore, the growth of cells *in vitro* requires the development of technologies to recreate some features of the natural microenvironment that cells experience in living tissues not only for optimal cell survival but also growth and function. Glass scaffolds coated with active peptide domain of proteins were used to examine the adherence of cultured cells to the surface under static and dynamic conditions. The results show that the combination of bioreactor culture and distinct ligand motifs further improved cell distribution and enhanced matrix production compared to gelatin-coated scaffolds.

A higher DNA content was observed in gelatin coated scaffolds compared to peptide-coated scaffolds on day 7 of culture (fig 5.6). However this was not reflected in the MTS data assayed on day 7 of culture (fig 5.5). This has also been observed by other researchers [31-33] and even with the reduction in DNA content for flow groups, cell distribution was much more homogeneous (fig 5.8) and as also seen in other studies [34-36]. As mentioned in previous chapters, cells can be concentrated along the periphery of the constructs in static cultures in certain scaffolds. This phenomenon is less observed in the presence of fluid shear stress. However it is worth noting that despite the low DNA content in flow groups, there are still a high number of cells on the constructs by day 14 of culture (fig 5.8). This could be due to a higher number of cells initially being attached to the peptide coated scaffold. The abundant cell adhesion on coated scaffolds is most likely mediated by the active peptide domains in comparison to gelatin-coated scaffolds. Furthermore, the way in which cells adhere and interact with the surrounding matrix is known to not only influence cell shape but also to control cell response and gene expression [37].

It is interesting to note that collagen and calcium production in static conditions for hES-MP cells on gelatin-coated scaffolds (fig 5.3) were similar to static conditions in flow experiments (fig 5.9) since these experiments were conducted at a similar time. However, there seems to be a discrepancy with regards to the collagen production and calcium deposition in samples cultured in static (fig 5.9) and for similar results obtained in chapter 4 (fig 4.8 & 4.9). The fact that these experiments were conducted at totally different time points could explain this variation. Although passage number of hES-MP cells were very similar at both time points, other factors including age of media, age of supplements (AA,  $\beta$ GP, and DEX), and seeding density could all have an effect on the biological response. It has been demonstrated that increasing the density of human umbilical cord mesenchymal stromal cells in polyglycolic acid scaffolds, have resulted in an increase in collagen and calcium production [38].

Cells seeded on gelatin and peptide-coated scaffolds under dynamic conditions produced a significantly ( $p < 0.05$ ) higher amount of collagen and calcium compared to cell in respective static conditions (fig 5.9). Furthermore, peptide-coated scaffolds enabled a higher collagen and calcium production than gelatin coated scaffolds. It has been shown that osteopontin is involved in bone cell attachment to ECM and also acts as a chemoattractant for bone cells during the early stages of bone development [39]. Early work demonstrated that the attachment of osteoblasts to osteopontin was dose dependant and mediated by a RGD peptide sequence [40]. Furthermore it was found that osteopontin plays an important role in adhesion, remodeling and osseointegration at the interface between a biomaterial and bone [41].

The ECM protein, Tenascin C is expressed in association with tissue remodeling during the development and pathogenesis in bone [42]. Osteoblasts have been shown to express Tenascin-C from the onset of bone formation and continue to do so in growing bone [10, 43]. In a recent study utilisng an osteosarcoma-derived osteoblast-like cell line, Tenascin C was found to stimulate ALP activity and antitenascin-C showed a reduction in ALP activity and collagen production, suggesting that Tenascin-C may play an important role in bone cell

differentiation [13]. In another study, heterogeneous bone marrow mononuclear cells showed a proliferative response in the presence of Tenascin C. Using recombinant fragments of human Tenascin C several mitogenic domains of the molecule was also identified. These effects suggest that Tenascin C plays a crucial role in proliferation and differentiation of hematopoietic cells within the bone marrow microenvironment [44].

As mentioned previously, BMPs belong to the TGF- $\beta$  superfamily and are known to induce and promote the differentiation of undifferentiated MSCs into osteogenic and chondrogenic cells [45]. *In vivo*, undifferentiated MSCs proliferate from the bone marrow, periosteum, and muscle surrounding the site of fracture and begin to migrate. This will eventually lead to new bone formation as a result of their differentiation into chondrogenic and osteogenic cells. Indeed BMPs have been demonstrated to be present at the initial stages of bone fracture healing and seem to play a key role in the events that results in the generation of new bone [46]. The results presented in this study with BMP-2 coatings are in agreement with previous work that have shown a synthetic BMP-2 peptide was able to induce alkaline phosphatase activity in C2C12 mouse osteoblast cells [47]. Although the glass scaffolds utilised in this study cannot be used for *in vivo* tissue engineering purposes, researchers have shown delivering BMP-2 using PLGA scaffolds over several weeks following implantation enhanced higher bone formation in rats [48], a canine model [49] and sheep [50] when compared to using a scaffold alone. Immobilised BMP-2 has previously been shown to support osteogenic differentiation *in vitro* [51, 52] using MC3T3-E1 cells. *Liu et al.* immobilised full-length BMP-2 to PEG hydrogels and demonstrated an increase in osteogenic MSC differentiation [53]. In another study, full-length BMP-2 was covalently linked to titanium implants in a canine model, which resulted in enhanced appositional bone growth [54]. The data presented in this study alongside previous studies indicate that BMP-2 remains biologically active when immobilised on 3D glass scaffolds. The osteogenic differentiation processes promoted by modular peptides in this study were very similar to MSC differentiation promoted by soluble BMP-2 protein in previous studies. It was shown that BMP-2 alone was not sufficient to induce ALP activity

by hMSCs however soluble BMP-2 promotes human MSC differentiation when presented to cells after pre-treatment with dexamethasone [55]. Due to the ability of BMPs to promote new bone formation, they have been widely used in bone tissue engineering applications [56, 57]. Human recombinant BMP-2 is an expensive growth factor which limits its clinical usefulness, therefore if a small BMP-2 peptide can be demonstrated to be as bioactive and full length BMP-2 this would be of strong interest to the bone graft substitute industry. This study also shows that hES-MP cells seeded on BMP-2 coated glass scaffolds and stimulated by flow perfusion can be used as a useful model for *in vitro* research on the biological and mechanical mechanisms associated with cell differentiation and cell organisation.

## **5.5 Conclusion**

In conclusion, the work presented in this chapter demonstrated that hES-MP cells cultured in serum-containing media had higher cell viability, greater collagen production and calcium deposition in comparison to samples cultured in serum-free media. Furthermore, peptide surface motifs of 3 proteins associated with bone cell attachment and differentiation promoted cell attachment of hES-MP cells. The application of oscillatory flow further accelerated cell growth and matrix production in comparison to gelatin-coated scaffolds, suggesting the application of the two can direct a cell phenotype in a target tissue. Therefore, this culturing system may provide a useful insight towards the development of *in vitro* bone formation and tissue engineering models, which can lead to improved strategies for the construction of bone graft substitutes.

## 5.6 References

- [1] Barnes D, and Sato G: Serum free culture: a unifying approach. *Cell*, 1980. 22: 649-655.
- [2] Cooke MJ, Phillips SR, Shah DSH, Athey D, Lakey JH, Przyborski SA: Enhanced cell attachment using a novel cell culture surface presenting functional domains from extracellular matrix proteins. *Cytotechnology* (2008) 56:71–79.
- [3] Spring J, Beck K, Chiquet-Ehrismann R. Two contrary functions of tenascin: dissection of the active sites by recombinant tenascin fragments. *Cell*. 1989 Oct 20;59(2):325-34.
- [4] Nies DE, Hemesath TJ, Kim JH, Gulcher JR, Stefansson K. The complete cDNA sequence of human hexabrachion (Tenascin). A multidomain protein containing unique epidermal growth factor repeats. *J Biol Chem*. 1991 Feb 15;266(5):2818-23.
- [5] Husmann K, Faissner A, Schachner M. Tenascin promotes cerebellar cell migration and neurite outgrowth by different domains in the fibronectin type III repeats. *J Cell Biol*. 1992 Mar;116(6):1475-86.
- [6] Wehrle-Haller B, Chiquet M. Dual function of tenascin: simultaneous promotion of neurite growth and inhibition of glial migration. *J Cell Sci*. 1993 Oct;106 ( Pt 2):597-610.
- [7] Jones PL, Boudreau N, Myers CA, Erickson HP, Bissell MJ. Tenascin-C inhibits extracellular matrix dependent gene expression in mammary epithelial cells. Localization of active regions using recombinant tenascin fragments. *J Cell Sci*. 1995 Feb;108 ( Pt 2):519-27.
- [8] Wirl G, Hermann M, Ekblom P, Fässler R. Mammary epithelial cell differentiation in vitro regulated by an interplay of EGF action and tenascin-C downregulation. *J Cell Sci*. 1995 Jun;108 ( Pt 6):2445-56.
- [9] Rüegg CR, Chiquet-Ehrismann R, Alkan SS. Tenascin, an extracellular matrix protein, exerts immunomodulatory activities. *Proc Natl Acad Sci U S A*. 1989 Oct;86(19):7437-41.
- [10] Mackie EJ, Thesleff I, Chiquet-Ehrismann R: Tenascin is associated with chondrogenic and osteogenic differentiation in vivo and promotes chondrogenesis in vitro *J Cell Biol*. 1987, 105: 2569–2579.

- [11] Mackie EJ, Ramsey S. Expression of tenascin in joint-associated tissues during development and postnatal growth. *J Anat.* 1996 Feb;188 ( Pt 1):157-65.
- [12] Thesleff I, Kantomaa T, Mackie E, Chiquet-Ehrismann R. Immunohistochemical localization of the matrix glycoprotein tenascin in the skull of the growing rat. *Arch Oral Biol.* 1988;33(6):383-90.
- [13] Mackie EJ, Ramsey S: Modulation of osteoblast behaviour by tenascin *J Cell Sci.* 1996, 109: 1597–1604.
- [14] Denhardt DT, Guo XJ. Osteopontin–A protein with diverse functions. *FASEB J* 1993;7:1475–1482.
- [15] Yokosaki Y, Matsuura N, Sasaki T, Murakami I, Schneider H, Higashiyama S, Saitoh Y, Yamakido M, Taooka Y, Sheppard D: The Integrin  $\alpha 9\beta 1$  bind to a novel recognition sequence (SVVYGLR) in the thrombin-cleaved amino-terminal fragment of osteopontin. *J Biol Chem* 1999, 274:36328-36334.
- [16] Liu YK, Nemoto A, Feng Y, Uemura T. The binding ability to matrix proteins and the inhibitory effects on cell adhesion of synthetic peptides derived from a conserved sequence of integrins. *J Biochem (Tokyo)* 1997;121:961–8
- [17] Lee YJ, Park SJ, Lee WK, Ko JS, Kim HM. MG63 osteoblastic cell adhesion to the hydrophobic surface precoated with recombinant osteopontin fragments. *Biomaterials.* 2003 Mar;24(6):1059-66.
- [18] Franzen A, Heinegård D. Extraction and purification of proteoglycans from mature bovine bone. *Biochem J* 1984;224:47–58.
- [19] Uludag H, D'Augusta D, Golden J, Timony G, Riedel R, Wozney JM. Implantation of recombinant human bone morphogenetic proteins with biomaterial carriers: a correlation between pharmacokinetics and osteoinduction in the rat ectopic model. *J Biomed Mater Res* 2000;50:227–38.
- [20] Smith E, Bai J, Oxenford C, Yang J, Somayaji R, Uludag H. Conjugation of RGD-peptides to thermoreversible polymers. *J Polym Sci Polym Chem* 2003;41:3989–4000.
- [21] Gao TJ, Uludag H. Effect of physiochemical properties of engineered thermoreversible polymers on retention of bone morphogenetic protein-2 in vivo. *J Biomed Mater Res* 2001;57:92–100.
- [22] Gao TJ, Kousinioris NA, Winn SR, Wozney JM, Uludag H. Synthetic thermoreversible polymers are compatible with osteoinductive activity of

rhBMP-2. *Tissue Eng* 2002;8:429–40.

[23] Saito A, Suzuki Y, Kitamura M, Ogata S, Yoshihara Y, Masuda S, Ohtsuki C, Tanihara M: Repair of 20-mm long rabbit radial bone defects using BMP-derived peptide combined with an alpha-tricalcium phosphate scaffold. *JBiomedMaterResA*2006,77:700-706.

[24] Lim TY, Wang W, Shi Z, Poh CK, Neoh KG: Human bone marrow-derived mesenchymal stem cells and osteoblast differentiation on titanium with surface-grafted chitosan and immobilized bone morphogenetic protein-2. *JMaterSciMaterMed*2009,20:1-10.

[25] Le Brun AP, Holt SA, Shah DS, Majkrzak CF, Lakey JH. Monitoring the assembly of antibody binding membrane protein arrays using polarized neutron reflection. *Eur Biophys J.* 2008 Jun;37(5):639-45.

[26] Lennon DP, Haynesworth SE, Young RG, Dennis JE, Caplan AI: A chemically defined medium supports in vitro proliferation and maintains the osteochondral potential of rat marrow-derived mesenchymal stem cells. *Experimental Cell Research.* 1995, vol. 219, no. 1, 211–222.

[27] Liu CH, Wu ML, and Hwang SM: Optimization of serum free medium for cord blood mesenchymal stem cells. *Biochemical Engineering Journal.* 2007, vol. 33, no.1, 1-9.

[28] Jung S, Panchalingam KM, Rosenberg L, Behie LA: Ex vivo expansion of human mesenchymal stem cells in defined serum-free media. *Stem Cells Int.* 2012;2012:123030.

[29] Parker AM, Shang H, Khurgel M, and Katz AJ: Low serum and serum-free culture of multipotential human adipose stem cells. *Cytotherapy.* 2007, vol. 9, no.7 pp.637-646.

[30] Jung S, Sen A, Rosenberg L, and Behie LA: Identification of growth and attachment factors for the serum-free isolation and expansion of human mesenchymal stromal cells. *Cytotherapy.* 2010, vol. 12, no. 5, pp. 637–657.

[31] de Peppo GM, Sjoval P, Lennerås M, Strehl R, Hyllner J, Thomsen P, Karlsson C: Osteogenic potential of human mesenchymal stem cells and human embryonic stem cell-derived mesodermal progenitors: a tissue engineering perspective. *Tissue Eng Part A.* 2010 Nov;16(11):3413-26.

[32] Vance J, Galley S, Liu DF, Donahue SW: Mechanical stimulation of MC3T3

osteoblastic cells in a bone tissue-engineering bioreactor enhances prostaglandin E2 release. *Tissue Eng.* 2005;11:1832–9.

[33] Grayson WL, Bhumiratana S, Cannizzaro C, Chao PH, Lennon DP, Caplan AI: Effects of initial seeding density and fluid perfusion rate on formation of tissue engineered bone. *Tissue Eng Part A.* 2008, 14: 1809-20.

[34] Cartmell SH, Porter BD, Garcia AJ, Guldborg RE: Effects of medium perfusion rate on cell-seeded three-dimensional bone constructs in vitro. *Tissue Eng.* 2003;9:1197–203.

[35] Janssen FW, Oostra J, Oorschot A, van Blitterswijk CA: A perfusion bioreactor system capable of producing clinically relevant volumes of tissue-engineered bone: in vivo bone formation showing proof of concept. *Biomaterials.* 2006;27:315–23.

[36] Jaasma MJ, O'Brien FJ: Mechanical stimulation of osteoblasts using steady and dynamic fluid flow. *Tissue Eng Part A.* 2008;14:1213–23.

[37] Saito A, Suzuki Y, Ogata S, Ohtsuki C, Tanihara M: Activation of osteoprogenitor cells by a novel synthetic peptide derived from the bone morphogenetic protein-2 knuckle epitope. *Biochim Biophys Acta* 2003, 1651:60-67.

[38] Wang L, Dormer NH, Bonewald LF, Detamore MS. Osteogenic differentiation of human umbilical cord mesenchymal stromal cells in polyglycolic acid scaffolds. *Tissue Eng Part A.* 2010 Jun;16(6):1937-48

[39] Butler WT, Ridall AL, Mckee MD Osteopontin. J.P. Bilezikian, J.G. Raisz, G.A. Rodan (Eds.), *Principles of bone biology*, San Diego, Academic Press (1996), 167–181.

[40] Somerman MJ, Prince CW, Butler WT, Foster RA, Moehring JM, Sauk JJ: Cell attachment activity of the 44 kilodalton bone phosphoprotein is not restricted to bone cells. *Matrix*, 9 (1989), 49–54.

[41] McKee MD, Nanci A: Osteopontin at mineralized tissue interfaces in bone, teeth and osseointegrated implantsultrastructural distribution and implication for mineralized tissue formation, turnover, and repair. *Microsc Res Tech*, 33 (1996), 141–164.

[42] Mackie E]: Tenascin in connective tissue development and pathogenesis. *Perspect Dev Neurobiol.* 1994, 2: 125–139.

- [43] Mackie EJ, Tucker RP: Tenascin in bone morphogenesis: Expression by osteoblasts and cell type-specific expression of splice variants *J Cell Sci.* 1992, 103: 765–771.
- [44] Seiffert M, Beck SC, Schermutzki F, Müller CA, Erickson HP, Klein G: Mitogenic and adhesive effects of tenascin-C on human hematopoietic cells are mediated by various functional domains. *Matrix Biol.* 1998 Apr;17(1):47-63.
- [45] Lind, M. Growth factors: possible new clinical tools. *Acta Orthop. Scand.* 1996, 67, 407.
- [46] Mundy GR, Boyce B, Hughes D, Wright K, Bonewald L, Dallas S, Harris S, Ghosh-Choudhury N, Chen D, Dunstan C, Izbicka E, and Yoneda T. The effects of cytokines and growth factors on osteoblastic cells. *Bone* 1995, 17, 71S.
- [47] Wiemann M, Jennissen HP, Rumpf H, Winkler L, Chatzinikolaïdou M, Schmitz I, Bingmann D: A reporter-cell assay for the detection of BMP-2 immobilized on porous and nonporous materials. *J Biomed Mater Res* 2002, 62:119-127.
- [48] Shimazu C, Hara T, Kinuta Y. Enhanced vertical alveolar bone augmentation by recombinant human bone morphogenetic protein-2 with a carrier in rats. *J Oral Rehabil.* 2006;33: 609–618.
- [49] Jones AA, Buser D, Schenk R. The effect of rhBMP-2 around endosseous implants with and without membranes in the canine model. *J Periodontol.* 2006, 77: 1184–1193.
- [50] Zheng YX, Zhao HY, Jing XB: Reconstruction of orbita floor defect with polylactideglycolide acid/recombinant human bone morphogenetic protein 2 compound implanted material in sheep. *Zhonghua Yan Ke Za Zhi*, 2006; 42: 535–539.
- [51] Winkler L, Bingmann D, Wiemann M: Heat treatment of BMP-2 depots on implant materials generates an immobilized layer of BMP-2 with pronounced bioactivity. *J Biomed Mater Res A* 2006, 79:895-901.
- [52] Mitchell EA, Chaffey BT, McCaskie AW, Lakey JH, Birch MA: Controlled spatial and conformational display of immobilised bone morphogenetic protein-2 and osteopontin signalling motifs regulates osteoblast adhesion and differentiation in vitro. *BMC Biol.* 2010 May 10;8:57.
- [53] Liu HW, Chen CH, Tsai CL, Lin IH, Hsiue GH. Heterobifunctional poly(ethylene glycol)-tethered bone morphogenetic protein-2-stimulated bone

marrow mesenchymal stromal cell differentiation and osteogenesis. *Tissue Eng.* 2007;13:1113–1124.

[54] Becker J, Kirsch A, Schwarz F, Chatzinikolaidou M, Rothamel D, Lekovic V, Laub M: Bone apposition to titanium implants biocoated with recombinant human bone morphogenetic protein-2 (rhBMP-2). A pilot study in dogs. *Clin Oral Investig.* 2006;10:217–224.

[55] Diefenderfer DL, Osyczka AM, Reilly GC, Leboy PS. BMP responsiveness in human mesenchymal stem cells. *Connect Tissue Res.* 2003;44 Suppl 1:305–311.

[56] Saito, N., and Takaoka, K. New synthetic biodegradable polymers as BMP carriers for bone tissue engineering. *Bio materials.* 2003, 24, 2287, 28.

[57] Saito, N., Okada, T., Horiuchi, H., Ota, H., Takahashi, J., Murakami, N., Nawata, M., Kojima, S., Nozaki, K., and Takaoka, K. Local bone formation by injection of recombinant human bone morphogenetic protein-2 contained in polymer carriers. *Bone.* 2003, 32, 381.

# Chapter 6: Primary cilia of bone cells and its response to 3D dynamic loading

## 6.1 Introduction

As discussed in chapter 1, bone tissue alters its mass and structure in response to mechanical and chemical stimulation both *in vivo* and *in vitro*. Therefore, increased loading results in greater bone formation, whereas reduced loading results in bone loss. The ability of bone to sense and translate the external force to biochemical signals depends on bone cells, including osteocytes, osteoblast and osteoclasts. Fluid flow in bone lacunar-canalicular network is believed to be one of the potential stimuli that trigger mechanotransduction in bone. Osteocytes have been proposed as a prime candidate mechanosensor because of their location within the bone matrix. They have been shown to respond to mechanical stimuli both in *in vivo* [1] and *in vitro* [2]. Osteoblasts and MSCs have also been shown to respond once subjected to an external force and also appear to play an important role in bone mechanotransduction [3, 4]. However the relative importance of different types of mechanical stimuli to which bone cells respond is still an active area of research.

One mechanical stimulus that can be applied to cells *in vitro* is oscillatory fluid flow. It has been suggested that oscillatory fluid flow may be the most representative of physiological fluid flow in bone *in vivo* [5] and as shown in chapter 4 oscillatory fluid flow promotes hES-MP cells commitment towards the osteogenic lineage. During dynamic loading of the bone, bending moments are created which lead to bone matrix deformation and pressure gradients. These pressure gradients force fluid flow from regions of high pressure to regions of low pressure within the canalicular network [6]. The cells are subjected to shear stress over their surfaces, cell processes and cell body that have been estimated to be around 0.8-3.0 Pa at the cell membrane [7].

The mechanisms by which cells sense and translate external forces is still not known, however recent evidence suggests that the primary cilia is mechanically sensitive in many cell types [8]. Interestingly, primary cilia have also been observed on osteocytes and osteoblasts [9-11] and are implied to be potential mechanosensors in these cells. Primary cilia have previously been shown to be flow sensitive in renal epithelial cells in which bending of the cilium causes an increase in intracellular calcium [12, 13]. Moreover, chondrocytes in cartilage have also been shown to exhibit primary cilia. It appears that the cilia can be attached to the ECM of cartilage integrins such that deformation of the matrix induces cilia bending [14, 15].

*Malone et al.*, applied continuous flow (0.036 Pa) to MC3T3-E1 osteoblasts and demonstrated the bending of primary cilia. It was shown that subjecting MC3T3-E1 osteoblasts and MLO-Y4 osteocytes to oscillatory fluid flow increased OPN and COX2 mRNA in comparison to no flow conditions. Furthermore, upon removal of the primary cilia (or inhibition of its formation), the fluid flow-induced response was no longer observed [8]. In another study, *Hoey et al.*, collected conditioned media from mechanically stimulated MLO-Y4 osteocytes and added it to MSCs. This resulted in a significant upregulation of OPN and COX2 in MSCs in comparison to statically cultured conditioned media. The upregulation of osteogenic genes in the MSCs did not occur once primary cilia formation was inhibited, suggesting the primary cilia as a sensory mechanism for fluid flow in bone cells [16].

It has been suggested that the primary cilia projecting from osteocytes might experience mechanical deformation, fluid flow shear stress, or pressure gradients depending on their size and orientation. Mechanical stimuli that might affect the primary cilia situated on preosteoblastic cells are less defined, since these cells are located on bone surfaces and within immature bone matrix rather than within the lacunae of the mature bone matrix.

It has been shown that long exposure to chloral hydrate will completely remove the cilia in MDCK cells (rat kidney cells) [17, 18], from the embryonic stem cells

of early embryo phase of the sea urchin [19] and also bone cells [8]. The mechanisms by which chloral hydrate destabilises the primary cilium is still unclear, however it has been proposed that it disrupts the junction between the cilium and basal body through disassembly of microtubules [19].

MLO-A5 cells were chosen to study the role the primary cilia since experiments performed by Dr. Delaine-Smith determined that they are very sensitive to different loading conditions by depositing a significant amount of matrix [20]. Furthermore, the mineral deposited by MLO-A5 cells has been characterized to be more like the mineral found in bone compared to that synthesized by other osteoblast cells such as MC3T3-E1 cells [21].

Dr. Delaine-Smith has recently studied the role of the primary cilia in MLO-A5 responses to fluid shear stress [20]. The experiments included seeding MLO-A5 cells on 6-well plates and subjecting them to back and forth rocking. In summary, he observed that subjecting MLO-A5 cells to fluid flow caused primary cilia length to shorten and that its removal (by application of CH) inhibited mineral deposition. Although the microtubule network seemed to be disrupted more with increase exposure time to CH, they returned to their normal state after 24hrs in fresh media regardless of exposure time. However it is not known if the primary cilia can still operate as a mechanosensor in 3D where the arrangement of cells is quite different from monolayer. In order to be able to compare the role of the cilium in 3D to that previously demonstrated in 2D, it was necessary to replicate the 2D loading regime as closely as possible.

Studies conducted on 2D plates to investigate the role of primary cilia as a sensory organelle do not represent well the mechanical environment experienced by cells in real bone tissue. In previous chapters, it was shown that subjecting progenitor cell-constructs to fluid shear stress significantly increased early markers of osteogenic differentiation and mineral deposition. Therefore, the aim of this chapter was to further understand mechanotransduction of cells in a 3D environment. It is possible that the application of flow could affect the movement of the primary cilia embedded deep in cell-seeded scaffolds. If the

primary cilium is responsible for sensing mechanical forces (such as the application of fluid flow), then mature cells lacking a cilium would become unresponsive and therefore unable to deposit mineral in response to mechanical stimulation.

## 6.2 Methodology

MLO-A5 cells between passages 25-28 were seeded at a density of 300,000 cells/scaffold on 0.1% gelatin coated glass scaffolds.  $\alpha$ -MEM media supplemented with AA and  $\beta$ GP was added on day 1 and changed every 2-3 days. Before subjecting the constructs to fluid flow, it had to be shown that the primary cilia does occur and project from MLO-A5 cells, where they would be capable of acting as a mechanosensor. This was the first attempt to image the primary cilia of MLO-A5 cells seeded on 3D glass scaffolds and the technique used was to stain the protein tubulin with specific anti-acetylated alpha tubulin antibody (described in chapter 2). To study the involvement of primary cilia in a 3D environment, MLO-A5 cells were exposed to 4mM chloral hydrate (CH) for 48 hrs and 72 hrs followed by a recovery period in which cell-seeded scaffolds were washed with PBS and cultured in fresh media (fig 6.1).

To study the response of primary cilia to mechanical loading, MLO-A5-constructs were subjected to oscillatory fluid flow (5 ml/min, 1 Hz, 1 hour loading session) on day 7 and 8, or cultured in static conditions. Media was collected for PGE2 assay two hours after the first loading session (day 7). Collagen production and calcium deposition were examined using Sirius red and alizarin red staining respectively on day 12 of culture. Cell viability was also quantified on day 7 to monitor any differences in cell activity.

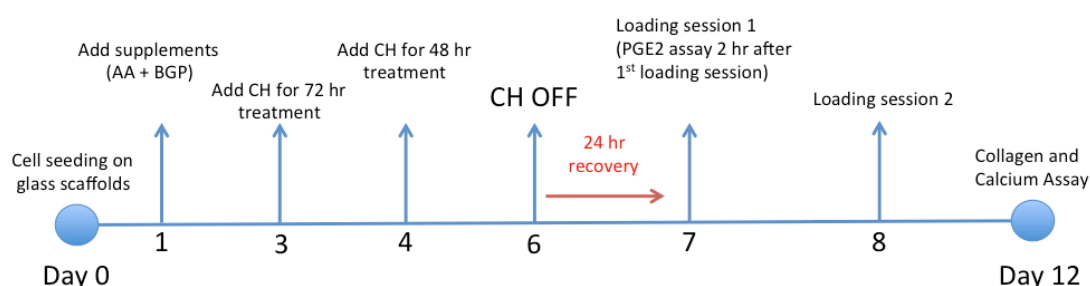


Fig 6.1; Experimental timeline used to study the effect of primary cilia damage on the fluid flow response of MLO-A5 cells. MLO-A5 cells were exposed to chloral hydrate (CH) for 48 and 72 hours on day 3 and 4 respectively. On day 6 of culture CH was removed and fresh media was added to samples. Cell-seeded scaffolds in control conditions were not treated with CH. Samples were then subjected to oscillatory fluid flow (1 hour at 1 Hz) on days 7 and 8 or cultured statically. Cell culture media was analysed for PGE2 release 2 hours after first loading session (day 7) and collagen production and calcium deposition was analysed on day 12.

## 6.3 Results

### 6.3.1 Cell viability quantified using Alamar Blue

Alamar Blue was utilised in this study to assess the effects of CH on MLO-A5 cell viability (fig 6.2). Samples were assayed on day 1 (blue bar) prior to CH treatment and again on day 7 (green bar) prior to dynamic loading. Cell seeded scaffolds not treated with CH had slightly higher cell viability on day 7 in comparison to day 1 of culture. Samples treated with CH for 48 and 72 h did not show any significant difference between day 1 and day 7 of culture. Although there were slightly fewer cells on day 7 of culture in samples treated with CH, these results were not significant and suggest that the application of CH did not have any important effect on MLO-A5 cell viability.

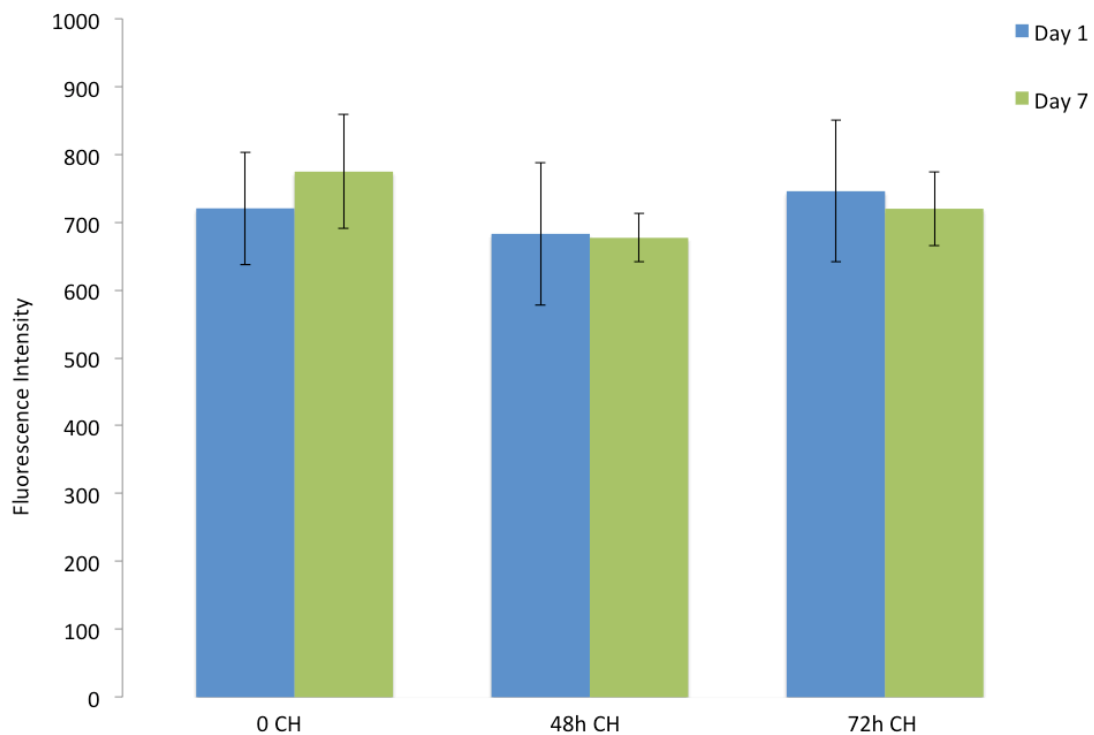


Fig 6.2; Alamar blue was used to quantify cell viability for samples treated with 0, 48 and 72 hour CH treatment on days 1 and 7 of static culture. All data is mean  $\pm$  SD (n = 4).

### 6.3.2 CH treatment and MLO-A5 response to FSS

On day 7 of culture, 2 hours after the first loading session, media from the samples was extracted and assayed for secreted PGE2. Cell seeded scaffolds subjected to fluid flow that were not treated with CH secreted more PGE2 into the media compared with statically cultured cells (fig 6.3). However, there were no significant differences in the levels of extracellular PGE2 for samples treated with 48 and 72 h CH and subjected to fluid flow compared to their static controls. Furthermore the PGE2 release from the CH treated cells in the FSS groups was significantly lower than for the non-treated FSS group.

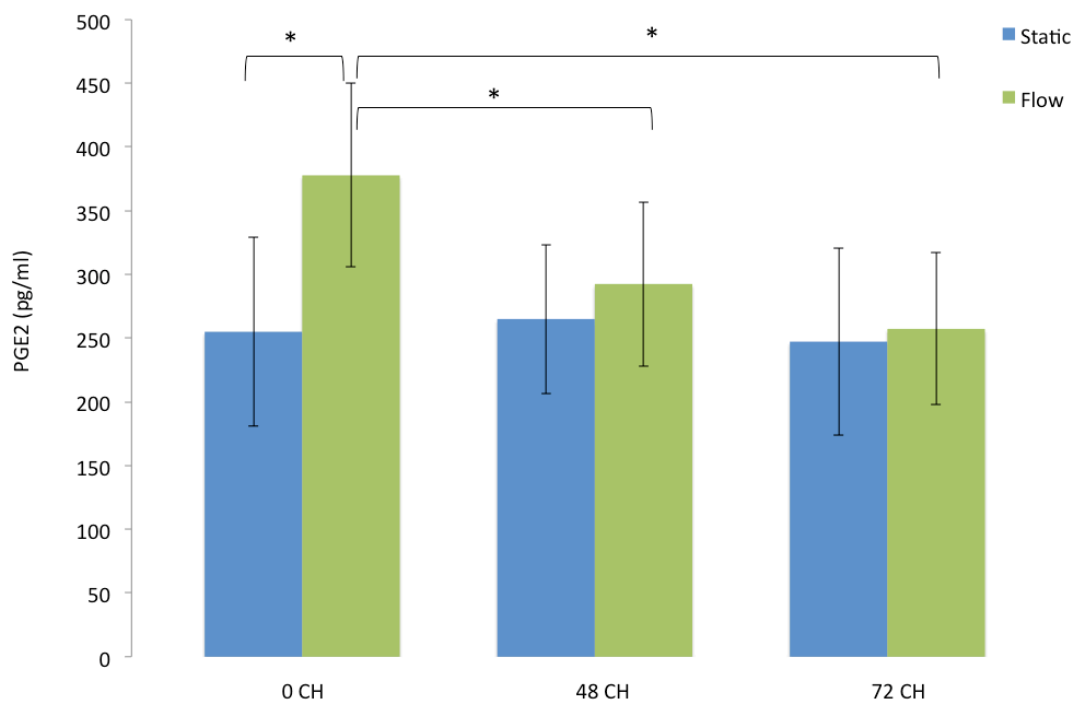


Fig 6.3; Extracellular PGE2 observed after 2 hours of loading on day 7 of culture for MLO-A5 constructs treated with 0, 48 and 72h CH. Data is mean  $\pm$  SD (n = 6). All data is mean  $\pm$  SD (n = 6). \* $P < 0.05$ .

### 6.3.3 Primary cilia of MLO-A5 cells treated with CH and subjected to fluid flow

MLO-A5 cells labeled with anti-acetylated  $\alpha$  tubulin can be seen in figure 6.4. It can be noted that the microtubule network (highlighted in green) was visualised within the cell cytoplasm and was well organised and surrounding the nucleus in control conditions (no exposure to CH). It is very difficult to image and focus on the primary cilia of cells seeded on scaffolds because of the cells being clustered in 3D and in multiple focal planes. As well as the microtubule network, a small bright protrusion was seen arising from cells which appeared to be the primary cilium.

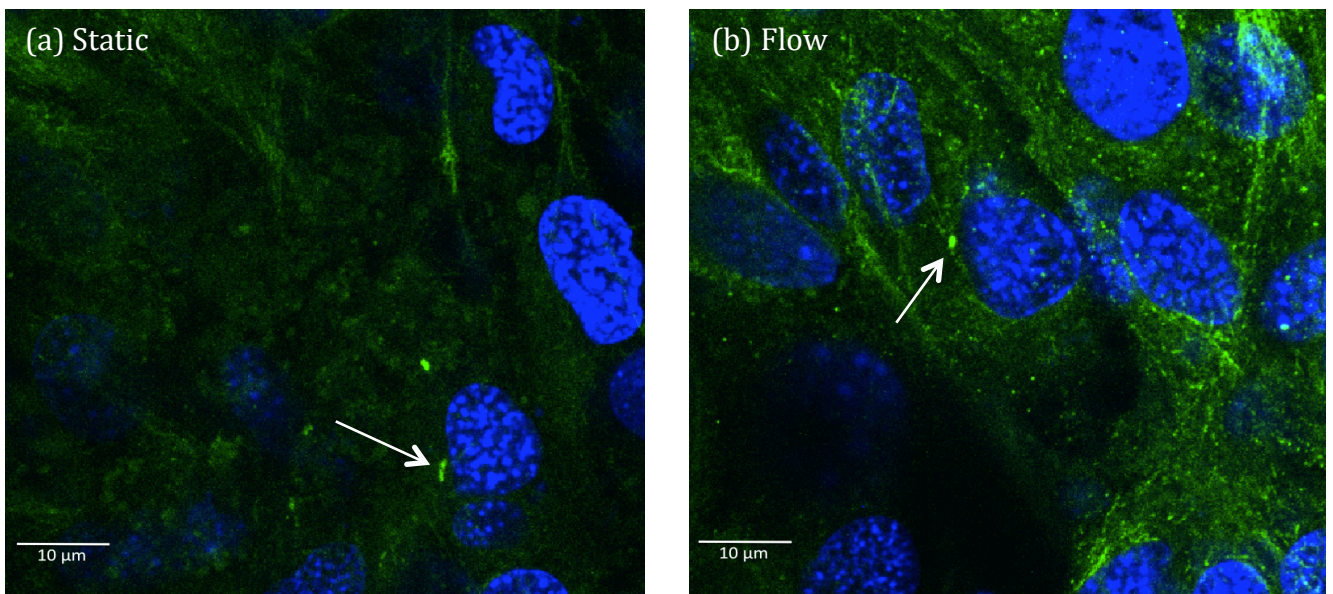


Fig 6.4; Cell nuclei (DAPI-blue) and anti-acetylated  $\alpha$  tubulin (green) staining of MLO-A5 cells with no CH treatment. The microtubule network can be seen surrounding the nucleus. Primary cilia seem to be projecting out of most cells and are located away from the cell nucleus indicated by the arrows. Images are representative of 3 experimental repeats.

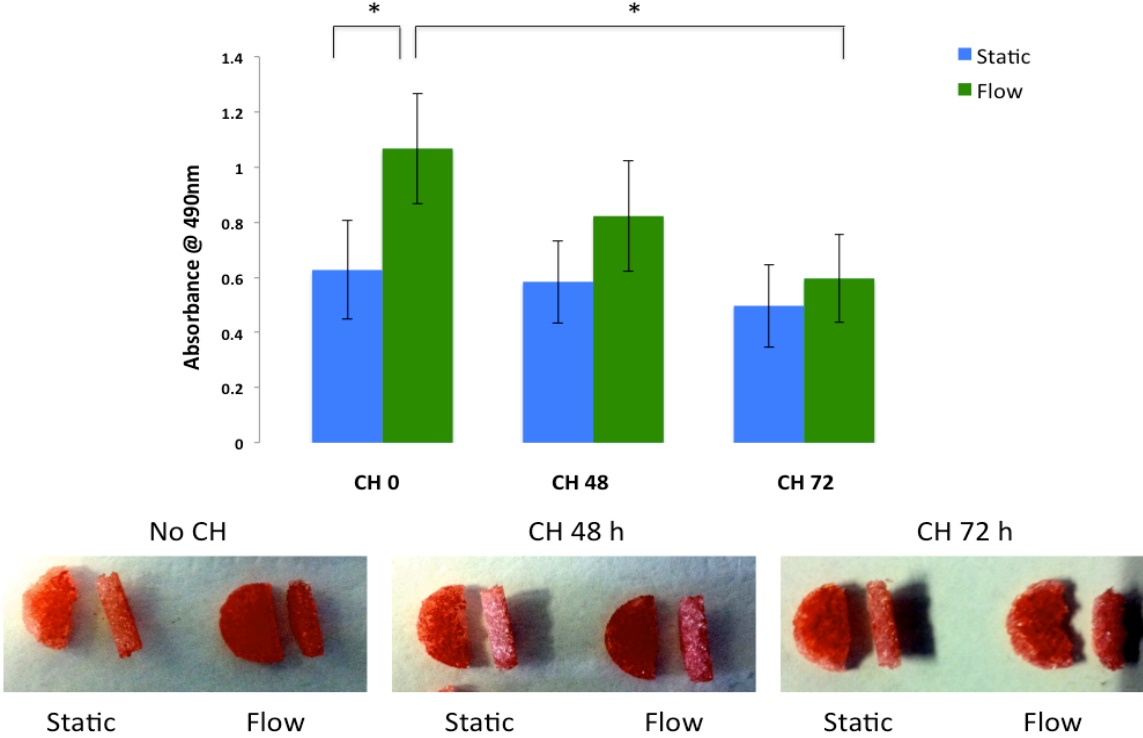
Dr. Delaine-smith imaged the same cell type but on 6 well plates and indicated that the primary cilium protrudes from the apical surface of the cell and is generally located on the side of the nucleus. When MLO-A5 cells were exposed to CH for 48 and 72 hrs, the microtubule network became increasingly disorganised

and the primary cilia were damaged or removed [20]. Therefore it can be assumed that the cilia was also disrupted in the current 3D model.

#### 6.3.4 Matrix production

Collagen production and calcium deposition measured by Sirius red and alizarin red staining respectively, were significantly higher in the dynamic control group (cells which were not exposed to CH and thus retained their cilia). Furthermore, the application of flow caused significantly more mineral production in the non CH treated group compared to static conditions. This confirmed that MLO-A5 cells responded to flow in the same way as reported for hES-MPs in the previous chapters. After exposure to chloral hydrate the ability of the cells to upregulate matrix in response to flow was reduced (fig 6.5). In both groups exposed to chloral hydrate (48 and 72 hrs) there was no significant difference in the collagen or calcium content between the static and flow groups.

### (a) Day 12 - Total Collagen



### (b) Day 12 - Total Calcium

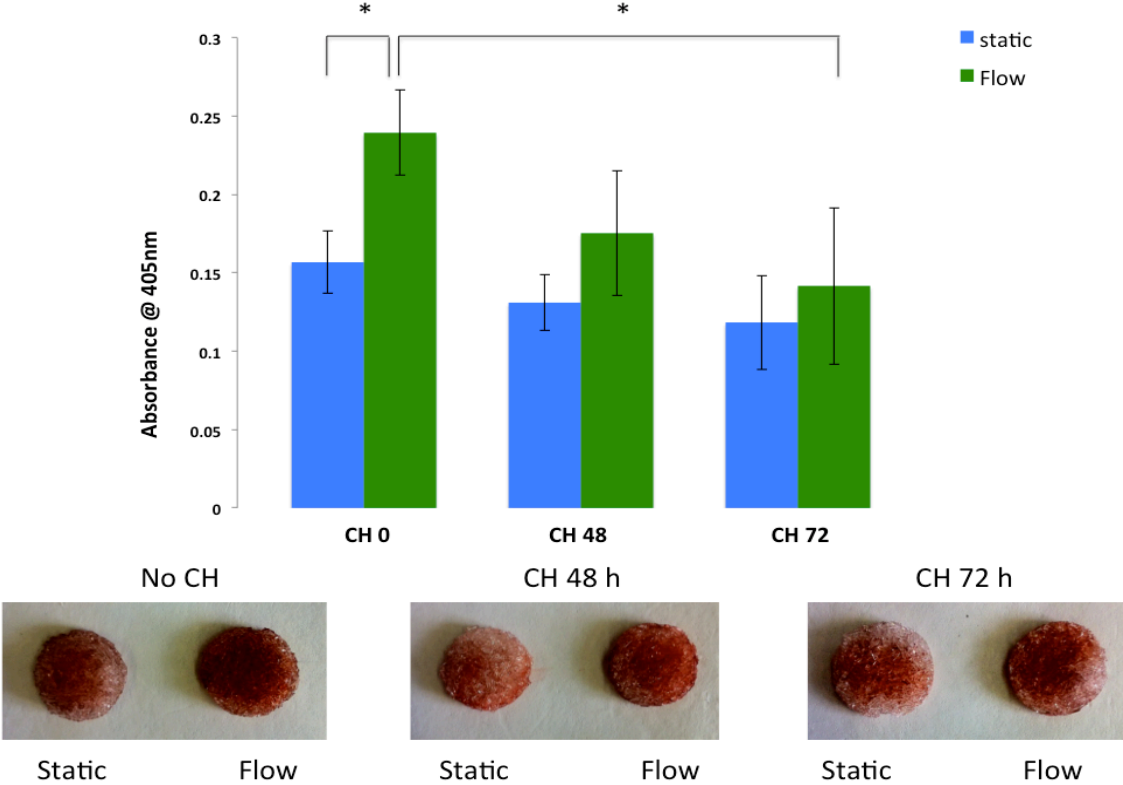


Fig 6.5; Collagen production (SR) and calcium deposition (AR) on day 12 of culture for MLO-A5 cells treated with 0, 48, and 72 hour CH treatment. Fluid flow caused cells to produce more collagen and calcium for 0 hour CH treatment, and produce less matrix in response to fluid flow with increasing CH treatment time. All data is mean ± SD (n = 6). \*P < 0.05.

## 6.4 Discussion

This is the first time that the primary cilia of MLO-A5 cells seeded on a porous glass scaffold have been reported and imaged *in vitro*. In other studies, it was shown that mouse renal epithelial cells had the primary cilia extended into the duct lumen and hence the primary cilium was always located near the cell nucleus [21]. In a recent study chondrocytes were seeded in a 3D agarose culture and it was shown that the length of chondrocyte primary cilia was reduced when samples were subjected to cyclic compressive strain in comparison to free-swelling culture [22]. In another study, rat-tail tendons were stress-deprived and it was demonstrated that cilia length increased in comparison to fresh controls. However once these samples were subjected to 24 hrs of cyclic loading, cilia length returned to normal levels supporting the concept that cilia are involved in the mechanotransduction response of tendon cells [23]. In this study there was some preliminary evidence based on confocal images that cells that had been subjected to fluid flow have slightly shorter cilia than those cultured in static conditions. However due to the irregular shape of the scaffold, it was difficult to obtain clear images of the primary cilia of MLO-A5 cells (fig 6.4). However this could be further investigated in the future by using transmission electron microscopy (TEM), reducing background staining or even higher magnification objectives.

MLO-A5 cells were chosen for this study since they have shown to be very sensitive to mechanical loading by producing a significant amount of collagen and calcium [20]. Furthermore, by using MLO-A5 cells it was possible to compare the response in this 3D model with Dr Delaine-Smith's 2D system, who also noticed a reduction in MLO-A5 cilia length once cells were subjected to fluid shear stress when compared to static cultures [20]. *Uzbekov et al.*, used transmission electron microscopy to study osteocyte centrosome morphology in relation to its mechanosensitive function. The spatial orientation of osteocyte centrosome was investigated and it was noticed that the primary cilium was mainly positioned perpendicular to the long axis of bone. Furthermore, it was observed that during osteocyte differentiation, mother and daughter centrioles

changed their original mutual orientation [24]. Due to the 3D nature of the scaffold it was difficult identifying and obtaining focused images of the primary cilia however it was shown that the primary cilia of MLO-A5 cells on a glass scaffold was generally to the side of the nucleus and it was not possible to image any particular organisation pattern of the primary cilium (fig 6.4). From the images it appears that the primary cilia are randomly organised in cultured cells. Therefore it maybe that type of mechanical stimulus, direction and force play an important role in cell migration and organisation.

Most of the work analysing primary cilia as mechanosensors has been demonstrated in the kidney and liver. *Praetorius and Spring* revealed that fluid flow within the kidney resulted in a deflection of the primary cilia which causes an extracellular calcium dependent increase in intracellular calcium [25]. This response was lost after the removal of the primary cilia. This mechanosensing mechanism has also been reported in liver cholangiocytes. It was found that the PC1/2 complex and the stretch activated ion channel TRPV4 are situated at the primary cilium and sense fluid shear stress and osmotic pressure respectively [26]. The application of flow not only resulted in an influx of calcium but also suppression of cAMP.

In bone cells, primary cilia are needed for cytokine release and changes in gene transcription in response to a mechanical stimulus. *Malone et al*, removed cilia in MC3T3-E1 osteoblasts using both siRNA against Polaris (a protein required for ciliogenesis) and chloral hydrate treatment. The results demonstrated that that the presence of a primary cilium in MC3T3-E1 cells was essential for OPN gene expression and PGE2 release by these cells when subjected to fluid flow, suggesting that primary cilia play an important role in transmitting the flow signal [8]. *Temiyasathit et al*. also investigated the role of primary cilia as mechanosensors in bone. This was demonstrated by using Cre-lox technology by cross-breeding mice that had floxed Kif3a gene (essential for ciliogenesis) and mice that express Cre under the control of the Col1 $\alpha$ 1 promoter. The results showed that after 3 consecutive days of axial compressive ulna loading, bone formation and mineral apposition was significantly increased for both the

knockout and control animals. However, in primary cilia knockout animals these increases were significantly reduced [27]. Hoey *et al.* also demonstrated that signalling molecules released into culture media by MC3T3 osteoblasts in response to fluid flow were primary-cilia dependent, suggesting that primary cilia play a role in osteogenic responses to flow in both osteoblasts and osteocytes [16].

In this chapter, it was shown that the primary cilium is needed for the upregulation of matrix production and PGE2 release. In the absence of primary cilia, MLO-A5 cells were less responsive and deposited less collagen and mineral in response to flow. In monolayer the cilia projects into the fluid flowing over the cells but in a 3D scaffold cell-cell and cell-matrix interactions may affect the cells position and ability to detect flow. Here it was demonstrated that even in a more complex environment of a 3D scaffold the cilia mediate the matrix-forming response of bone cells to fluid flow.

PGE2 has been shown to play an important role in osteoblast differentiation and in bone cell mechanotransduction. Bone cells *in vivo* subjected to fluid shear stress have been shown to induce PGE2 secretion, which stimulates the production of new bone [28]. In 2D studies it was shown that PGE2 was released when subjected to continuous and short-term rest-inserted fluid flow, a finding which is much the same in 3D case studies [29]. In this study, PGE2 secretion by MLO-A5 cells subjected to FSS was significantly higher compared to static cultures. Dr Delaine-Smith also presented the same findings for cells subjected to FFS in monolayer. In his studies the application of FSS combined with CH for only 24 hrs did not inhibit the PGE2 response; there was a 1.6-fold increase in PGE2 levels [20]. Furthermore, in this 3D system cell response was removed when samples were treated with 48 and 72 hrs CH suggesting that the primary cilium plays an important role in response to loading. In a similar study, the load-induced PGE2 production of immature osteoblasts (MC3T3-E1) and osteocytes (MLO-Y4) was removed when primary cilia formation was inhibited [8].

The technique to remove primary cilia used in the present study was to expose MLO-A5 cells to chloral hydrate. There is evidence that chloral hydrate not only weakens the attachment of the primary cilium, it also causes substantial alterations in microtubules and associated processes [18], and also interferes with mitosis [30]. The 24 hour recovery period should allow microtubule recovery as previously seen in 2D culture, so that at the time of flow only the cilia and not the microtubules were damaged. Although the prolonged exposure times required to remove the cilia may cause undesirable side effects related to microtubule damage, at present chloral hydrate is the only pharmacological technique for removal of MLO-A5 cilia. The treatment used in these experiments did not seem to adversely affect cell viability, probably because the cells were seeded at high density and there is not a large increase in cell number over time even in non-treated cells in this culture condition.

Other techniques used for the removal of primary cilia include siRNA-mediated depletion of the intraflagellar transport (IFT) component polaris (a protein for primary cilia biogenesis and function) [8]. In a recent study it was shown that after polaris siRNA treatment, only 50% fewer MLO-Y4 cells had primary cilia than control cells and a complete loss of flow response was observed in these cells. This is because the efficiency of IFT will probably decrease upon reduction of polaris protein levels, which will prevent delivery of functional ciliary components to some fraction of the remaining cilia [8]. In addition, this technique is expensive, more complicated and also needs to be optimised since it can inhibit other mechanosensory mechanisms [31].

Other pathways exist in which mechanical stimulation is transduced and modulated. When a cell is subjected to some form of mechanical stimuli, alterations in the cytoskeleton can occur. These include actin reorientation, microtubule polymerisation/depolymerisation and reorganisation of focal adhesion sites [32, 33]. There is also evidence that the cell glycocalyx plays a sensory role in bone cells. In a previous study, *Reilly et al* inhibited the ability of osteocyte-like cells to upregulate PGE2 release in response to oscillatory fluid flow by removal of hyaluronan (HA, a key glycocalyx component) [34]. In a more

recent study, *Morris et al* used laminar flow on mature bone cells as a stimulus to increase collagen production, however this response was absent upon removal of HA [35].  $\beta 1$  integrin has also been demonstrated to play an important role in both osteoblasts and osteocytes. *Zimmerman et al.*, demonstrated that the expression of an osteoblast-specific dominant negative form of  $\beta 1$  in long bones of mice lead to reduced bone mass and increased cortical porosity [36]. Bone cells also express different ion channels which are involved in mechanosensitive pathways including; the gadolinium-sensitive stretch-activated cation channels [37], the multimeric voltage sensitive calcium channels (VSCC) [38, 39], and transient receptor potential (TRP) channels [40]. As a response to membrane strain, stretch-activated cation channels cause a change in membrane potential leading to local depolarisation sufficient to activate VSCCs. *Li et al.*, demonstrated that VSCCs are mechanosensitive in rat tibia when mice treated with VSCC inhibitors exhibited significantly suppressed load-induced bone formation [41]. It may be possible that multiple mechanosensitive mechanisms are present within bone cells and they are activated at different levels of stimulus.

## **6.5 Conclusion**

This is the first time that MLO-A5 cells seeded on glass scaffolds were used to study flow and mechanical sensing of the primary cilia in bone. It was shown that the primary cilium is present on MLO-A5 bone cells in a 3D porous scaffold. Treatment with chloral hydrate (CH) proved to be an effective method to disrupt/damage primary cilia in a 3D environment. Furthermore, 48 and 72 hours exposure to chloral hydrate was enough to reduce matrix production in response to flow by MLO-A5 cells in 3D glass scaffolds. The present study demonstrates that the presence of intact primary cilia is essential for load sensing and the absence of the cilium (or changes in its morphology), can influence cellular responses to fluid flow.

## 6.6 References

- [1] Robling AG, Bellido T, Turner CH: Mechanical stimulation in vivo reduces osteocyte expression of sclerostin. *J Musculoskelet Neuronal Interact* 2006, 6:354.
- [2] Klein-Nulend J, van der Plas A, Semeins CM, Ajubi NE, Frangos JA, Nijweide PJ, Burger EH: Sensitivity of osteocytes to biomechanical stress in vitro. *FASEB J*. 1995, 9:441–445.
- [3] Reich KM, Frangos JA: Protein kinase C mediates flow-induced prostaglandin E2 production in osteoblasts. *Calcif Tissue Int*. 1993, 52:62–66.
- [4] Meinel L, Karageorgiou V, Fajardo R, Snyder B, Shinde-Patil V, Zichner L, Kaplan D, Langer R, Vunjak-Novakovic G: Bone tissue engineering using human mesenchymal stem cells: effects of scaffold material and medium flow. *Ann Biomed Eng*. 2004, 32:112–122.
- [5] Jacobs CR, Yellowley CE, Davis BR, Zhou Z, Cimbala JM, Donahue HJ: Differential effect of steady versus oscillating flow on bone cells. *J Biochem*, 1998. 31(11): 969-76.
- [6] Knothe Tate ML, Knothe U, Niederer P: Experimental elucidation of mechanical load-induced fluid flow and its potential role in bone metabolism and functional adaptation. *Am J Med Sci*. 1998, 316:189–195.
- [7] Weinbaum S, Cowin SC, and Zeng, Y: A model for the excitation of osteocytes by mechanical-induced bone fluid shear stresses. *J Biochem*, 1994. 27(3): 339-60.
- [8] Malone AM, Anderson CT, Tummala P, Kwon RY, Johnston TR, Stearns T, Jacobs CR: Primary cilia mediate mechanosensing in bone cells by a calcium-independent mechanism. *Proc Natl Acad Sci USA*. 2007, 104:13325–13330.
- [9] Matthews JL, Martin JH: Intracellular transport of calcium and its relationship to homeostasis and mineralization. An electron microscope study. *Am J Med*. 1971, 50:589–597.
- [10] Tonna EA, Lampen NM: Electron microscopy of aging skeletal cells. I. Centrioles and solitary cilia. *J Gerontol*. 1972, 27:316–324.
- [11] Xiao Z, Zhang S, Mahlios J, Zhou G, Magenheimer BS, Guo D, Dallas SL, Maser R, Calvet JP, Bonewald L, Quarles LD: Cilia-like structures and polycystin-1 in

osteoblasts/osteocytes and associated abnormalities in skeletogenesis and Runx2 expression. *J Biol Chem.* 2006, 281:30884–30895.

[12] Liu W, Murcia NS, Duan Y, Weinbaum S, Yoder BK, Schwiebert E, Satlin LM: Mechanoregulation of intracellular Ca<sup>2+</sup> concentration is attenuated in collecting duct of monocilia-impaired *orpk* mice. *Am J Physiol Renal Physiol.* 2005, 289:978–988.

[13] Schwartz EA, Leonard ML, Bizios R, Bowser SS. Analysis and modeling of the primary cilium bending response to fluid shear. *Am J Physiol.* 1997, 272:132–138.

[14] Jensen CG, Poole CA, McGlashan SR, Marko M, Issa ZI, Vujcich KV, Bowser SS: Ultrastructural, tomographic and confocal imaging of the chondrocyte primary cilium in situ. *Cell Biol Int.* 2004, 28:101–110.

[15] McGlashan SR, Jensen CG, Poole CA: Localization of extracellular matrix receptors on the chondrocyte primary cilium. *J Histochem Cytochem.* 2006, 54:1005–1014.

[16] Hoey DA, Kelly DJ, Jacobs CR. A role for the primary cilium in paracrine signaling between mechanically stimulated osteocytes and mesenchymal stem cells. *Biochem Biophys Res Commun.* 2011 Aug 19;412(1):182-7.

[17] Praetorius HA, and Spring KA: The renal cell primary cilium functions as a flow sensor. *Curr Opin Nephrol Hypertens*, 2003. 12(5): 517-20.

[18] Praetorius HA, and Spring KA: Removal of the MDCK cell primary cilium abolishes flow sensing. *J Membr Biol*, 2003. 191(1): 69-76.

[19] Chakrabarti A, Schatten H, Mitchell KD, Crosser M, Taylor M: Chloral hydrate alters the organization of the ciliary basal apparatus and cell organelles in sea urchin embryos. *Cell Tissue Res*, 1998. 292(3): 453-62.

[20] Delaine-Smith RM: Mechanical and physical guidance of osteogenic differentiation and matrix production. 2013, PhD thesis, University of Sheffield.

[21] Alieva IB, and Vorogjev IA: Vertebrate primary cilia: a sensory part of centrosomal complex in tissue cells, but a “sleeping beauty” in cultured cell? *Cell Nio. Int.*, 2004. 28: 139-150.

[22] McGlashan SR, Knight MM, Chowdhury TT, Joshi P, Jensen CG, Kennedy S, Poole CA: Mechanical loading modulates chondrocyte primary cilia incidence and length. *Cell Biol Int* 34:441-446.

- [23] Gardner K, Arnoczky SP, and Lavagnino M: Effect of In vitro Stress-Depreavation and Cyclic Loading on the Length of Tendon Cell Cilia in situ. *J Orthop Res.* 2011, 29(4):582-587.
- [24] Uzbekov RE, Maurel DB, Aveline PC, Pallu S, Benhamou CL, Rochefort GY. Centrosome fine ultrastructure of the osteocyte mechanosensitive primary cilium. *Microsc Microanal.* 2012 Dec;18(6):1430-41.
- [25] Praetorius HA, Spring KR: Bending the MDCK cell primary cilium increases intracellular calcium. *Journal of Membrane Biology.* 2011, 184, 71–79.
- [26] Gradilone SA, Masyuk AI, Splinter PL, Banales JM, Huang BQ, Tietz PS, Masyuk TV, Larusso NF: Cholangiocyte cilia express TRPV4 and detect changes in luminal tonicity inducing bicarbonate secretion. *Proceedings of the National Academy of Sciences USA.* 2007, 104, 19138–19143.
- [27] Temiyasathit S, Tang WJ, Leucht P, Anderson CT, Castillo AB, Helms JA, Stearns T, Jacobs CR, editors. Primary cilia mediate loading-induced bone formation in vivo. *Orthopaedic Research Society; 2010. New Orleans, US; 2010.*
- [28] Bakker AD, Joldersma M, Klein-Nulend J, and Burger EH: Interactive effects of PTH and mechanical stress on nitric oxide and PGE2 production by primary mouse osteoblastic cells. *Am J Physiol Endocrinol Metab.* 2003 Sep;285(3):E608-13.
- [29] Vance J, Galley S, Liu DF, Donahue SW: Mechanical stimulation of MC3T3 osteoblastic cells in a bone tissue-engineering bioreactor enhances prostaglandin E2 release. *Tissue Eng.* 2004. 10(5-6): 1832-9.
- [30] Lee GM, Diguseppi J, Gawdi GM, Herman B. Chloral hydrate disrupts mitosis by increasing intracellular free calcium. *J Cell Sci.* 1987 Dec;88 ( Pt 5):603-612.
- [31] Jackson AL, Bartz SR, Schelter J, Kobayashi SV, Burchard J, Mao M, Li B, Cavet G, Linsley PS: Expression profiling reveals off-target gene regulating by RNAi. *Nat Biotechnol.* 2003. 21(6): 635-7.
- [32] Geiger RC, Kaufman CD, Lam AP, Budinger GR, Dean DA: Tubulin acetylation and histone deacetylase 6 activity in the lung under cyclic load. *American Journal of Respiratory Cell and Molecular Biology.* 2009, 40, 76–82.
- [33] Pavalko FM, Chen NX, Turner CH, Burr DB, Atkinson S, Hsieh YF, Qiu J, Duncan RL: Fluid shear-induced mechanical signaling in MC3T3-E1 osteoblasts requires cytoskeleton-integrin interactions. *American Journal of Physiology.*

1998;275(6 Pt 1):1591–1601.

[34] Reilly GC, Haut TR, Yellowley CE, Donahue HJ, Jacobs CR: Fluid flow induced PGE2 release by bone cells is reduced by glycocalyx degradation whereas calcium signals are not. *Biorheology*. 2003;40(6):591-603.

[35] Morris HL, Reed CI, Haycock JW, Reilly GC: Mechanisms of fluid-flow-induced matrix production in bone tissue engineering. *Proc Inst Mech Eng H*. 2010 Dec;224(12):1509-21.

[36] Zimmerman D, Jin F, Leboy P, Hardy S, Damsky C. Impaired bone formation in transgenic mice resulting from altered integrin function in osteoblasts. *Developmental biology* 2000; 220:2–15.

[37] Duncan RL, Hruska KA. Chronic, intermittent loading alters mechanosensitive channel characteristics in osteoblast-like cells. *The American journal of physiology*. 1994;267:F909–16.

[38] Li J, Duncan RL, Burr DB, Turner CH. L-type calcium channels mediate mechanically induced bone formation in vivo. *Journal of bone and mineral research : the official journal of the American Society for Bone and Mineral Research*. 2002;17:1795–800.

[39] Shao Y, Alicknavitch M, Farach-Carson MC. Expression of voltage sensitive calcium channel (VSCC) L-type Cav1.2 (alpha1C) and T-type Cav3.2 (alpha1H) subunits during mouse bone development. *Developmental dynamics : an official publication of the American Association of Anatomists*. 2005;234:54–62.

[40] Abed E, Labelle D, Martineau C, Loghin A, Moreau R. Expression of transient receptor potential (TRP) channels in human and murine osteoblast-like cells. *Molecular membrane biology*. 2009;26:146–58.

[41] Li J, Duncan RL, Burr DB, Gattone VH, Turner CH. Parathyroid hormone enhances mechanically induced bone formation, possibly involving L-type voltage-sensitive calcium channels. *Endocrinology*. 2003; 144:1226–33.

## Chapter 7: Conclusion and Future Work

The main aim of this project was to investigate the effects of a perfusion bioreactor system on progenitor cell differentiation (towards an osteogenic lineage) and matrix mineralisation. The overall goal was to study which parameters within a bioreactor can accelerate cell differentiation and matrix production in order to direct cell phenotype and speed up development time. Here it was shown that direct perfusion in combination with oscillatory fluid flow improves cell distribution throughout the scaffold structure, enhances proliferation and upregulates the enzyme ALP and extracellular matrix components associated with osteogenic differentiation by hES-MP cells seeded on a novel glass scaffold. The system designed in this report not only provides insight into cell mechanotransduction but also provides information regarding the relationship between fluid shear stress, cellular function and tissue development. The system was further used to investigate whether peptide-coated scaffolds (developed by our industrial collaborators) would support cells and whether there was a synergistic effect of protein coating and fluid flow conditions. Furthermore the flow parameters shown to upregulate bone matrix were used to identify a potential mechanotransduction mechanism. The work presented in this thesis provides a useful 3D model with which to understand the mechanical response of differentiating bone cells and can be applied to further *in vitro* studies of bone mechanotransduction or be used to further develop and optimise bioreactor parameters for clinical bone tissue engineering applications.

### 7.1 Optimal culturing strategy

In this study it was shown that hES-MP-constructs subjected to short bouts of fluid flow can greatly enhance matrix production and genes associated with osteogenic differentiation. As suggested by a number of other research groups in the field, the reason for an upregulation in matrix production could be because of a better and more efficient nutrient transport, alongside biochemical cues which can ultimately create a suitable microenvironment for the development of

functional 3D constructs. However the improved nutrient flow would have only occurred for short time periods in this experimental set up since the samples were in static culture between flow sessions, which were of only 1 hours duration. Therefore, it seems likely there was a specific response to the shear stress that induced long-term changes in the cells. However, a big question still remains regarding the ultimate strategy for directing the differentiation of progenitor cell lines through the use of mechanical cues such as shear stress. Many important parameters including flow type, insertion of rest periods, duration, frequency and magnitude of shear stress can all influence cell response. With respect to flow duration, there is evidence suggesting that constant stimulation of cells (irrespective of flow type) can lead to cellular desensitisation and switching off the cells response. In order to overcome this problem, rest insertions between loading sessions have been explored by a number of researchers. This appears to enhance the expression of certain genes such as osteopontin [1], bone sialoprotein [2] and PGE2 [3]. The timing of mechanical loading is also an important factor to consider. Cells tend to respond to the application of flow within seconds (influxes in calcium) to weeks (mineralised matrix deposition). In this investigation, fluid flow was subjected to samples on day 4 and analysed on day 7 of culture for short-term experiments. For long-term experiments, samples were subjected to loading on days 4, 7, and 10 and markers of osteogenesis were analysed on day 14. These time points were chosen following a successful project conducted by a previous student [4]. However, the duration and frequency of flow required to commit cells towards a specific lineage is still an active area of research.

Future work:

- Measuring ALP activity at several time points (day 5, 6, etc) soon after the application of flow
- Studying how a range of frequencies (<1 Hz <) and loading durations (<1 hr <) can effect cell phenotype

## **7.2 Bioreactors for cell seeding**

In this study cells were seeded onto glass and PU scaffolds by directly adding the cell suspension to the scaffold. Although this method is the simplest since it avoids the use of tubing, pumps and large volumes of media, it can result in non-homogeneous cell distribution and low seeding efficiency. In previous studies that have utilised PU scaffolds (10 mm x 10 mm), this seeding method seemed to cause cells to settle in the centre of the scaffold and be absent from the periphery. Low seeding efficiency can be improved by placing scaffolds in spinner flasks. However direct perfusion bioreactors have shown to further improve seeding efficiency [5-9]. It has been demonstrated that loading efficiency for bone marrow stromal cells and chondrocytes in a perfusion bioreactor was 20% higher in comparison to static loading. Furthermore, cells were significantly more uniformly distributed [10]. Studies that have utilised direct perfusion for cell seeding have also been shown to yield higher cell attachment compared to statically loaded cells. In another study, oscillatory flow was used to seed preosteoblastic cells onto polystyrene and PLLA scaffolds. As a result higher seeding efficiency and higher cell attachment was achieved under dynamic loading in comparison to statically loaded cells [11]. The bioreactor system developed in this study can be modified to seed cells onto a range of scaffold shapes, however further experiments will need to be carried out in order to determine a flow rate for initial cell seeding.

## **7.3 Bone tissue engineering scaffolds**

Scaffolds used in bone tissue engineering are typically made of porous degradable materials that supply the mechanical support during repair and regeneration of damaged or diseased bone. Ideally a scaffold for bone tissue engineering should be bioresorbable, biocompatible, have the mechanical properties to match host bone properties and have an interconnected porosity for successful diffusion of nutrients. Bioglass based bioresorbable scaffolds [12], polymeric scaffolds [13], composite scaffolds [14] and metallic scaffolds [15] have been demonstrated to enhance osteogenic differentiation of MSCs when

used for bone repair *in vivo*. The borosilicate glass scaffolds utilised in this study are biocompatible in which cells can attach and proliferate, however they cannot be used for clinical applications. The reason glass scaffolds were utilised in this study is that they have good light transmissibility used for cell staining, are supplied uncoated or peptide coated which can both promote cell attachment and provide a foundation for studying various aspects of cell matrix interaction, mechanotransduction and cell behavior relevant *in vitro* three-dimensional (3D) culture systems.

Organisation of porosity has also been shown to play a key role in the quality of bone formation. In a recent study, an ordered and confined geometry of hydroxyapatite (HA) foams led to self-assembly of collagen in the pores which resulted in compact lamellar bone [16]. In comparison, when progenitor cells were loaded onto a HA/collagen composite, collagen fibres were distributed in a nematic phase and resulting in woven isotropic bone. Porosity for most bone tissue engineering scaffolds is uniformly distributed throughout scaffold structure. However, the scaffold may not be uniformly porous as demonstrated by the borosilicate glass scaffolds. Natural bone has higher porosity in the core with a strong and dense outer shell, hence it does not have a uniform distribution of porosity. Since the shear stress distribution can be affected by pore geometry, a parallel study comparing the glass scaffolds with other scaffolds with different pore architecture would further provide insight into osteoblastic differentiation and ECM mineralisation.

#### **7.4 Primary cilia of bone cells**

The data from chapter 6 supports the hypothesis that oscillatory fluid shear stress can mediate mechanosensation in MLO-A5 osteoblastic cells via the primary cilium. In summary it was shown that primary cilia translate dynamic fluid flow signals into upregulation of collagen, calcium and PGE2 in MLO-A5 cells. However it is still unclear how the primary cilia transmits the external force to the inside of the cell and how it interacts with the mineralised matrix of bone. One possible reason could be the mechanical stimulus is converted into a

chemical signal that initiates a cellular response such as a change in gene expression or cytokine release. However, as mentioned previously in chapter 1, the only characterised mechanosensory mechanism in the cilium involves the polycystins [17]. Adenylyl cyclases have also been found in the primary cilia, suggesting that cAMP could be a second messenger in ciliary signaling [18]. As has been proposed for Shh signaling, IFT could also traffic activated signaling proteins from the ciliary compartment to the cytoplasm [19], all of which suggests that the primary cilium can be coupled with other signaling pathways. To further characterise the role of the primary cilium in bone, conditional knockout of genes required for primary cilium in osteocytes, osteoblasts and osteoclasts can be undertaken [20]. Since the primary cilia play different signaling roles depending on developmental stage, in depth investigation of primary cilia function in these cells at different stages of differentiation could provide further insight into how cells sense and respond to environmental stimuli. Future studies could involve integrating ciliary signaling with other cellular sensory systems to provide a comprehensive picture of ciliary function in response to mechanical loading. Thus, for clinical applications it would be worth investigating mechanotransduction of osteoprogenitors considering that it was recently demonstrated by Hoey *et al.*, that the primary cilia is essential for load-induced gene responses in MSCs [21].

## **7.5 Computational Modeling**

In the field of bone tissue engineering, growing interest has been given to analysing shear stress distribution in complex 3D scaffolds. In this study it was shown that the action of fluid flow entering the scaffold is a potent mechanical stimulus, which can control the phenotype of the 3D construct. It is evident that scaffold architecture and geometry determined by pore size, shape and distribution are key design parameters [22-24]. The combination of micro-CT (fig 7.1) and Computational Fluid Dynamics (CFD) can be very useful in order to obtain local shear stresses within porous structures. This can help determine loading conditions at the cellular level and provide further insight that relates mechanical stimuli with osteogenesis. Predictive models developed in this

manner are a powerful tool for better understating constructs subjected to perfusion flow prior to transplantation. [25-28]. Flow patterns within the flow perfusion bioreactor need to be better characterised to further understand the relationship between fluid shear stress and cell differentiation for creating the ideal scaffold/culture combination.

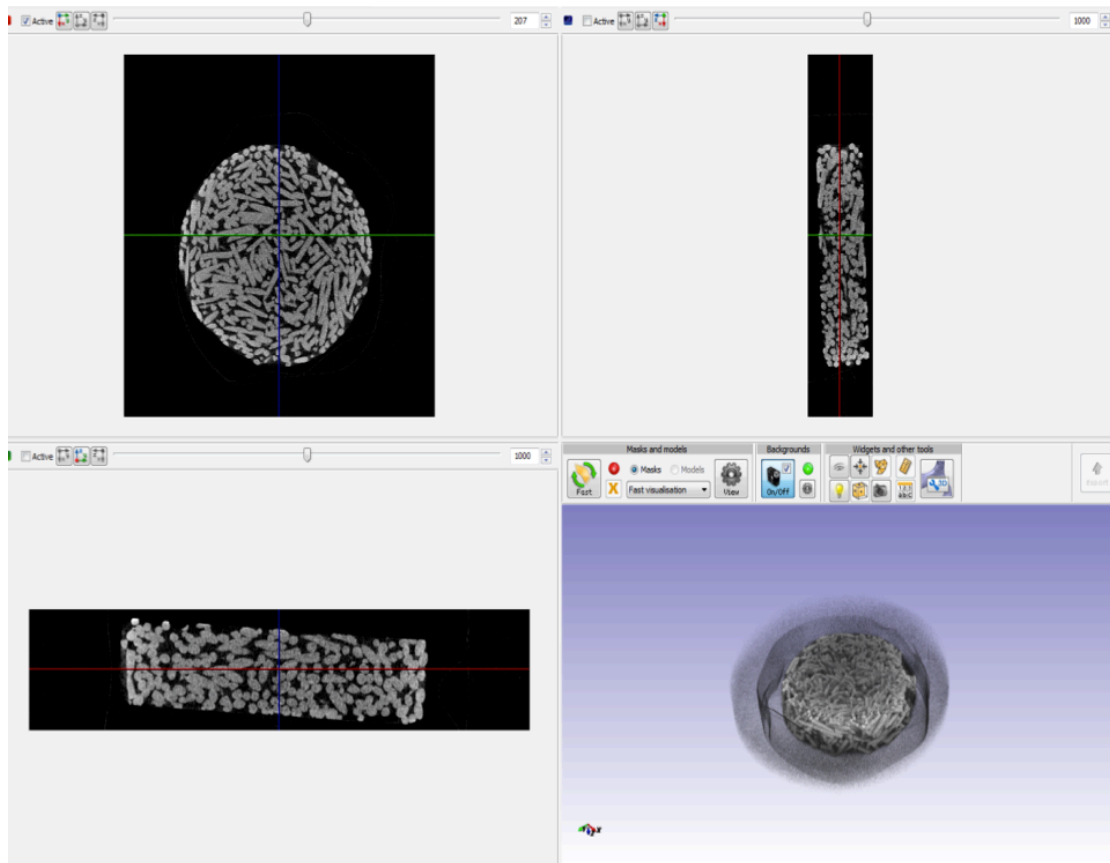


Fig 7.1; Micro-CT images of the glass scaffold was obtained by placing the scaffold in a SKYSCAN 1172 micro-CT machine. This resulted in a total of 415 images taken from top to bottom of glass scaffold. Images were compiled in ScanIP to create a 3D model.

## 7.6 Mesenchymal Progenitors

The choice of an optimal cell source is of great importance for the successful culture of functional constructs to be used for the repair of skeletal defects. Results from this project demonstrated that the use of a perfusion bioreactor in combination with hES-MP cells on 3D porous scaffolds, strongly promoted cell

proliferation and osteogenic differentiation. Other factors including surface chemistry and scaffold composition have also been identified to enhance MSC differentiation into a variety of tissue-specific cells. This makes MSCs an attractive cell source for tissue engineering and regenerative medicine purposes. However, there are still a number of questions that need to be addressed before MSCs can be utilised in a clinical setting. Limited availability and poor proliferative properties are of major concern. Moreover the timing and differentiation process of MSCs to a specific cell is still unclear and requires further investigation. Even though it was shown that some osteogenic markers were upregulated in this study, further research regarding the differentiation of hES-MP cells under perfusion is still required. These could include cytokines and expression of other osteogenic markers in order to confirm the existence of differentiated osteoblasts. Additionally, use of histological and mineral analysis (FTIR) can contribute to understanding the structural and mechanical properties of the hES-MP/scaffold construct. In the meantime the stable, easily handled and highly osteogenic pluripotent stem cell derived-mesodermal progenitors used here have a great potential as a cell source for the fabrication of bone substitutes in a clinical context.

### **7.7 Co-culture of Osteoprogenitor Cells with Endothelial Cells**

The repair of skeletal defects involves many different events and multiple cell types. The main limitation in creating large scale implantable constructs is the lack of a vascular network. In particular, the survival of bone tissue relies on the development of blood vessels since they transport nutrients, oxygen and soluble factors to the tissue. Researchers have suggested to incorporate endothelial cells supplemented with angiogenic factors (vascular endothelial growth factor) into the tissue engineered construct in order to achieve a vascular network and understand more about the relationship between the vasculature and bone. Since osteoprogenitor and endothelial cells have been shown to be mechanosensitive, a coculture system could be developed to study the effect of fluid flow on the interactions between both cell types. Cultures can be analysed

for OPN, OC and BSP to determine osteogenic differentiation. Signaling mechanisms could be studied to provide further insight into the cellular and molecular interactions between blood cells and blood vessels.

## **7.8 Final Conclusions**

- In chapter 3 it was shown that hES-MP and mouse MSC cells were able to survive and distribute throughout a PU foam and novel glass scaffold for up to 14 days in static culture. Furthermore, short bouts of fluid flow was shown to increase cell viability and calcium deposition of hES-MP-glass constructs.
- The effect of flow type (unidirectional Vs oscillatory) and scaffold orientation on human mesenchymal progenitor cell differentiation and matrix production was investigated in chapter 4. It was shown that direct perfusion in combination with oscillatory fluid flow creates a more uniform cell distribution and an upregulation of ALP collagen and calcium associated with osteogenesis.
- The methods developed in chapter 4 were used to study the cell's response to a combination of peptide coated scaffolds and bioreactor culture. In chapter 5 it was shown that the combination of peptide coated scaffolds and oscillatory flow improves cell distribution and further enhances early and late markers of bone formation.
- The role of the primary cilia as a mechanosensory organelle was investigated in chapter 6. It was demonstrated that MLO-A5 cells were less responsive and synthesised less matrix in response to fluid shear stress in the absence of the primary cilium.

## 7.9 References

- [1] Partap, S., Plunkett, N., Kelly, D., and O'Brien, F. Stimulation of osteoblasts using rest periods during bioreactor culture on collagen-glycosaminoglycan scaffolds. *J Mater Sci Mater Med* 21, 2325, 2010.
- [2] Kreke, M.R., Huckle, W.R., and Goldstein, A.S. Fluid flow stimulates expression of osteopontin and bone sialoprotein by bone marrow stromal cells in a temporally dependent manner. *Bone* 36, 1047, 2005.
- [3] Jaasma, M.J., and O'Brien, F.J. Mechanical stimulation of osteoblasts using steady and dynamic fluid flow. *Tissue Eng Part A* 14, 1213, 2008.
- [4] Sittichokechaiwut A. Dynamic Mechanical Stimulation for Bone Tissue Engineering. 2009. PhD thesis, University of Sheffield.
- [5] Zhao F, Pathi P, Grayson W, Xing Q, Locke BR, Ma T: Effects of oxygen transport on 3-D human mesenchymal stem cell metabolic activity in perfusion and static cultures: experiments and mathematical model. *Biotechnol Prog* 2005;21:1269–80.
- [6] Li Y, Ma T, Kniss DA, Lasky LC, Yang ST: Effects of filtration seeding on cell density, spatial distribution, and proliferation in nonwoven fibrous matrices. *Biotechnol Prog* 2001;17:935–44.
- [7] Kitagawa T, Yamaoka T, Iwase R, Murakami A: Three-dimensional cell seeding and growth in radial-flow perfusion bioreactor for in vitro tissue reconstruction. *Biotechnol Bioeng* 2006;93:947–54.
- [8] Kim SS, Sundback CA, Kaihara S, Benvenuto MS, Kim BS, Mooney DJ: Dynamic seeding and in vitro culture of hepatocytes in a flow perfusion system. *Tissue Eng* 2000;6:39–44.
- [9] Vunjak-Novakovic G, Obradovic B, Martin I, Bursac PM, Langer R, Freed LE: Dynamic cell seeding of polymer scaffolds for cartilage tissue engineering. *Biotechnol Prog* 1998;14:193–202.
- [10] Wendt D, Marsano A, Jakob M, Heberer M, Martin I: Oscillating perfusion of cell suspensions through three-dimensional scaffolds enhances cell seeding efficiency and uniformity. *Biotechnol Bioeng* 2003;84:205–14.

- [11] Alvarez-Barreto JF, Linehan SM, Shambaugh RL, Sikavitsas VI: Flow perfusion improves seeding of tissue engineering scaffolds with different architectures. *Ann Biomed Eng* 2007;35:429–42.
- [12] Jones, JR: Optimising bioactive glass scaffolds for bone tissue engineering. *Biomaterials*. 2006, 27, 964–973.
- [13] Lee SH, and Shin H: Matrices and scaffolds for delivery of bioactive molecules in bone and cartilage tissue engineering. *Adv. Drug Deliv. Rev.* 2007, 59, 339–359.
- [14] Laschke MW, Strohe A, Menger MD, Alini M, Eglin D: In vitro and in vivo evaluation of a novel nanosize hydroxyapatite particles/poly(ester-urethane) composite scaffold for bone tissue engineering. *Acta Biomater.* 2010 Jun;6(6):2020-7.
- [15] Dabrowski B, Swieszkowski W, Godlinski D, Kurzydowski KJ: Highly porous titanium scaffolds for orthopaedic applications. *J Biomed Mater Res B Appl Biomater.* 2010 Oct;95(1):53-61.
- [16] Scaglione S, Giannoni P, Bianchini P, Sandri M, Marotta R, Firpo G, Valbusa U, Tampieri A, Diaspro A, Bianco P, Quarto R: Order versus disorder: in vivo bone formation within osteoconductive scaffolds. *Sci. Rep.* 2, Article no. 274.
- [17] Nauli SM, Alenghat FJ, Luo Y, Williams E, Vassilev P, Li X, Elia AE, Lu W, Brown EM, Quinn SJ, Ingber DE, Zhou J: Polycystins 1 and 2 mediate mechanosensation in the primary cilium of kidney cells *Nat Genet.* 2003 Feb;33(2):129-37.
- [18] Masyuk AI, Masyuk TV, Splinter PL, Huang BQ, Stroope AJ, LaRusso NF: Cholangiocyte cilia detect changes in luminal fluid flow and transmit them into intracellular Ca<sup>2+</sup> and cAMP signaling. *Gastroenterol.* *Gastroenterology.* 2006 Sep;131(3):911-20.
- [19] Haycraft CJ, Zhang Q, Song B, Jackson WS, Detloff PJ, Serra R, Yoder BK: Intraflagellar transport is essential for endochondral bone formation. *Development.* 2007 Jan;134(2):307-16.
- [20] Haycraft, C.J. & R. Serra. 2008. Cilia involvement in patterning and maintenance of the skeleton. *Curr. Top. Dev. Biol.* 85: 303–332.

- [21] Hoey DA, Tormey S, Ramcharan S; O' Brien FJ, Jacobs CR. Primary Cilia Mediated Mechanotransduction in Human Mesenchymal Stem Cells. *STEM CELLS*, 2012, Vol.30(11), pp.2561-2570.
- [22] Hollister SJ, Maddox RD, Taboas JM: Optimal design and fabrication of scaffolds to mimic tissue properties and satisfy biological constraints. *Biomaterials* 2002;23:4095–103.
- [23] Boschetti F, Raimondi MT, Migliavacca F, Dubini G: Prediction of the micro-fluid dynamic environment imposed to three-dimensional engineered cell systems in bioreactors. *J Biomech* 2006;39:418–25.
- [24] Adachi T, Osako Y, Tanaka M, Hojo M, Hollister SJ: Framework for optimal design of porous scaffold microstructure by computational simulation of bone regeneration. *Biomaterials* 2006;27:3964–72.
- [25] Alvarez-Barreto JF, Linehan SM, Shambaugh RL, Sikavitsas VI. Flow perfusion improves seeding of tissue engineering scaffolds with different architectures. *Ann Biomed Eng* 2007; 35(3): 429-42.
- [26] Zhang ZY, Teoh SH, Teo EY, Khoon CMS, Shin CW, Tien FT: A comparison of bioreactors for culture of fetal mesenchymal stem cells for bone tissue engineering. *Biomaterials* 2010; 31(33):8684-95.
- [27] David B, Bonnefont-Rousselot D, Oudina K, Degat MC, Deschep- per M, Viateau V, et al. A perfusion bioreactor for engineering bone constructs: An in vitro and in vivo study. *Tissue Eng Part C Methods* 2011; 17(5): 505-16.
- [28] Cioffi, M., Boschetti, F., et al., 2006. Modeling evaluation of the fluid-dynamic microenvironment in tissue-engineered constructs: a micro-CT based model. *Biotechnology and Bioengineering* 93 (3), 500–510.

# Appendix 1

## Conferences

- SPRBM/BMES conference on Cellular and Molecular Bioengineering – Miami, January 2010 (presented poster: Mechanical stimulation of mesenchymal stem cells in 3D scaffolds using oscillating fluid flow. M.Shaeri, S. Philips, D.Athey and G.C. Reilly)
- The 12th Annual White Rose Biomaterials and Tissue Engineering Working Progress Meeting – Leeds University, November 2010 (presented poster: Mechanical stimulation of mesenchymal stem cells in 3D scaffolds using oscillating fluid flow. Shaeri M, Reilly, G C)
- The 13th Annual White Rose Biomaterials and Tissue Engineering Working Progress Meeting- University of Sheffield Sheffield, November 2011 (oral presentation: Mechanical stimulation of mesenchymal stem cells in a 3D glass scaffold using oscillating and unidirectional flow. M. Shaeri, S. Phillips, D. Athey, C.K. Chong and G.C. Reilly)
- Bioengineering 11 Conference-Queen Mary University, February 2012 (presented poster: Mechanical stimulation of mesenchymal stem cells in 3D scaffolds using oscillating fluid flow M. Shaeri, S. Phillips, D. Athey and G.C. Reilly)
- European Society of Biomechanics (ESB), Lisbon, July 2012 (Oral presentation: mechanical stimulation of mesenchymal stem cells in a 3D glass scaffold using oscillating and unidirectional flow. M. Shaeri, S. Phillips, D. Athey, C.K. Chong and G.C. Reilly)